

SIXTH INTERNATIONAL WORKSHOP

ON LASER RANGING INSTRUMENTATION

ANTIBES JUAN-LES-PINS



6^e COLLOQUE INTERNATIONAL
SUR L'INSTRUMENTATION
DE LA TELEMETRIE LASER

EDITED BY / EDITE PAR :

- JEAN GAIGNEBET
- FRANCOISE BAUMONT

WE WISH HEREBY TO EXPRESS OUR THANKS TO /
NOUS TENONS A REMERCIER ICI :

- MINISTERE DES AFFAIRES ETRANGERES
- ASSOCIATION INTERNATIONALE DE GEODESIE
- UNION GEODESIQUE ET GEOPHYSIQUE INTERNATIONALE
- INSTITUT NATIONAL DES SCIENCES DE L'UNIVERS
- CENTRE NATIONAL D'ETUDES SPATIALES
- AEROSPATIALE
- BRASSARD MICHELET INDUSTRIES
- QUANTEL
- SOCIETE D'ETUDES ET DE CONSTRUCTION D'INSTRUMENTS ASTRONOMIQUES

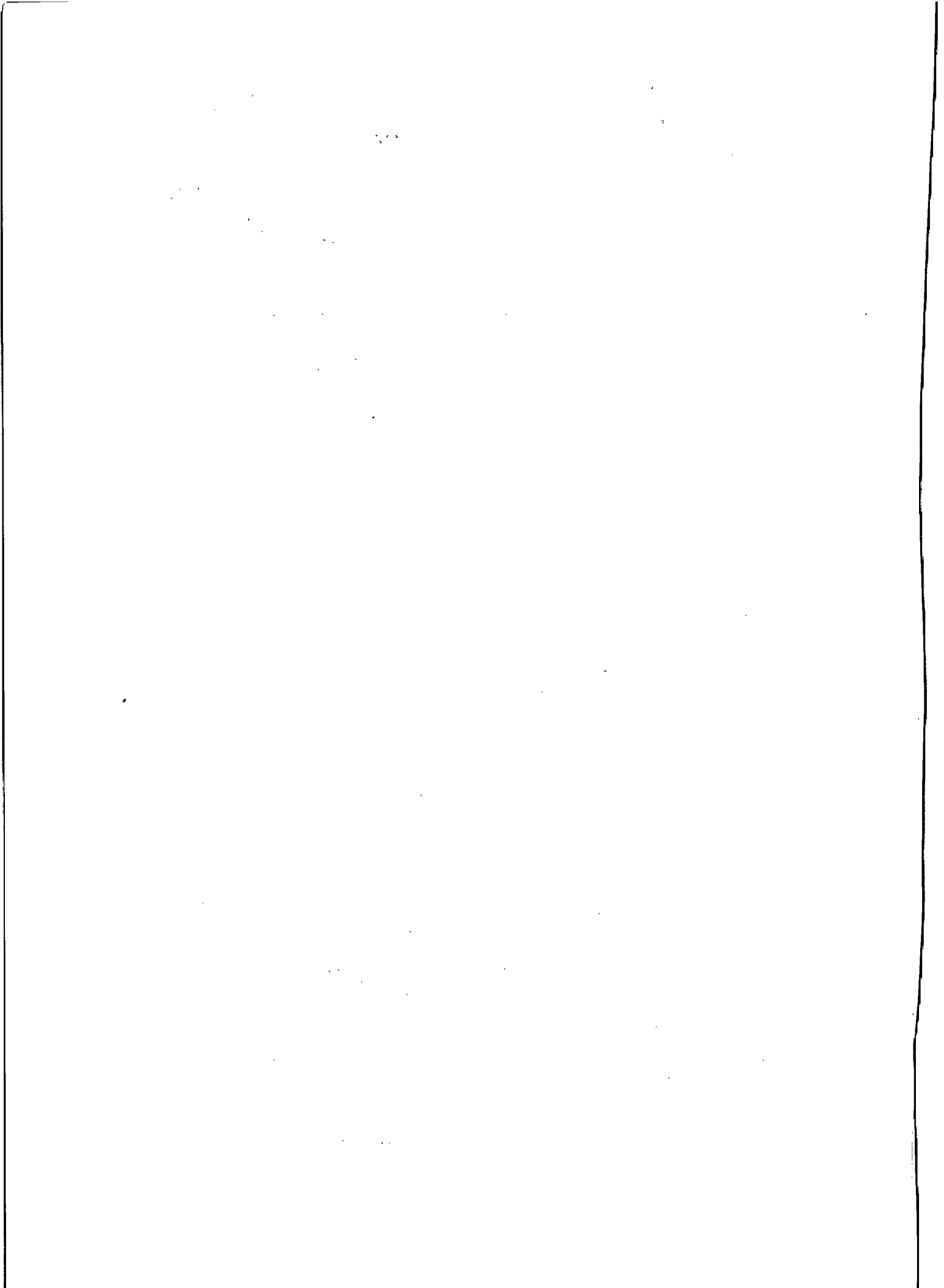


TABLE OF CONTENTS

=====

	PAGE
WELCOMING ADDRESS J.P. Rozelot	V
PREFACE J. Gaignebet	VII
RESOLUTIONS	XI
LIST OF PARTICIPANTS	XVI
 <u>SCIENTIFIC RESULTS AND FUTURE GOALS OF LASER RANGING</u>	
Chairman : F. Barlier (Invited Papers)	
 I. Ciufolini	
New Relativistic Measurements With Laser Ranged Satellites	1
 <u>NORMAL POINTS</u> Chairman : D. Lelgeman	
 R. Kolenkiewicz et al.	
Comparison Of Lageos Satellite Ranging Normal Points	11
 <u>SATELLITE MOBILE STATIONS</u> Chairman : P. Wilson	
 T. Varghese, M. Hernick	
Sub Cm Multiphotoelectron Satellite Laser Ranging	21
 T. Varghese et al.	
TLRS-1 ; System Upgrade And Performance Results	33
 N. Sasaki, Y. Suzaki	
Satellite Laser Ranging System At The Simosato Hydrographie Observatory And The Transportable system, HTLRS	45
 Z. Wen-Yao, T. De Tong	
Progress In SLR At Shanghai Observatory	59
 K. Hamal et al.	
Interkosmos Laser Radar, Version Mode Locked Train	69
 F. Pierron et al.	
Upgrades And New Developments On Satellite Laser Ranging Station From Grasse	73
 L. Grunwaldt et al.	
The SBG Laser Radar Stations Potsdam And Santiago De Cuba Status And Performance Report	93
 K. Hamal et al.	
3. Generation Laser Radar, Version Mode Locked Train Proposal	109
 A. Banni, V. Capoccia	
The New Satellite Laser Ranging System At Cagliari Observatory	113
 P. Kloeckler, Th. Schildknecht	
Zimmerwald Satellite Observation Station	123

LUNAR AND COMBINED Chairman : K. Hamal

Ch. Veillet et al.
The New CERGA LLR Station 129

M.L. White
Recent Improvements And Future Plans At The University Of
Hawaïi Lunar And Satellite Ranging Station 135

J.R. Wiant, P.J. Shelus
The McDonald Observatory Laser Ranging Station : MLRS 139

DETECTORS : SOLID STATE AND PMT Chairman : S.R. Bowman

I. Prochaska
Start Detector For The Mode Locked Train Laser Radar 145

R. Neubert et al.
Ambiguity And Resolution of A Mode Locked Pulse
Train Laser Radar 149

I. Prochaska, J. Gaignebet
Microchannel/Dynode Photomultipliers Comparison Experiment 161

Z. Neumann
Detectors For III Generation Laser Ranging Systems 165

S.R. Bowman et al
The Use Of Geiger Mode Avalanche Photodiodes For Precise
Laser Ranging At Very Low Light Levels : An Experimental Evaluation 173

K. Hamal et al.
Single Photon Solid State Detector For Ranging At Room Temperature 185

W.A. Kielek
"Constant Fraction" Discriminators In Few And Multiphotoelectron
Laser Ranging 189

TIMING AND EPOCH Chairman : C.A. Steggerda

B.A. Greene
Calibration Of Sub-Picosecond Timing Systems 197

P. Dachel et al.
Recent Advances In The GLTN Timing And Frequency Instrumentation 205

C.A. Steggerda
The Development Of A Dual Frequency Event Timer 225

LASERS Chairmen : F. Moya, H. Jelinkova

K. Hamal, H. Jelinkova
Saturable Dye For 1.06 μ m 243

H. Jelinkova et al.
Spatial Structure Of The Doubled Nd:YAG Laser Transmitter Beam 251

L. Jiyu
Some Special Requirements To Lasers For Satellite Laser Ranging 261

OPTICS, TRACKING AND MOUNTS Chairman : M.L. White

S.R. Bowman et al. Analysis And Performance Of A Passive Polarization Telescope Coupling Switch For Lunar Laser Ranging	273
H. Feng et al. An Accurate Test Of The Azimuth Axis Of A 1.2M Alt-AZ Telescope Mount For The Lunar Laser Ranging And The Analysis Of The Results	281
M.L. White Double Peak Polarized Interference Filters	289
R. Korakitis Effects Of Telescope Design On Laser Beam Pointing Accuracy	297

CALIBRATION Chairman : M. Pearlman

T. Varghese System Characterization Of Moblas-7 For Colocation With TLRS-1 & 2	311
R. Appler Calibration Error Sources	323
B.A. Greene Calibration Of Sub-Millimeter Precision Satellite Laser Ranging Systems	331
P. Kloeckler, T. Schildknecht Measuring And Modelling Pulse Discriminator Amplitude Dependence	343
H. Junginger MTLRS Ground Tests	357
J.D. Rayner et al. Zero Range Realtime Calibration	373
K. Hamal, I. Prochaska System Stability Using Mode Locked Train	377
L. Jiyu Satellite Laser Ranging Errors	379

SOFTWARE BENCHMARKING AND COLOCATION Chairman : E. Vermaat

M.R. Pearlman Some Current Issues On Laser Collocations	399
A. Cenci Management Of The Laser Ranging Systems Colocation	409
D.L.F. Van Loon Eccentricity Vectors For Colocation Purposes	441
V. Husson, D. Edge Polyquick Collocation Analysis	453
A. Caporali Colocation Data Analysis : Dynamical Approach	467
R. Kolenkiewicz Geodyn Collocation Analysis And Its Comparison With Polyquick	481

RAPID ON SITE DETERMINATION OF THE EARTH ROTATION

Chairmen : D. Smith, Ch. Veillet

- P.J. Shelus, R. Ricklefs
Real Time, On Site Earth Orientation Parameter Generation At
The MLRS Using Laser Ranging Data 493
- G.M. Appleby, A.T. Sinclair
A Note On The Use Of The CRS Lageos Ephemerides 499
- Ch. Veillet et al.
Real Time UT0 Determination At CERGA LLR Station 507
- P.J. Shelus
A Simple Software Scheduling Tool For Efficient Observing
Operations At A Lunar/Lageos Laser Ranging Station 511

HIGHT AVERAGE POWER AND NEW LASERS, NEW SATELLITES

Chairman : C.O. Alley

- S.R. Bowman et al.
A Neodimium YAG Active Mirror For The Amplification Of Mode
Locked Laser Pulses 523
- M. Sasaki
Japanese Geodetic Satellite "AJISAI" Launched In August 1986 527
- F.M. Yang
The Proposal Of Strictly Simultaneous Satellite Laser Ranging 549

TWO WAVELENGTH SYSTEMS AND STREAK CAMERA Chairman : B. Greene

- I. Prochaska, K. Hamal
Streak Camera Based Laser Radar Receiver. Its Performance and
Limitations 559
- J. Gaignebet et al., K. Hamal et al.
Two Wavelength Ranging On Ground Target Using Nd:YAG 2HG and
Raman 0.68 μ m Pulses 565
- I. Prochaska, K. Hamal
Picosecond Laser Ranging Using Photodiode 577
- B.A. Greene
Multiple Wavelength Laser ranging 581
- F. Guerin, G. Cerutti-Maori
Problems Induced By Multicolor Telemetry On Laser Retroreflector
Development 593

SPECIAL STUDY GROUP ON LUNAR LASER RANGING

Report prepared by Ch. Veillet 623

LUNAR AND COMBINED (Additive)

- C.O. Alley et al.
First Lunar Ranging Results From The University Of Maryland
Research Station At The 1.2M Telescope Of The GSFC 625

The Vith International Workshop on Laser Ranging Instrumentation

recognizing the many contributions of the Centre d'Etudes et Recherche en Geodynamique et Astronomie to the success of the Workshop through its sponsorship and local supporting organization,

and further recognizing the exceptionally effective and untiring efforts of the Chairman of the Local Organizing Committee for the Workshop, Jean Gaignebet and its Scientific Secretary, Francoise Baumont,

Wishes to express its deep appreciation to the members of CERGA and especially to Dr. Gaignebet and Dr. Baumont for selecting such an attractive location and for providing excellent support.

PAPERS PRESENTED BUT NOT PUBLISHED

SCIENTIFIC RESULTS AND FUTURE GOALS OF LASER RANGING INVITED PAPERS

- X.X. Newhall et al.
Lunar Laser Ranging Results Review
- D.E. Smith
Tidal Dissipation With Lageos
- C. Yoder
Implication Of Tidal Dissipation On G'
- B.D. Tapley et al.
Lageos Results Review

LASERS

- R. Dewhurst et al.
A Passively Mode Locked Nd:YAG Laser Using A Half Symetry Unstable Resonator With Continuous Output Coupling
- B.A. Greene
Laser Design For Fifth Generation SLR System

OPTICS, TRACKING AND MOUNTS

- K. Hamal
Transmit Receive Switch

HIGH AVERAGE POWER LASERS AND NEW LASER SPACE BORNE SYSTEMS AND NEW SATELLITES

- D.M. Smith
Topex, Poseidon And ERS-1 Satellite For Laser Tracking
- I. Ciufolini et al.
The Status Of Lageos 2 ; Informal Discussion Prospects For A Lageos 3.

SYSTEM CHARACTERIZATION OF MOBLAS-7 FOR COLLOCATION WITH TLRS-1 & -2

T. Varghese
Allied Bendix Aerospace
BFEC, GLTN
Seabrook, MD 20706 - USA -

Telephone (301) 7318916 - 2867743
Telex 197700 GLTN

ABSTRACT

The Moblas 4-8 systems are characterized by separate transmission reception axial geometry and hence produce parallax in ranging to short range targets. The conventional targets for these systems are located at distances of approximately 3 km and produces significant errors during survey as well as range measurements due to terrain and environmental features. An optical package with dual capability for parallax-free short/long external ranging and internal calibration at levels better than 1 mm was designed and performance evaluated on the system. This paper describes the system characterization test results performed with the above configuration.

1.0 INTRODUCTION:

A major collocation effort has been under-way at the NASA Goddard Optical Research Facility between the Goddard Laser Tracking Network (GLTN) " standard " Moblas-7 (Mobile optical Laser ranging System) and TLRS-1 & 2 (Transportable Laser Ranging System) since May 1986. The goal of NASA Crustal Dynamics program is to obtain ranging agreement between these stations on simultaneously collocated passes under 1cm. This may appear to be an ambitious goal considering the complexity of the number of parameters involved. However, the technology incorporated into these systems are robust enough to yield results comparable to the set goals provided, sufficient care is taken in the calibration and satellite operation of the system. Considering the number of error sources ,systematic and otherwise, present in the system it was recognized to be important to characterize the system at the mm level to meet the above goal. The precision of the system has been considerably improved after receiver upgrade(1,2) whereby calibration RMS is typically 4-5mm and satellite RMS 7-8mm.

This paper describes some of the recent improvements in our calibration techniques to establish systematic errors at the few mm level. The results presented in this paper are preliminary; refinements in techniques and analyses will be published(3) elsewhere at a future time.

2.1 SYSTEM DESCRIPTION

The schematic of the data-loop comprising the transmitter and receiver is shown in fig.2-1 and the corresponding optical layout in fig.2-2. A beam splitter reflects part of the output onto a photodiode(PD) which initiates the time interval counting process. The receive optics consists of a 30 inch telescope (Cassegrain with a f/1.5 primary mirror) which images the target return-optical beam onto the MCP-PMT after collimation and spectral bandpass filtering (used only for daytime tracking) The output from PD/PMT is allowed to undergo constant fraction discrimination in the Tennelec TC 454 CFD which provides a NIM pulse output for the HP5370 to start/stop counting. A part of the output is also fed to the LeCroy224 Quad Integrator for energy measurement.

The separate transmission reception geometry of the ranging system reduces the effectiveness of the system for horizontal ranging on short range targets due to problems of parallax. The system has been traditionally ranging to targets 3 km away for calibration purposes.

The meteorological measurements are performed on station and can be significantly different from the target location. The topological constraints dictated putting up the target at heights of about 40 ft which when subject to temperature, wind and solar loading produces variations of several mm. The overall error due to all the above problems were around a cm. By establishing a target close to the station on a stable structure the above problems can be significantly reduced provided ranging can be performed without parallax.

2.2 PARALLAX-FREE OPTICAL RANGING

The schematic for parallax-free optical ranging is illustrated in fig.2.3. It consists of two mirrors M1 and M2 mounted on mirror mounts and are aligned parallel to each other within few arc-secs. The mirrors are mounted such that the line joining their centers makes an angle of 45 degrees with the reflecting surfaces of the mirrors and is orthogonal to the transmit receive axes. This arrangement is held together in a rotary fixture and can be swung into position for calibration and moved out of the way for satellite ranging. The reflectivity of M1 is 50% while that of M2 is 100%.

The partially transmitted beam leaving the system hits the target and retro-reflected to M1. M1 reflects part of the return beam to M2 which couples the light into the telescope and from there to the detector. A target can also be mounted on the system as a reference for internal calibration. The distance from the center of rotation to the internal target can be accurately measured using a vernier to better than a mm and thus provides a powerful tool to examine survey inaccuracy. This arrangement also provides a means to measure any changes in the path length of the system as a function of mount pointing angles and apply the corresponding correction to the satellite data.

2.3 RESULTS AND DISCUSSION

Fig.2.4 illustrates the system delay as a function of time for two targets measured over a period of two hours. Each division on the vertical axis is 1.5mm. The number shown along with each box is the ambient temperature in fahrenheit. The displacement of the two data sets is due to the wrong range value used in station processing of the data for internal calibration. The pertinent feature to examine here is the close agreement between internal and external calibration as a function of time. The difference between the system delays stays as a constant over the time interval of the experiment. When the system was stabilized over a period of time, the system delay did not vary more than a mm and this feature is depicted in fig.2.5.

The variation of system delay as a function of elevation and azimuth were also studied. Fig.2-6 &-7 illustrates the Az-El dependence under two alignment conditions of the coelostat which holds the coude optics. Although the nature of response differed, the magnitude of variation remained essentially the same.

Satellite passes were simulated using the target mounted on the telescope. Fig.2.8 illustrates the plot of system delay as a function of elevation angle for a 66 degree (PCA) elevation Lageos pass. It is clear that for the particular geometry of this pass, the system delay is a monotonically decreasing function (within the uncertainty of measurement) of elevation. Further experiments are planned for future to examine mm problems due to mount pointing angles and apply appropriate correction to the satellite data.

2.3 SUMMARY

The demonstration of a parallax-free optical ranging scheme has been accomplished with the means to study mm problems in horizontal ranging. The optical closure that can be realized between the transmit and receive axes can be used for the alignment of optical components following the telescope. The ability to verify survey ranges and characterize mm problems due to mount orientation angles are unique advantages of the system.

2.4 REFERENCES

- (1) "Sub-cm Multiphotoelectron Satellite Laser Ranging", Thomas Varghese, Michael Heinick, Sixth International Workshop on Laser Ranging Instrumentation, Antibes, France, Sept.1986.
- (2) Thomas Varghese, Technical Report, Allied-Bendix Aerospace, BFEC, #1909A-B-05/10/85-S-C.
- (3) Thomas Varghese (to be published)

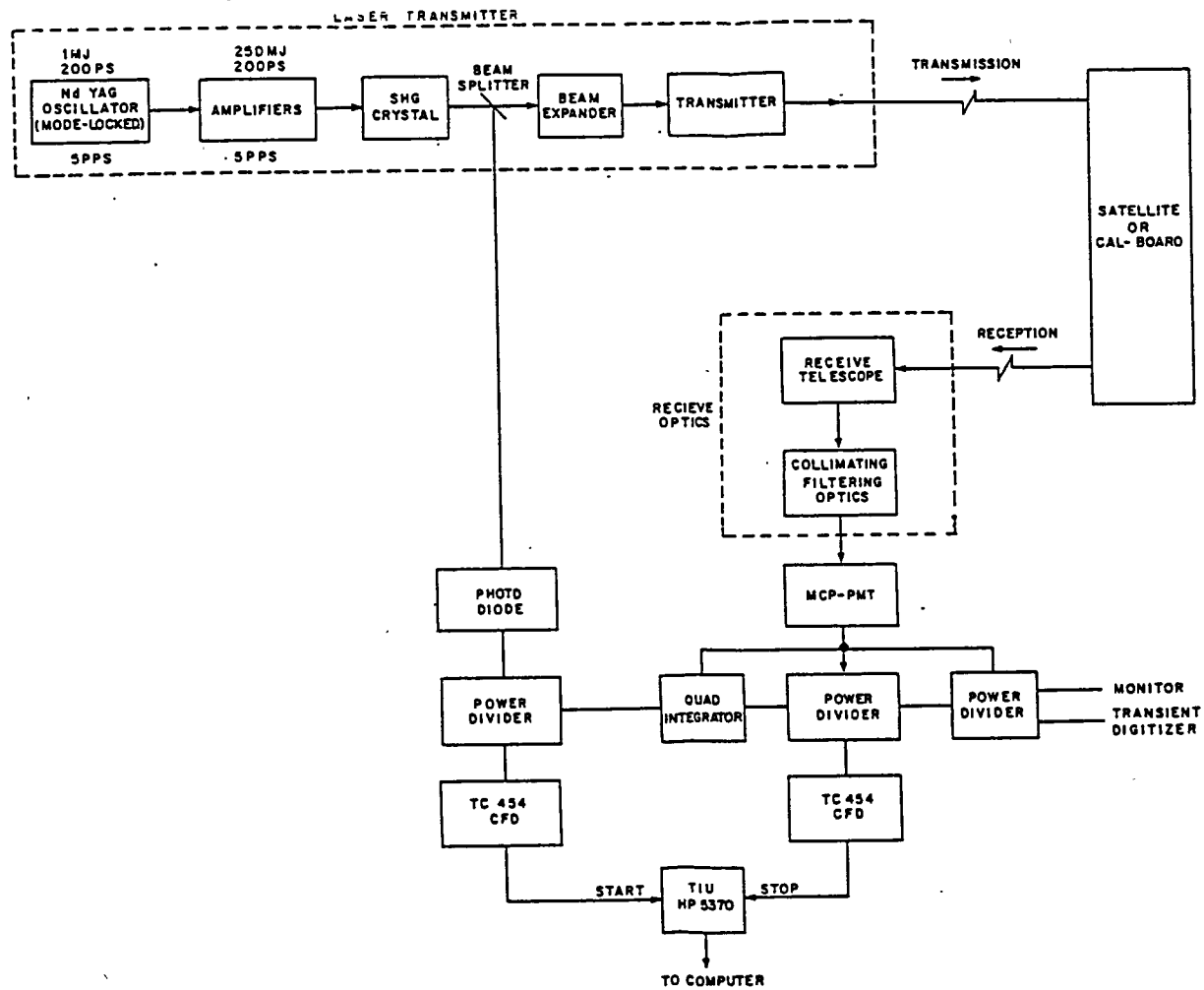


FIG. 2-1

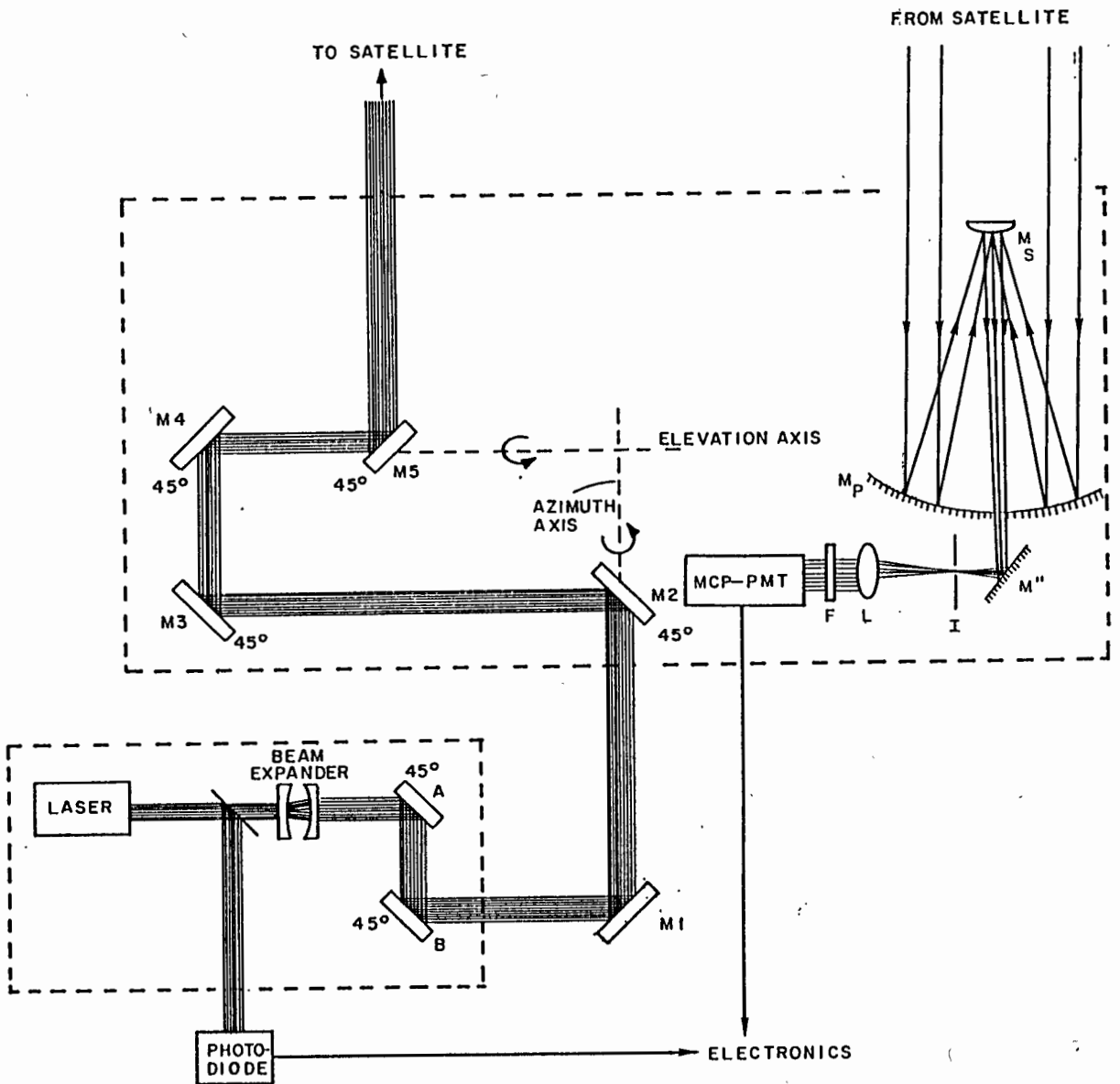


FIG. 2-2 SCHEMATIC OF OPTICAL LAYOUT

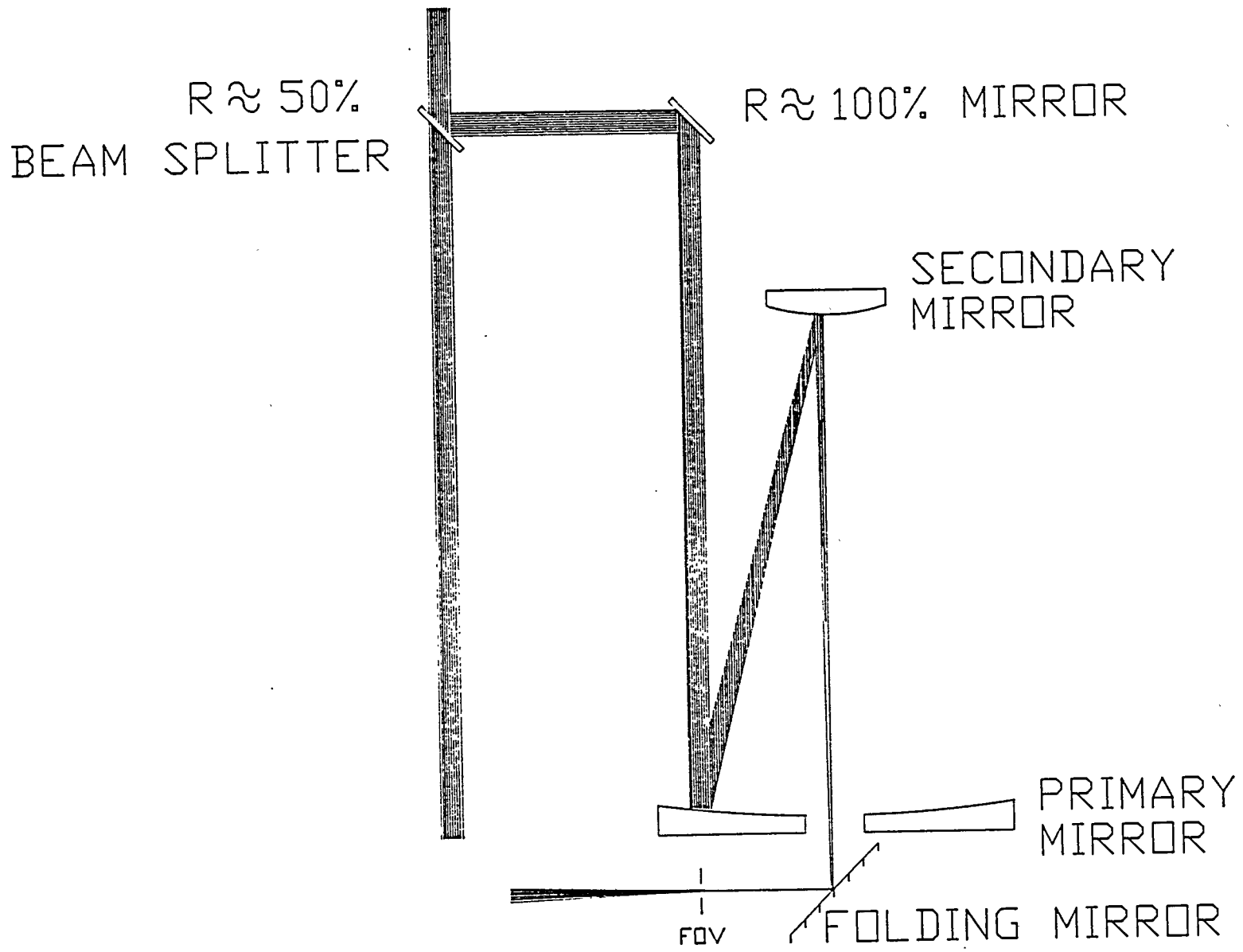
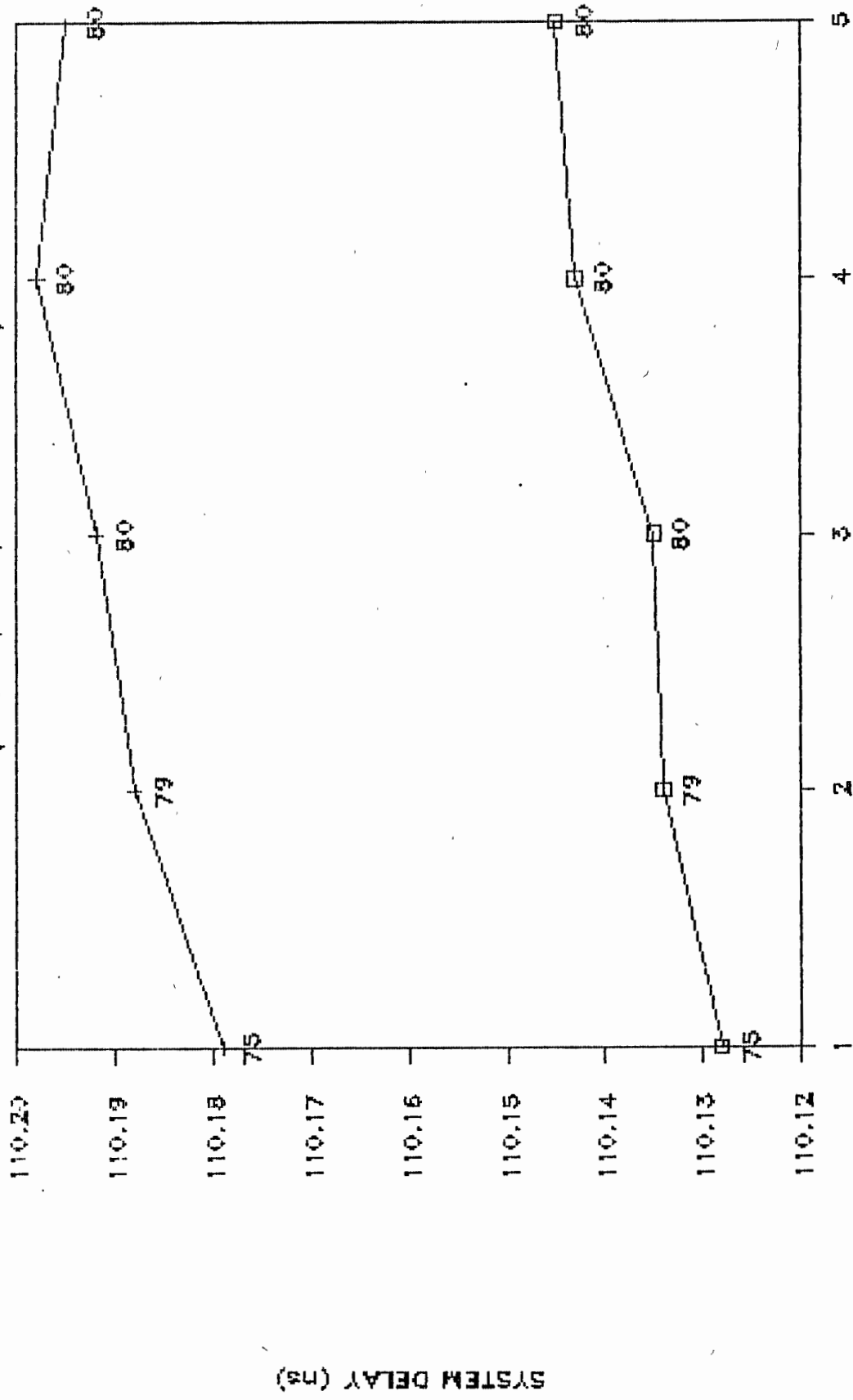


FIG. 2-3

MOBLAS-7 SYSTEM DELAY STABILITY VS TIME

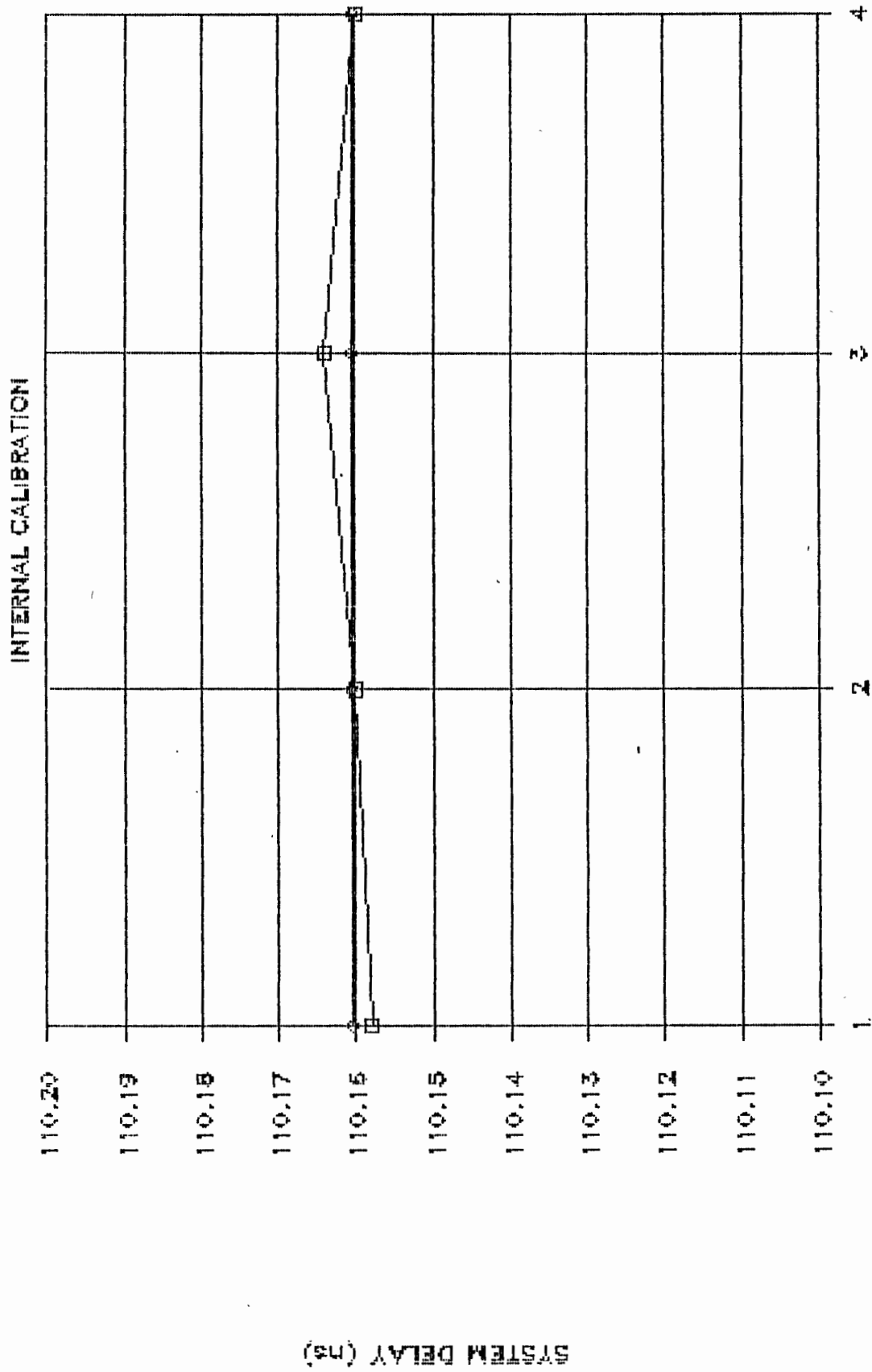
(SEP 18, 1986, 6 PM TO 8 PM)



□ IC + TGT #3 (RANGE 80 M)

FIG. 2-4

MOBLAS-7 SYSTEM DELAY VS TIME



◇ AVG

FIG. 2-5

MOBLAS-7 SYSTEM DELAY VS AZIMUTH

IC (ELEVATION 0-90)

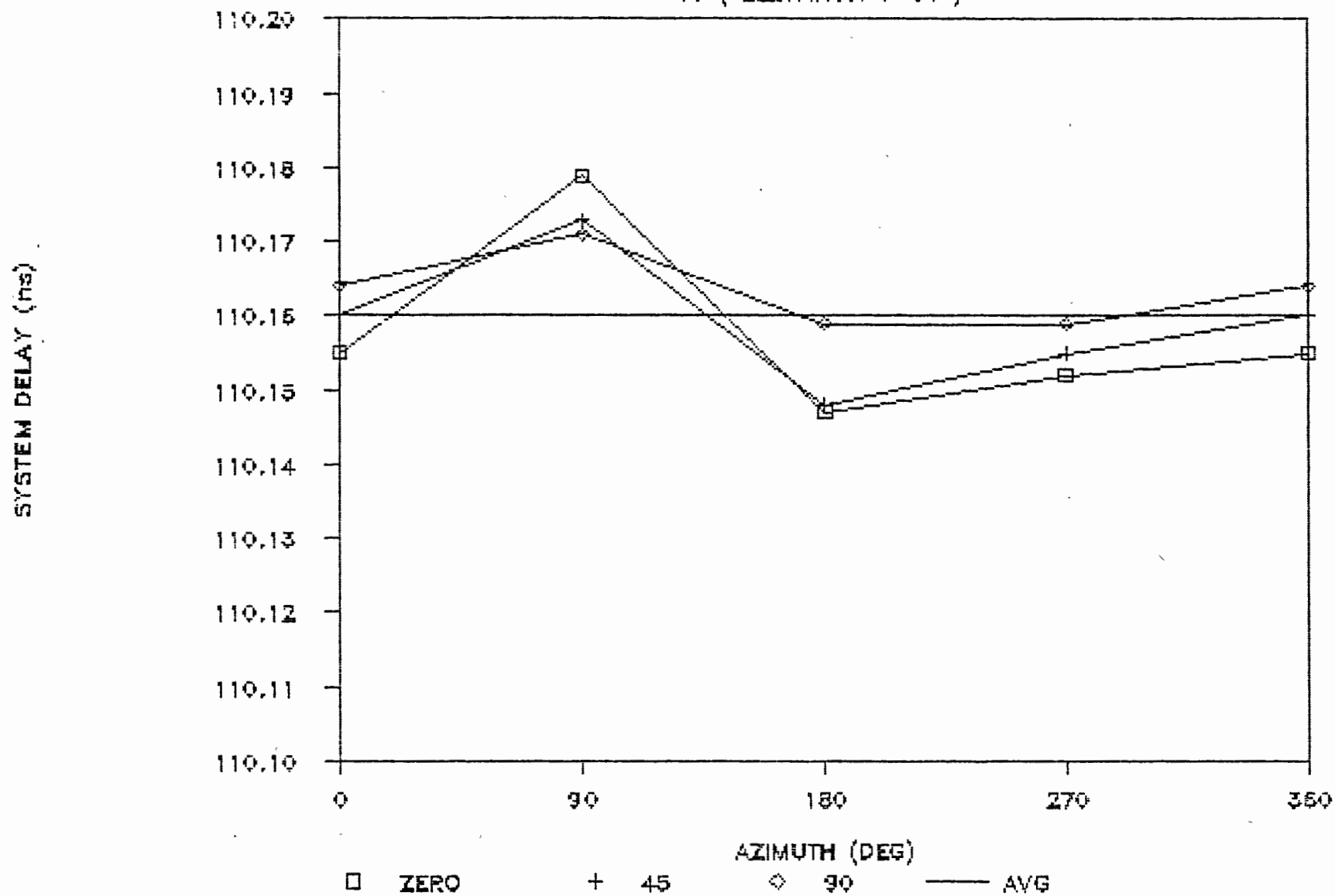


FIG. 2-6

MOBLAS-7 SYSTEM DELAY VS AZMUTH (EL 0 - 90)

INTERNAL CALIBRATION ON SEP 17, 1986

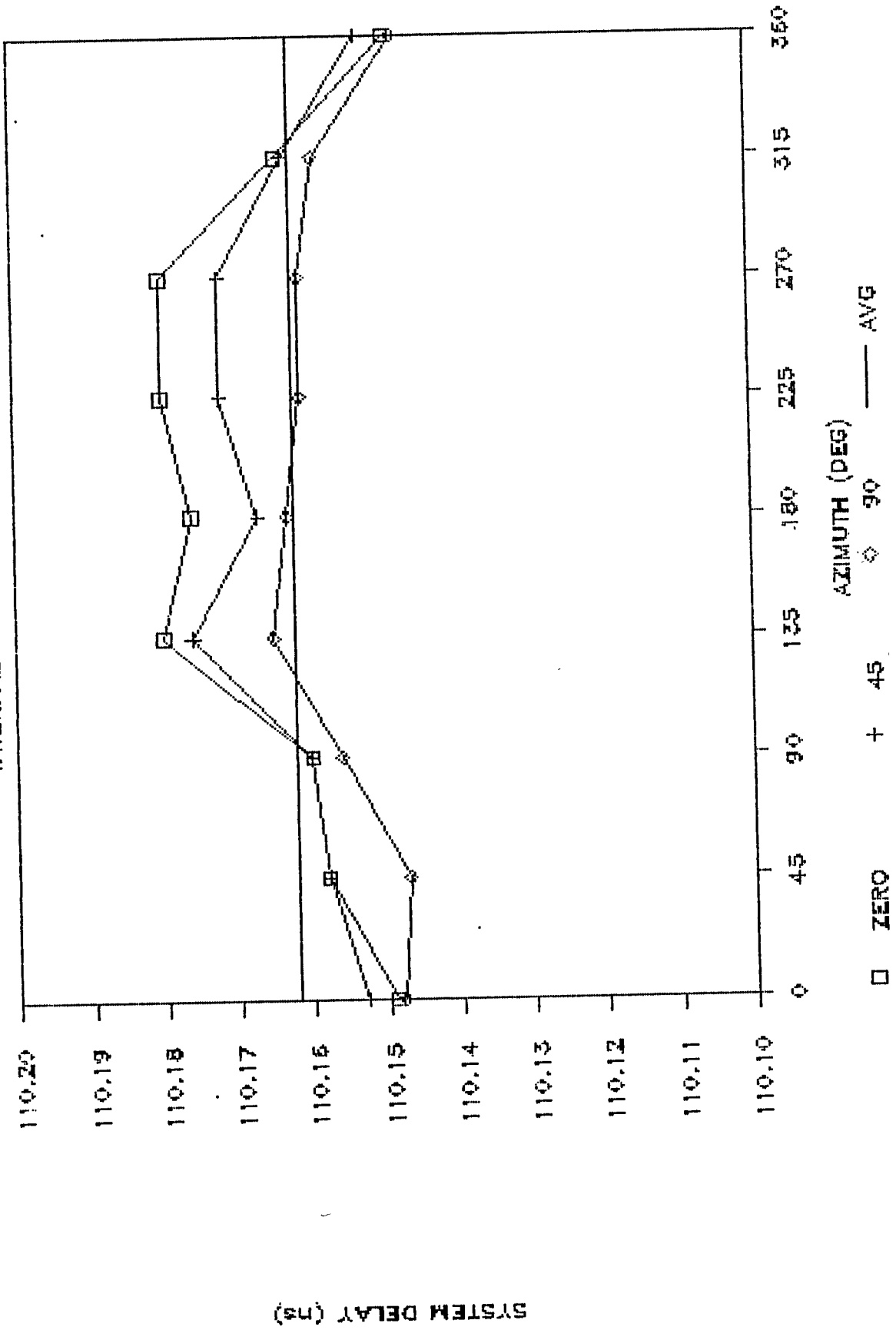
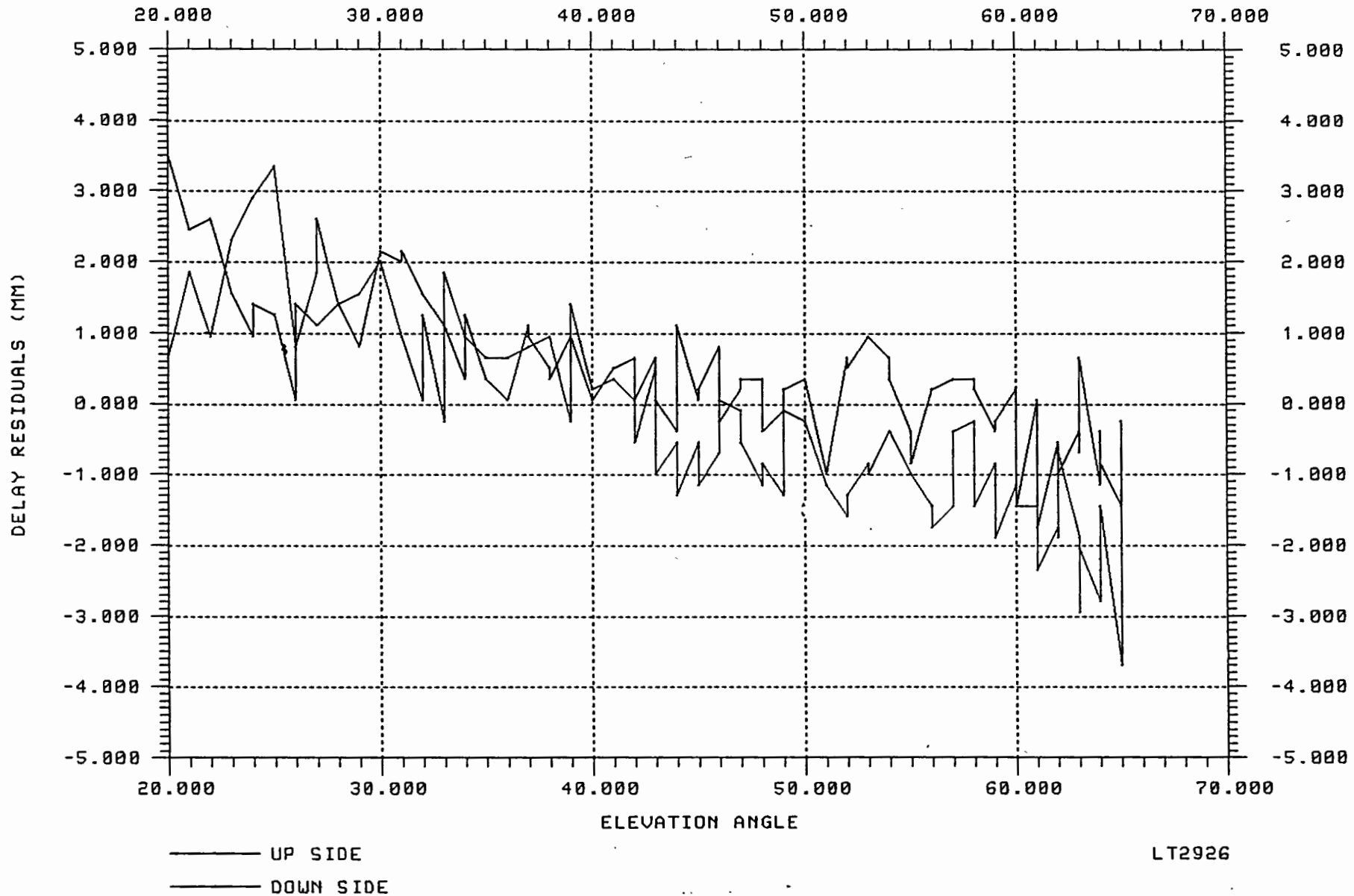


FIG. 2-7

M7 IC VS. EL



LT2926

FIG. 2-8

CALIBRATION ERROR SOURCES

R.L. Appler
NASA/Goddard Space Flight Center
Greenbelt, Maryland 20771

Telephone (301) 286 8119
TWX 2579559 CDPO UR

ABSTRACT

Through gradual improvement in laser ranging hardware and software, we have reached an era where sub-centimeter ranging precision and two-minute normal point data at the millimeter level are routinely obtained at Moblas 7. Systematic error sources, once buried in the noise of measurements, are now being identified and investigations are underway to determine the means through which we can minimize these errors with sub-centimeter ranging accuracy as our near-term goal. An overview of some of the error sources and possible means to reduce their effect is presented.

CALIBRATION ERROR SOURCES

Robert L. Appler
NASA/Goddard Space Flight Center
Greenbelt, Maryland 20771

Telephone (301) 286-8119
TWX 2579559 CDPO UR

ABSTRACT

Through gradual improvement in laser ranging hardware and software, we have reached an era where sub-centimeter ranging precision and two-minute normal point data at the millimeter level are routinely obtained at Moblas 7. Systematic error sources, once buried in the noise of measurements, are now being identified and investigations are underway to determine the means through which we can minimize these errors with sub-centimeter ranging accuracy as our near-term goal. An overview of some of the error sources and possible means to reduce their effect is presented.

1. Introduction

Substantial hardware changes directly and/or indirectly influencing the time-of-flight measurements in satellite laser ranging have been incorporated into laser ranging instrumentation within the Goddard Laser Tracking Network. Laser pulse widths have been reduced to 200 picoseconds or less. Timing is within 100 nanoseconds of Universal Time. The jitter in the measurement of system and satellite delay is less than 30 picoseconds. Discriminator time walk as a function of signal amplitude at signals greater than three photoelectrons is negligible. Signals at three photoelectrons or less are rejected by gating. Photomultiplier time walk as a function of image position and signal level is virtually nonexistent. Better alignment techniques have been initiated. Multi-photoelectron ranging has substantially increased the signal-to-noise ratio. These and a multitude of other refinements in instrumentation and technique have brought the single-shot precision even in daylight LAGEOS ranging to the eight millimeter level on a regular basis at Moblas 7. Similar results should be seen on Moblas 4, 5, 6, and 8 after the installation of the microchannel plate detector and the Tennelec discriminator on these systems.

The enhanced ranging precision brought about by events discussed above increases our ability to identify the sources of systematic errors that exist. We are making an in-depth effort to uncover and diminish the effects of known error sources and we are constantly on the look out for new error sources to be identified and eliminated. The following areas are being scrutinized to determine whether systematic errors

leading to range biases are present or whether they indirectly cause range biases in other data loop optics, mechanics, or electronics:

- * System Timing
- * Optical/Mechanical Path
- * Data Processing Software
- * Atmospheric Model
- * Atmospheric Monitoring
- * Temperature and Humidity Control
- * System Calibration

As new sources of error are uncovered, these too, will be investigated and attempts will be made to eliminate, or at least, reduce them.

I. System Timing

Cesium clocks used in the network are known to have excellent long term stability but to exhibit significant short term phase and frequency jitter which may or may not translate into a systematic range bias. Distribution amplifiers and time code generators currently used in conjunction with the cesium clock were installed in the network during an era of much lower system precision and have looser specifications than is desired. The output of these devices provides epoch time to 100 ns when locked to epoch time obtained from the GPS receiver. The cesium also provides the clock frequency input to the time interval units used to measure system delay and the round trip time of flight to the satellite.

In an attempt to determine whether any systematic bias is contributed by the timing system, a spectrally pure disciplined crystal oscillator will be purchased, tested against a hydrogen maser, and then used as a standard of comparison against timing electronics presently in the network. If results indicate the need, network timing electronics will be upgraded to meet the more stringent performance requirements needed to achieve sub-centimeter system accuracy.

The time interval counters used in the GLTN will also be investigated to determine what timing error is introduced by its electronics when driven by the disciplined oscillator. Measures will be taken to correct resulting systematic biases.

II. Optical/Mechanical Path

Every system alignment of the optical path to the mechanical axes is subject to some alignment error which is difficult to routinely measure to an accuracy of a few millimeters. Systems where the transmit and receive optical paths are separated and especially in those systems using a Coude' path having four or five mirrors, are subject to translational errors as a function of mount pointing because of the very difficult task of aligning the optics to the mechanical axes exactly. Certainly, routine alignment which is necessary due to thermal and other shifts during operations does not permit the time necessary to achieve a "perfect" alignment, if indeed, a "perfect" alignment were possible to achieve.

Solar loading and other thermal effects, minor misalignment during laser repair and/or alignment, mechanical disturbances to the laser and mount, deviations of the azimuth axis from vertical due to settling and other causes, inadvertent relaxation of spring load when adjusting spring-loaded optical mounts represent some additional probable causes for alignment errors. Care must be taken to minimize most of these problems through proper mount design.

Some steps that can and must be taken to improve system alignment integrity include the use of special paints and/or shielding of critical mechanical components from the sun to minimize the effects of solar loading, making adjustments against spring loads, and designing adjustment mechanisms to work with gravity wherever possible.

III. Data Processing

A thorough investigation must be made to insure that all measurement resolution available by the hardware is used during the processing of data. For instance, is epoch time analyzed to a resolution of 100 ns? Is atmospheric pressure analyzed to a resolution of 0.1 millibar? Are temperature effects on range analyzed at a resolution of 0.1 degree C? If the answer to any of these and/or similar questions is no, immediate steps must be taken to see that all available resolution is used in processing data.

Similar questions relate to correction during data processing for known sources of range biases such as:

- * Use of neutral density filters during system calibration.
- * Correction for parallax resulting from the use of near-in calibration targets.
- * Minor changes in optical path caused by residual alignment errors after system alignment.
- * Range bias as a function of return signal amplitude.

Care must be taken in all of these areas to eliminate these and other similar sources of data processing error as well as in the verification of system and data processing software to ensure that avoidable errors are not introduced.

IV. Atmospheric Model

Marini and Murray of NASA Goddard Space Flight Center developed an atmospheric model for refraction which has been the Network standard for many years. Dr. Jim Davis and Dr. Tom Herring of the Massachusetts Institute of Technology have added coefficients to the Marini-Murray model which improve the model from an accuracy of approximately 1 centimeter to one of approximately 0.5 centimeters.

Although not a source of ranging system error, the error in the atmospheric model still produces a systematic error in the range value. Until such time that two color ranging can be implemented into the network, at least the updated Davis-Herring version of the model must be used in satellite range determination.

V. Atmospheric Monitoring

Care must be taken in regard to the location of atmospheric monitoring instrumentation on a site and in the calibration of that instrumentation. The pressure sensor should be placed as close to the elevation axis as possible and any tubing required between the sensor and the axis should have its open end pointed upward in order to avoid the trapping of air in the tube--thereby introducing an error in the actual pressure. Temperature sensors should be placed sufficiently far from artificial heat sources and protected from direct incidence of the sun so as to avoid an error in the reading in the ambient temperature. Significant range biases have been introduced in the past because of improper placement of these instruments.

VI. Temperature and Humidity Control

In order to minimize their effects on wavefront propagation, laser alignment and power, data loop electronic stability, etc., it is imperative that environmental control be given high priority. Errors in range measurement can be significant if the environment is not maintained to high tolerances. The effect of heat on instrument reliability is already well known. Temperature and humidity control is being heavily stressed now in the network and measures have already been taken or are being taken to hold these parameters constant to practical levels.

VII. Calibration

System calibration errors are deeply interwoven with the error sources discussed above. Station timing, optical/mechanical alignment, data processing, etc., when combined, lead to an unacceptable level of systematic errors. In addition to these errors, which are internal to the system, another perhaps larger source of error lies in the system calibration, itself.

Target boards and corner cubes are traditionally placed at distant ranges in order to minimize parallax problems encountered in those systems which transmit on one path and receive on another. Newer systems having a common transmit and receive path, perhaps by tradition rather than for any other reason, have continued using these distant targets. As a consequence, atmospheric ambiguities continue to compromise the measurement range to the target during the surveying process and during system calibration. In addition to atmospheric concerns, the target heights have been excessive in order to accommodate site conditions. As a consequence, small, random changes

in target verticality have led to significant calibration biases. Errors in the survey of a station monument as well as errors in the determination of system eccentricities compound the problem.

Recent steps have been taken to minimize the effects of parallax and atmosphere. Unfortunately, only preliminary data has been taken and it is too early to report on the results at this time, although the data appears encouraging. Dr. Thomas Varghese of Bendix Field Engineering has developed an anti-parallax attachment for Moblas 7 to demonstrate the enhanced precision possible with such a device. This device can be used for near-in ranging as well as for internal calibration (IC) wherein the IC feedback optics covers the total optical path so as to avoid any subtle alignment errors leading to an incorrect determination of system delay via internal calibration itself. It provides an independently calibratable optical path which can be subtracted from the total time of flight from transmit start to detect stop so as to be able to accurately determine true system delay. This can be done in all pointing directions. The system delay thus determined can be compared against near targets as a redundant check on calibration.

In addition to the parallax-free internal calibration system discussed above, short, concrete reinforced piers are gradually being installed in the network to minimize the atmospheric and target instability problems. These piers are virtually identical to the first order surveying monuments which have proved to be very stable at the millimeter level. When used at the Goddard Optical Research Facility, each system ranges on the same corner cube with negligible parallax. As a result, any minor changes in the target position does not negate the use of the target as a valuable means to achieve system intercomparisons.

An open corner cube has been developed by NASA Goddard to provide another means to check system calibration. This cube has an effective aperture of 0.5 m to permit ranging by Moblas 7 without parallax. great care has been taken in the design to insure that the range between the vertex point and the laser system reference point can be surveyed to an accuracy of about 1 mm. Unfortunately, there has not yet been time available to check out this device.

VIII. Summary

As discussed above, ranging precision is currently at the subcentimeter level on Moblas 7. Some sources of error known to exist include:

- System Timing
- Optical/Mechanical Alignment
- Time Tagging
- Data Processing
- Atmospheric Model
- Atmospheric Measurements
- System Calibration

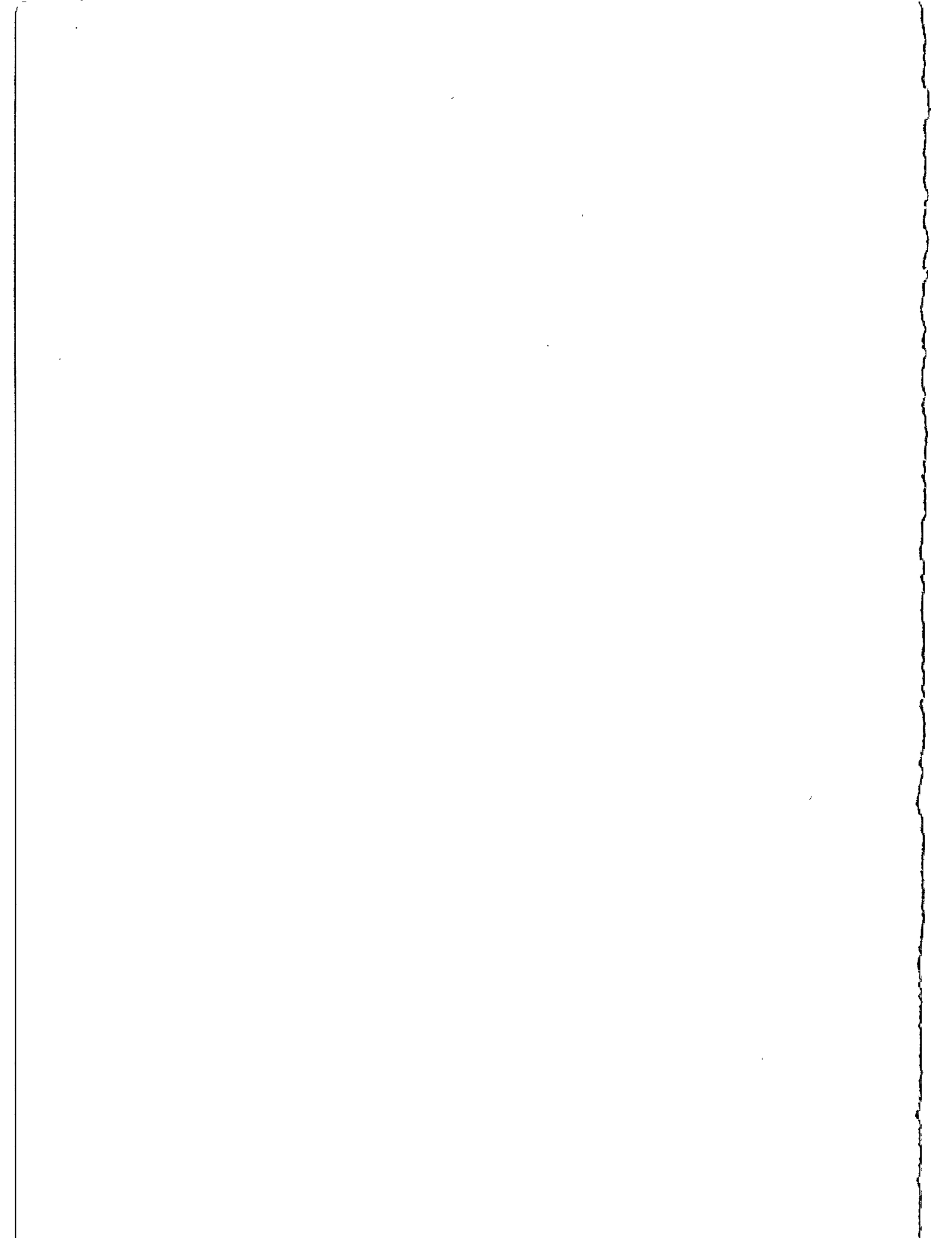
The measures being taken to implement hardware/software changes are discussed.

It is clear that the degree to which system accuracy can approach system precision depends upon the amount of success achieved in the elimination of these and other errors.

It is hoped that this paper will assist anyone who is not aware of the potential problems mentioned to take advantage of the experience of others to avoid known pitfalls during the development or modification of a laser ranging system.

ACKNOWLEDGMENT

Special thanks go to Dr. Tom Varghese of Bendix Field Engineering Corporation and Dr. Mike Pearlman of the Smithsonian Astrophysical Observatory who through their work or through useful suggestions have helped in providing information included herein. Also to be thanked are other members of the Bendix Engineering and Data Services teams and to Dr. Robert Coates, Manager of the Crustal Dynamics Project who made possible the presentation of this paper at the Sixth International Workshop on Laser Ranging Instrumentation.



CALIBRATION OF SUB-MILLIMETRE PRECISION SATELLITE
LASER RANGING SYSTEMS

B.A. Greene
Division of National Mapping
P.O. Box 31
Belconnen ACT 2616 - Australia -

Telephone (6162) 525095
Telex AA 62230

ABSTRACT

The deficiencies of the calibration procedures in general use by SLR stations are examined in the context of sub-millimetre precision systems and their calibration requirements. It is shown that calibration accuracies of a few millimetres are possible if great care is taken with conventional procedures. Two new calibration techniques which yield sub-millimetre accuracy are proposed, and the results of applying one of these to a fully operational SLR station are presented.

CALIBRATION OF SUB-MILLIMETRE PRECISION SATELLITE LASER RANGING SYSTEMS

B.A. Greene

1. Introduction

The precision of satellite laser ranging systems has improved dramatically over the past 10 years. It is now possible to obtain, within 2 minutes, over 400 range measurements to satellites 1-10 000 km distant, with each measurement having associated with it an uncertainty of only 8 mm. Data of this quality and quantity allow the satellite position to be described with a statistical uncertainty of 0.4 mm each 2 minutes ('normal' points). Even better performance can be expected in the future.

Clearly, the accuracy of the measurement will depend on systematic error terms which must be removed from the data by means of system calibration. In this paper the characteristics and in particular the deficiencies of existing calibration techniques are reviewed. It is found that no existing technique can provide sub-millimetre accuracy and thus allow removal of all systematic errors to below the noise level of the 2-minute satellite range normal point presently being obtained.

Two new techniques for calibration are then proposed.

2. Current Calibration Techniques

There are currently two modes of calibration in general use in operational laser ranging systems. These are:

- . target board calibration
- . real-time calibration

Target board calibrations utilise a sequence of range measurements to a fixed terrestrial target to determine the system constant delay. These calibrations are normally carried out to a target 0.2 - 4.0 km distant on a regular basis, and always before and after a ranging operation (satellite pass). This technique is deficient in several ways:

- . It includes a component of system delay which is not replicated in ranging mode - the horizontal path;
- . It gives the system delay before and after the pass, not during the pass, which is the time of interest;
- . Because the range is short, critical errors in elapsed time measurement are not sampled in those systems utilising time-interval techniques;
- . The technique is limited by survey accuracy, which is sometimes poor because of inaccessibility of system reference points;

- . Because the range measured is so short, the return signal enters an electromagnetic environment which can be different from that experienced by a satellite return (electromagnetic asymmetry);
- . Because of the way calibrations are made, the system is very open to abuse. It is not rare for post-ranging calibrations to be continued by operational crews until a 'satisfactory' result is obtained.

To overcome these disadvantages, the real-time calibration (RTC) technique was pioneered by the University of Texas. This technique uses real-time optical feedback to the detector, via the same (identical) path as the range measurement uses, to determine on a shot-by-shot basis the system delay. A great benefit of the technique is that any system hardware element, even in the measurement chain, can be modified, repaired, or replaced without adversely affecting the system delay or the calibration accuracy, as the system delay is measured during the ranging process each time. Another major benefit is that the calibration data is securely written into the 20-30 000 long record of ranging, and is virtually tamper-proof, so a true record of station calibration is assured.

The RTC technique also has several disadvantages:

- . the range is still very short, so electromagnetic asymmetry will apply;
- . the calibration (feedback) path does not usually include all of the transmit and receive optics, so some categories of system delay associated with (e.g.) misalignment of optics may pass undetected, and cause systematic errors.

Figures 1-4 show the result of real-time calibration of a state-of-the-art SLR system, the Natmap/NASA Laser Ranging System at Orroral (Australia). The time walk of this system is evident in these figures, which show actual RTC results for 4 consecutive LAGEOS passes taken in July 1986, plotted as 1 minute normal points. Also clearly evident is that pre- and post-calibration techniques would show differences of up to 2 mm, with no indication possible of how the system temporal drift took place in terms of time distribution.

According to the theory of RTC, time walk in a system monitored by RTC is irrelevant, since RTC gives the system delay as a function of time. However, it is not common for analysis centres of SLR data to allow a time-varying system delay, despite the physical impossibility of it being anything other than time-varying. This has been because very few stations can determine time-dependent system delay during ranging, and also because errors arising from taking system delay as a constant are rarely greater than 5 mm. A 5 mm maximum error has, until recently, been acceptable.

3. Real Time Differential Range Calibrations

The data shown in Figures 1-4 is typical of Orroral calibration (RTC) data. It contains some interesting features which suggest fine temporal structure within the system delay at the 1-2 minute scale. A second real-time calibration, to a target at a different range from that used for the existing RTC, should reflect all real temporal structure in the RTC estimate of system delay. In addition, if the range difference between the two targets was known, then the accuracy of the system can be

determined, since the difference in system delays should equal the range difference between targets.

Since it is trivial to obtain optical mounts, rails, and components which can be positioned to 0.1 mm or better, an extremely precise accuracy calibration of the system is possible, if the system is based on epoch timing, as all submillimetre systems must be. Epoch timing is essential because even events closely spaced in time, such as two calibration pulses, will be jointly random in phase with respect to the epoch timing system timebase, and so will sample the error space randomly, as desired. If the differential range is never varied, some sectors of error space are never sampled due to the fixed phase relationship between calibration pulses. That is, the first event is random in phase with respect to the system time base, but the phase of the second is completely determined. In practice it has been found that only a few differential range settings are required to establish accuracy, with occasional changes to the differential delay sufficing to maintain it. For a properly designed timing system the error due to completely ignoring the fact that the two calibration epochs are correlated is never more than 0.5 mm RMS.

The result of applying real-time differential range (RTDR) calibration to the NLRS is shown in Figures 5 and 6. The range difference used was 19.0 picoseconds, and the two real time calibrations can be seen together in Figure 5 against elapsed time. In Figure 6 the difference between the two calibrations minus the known range difference (system error) is plotted against elapsed time. The accuracy specification of the NLRS at this time was 0.5 mm, and the calibration data for this pass gives:

True range difference	:	19	ps
Average measured difference	:	17.95	ps
Standard deviation	:	3.0	ps
Mean error	:	1.05	ps

Clearly, despite the evident loss of calibration after approximately 20 minutes of ranging, the specification is met. The error from 20 minutes onwards was due to a temperature change in one part of the timing system. When these excursions can be controlled, a specification of 0.25 mm RMS is achievable, as can be seen from the initial data segment of Figure 6. Absolute calibration using RTDR methods is contributing significantly to the refinement of timing circuits and techniques for SLR.

The RTDR method allows tracking of system delay to 0.1 mm accuracy. However, it suffers from the same principal deficiencies as the conventional RTC method from which it was derived, i.e.

- . electromagnetic asymmetry
- . some potential errors (optical) not sampled.

Testing using the actual ranging environment whilst electrically and magnetically shielding detector and timing systems can determine the impact of transient electromagnetic fields on the SLR system. Independent tests can be made by generating optical pulses using high speed laser diodes to avoid electromagnetic transients, and observing the performance of the SLR system under calibration. As a result of such testing at the NLRS, conventional PMTs are completely magnetically shielded in mu-metal cases for operations. At the 0.5 mm level MCP PMTs do not exhibit bias in magnetic fields such as are generated by typical SLF laser systems.

The sampling of all possible errors in a SLR system requires additional calibration techniques.

4. Terrestrial Target Array Calibration

SLR systems normally define their site coordinates in relation to a number (at least three) of intervisible prime geodetic marks within 100 m of the SLR system. It is normal for all marks on the site, or in the case of a mobile SLR, on the pad, to be subordinate to these prime marks, which can be surveyed and located to 1 mm RMS in 3 coordinates.

State-of-the-art SLR systems can provide 0.5 mm precision over virtually any range, as well as possessing sub-arcsecond precision readout of angular position. If these capabilities were utilised to connect the SLR system directly to the prime geodetic markers, many advantages could be obtained:

- . The accuracy of the SLR system could be determined in the context of conventional geodetic measurements. Although the SLR system can be accurately calibrated by RTDR, a second calibration is afforded by the closure calculations when surveying the control marks. In this application the marks are used as ultra-high precision terrestrial targets, the redundancy in which yields a measure of system accuracy.
- . Monitoring of tilt, subsidence, and local movement is automatic. This is useful for fixed stations, and for mobile systems allows the concept of a highly mobile 'padless' design. That is, a mobile SLR which does not require a concrete pad or the normal marks contained in/on it. This greatly enhances mobile SLR productivity and flexibility.
- . A proliferation of instruments (and errors) is avoided, as the ranging system surveys itself onto the site, and maintains its own coordinates.
- . If the geodetic markers are fixed in any major datum, very good initial offsets for mount modelling of the telescope can be obtained from the terrestrial targets alone. Similarly, mount model recovery can be expedited, even if the marks have not been fixed.
- . Any desired reference point in the SLR system can be solved for.

In practice, a specially constructed target must be placed very precisely on each marker. Ranging to at least 3 targets produces a sub-millimetre solution for horizontal coordinates. The 3-D error ellipsoid is elongated in the vertical direction, because all targets are approximately coplanar. However, arcsecond precision elevation angle observations readily produce sub-millimetre vertical coordinates over 100 m distances. Once angle and range observations have been combined, the solution can be obtained. Six targets, randomly distributed in azimuth, are recommended. This allows for one or two marks to be damaged, obscured, or inaccessible at any time, whilst still providing adequate redundancy for sub-millimetre solution.

The technique is clearly sensitive to survey errors in the ground geodetic marks. In practice it is not difficult to isolate one or two errors from the solutions. Scale errors can also be easily detected, although not attributed. In general, if a sub-millimetre solution is not possible

initially, with the geodetic marks constrained in 3 dimensions by the ground survey results, then the mark coordinates must be unconstrained, and small adjustments made as the optimum solution for station coordinates is sought. Releasing the constraint on the marker coordinates is not done unless the SLR system has successfully calibrated at all other levels. This procedure could be necessitated by ground survey error, target installation (on mark) error, or atmospheric model error. Standard geodetic techniques can apply to the establishment and maintenance of the station coordinates and system delay determined by this technique.

The single weakness in this technique is that elevation-dependent misalignments which can cause systematic error are not sampled. An additional, infrequent, calibration technique must be applied to measure these errors. This technique involves the erection of a simple calibration jig which allows retroreflectors to be placed at any point in the transmitted beam, and RTC to be executed as elevation angle is altered. Rigorous testing is tedious and time consuming, but is required very infrequently. Mobile systems could be taken to a standard calibration facility, whilst fixed systems can more readily program the effort required on-site.

References

1. E.C. Silverberg, "The feedback calibration of the TLRS ranging system", in Proc. Fourth International Workshop on Laser Ranging Instrumentation, (University of Texas, Austin, Oct 12-16 1981). Bonn: Geodetic Institute, University of Bonn, 1982, pp. 338-351.
2. B.A. Greene, "Epoch timing for laser ranging", in Proc. Fifth International Workshop on Laser Ranging Instrumentation, (Herstmonceux Castle, September 10-14, 1984). Geodetic Institute, University of Bonn, 1985, pp. 247-250.

Figure 1

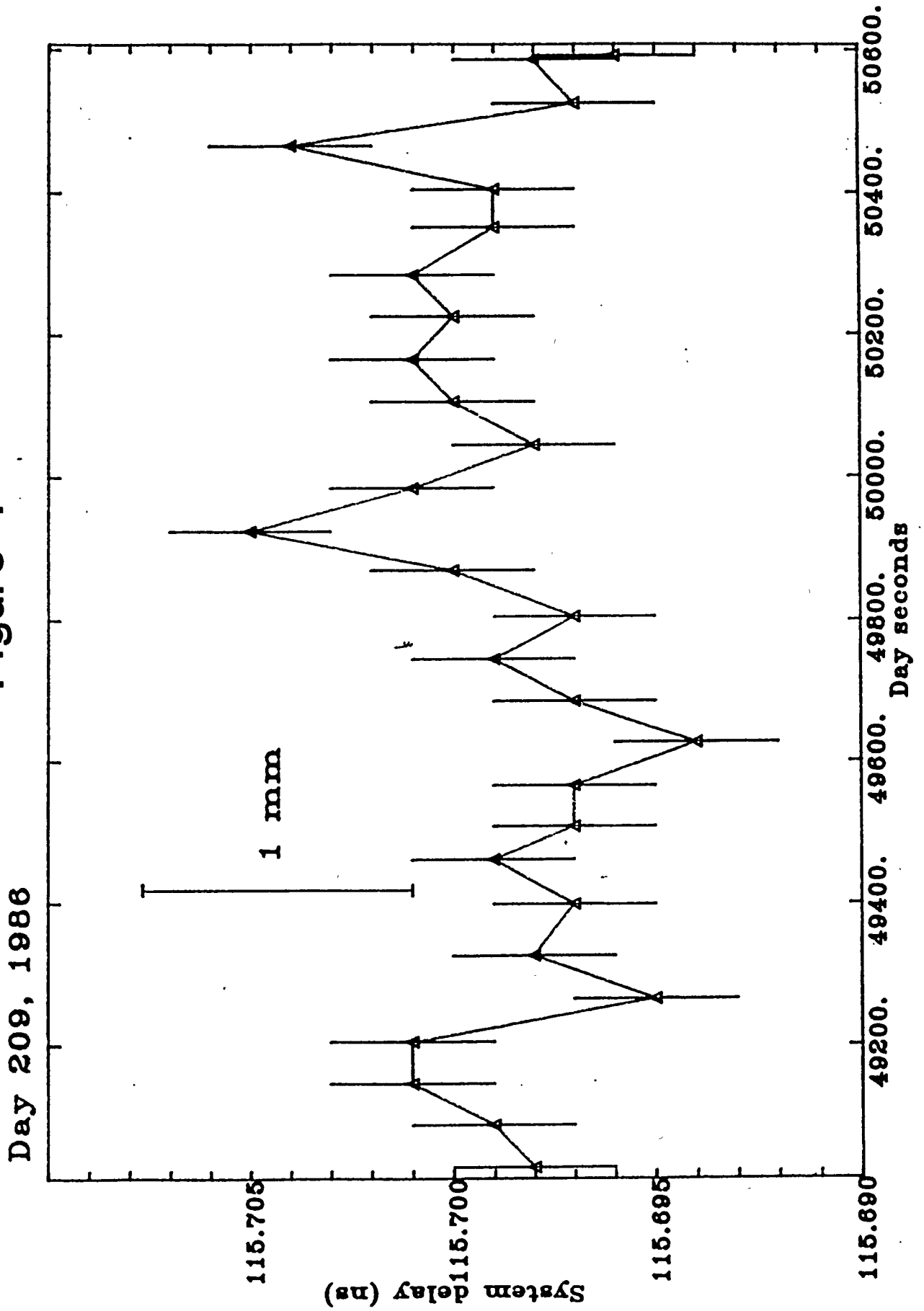


Figure 2

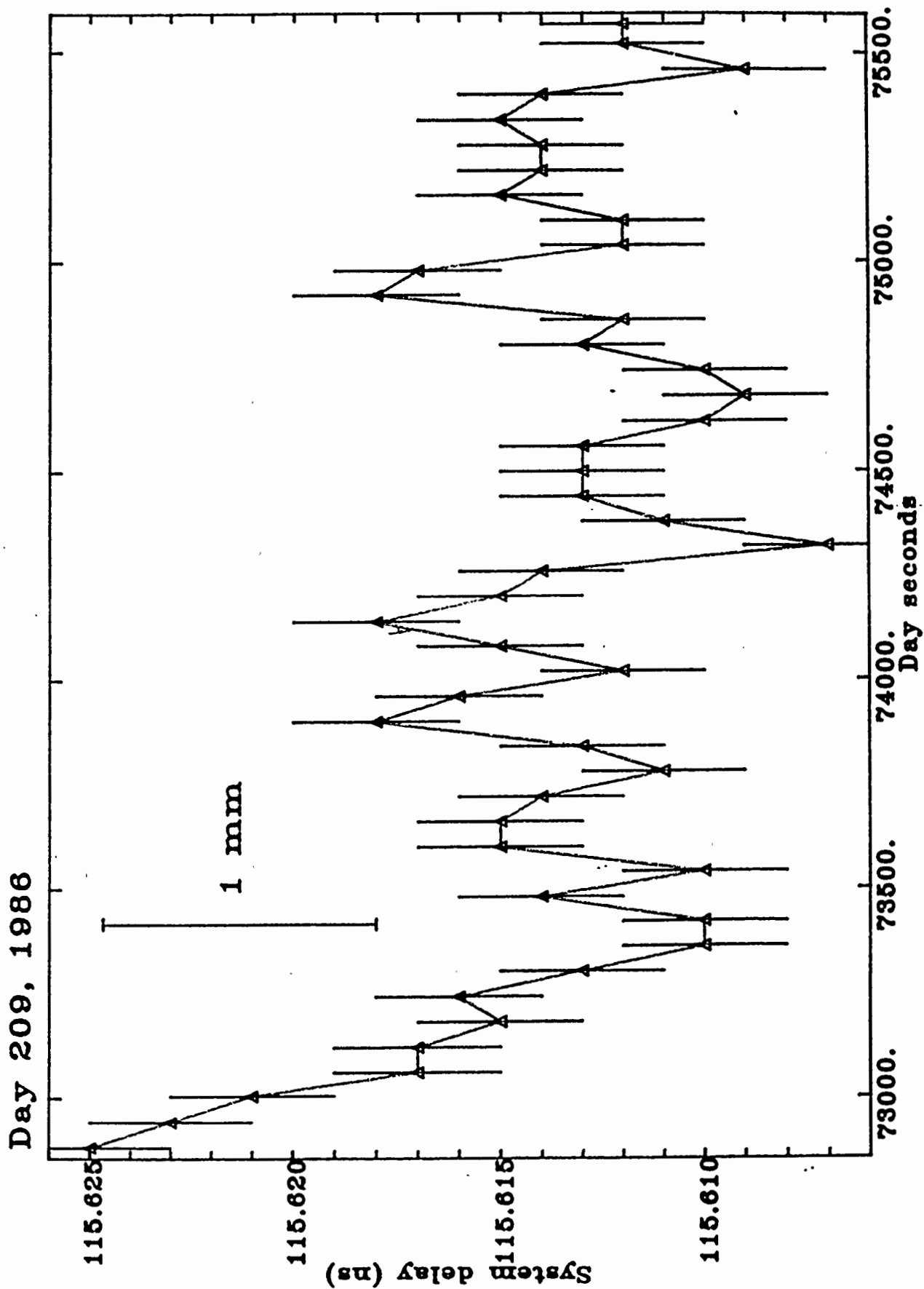


Figure 3

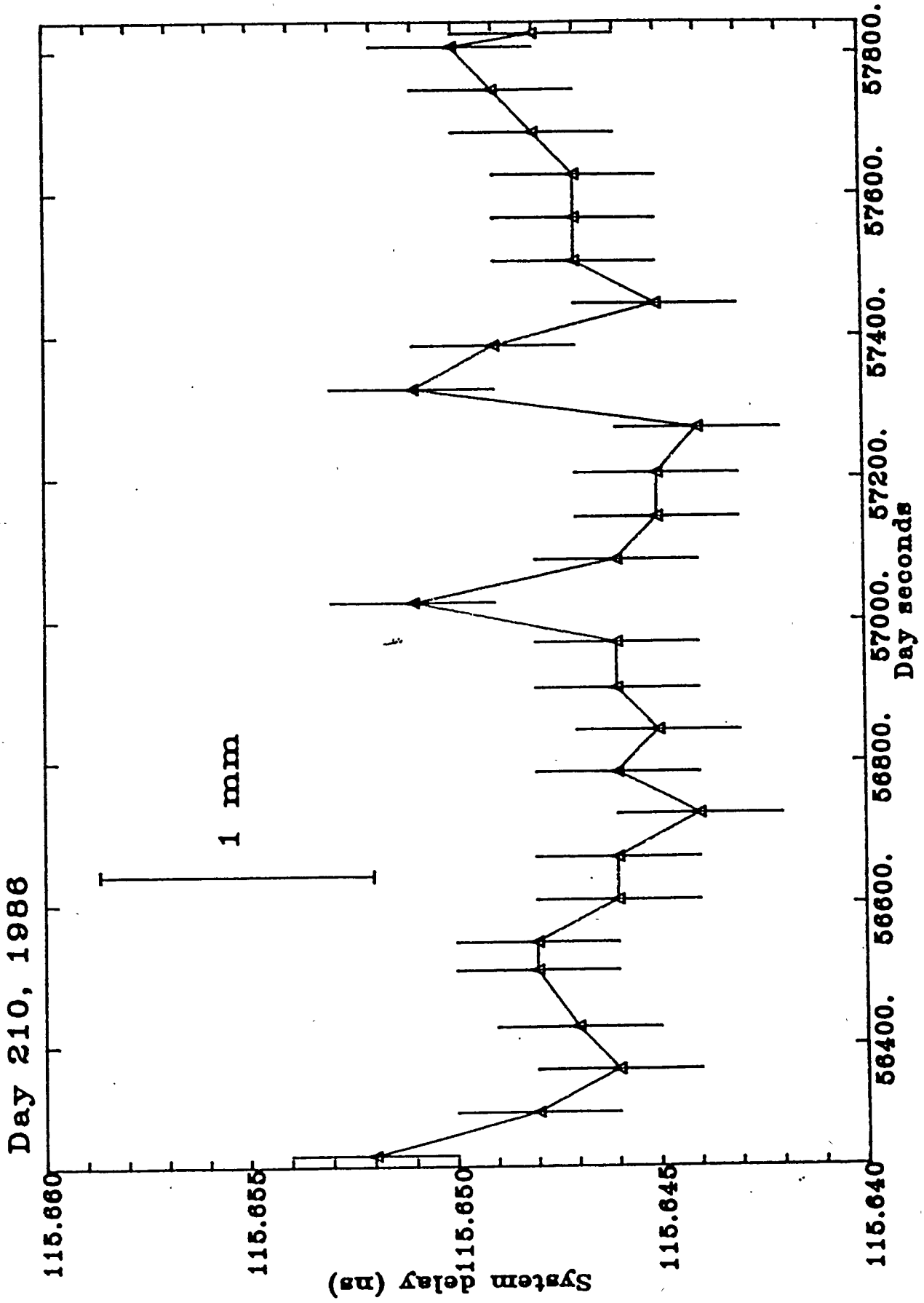
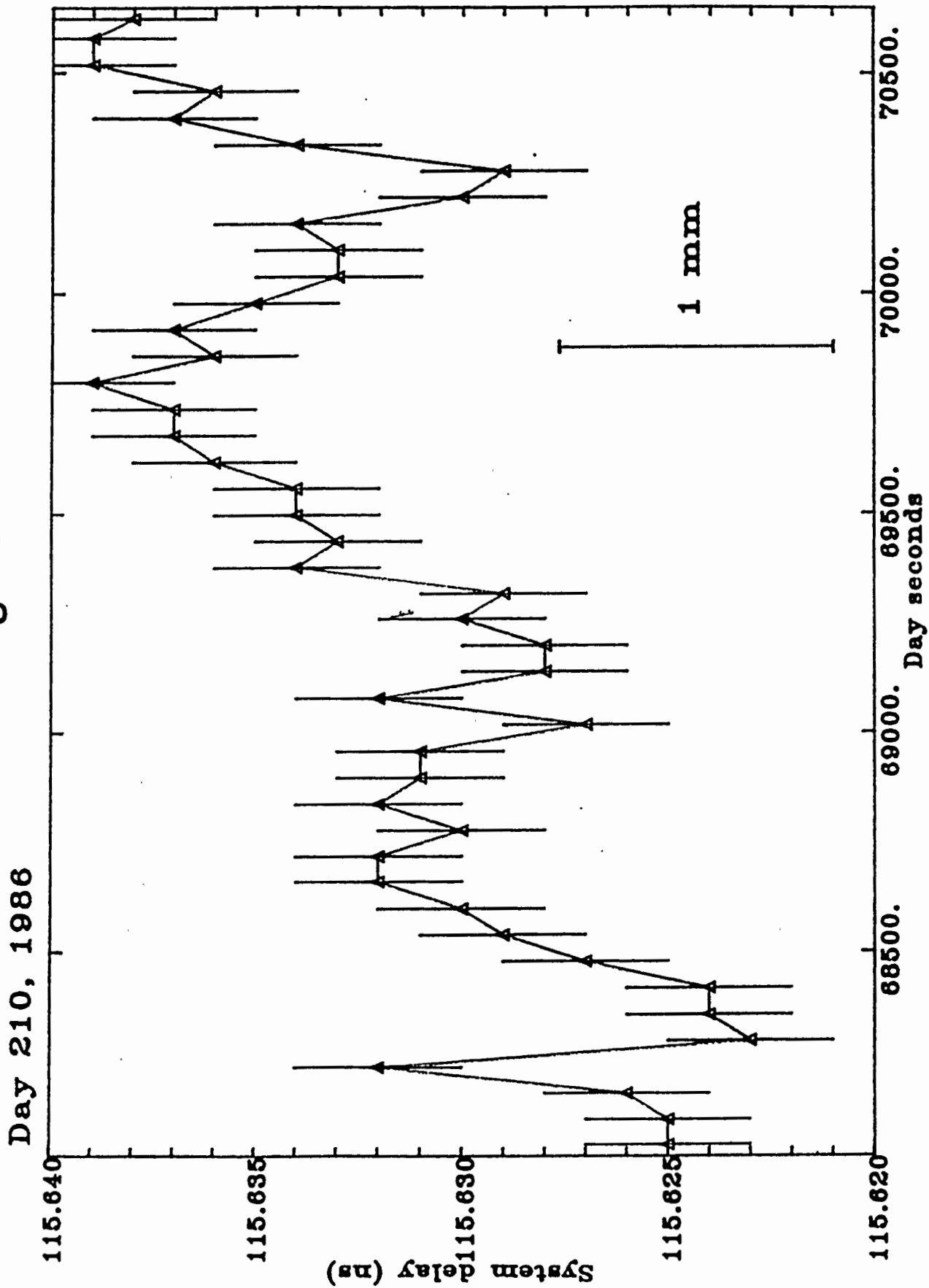


Figure 4



Calibrations

Real-Time Differential Range (RTDR)

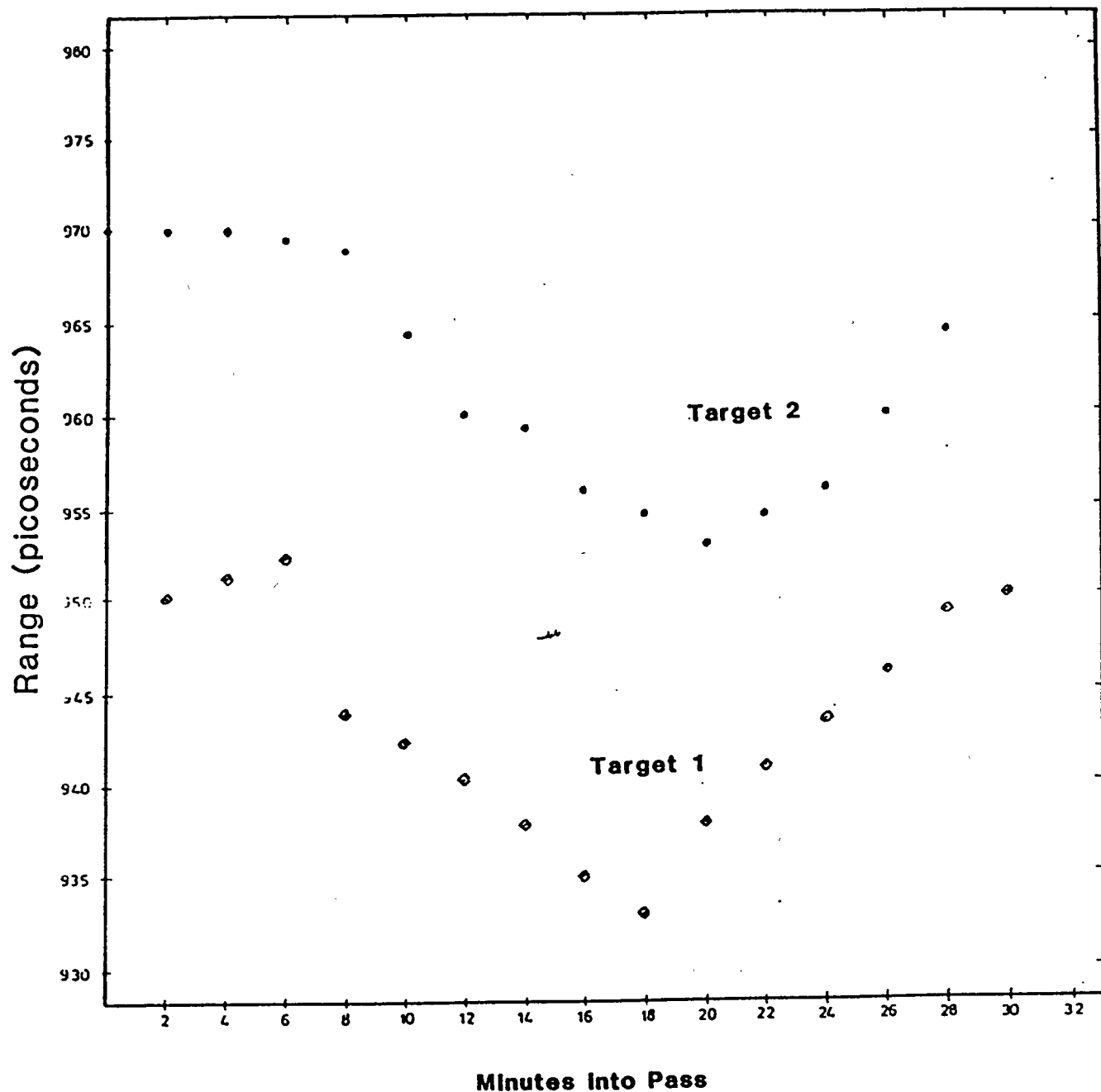


Figure 5

NLRS ACCURACY

Determined by Real-Time Differential Range Calibrations

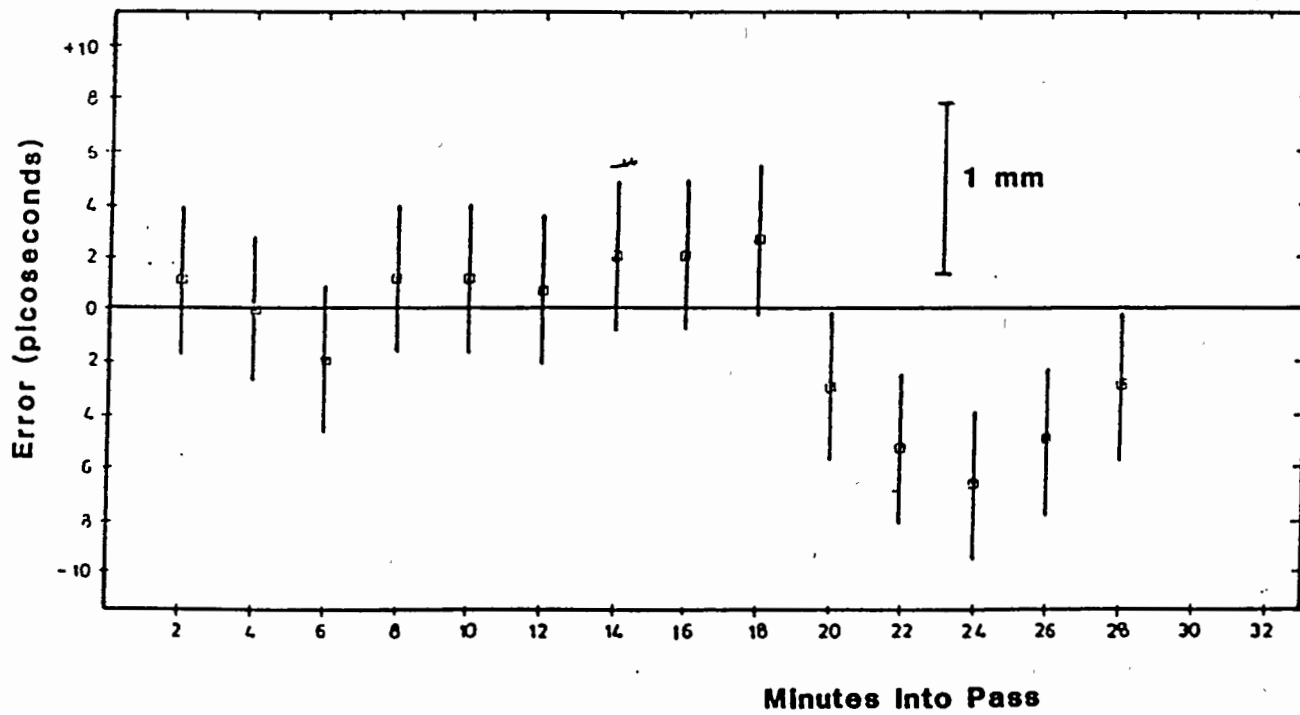


Figure 6

MEASURING AND MODELLING PULSE DISCRIMINATOR AMPLITUDE DEPENDENCE

P. Kloeckler, Th. Schildknecht
Zimmerwald Satellite Observation Station
Astronomisches Institut
Sidlerstasse 5,
CH - 3012 BERNE - Switzerland -

Telephone 4131 65 85 91
Telex 912643 PIBE CH

ABSTRACT

Amplitude dependence of the return pulse discriminator contributes significantly to the ranging-machine error budget, if multiphoton ranging is considered. Constant fraction discriminators of improved design are most commonly used to reduce this dependence, yet these must be - and remain - well adjusted. Even then, a rest of doubt remains, because characterizations are often done in an ideal, not real, test environment.

The present paper introduces a characterization method which confronts the discriminator under test with a real ranging environment. The same setup is also used to monitor the performance during the ranging session.

Several discriminator types have thus been investigated, and attempts undertaken for computer-modelling of remaining systematic errors.

1. AGAIN: THE TIME-WALK PROBLEM

This problem, as illustrated in Fig.1 for a simple fixed-threshold discriminator, seemed solved when the stations changed to picosecond lasers and single-photon ranging. This resulted in a very limited dynamic range of echo-pulse amplitudes; multi-photon events were deliberately purged from the data by signal attenuation and data screening. Any remaining amplitude dependence was taken care of by a constant fraction discriminator and hence deeply buried in the timing noise caused by the photomultiplier. (5..15 cm r.m.s.)

However, after some operational experience with the new or upgraded systems it was found that multiphoton-events were sometimes quite numerous -perhaps caused by "hot spots" in the laser beam- and operators had to be alert to react accordingly.

With the advent of microchannel-plate photomultipliers, the situation changed again. The r.m.s. values dropped to the 1..3 cm level, and millimetre precision ranging to satellites became feasible. Systematic errors had to be reduced accordingly: better constant-fraction discriminators were selected | 2 |.

Another trend that became apparent was the revival of multi-photon ranging with stations affording large telescope apertures and more powerful lasers: the dynamic range of the received signal became larger again and had to be well controlled for the ultimate in precision.

The japanese satellite AJISAI with its great effective cross-section and diameter imposes such a pulse distortion (Fig.2), so that it was suggested to use some sort of leading edge detection to preserve the inherent ranging precision of the observing stations.

To conclude this brief review, we suggest that the discriminator problems are far from solved, and it is certain that new products and concepts will continue to be introduced into the LRS's. Prior to their introduction, however, they have to be sufficiently well characterized to make sure that no additional systematic errors will bias the low r.m.s. data.

2. CHARACTERIZATION OF TIMING CHANNELS

CHARACTERIZATION MEANS DETERMINATION OF ALL RELEVANT SYSTEM PARAMETERS WITH REGARD TO ALL RELEVANT VARIABLES (TIME, TEMPERATURE, GEOMETRY, AMPLITUDE, NOISE ETC.).

In practice, though, only a few parameters are characterized, while others are either thought to be less relevant, have been measured once by some reputed agency | 2 |, or it is depended upon the manufacturer's specifications. This attitude is possible because a total system delay is elaborated frequently in which all individual parameters are lumped together. Nevertheless, we sometimes would like to determine individual parameters for optimization.

An ideal setup for characterizing a typical timing channel (consisting of: optoelectronic detector, solid-state amplifiers, cables, pulse discriminator and time-interval digitizer) would include an optical pulse source, a variable attenuator, some pulse amplitude measuring device, a background events counter, an oscilloscope or pulse digitizer and a computer. (Fig.3)

Our practical installation, though presented earlier | 3 |, is depicted in Fig.4. We use our actual ranging equipment for the characterization, with only a few additions: a lid on the receiving telescope with an iris diaphragm for control of background illumination, a counter and a second fast photodiode to provide an additional, low jitter stop-channel. A pulse generator for simulating pulses of variable width (from 1 ns FWHM) exists, but is not used for amplitude characterizations because of inevitable time shifts when attenuating the pulse. The internal feedback path used for in-pass calibration readily can be used for characterizing a chain of devices, which are intended to work together. The advantages against testing individual devices separately in the laboratory are numerous:

- *A similar electro-magnetic environment is effective as when actually ranging to satellites
- *Optical attenuation introduces no variable delays (as electrical attenuation might do)
- *Possibility of verification any time and on site
- *Pulse shapes¹, amplifier distortions, cable bandwidth limitations and background noise as in real LRS

3. TESTS

3.1 DEVICES UNDER TEST

Two types of discriminators have been tested so far:

-FIXED THRESHOLD: Various models (LeCroy 120, 623 and 4202, the latter included in the time digitizer) differ mainly in the number of channels and the minimal thresholds available. Threshold in the 4202 can be set as low as -5 mV, thus affording additional receiving gain. Their amplitude response is smooth and naturally reflects the leading edge of the input signal. It easily can be modelled (viz. Appendix). They behave well also with sub-nanosecond pulses.

¹ One fundamental limitation of the concept is the failure to simulate the target depth function. We have to trust that the transmitted pulse shape is only slightly altered by the satellite's reflectors.

-CONSTANT FRACTION: The earlier "network-standard" Ortec model 934 has caused serious time-walk problems even with the 3 ns FWHM pulses of our conventional photomultiplier | 3 |. The device is not specified for sub-nanosecond pulses. Minimum threshold is -30mV, but it was found that up to -100 mV operation was not satisfactory. Adjustment of minimum walk is a cumbersome procedure.

A successor (ETL 103 model) features an automatic walk adjustment utilizing a slow feedback loop to keep the DC/level at the input zero. It also allows a minimum threshold setting of -5 mV, and contains a faster trigger circuit.

The new Tennelec 454 model arrived just recently; hence we cannot comment much on its merits. Initial tests indicate a significant improvement in performance and ease of adjustment. However, it was noted that a slewing effect near threshold also exists.

3.2 TEST PROCEDURE

The program for internal calibration was run, which operates the laser and data acquisition. The stop ND-filter was placed in an initial position, attenuating the laser pulse to single-photon level. Then a short calibration run was performed to aid adjustment of the start ND-filter(to make sure that the start detector was operating in its specified amplitude range). After this, a few hundred calibration points were taken while opening the stop-ND filter to run through the dynamic amplitude range at the receiving side. After completion, the relevant variables were noted and the data-set screened. A following computer evaluation yielded the time-delay vs. amplitude curve.

As an optoelectronic detector, both photomultipliers and a PIN diode were used. Time intervals were measured with the LeCroy 4202 TDC and not with the HP counter for practical reasons.

3.3 RESULTS OF MEASUREMENTS

Some results are summarized in the table below and plotted in Figures 5-12:

Figs. 5 and 6 reflect the amplitude dependence of a typical constant-fraction and leading-edge discriminator, respectively. They were taken using a conventional photomultiplier.

In Figs.7 and 8, the effect of modelling the amplitude dependence of a fixed-threshold discriminator is shown. Here, the microchannel- detector was used.

Fig. 9 shows the effect of linearly modelling the same constant-fraction discriminator as in Fig.5. The slewing near threshold still visible in Fig. 5 was removed by raising the threshold.

In Fig. 10 the improved constant-fraction discriminator is characterized, using the diode detector.

Figs. 11 and 12 show the effect of modelling on the residuals of a satellite pass, which was AJISAI, observed by microchannel-plate.

The results of the amplitude dependence characterizations are summarized in the following table:

SUMMARY OF RESULTS

T I M E - W A L K
(ALL VALUES IN PICOSECONDS PEAK)

DETECTOR TYPE:	D341 (PM)	R1294 (MCP-PM)	HP-5082 (DIODE)
METHOD:			
CONSTANT FRACTION (NO MODEL)			
ORT 934	±210 @ 1:10		
	±650 @ 1:50		
ETL 103	±460 @ 1:10		
	±630 @ 1:30		
TENN 454		±125 @ 1:10	± 55 @ 1:5
		±175 @ 1:50	±285 @ 1:10 s
CONSTANT FRACTION (LINEAR MODEL)			
ORT 934	±200 @ 1:10		
	±200 @ 1:50		
ETL 103	±210 @ 1:10		
	±210 @ 1:30		
FIXED THRESHOLD (NO MODEL)			
LCR 4202	±780 @ 1:10	±120 @ 1:10	
LCR 623	±725 @ 1:10		
FIXED THRESHOLD (LINEAR MODEL)			
LCR 4202	±325 @ 1:10		
FIXED THRESHOLD (GAUSS MODEL)			
LCR 4202		± 80 @ 1:10	

s Note: TIME "SLEWING" NEAR THRESHOLD

4. REFERENCE

| 1 | J. J. DEGNAN

SATELLITE LASER RANGING: CURRENT STATUS AND FUTURE PROSPECTS
IEEE TRANS. ON GEOSCIENCE AND REMOTE SENSING
VOL. GE-23, NO. 4, JULY 1985, P. 398

| 2 | M. R. PEARLMAN

SLR GROUND TESTS
CIRCULAR DATED AUGUST 2, 1985

| 3 | P. KLOECKLER, I. BAUERSIMA

IN PASS CALIBRATION DURING LASER RANGING OPERATION
PROC. OF THE FIFTH INTERNATIONAL WORKSHOP ON LASER RANGING
INSTRUMENTATION, HERSTMONCEUX CASTLE, SUSSEX, ENGLAND
VOL. I, P. 194

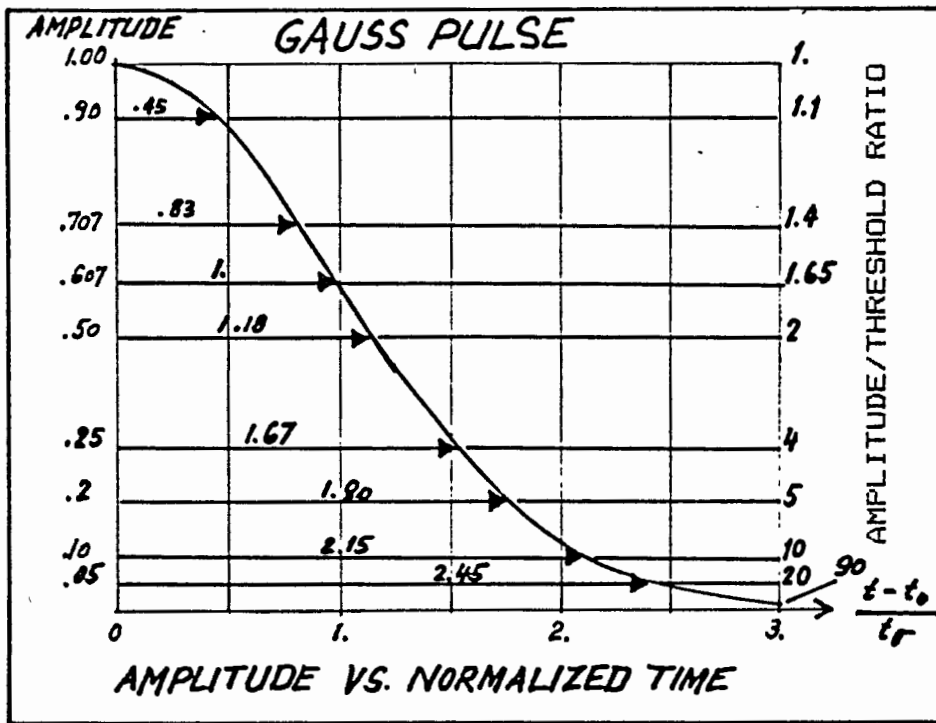


FIG. 1 CORRECTIONS FOR AMPLITUDE DEPENDENT ERROR:
(FIXED THRESHOLD DETECTION)
1 ns t_0 Pulse Width assumed

A/T ratio:	correction in ns:
1.0	0
1.65	1.00
5.0	1.80
10.0	2.15
90.0	3.00

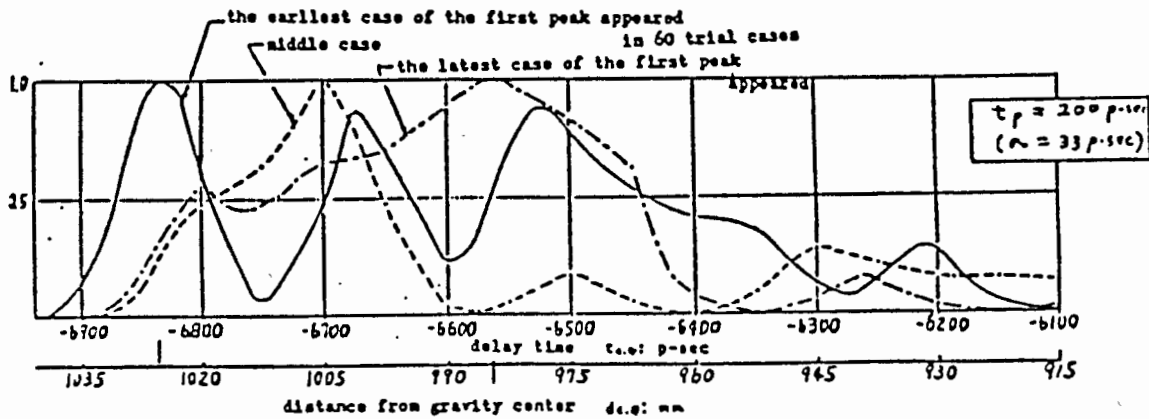


FIG. 2 RETURN PULSE FROM "AJISAI"
Results of Computer Modelling

Courtesy:
M. SASAKI
HYDROGRAPHIC DEPT.
OF JAPAN

FIG. 3 IDEAL SETUP FOR AMPLITUDE DEPENDENCE CALIBRATION

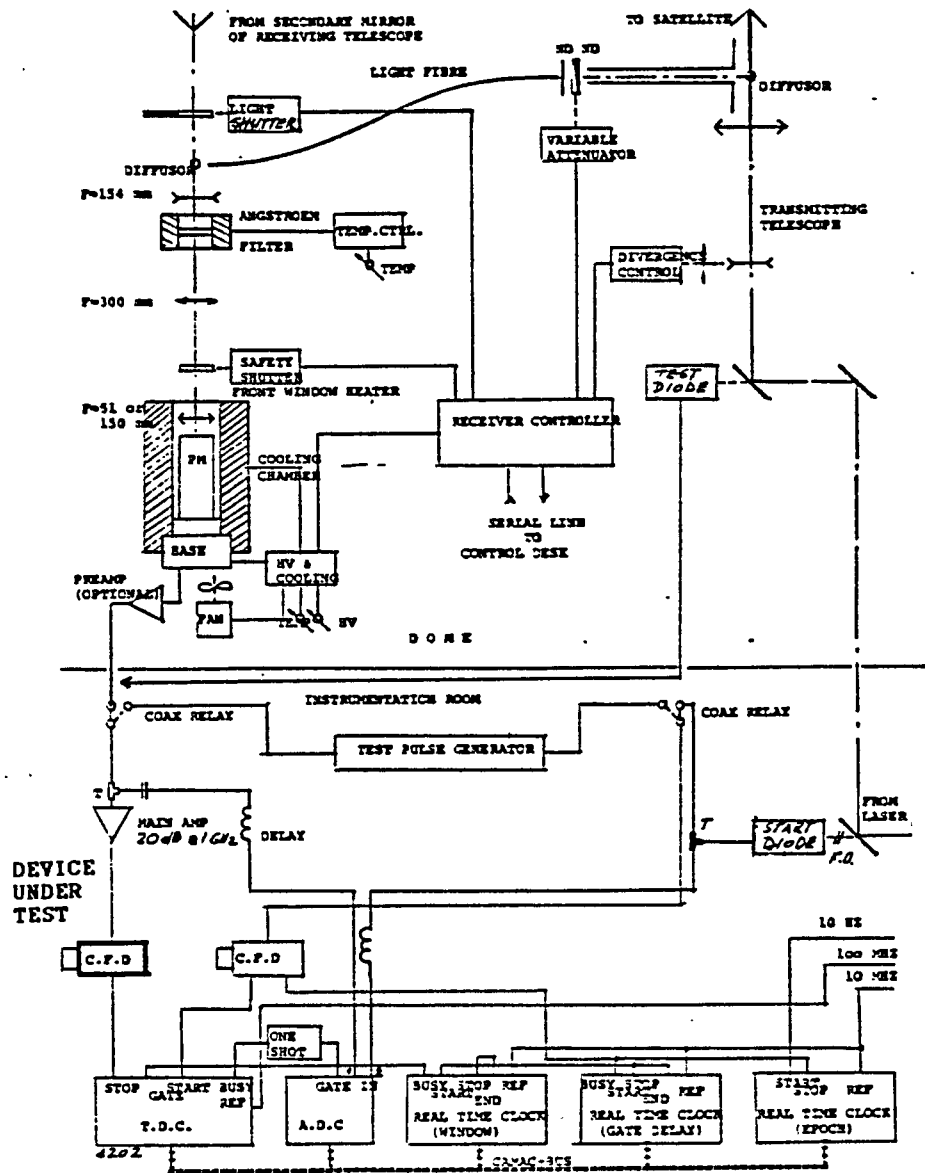
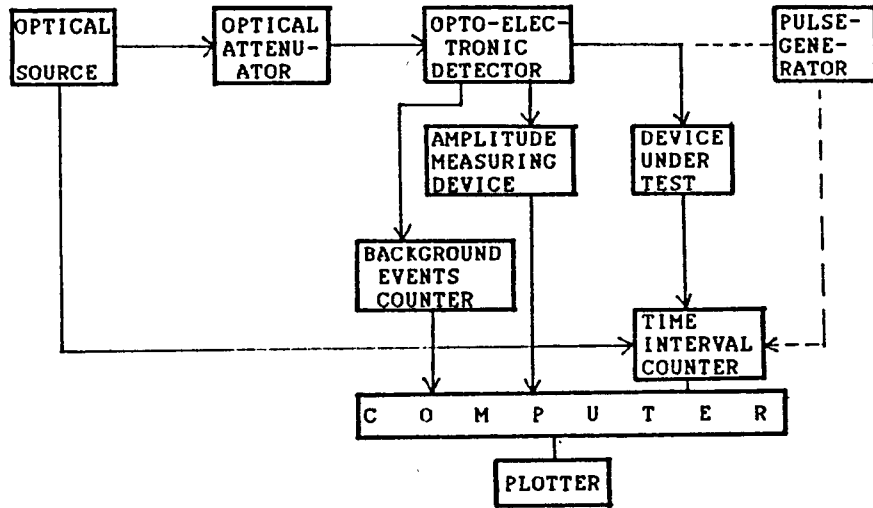
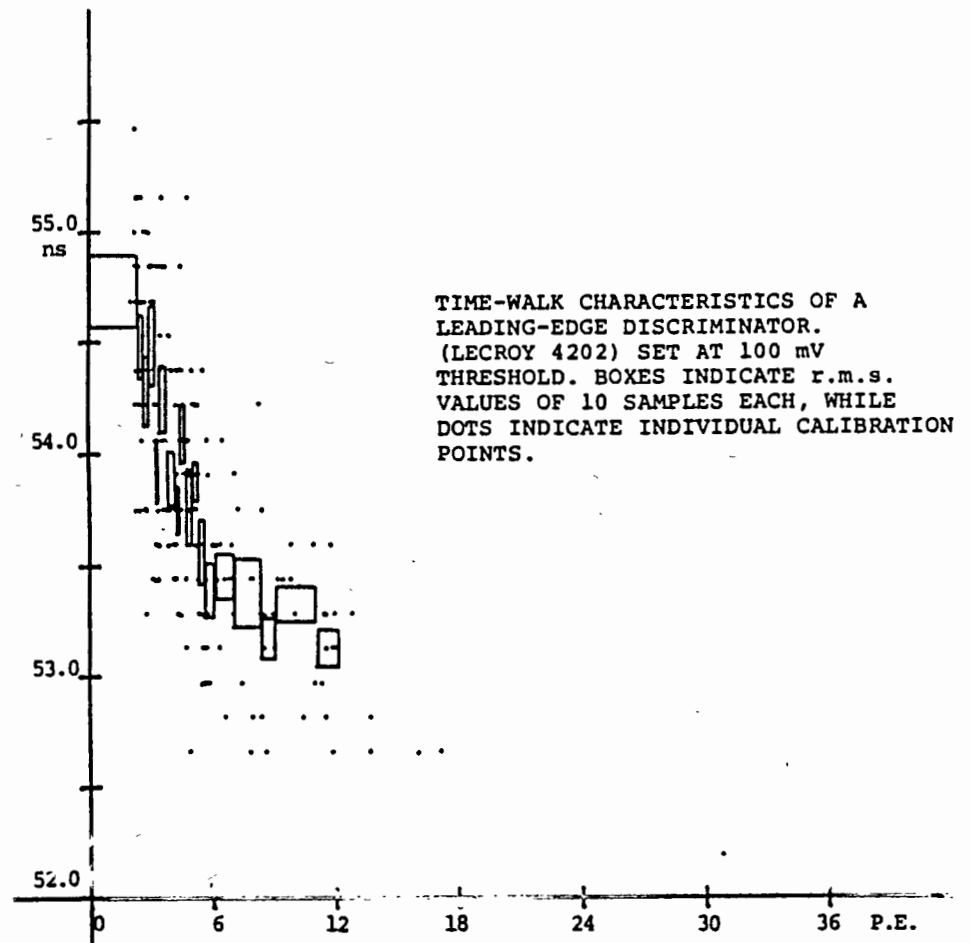
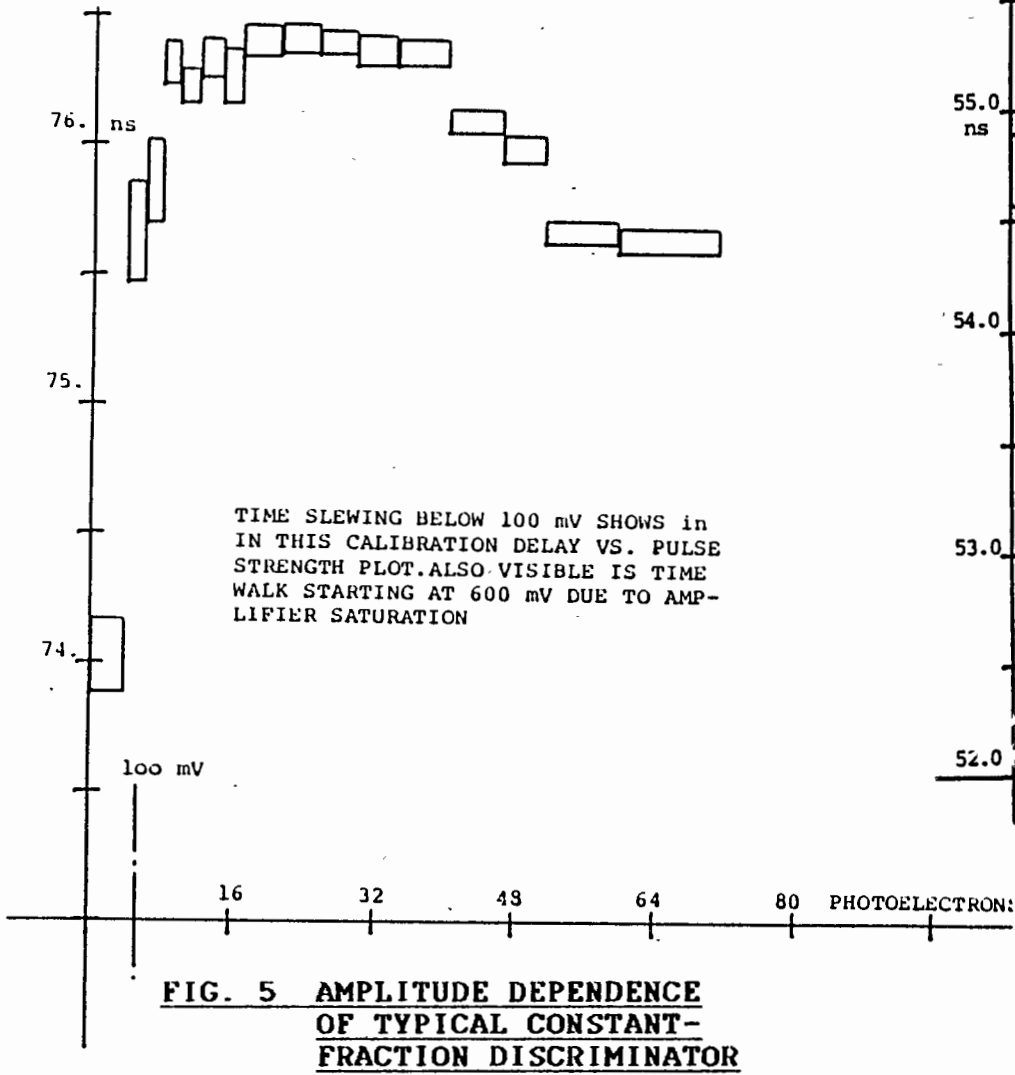


FIG. 4 CALIBRATION SETUP USING INTERNAL OPTICAL FEEDBACK



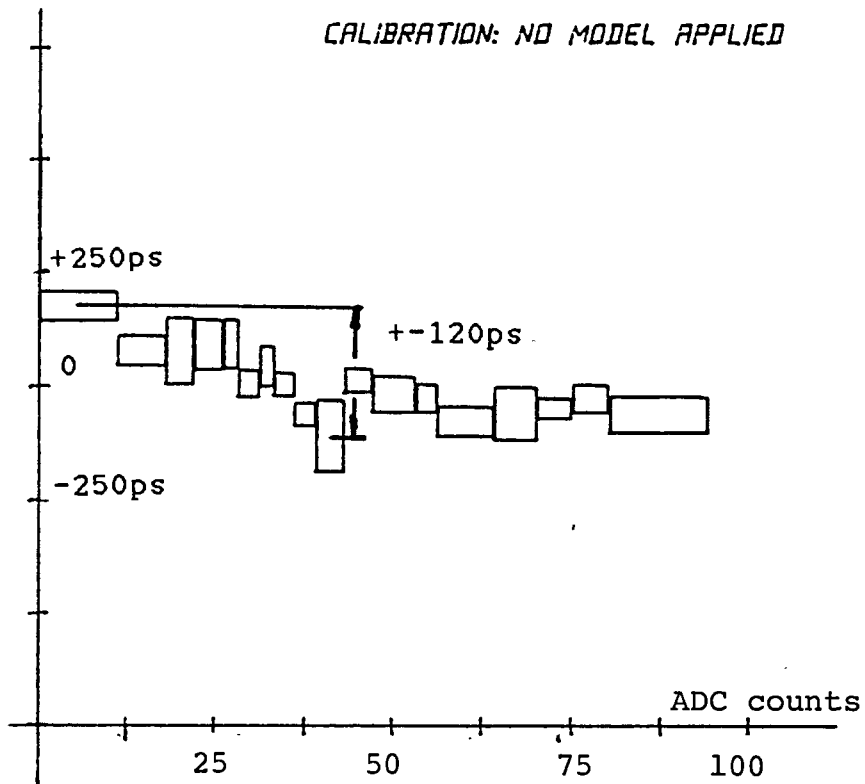


FIG. 7 FIXED-THRESHOLD DISCR.:
UNMODELLED

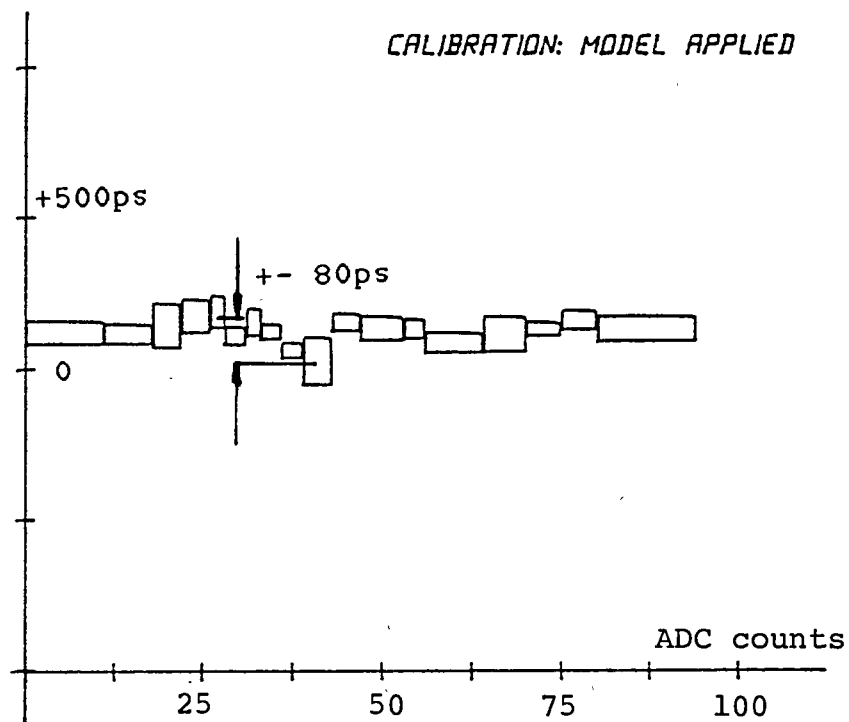
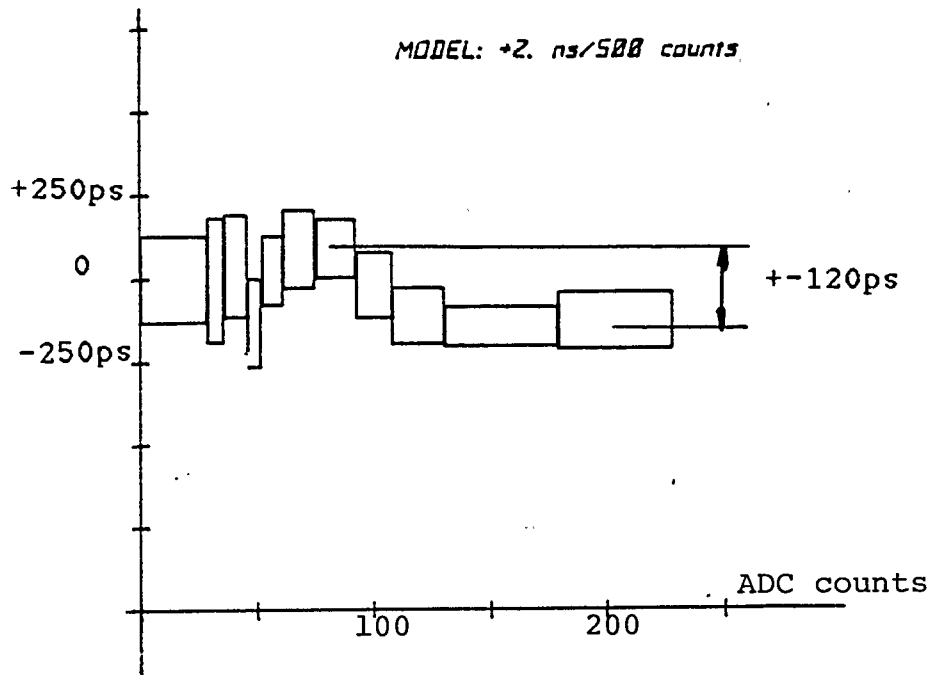
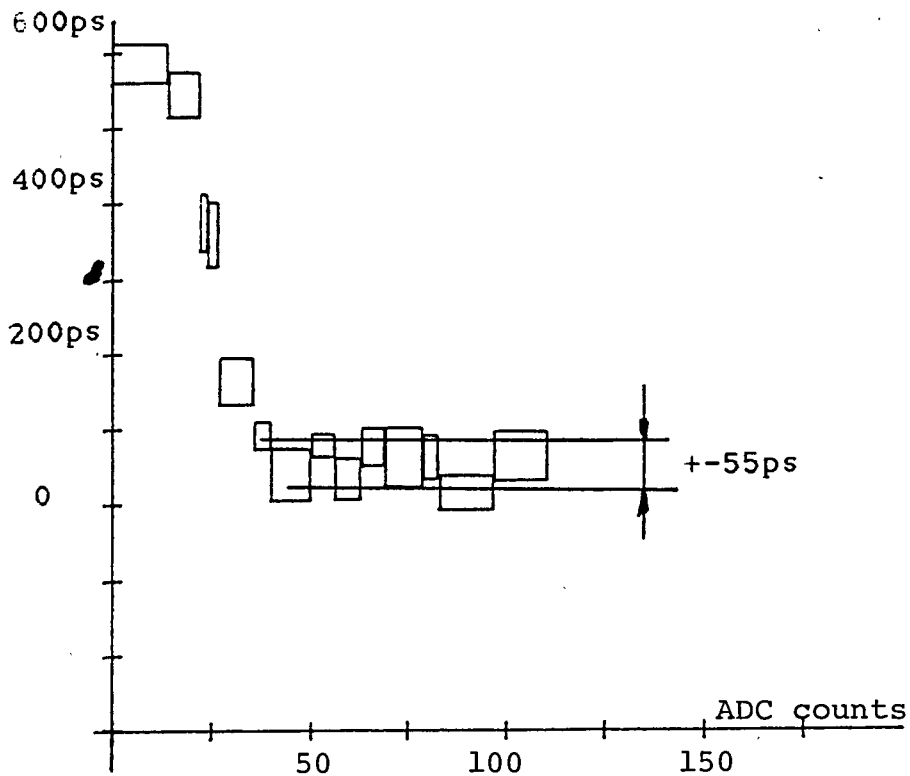


FIG. 8 FIXED-THRESHOLD DISCR.:
MODELLED



**FIG. 9 CONSTANT FRACTION DISCR.:
MODELLED**



**FIG. 10 IMPROVED CONST. FRAC. DISCR.
NOTE 'SLEWING' NEAR THRESHOLD**

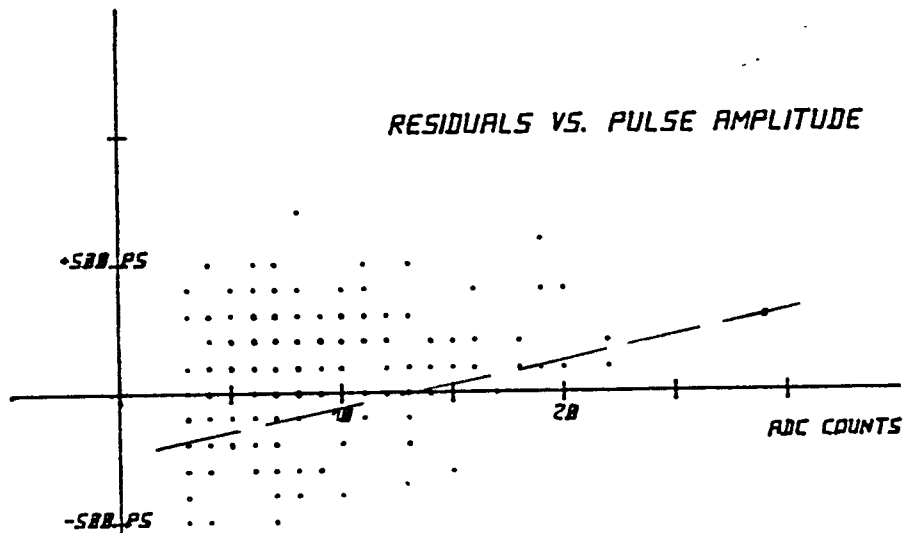


FIG. 11 "AJISAI" PASS
AFTER SCREENING:
FIXED THRESHOLD
NO MODEL

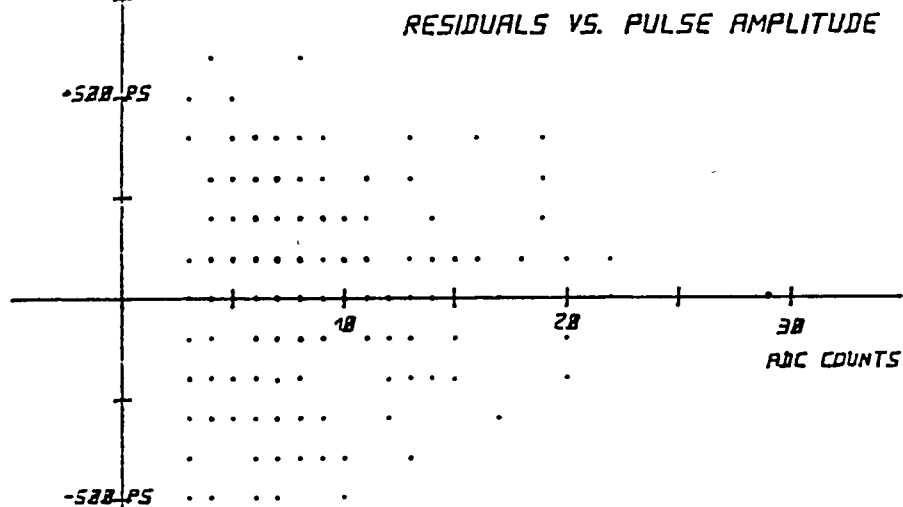


FIG. 12 SAME PASS
FIXED THRESHOLD
GAUSS-MODEL

APPENDIX COMPUTER MODELLING OF DISCRIMINATOR AMPLITUDE DEPENDENCE

A) LEADING EDGE

If Gaussian pulse is assumed:

$$u(t) = U_{th} = A * \exp - \frac{(t - t_0)^2}{(2 t_0)^2}$$

with: U_{th} threshold voltage
 A amplitude
 $t - t_0$ time correction to centroid
 t_0 half pulse width at $.607 * A$

we get for the time correction:

$$t - t_0 = .60 * t_{FWHM} \sqrt{-\ln(U_{th}/A)}$$

with: t_{FWHM} full pulse width at $.5 * A$

In the above formula, the term U_{th}/A must not become greater than 1. Threshold usually is defined as the amplitude where 50% firings occur. Here, care must be taken to use the smallest amplitude value permitted to fire the discriminator as U_{th} . Correction is most prominent with low amplitudes, and becomes very small above tenfold threshold. (viz. Fig. 1)

When the calibration values are evaluated, a table is created which contains correction values vs. amplitude. Intermediate values are linearly interpolated. For the whole procedure note Table A.1.

B) CONSTANT FRACTION

A linear correction, removing the slope, was applied. It then was found, that the remaining "roughness" was possibly of systematic nature, but its law is not easily found from the electronic circuitry involved.

FINAL REMARK

The chosen approach utilizing a table of correction data allows an empirical model which can be tested immediately. We finally wish to point out that all observation data remain unchanged; in particular the in-pass calibration points can be used at any time later-on to adjust or test the applied model.

CALIBRATION PROCEEDURE

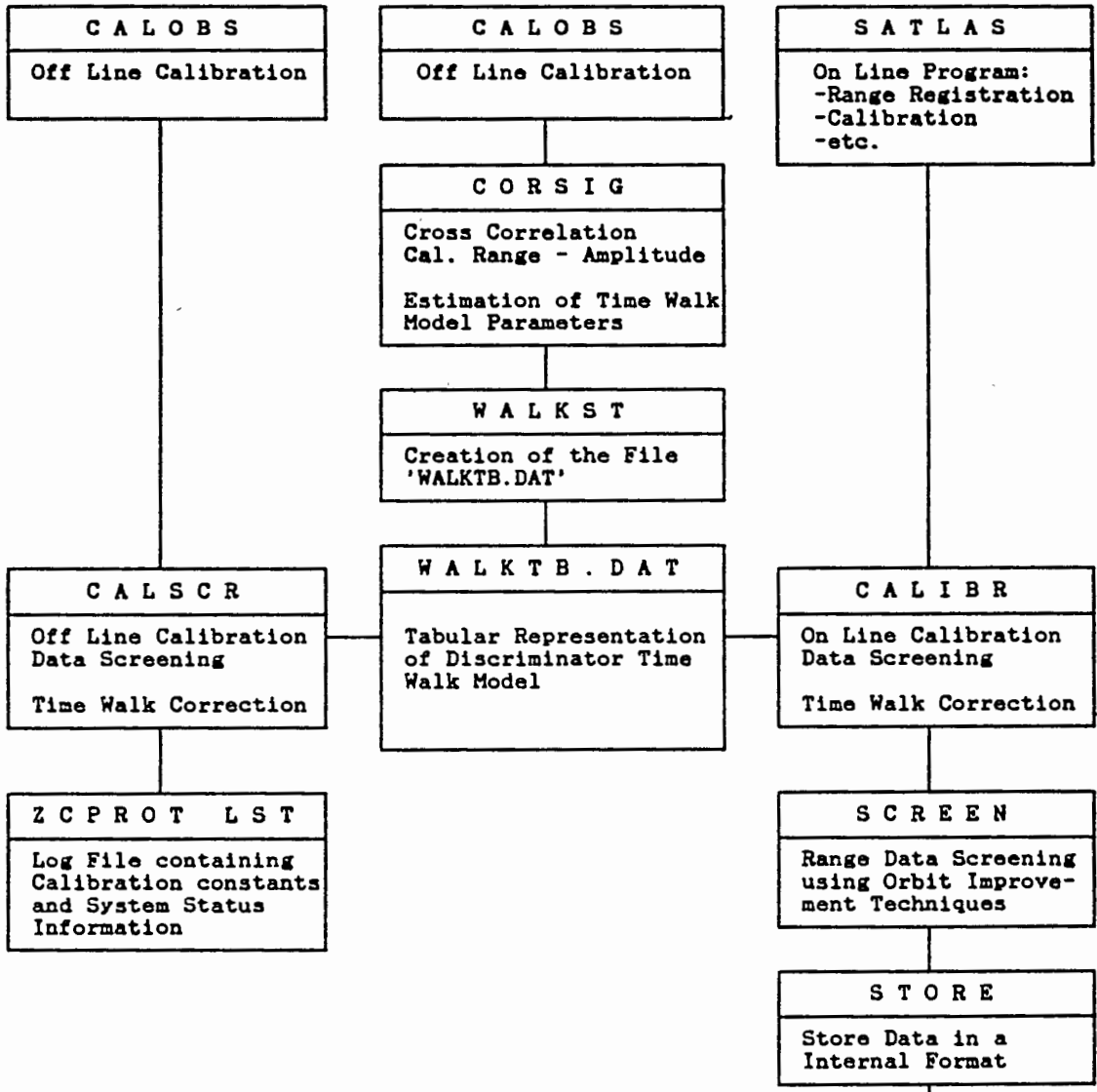
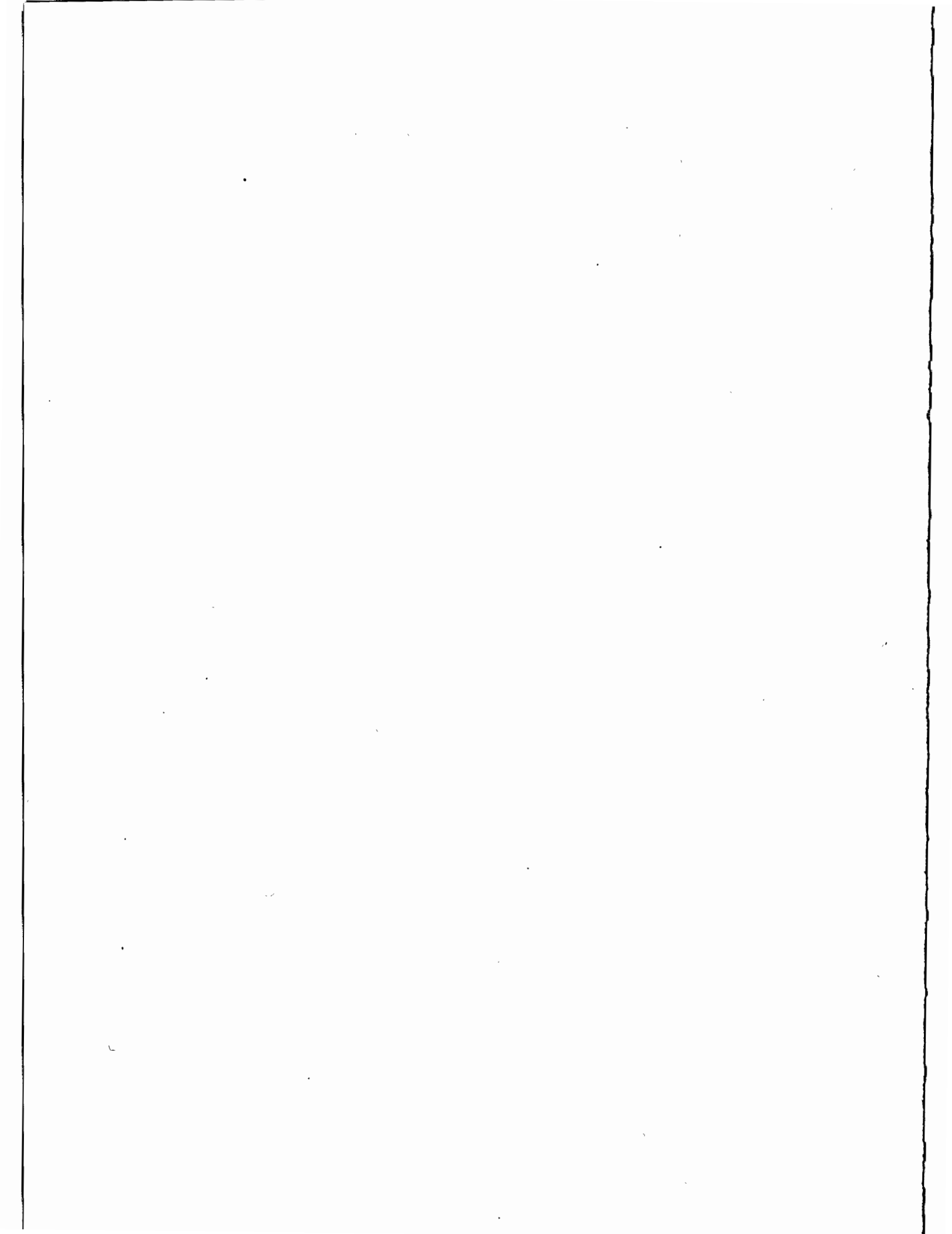


TABLE A.1 FLOWCHART FOR MODELLING OF AMPLITUDE DEPENDENCE



MLRS GROUND TESTS

H. Junginger
Institut für Angewandte Geodäsie
Satellitenbeobachtungsstation Wettzell
D-8493 Kötzing

Telephone (9941) 8643
Telex 69937 WESAT D

W. Beek
Delft University of Technology
Observatory for Satellite Geodesy
Postbox 581
NL-7300 AN Apeldoorn

Telephone (5769) 341
Telex 36442 SATKO NL

ABSTRACT

MLRS-1 and MLRS-2 performed a series of ground tests in 1985/86. Thereby they were using their internal as well as this target calibration capabilities. Five different test procedures are described and data are presented for each procedure at least from one MTLR-System. The mean RMS of MTLRS calibration normal points was found to range between less than .4 and 1 cm, well within the system specifications. No indications for systematic biases at the 1 cm level could be found under normal MTLRS operation conditions.

1. Introduction

The two European Modular Transportable Laser Ranging Systems [1] operated by the Institut für Angewandte Geodäsie in Frankfurt / Federal Republic of Germany (MTLRS-1) and the Delft University of Technology / The Netherlands (MTLRS-2) were for the first time collecting data in Italy and Greece in 1986. Before the systems were shipped to these countries to start the WEGENER-MEDLAS observation campaign (Working Group of European Geo-Scientists for the Establishment of Networks for Earthquake Research - MEDiterranean LASer Project) they went through a series of collocation and performance verification tests. It is the purpose of this paper to report on the results of ground measurements done during this testing period.

The paper is organized as follows: In section 2 the internal calibration procedure for the MTLR-Systems is described because most of the tests are based on this capability. Furthermore an overview is given on the electronical devices in the time of flight detection circuits. Section 3 starts with a discussion of system stability over time periods typical for LAGEOS passes. Temporal variations of the time of flight caused by internal noise sources are superimposed to all data. For this reason they have to be well known before in the remaining parts of section 3 systematic dependences of range data on the PMT voltage, the laser beam wave front, the pointing direction of the mount, and on the signal strength can be studied. In section 4 the results of the ground tests are critically summarized.

2. Internal Calibration and Brief System Overview

In Fig. 1 the optical and opto-electronic components of the MTLR-Systems and the pathes of transmitted and received light are shown schematicly. Light pulses originating in the Nd:YAP Laser are transmitted through a neutral density filter package (which optionally allows attenuation), through various mirrors and prisms to the beam splitter assembly. There the laser beam is divided into two symmetric semi-circular beams which are guided through the mount into the telescope. A cross section of the emitted laser beam at the telescope exit is shown schematicly in Fig. 2.

The tiny fraction of the transmitted light pulses which is reflected at any target is received by the same telescope. It follows a light pass common to the transmitted light up to the beam splitter assembly. There it is separated and guided into the detection package.

The MTLR-Systems are calibrated by fixing a retroreflector in the laser beam at the telescope entrance (see Figs. 1 and 2). The retroreflector is mechanically integrated in a cover which can be screwed on the entrance. During calibration and

MTLRS COUDE TELESCOPE

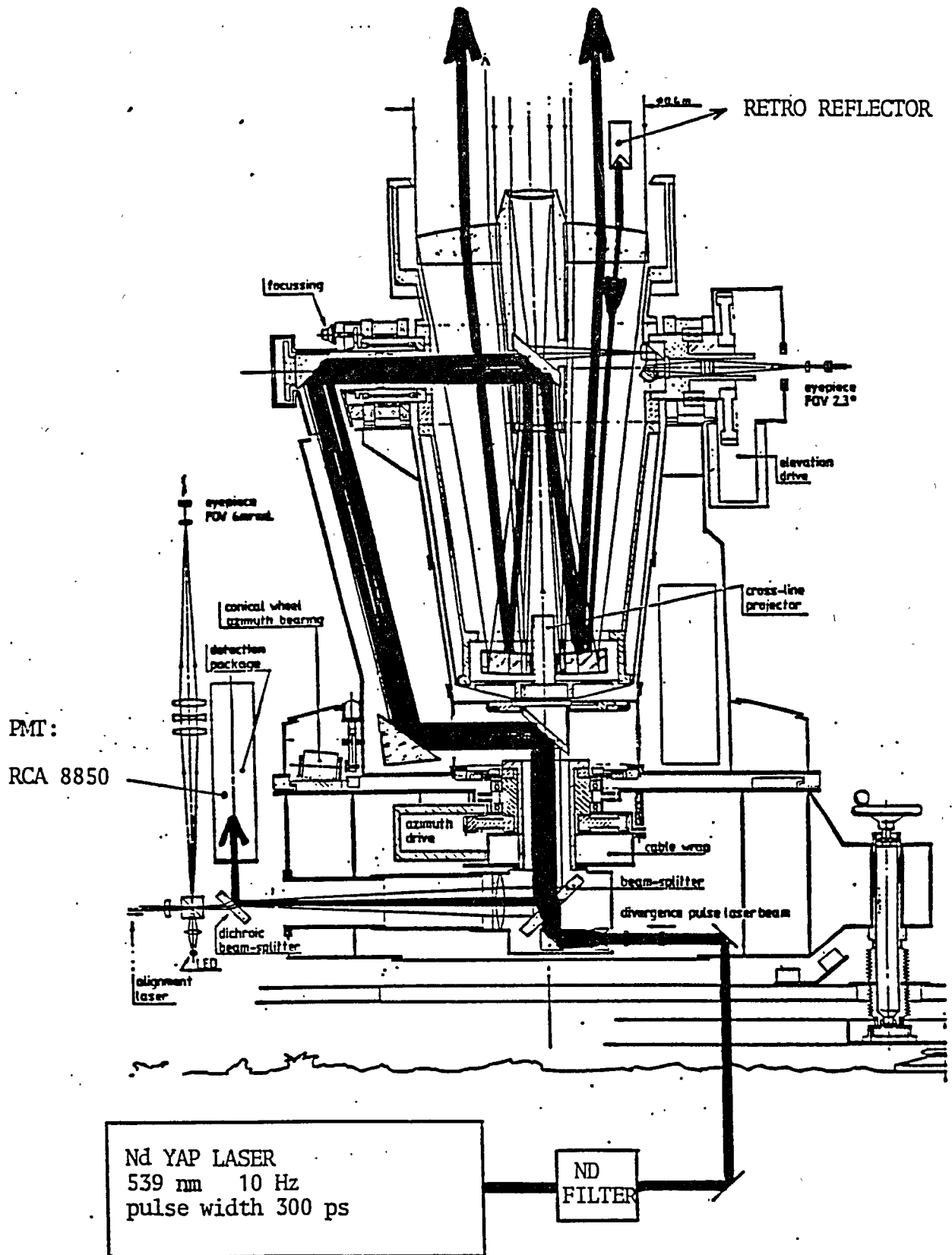


FIG 1 Light pathes through the MTLRS Coudé Telescope

during ground target measurements the transmitted light is attenuated by 8 to 12 orders of magnitude.

Since the retroreflector is fixed with respect to the telescope, the emitted laser beam rotates relative to the reflector when the mount is moved. This is evident from the optical design. In Fig. 2 a 90° rotation is shown. It can be achieved in three different ways: Either the azimuth of the mount is rotated by 90°, or the elevation is changed by -90°, or the elevation is moved by X° and the azimuth by X° - 90°. The rotation of the semi-circular beam halves with respects to the retroreflector puts constraints on the possible mount pointing directions during calibration. These constraints are important for the tests described in section 3.4.

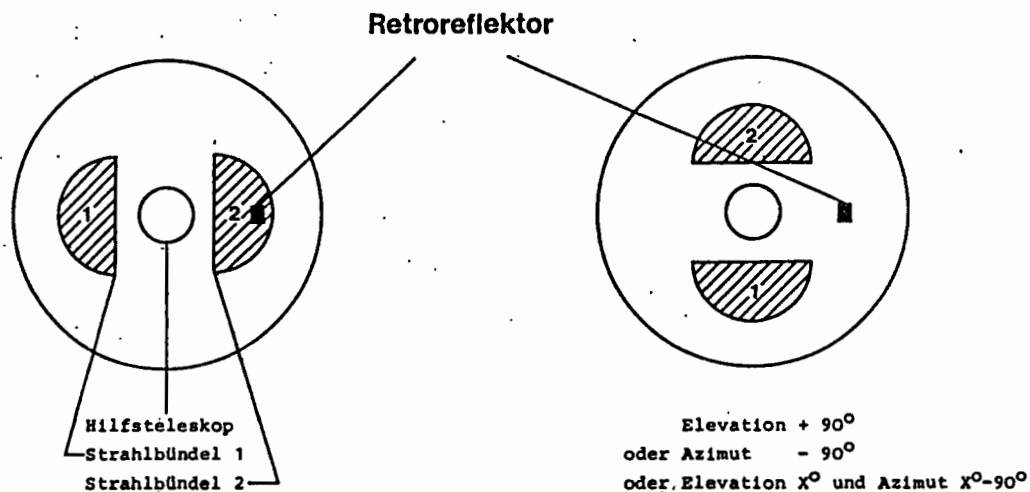


Fig. 2: Cross section through laser beam (hatched areas) at the telescope entrance in two different telescope positions.

Nearly all electrical and opto-electronic components of the MTLRS time of flight detection circuits are commercially available. As a reference their types are given in Table I.

TABLE I

Start-Detector	HP 5082-4207
Constant Fraction Discriminators	ORTEC 934
Range Counters	HP 5370A/B
Photo Multiplier Tube (PMT)	RCA 8850
PMT High Voltage Supply	LABEN 8122
PMT Amplifier	TRONTECH W500F
Frequency Standards	Cs (FTS 4010) or Rb (EFRATOM FRK)

Table 1: Commercially available components of the MTLRS time of flight detection circuits.

3. Ground Tests

3.1 Stability Tests

During the collocation period in Matera starting in January and ending in March 1986, MTLRS-1 and MTLRS-2 went through a stability test which was done by calibrating continuously to the retroreflectors (as described in the previous section) for a bit less than one hour. Times of flight measured in this way are shown in Fig. 3 as a function of time together with single shot RMS-values and return rates. In the upper part of the figure data from MTLRS-1 are displayed, whereas the lower part shows data from MTLRS-2.

The full and dashed lines in the first panel of the figure distinguish average calibration values measured by the two MTLRS-1 range counters 1 and 2 within 5 minute bins. The RMS of the average calibration values is .03 ns which corresponds to .45 cm. The difference between the maximum and minimum bin averaged time of flight is .09 ns which corresponds to a range difference of 1.35 cm. The mean calibration value for MTLRS-1 is about 116.10 ns.

In the second panel single shot RMS-values are shown for each 5 minute bin and for each range counter. The RMS-values vary between .30 and .42 ns. There is a weak indication for about 20 ps greater RMS-values for counter 1. This could be caused by a quartz of inferior quality installed in this counter.

The third panel shows the mean return rates per bin measured by counters 1 and 2. They are defined as the number of accepted data points in one bin (for each individual counter), divided by the number of laser shots in the same bin. Because MTLRS lasers usually operate with a pulse frequency of 10 Hz, a return rate of 5% in a 5 minute bin means that 150 measurements contributed to a bin averaged calibration value. During the stability test the return rate was fluctuating between 5% and 8%.

The variations of the mean calibration values and of the single shot RMS-values in the MTLRS-2 data shown in the lower part of the figure are smoother than those for MTLRS-1. The mean calibration point RMS is .01 ns corresponding to .15 cm. The mean calibration value for MTLRS-2 is about 138.5 ns, the mean single shot RMS .36 ns, in agreement with the value characterizing MTLRS-1. The return rate varied during the MTLRS-2 stability test between 10% and 14%. Eventhough this is twice the MTLRS-1 return rate, both systems were testing at the same light intensity levels. MTLRS-2 has only one counter, therefore its return rate has to be compared with the sum of the MTLRS-1 return rates.

The differences in scatter of the MTLRS-1 and MTLRS-2 mean calibration- and single shot RMS-values have possibly statistical reasons. The numbers of data points contributing to the mean calibration values shown in Fig. 3 differ by a factor of 4 approximately between MTLRS-1 and MTLRS-2. A factor of 2 comes from the fact that MTLRS-1 data were measured with two counters whereas MTLRS-2 was only using one counter. Another factor of 2 is caused by the bin size which was chosen to be 5 minutes for MTLRS-1 and 10 minutes for MTLRS-2.

Assuming Gaussian statistics the RMS of bin averaged calibration values should be smaller than the single shot RMS by a factor of $1/\sqrt{N}$ (where N is the number of accepted data points within a bin). This leads (for the bin sizes and return rates shown in Fig. 3) to an expected RMS for bin averaged calibration values of .2 and .4 cm for MTLRS-2 and MTLRS-1 respectively, in reasonable agreement with the data.

Another meaningful number characterizing the temporal stability of Laser ranging systems over time periods typical for LAGEOS passes is the mean pre- minus post-calibration value. Before and after each measurement the MTLR-Systems are calibrated as described in section 2. The difference between these calibration values is the pre- minus post-calibration value.

For all measurements made during the Matera collocation period the mean pre- minus post-calibration values were found to be .8 cm and 1.0 cm for MTLRS-1 and MTLRS-2 respectively. They are slightly larger than those found during the Matera stability tests. However, they are within the system specifications.

3.2 PMT Test

In Fig. 4 mean calibration values, single shot RMS and return rates are shown as a function of the voltage applied to the MTLRS-1 and MTLRS-2 photo multiplier tubes (PMT). The voltage was changed from 30 V below the nominal PMT voltage (which is -2000 V for MTLRS-1 and -1900 V for MTLRS-2) to 30 V above the nominal voltage in steps of 10 V. It was the intention of this test to estimate the influence of instabilities in the high voltage power supply on range measurements.

The calibration values of both systems decrease with decreasing PMT voltage. This is in accordance with our expectations because the transit times of primary and secondary electrons in the PMT should decrease with increasing potential differences inside the tube.

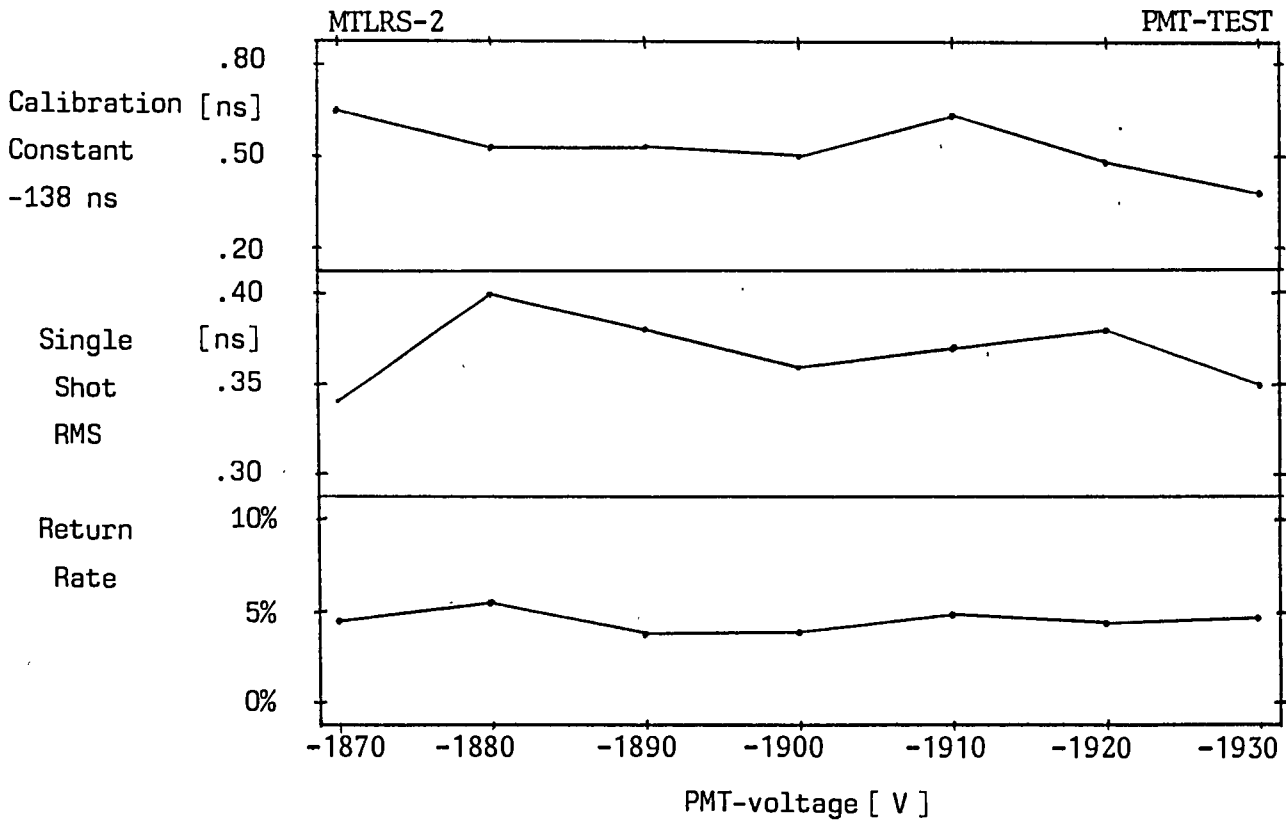
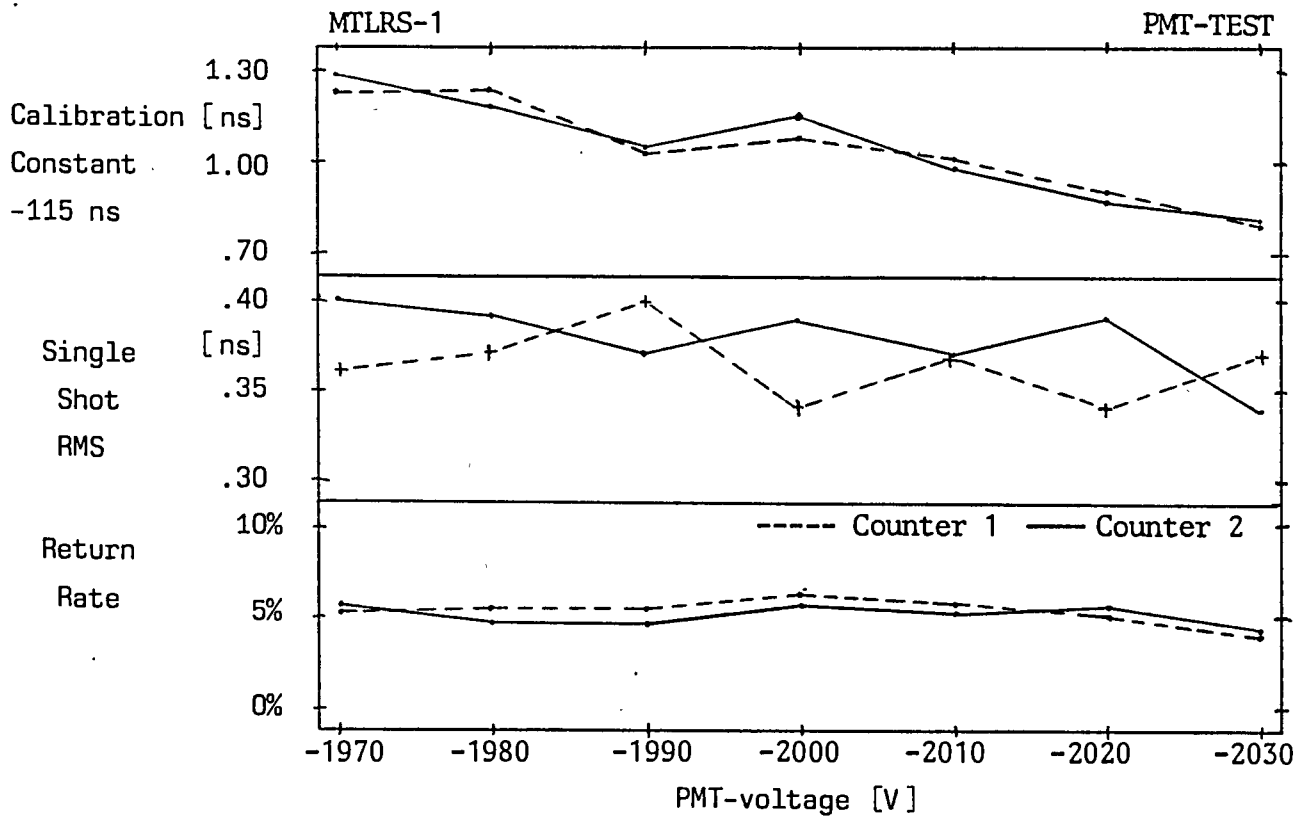


FIG 4 Influence of the PMT-voltage on the calibration constant. The nominal PMT-voltage is -2000 V for MTLRS-1 and -1900 V for MTLRS-2.

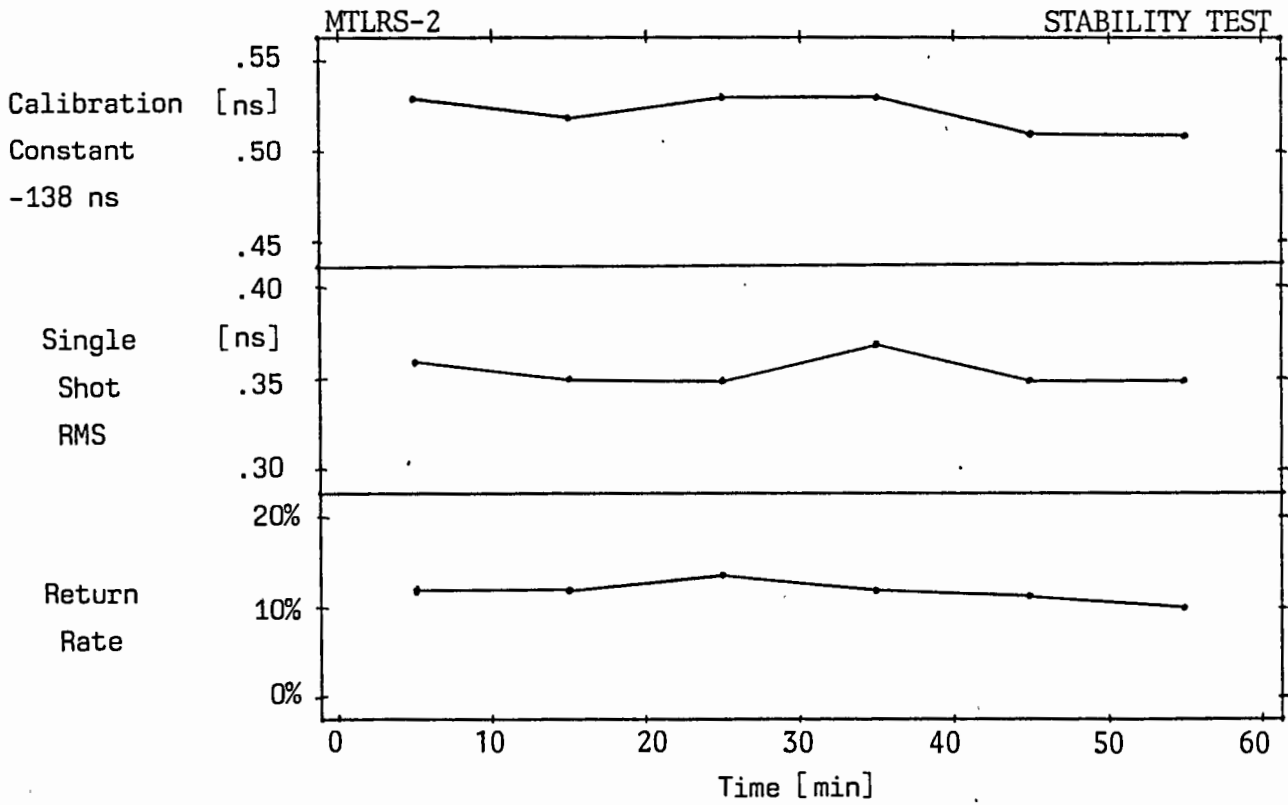
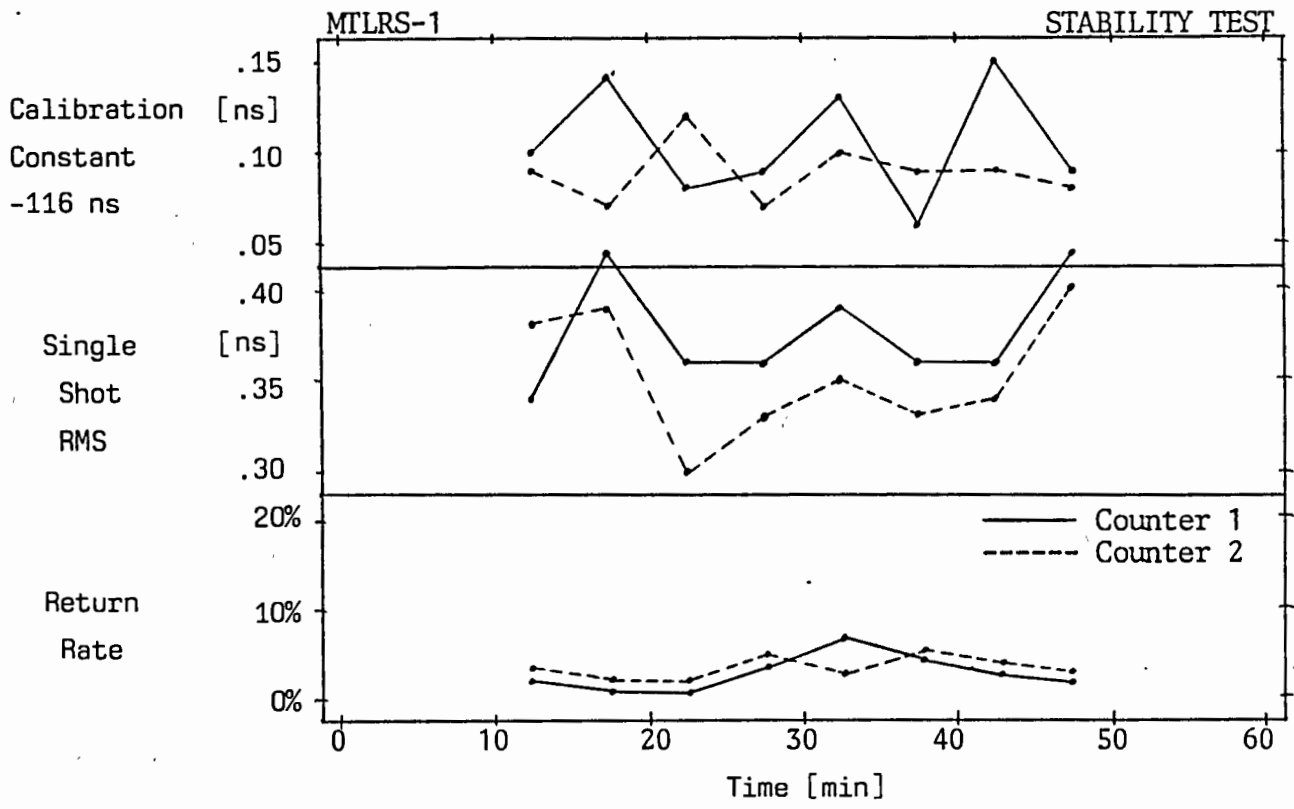


FIG 3 Calibration constant, single shot RMS, and return rate versus time. For MTLRS-1 5 min bins have been used. MTLRS-2 data were evaluated in 10 min bins.

The decrease of the calibration values with decreasing PMT voltage is not as smooth and steady (in particular for MTLRS-2) as might be expected. This can not be fully attributed to statistics. The main reason could be the uncertainty of the PMT voltage actually applied. It was adjusted in both systems with the adjustment knobs at the high voltage power supplies and not verified with a volt meter.

The calibration values changed by about .4 ns and .3 ns for MTLRS-1 and MTLRS-2 over 60 V. This corresponds to range differences of the order of 1 cm per 10 V deviation of the PMT voltage from its nominal value for both systems.

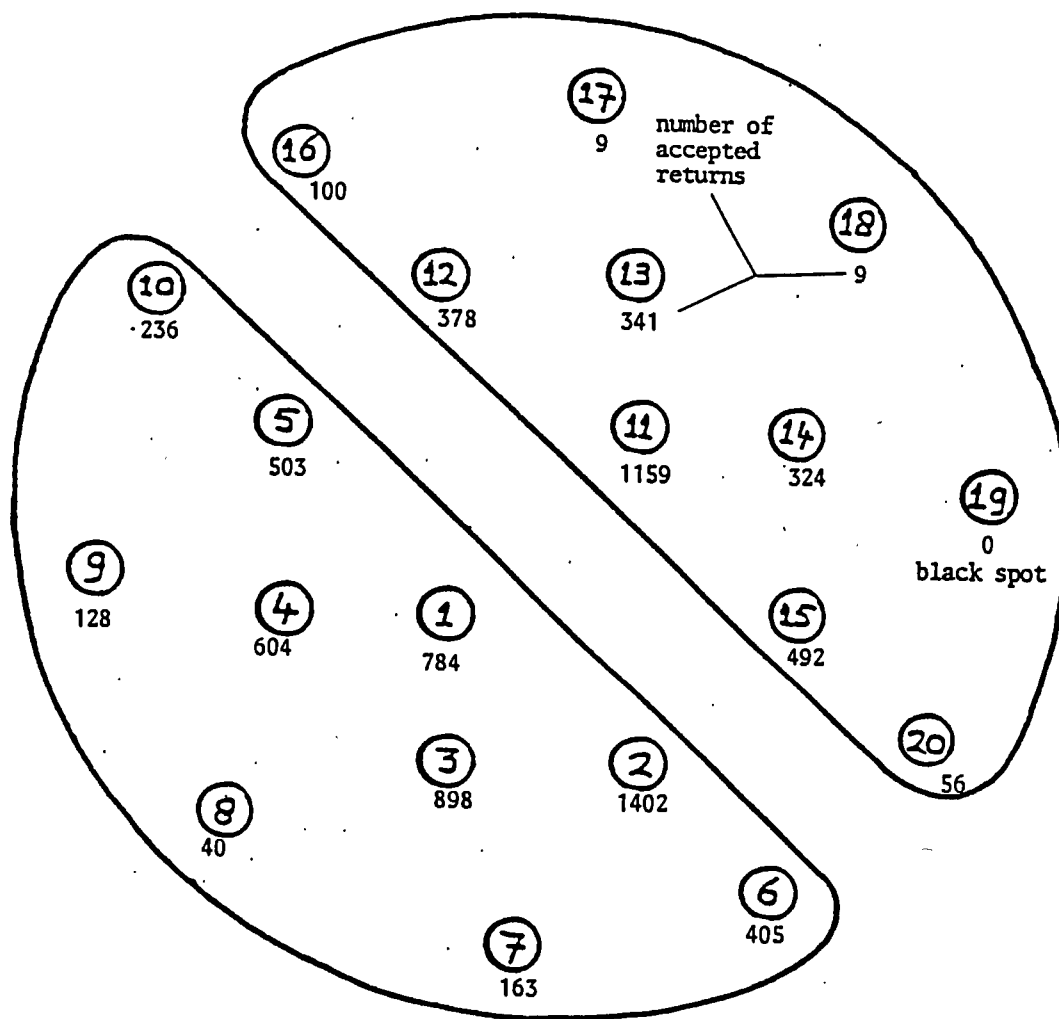


Fig. 5: Retroreflector positions in the MTLRS-2 beam during the Matera cube map test. The beam had a diameter of about 1.5 m at the target 1146 m from the system. The retroreflector positions are labeled with numbers between 1 and 20.

In order to estimate the influence of the PMT high voltage power supply on system stability we will investigate in the near future the temperature coefficient, switch on effects, and the long term stability of this device.

The single shot RMS values were not affected by the PMT voltage changes. For both systems the return rates during the PMT test were about 5%, indicating that MTLRS-1 was testing at about twice the light intensity used by MTLRS-2.

3.3 Cube Map Test

Wave front distortions originating very often from multi-mode laser operation can lead to biases which depend on the location of the target inside the transmitted laser beam. It is the purpose of the cube map test to detect these kind of biases.

MTLRS-2 tried a cube map test during the Matera collocation period. The test was originally planned to take place in two steps. The aim of the first step was to measure an intensity map of the beam. In a second step ranges as a function of the target location inside the beam should have been measured. Thereby it was foreseen to use the intensity information to compensate for intensity differences within the beam with the ND-filters.

The retroreflector used for the cube map test was at a distance of 1146 m from MTLRS-2. With maximum beam divergence the diameter of the beam at the target was about 1.5 m. In Fig. 5 the cross section of the beam at the target is shown schematically. The distribution of retroreflector positions inside the laser beam (seen towards MTLRS-2) is indicated. All positions are labeled by numbers between 1 and 20. The ranging time to one position was 2.5 minutes. Positions were changed by redirecting the mount. The number of accepted returns from each retroreflector position is also indicated in Fig. 5.

Mean times of flight, single shot RMS values, and total numbers of accepted returns are shown in Fig. 6 for the retroreflector positions indicated and labeled in Fig. 5. The sequence in which the data are presented was defined by the number of accepted returns contributing to a mean range.

Mean times of flight calculated for positions with more than 100 returns show an extremely smooth behaviour. All of them differ by less than 100 ps from each other, indicating no biases, eventhough the light intensity during these measurements varied by $1\frac{1}{2}$ orders of magnitude.

The deviations of the times of flight for positions with less than 100 returns are larger. The maximum deviation is 300 ps for position 20 with 56 returns. All these positions are located on the outer semi-circle of the right beam half in Fig. 5.

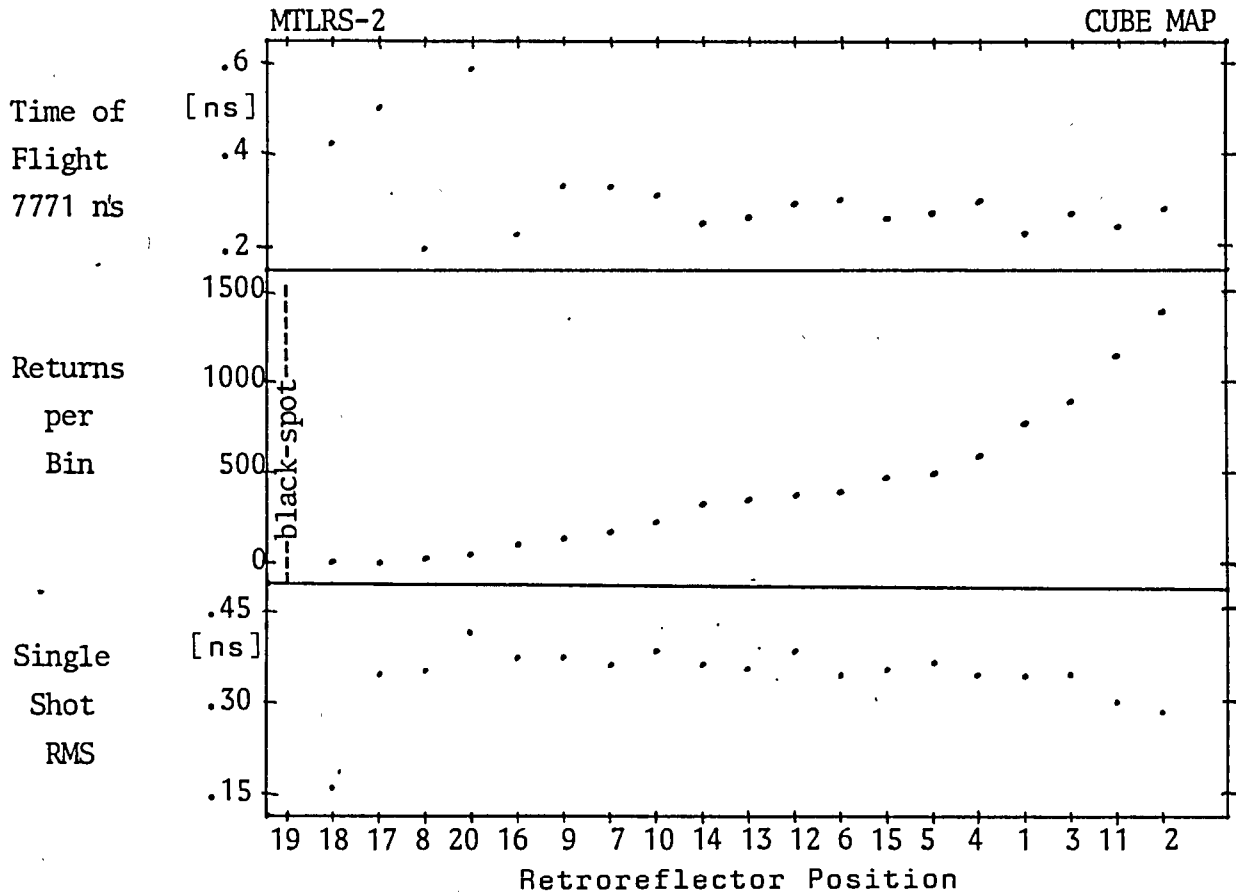


FIG 6 Range, single shot RMS, and number of returns measured during 2.5 min at the retroreflector positions marked and labeled in Fig. 5.

In order to verify whether there is or there is not a wave front distortion problem on the outer semi-circle, the second part of the test was planned, as described above. Unfortunately it was impossible to complete this step in Matera because of instrumental problems.

3.4 Mount Biases

Fig. 7 shows mean calibration values as a function of universal time which were measured by MTLRS-1 at the Goddard Optical Test Facility in June 1985. During the test which lasted for nearly 4 hours the mount was moved. Dots represent mean calibration values calculated from data within 51 sec bins. Vertical dashed lines separate intervals of different system states. System states are characterized by three parameters which are also indicated in Fig. 7: Azimuth and elevation of the telescope pointing direction and mean number of accepted calibration points per 51 sec bin. Horizontal dashed lines mark mean calibration values for each system state.

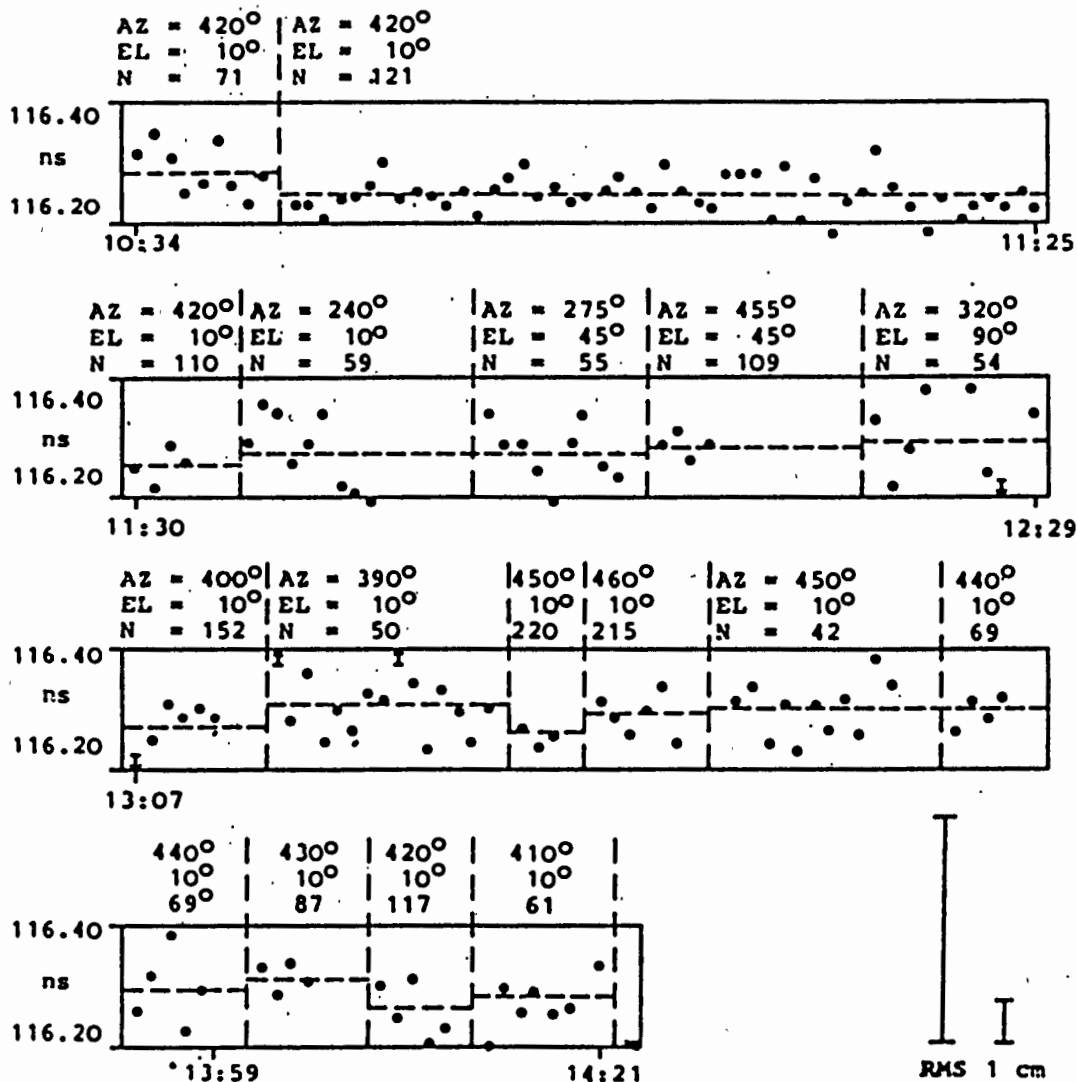


Fig. 7: MTLRS-1 calibration constants measured at GORF in June 1985. See text for details.

The test was done in three phases. In the first phase the telescope was in the normal calibration position and the system was runing for about one hour. In the second phase the mount was moved in a way that the retroreflector for internal calibration was either at the same position within the beam as during normal system calibration, or at the conjugate position which is reached after a 180° rotation of the reflector (see Fig. 2). Thereby the constraints discussed in section 2 were taken into account. In the third phase of the test one beam half (see Figs. 2 and 5) was scanned azimuthally by the retroreflector in steps of 10°.

The difference between the maximum and minimum mean calibration value for the system states shown in Fig. 7 is 70 ps corresponding to a range difference of 1 cm. This is in excellent agreement with the tests discussed in sections 3.1 and 3.3. No significant systematic variation could be found in the data which is associated with the mount pointing direction.

3.5 Signal Strength

MTLR-Systems up to now do not directly measure pulse heights of PMT signals. Therefore indirect means have to be applied to infer the intensity level of light pulses received in the detection package. A number related to the received light intensity is the return rate defined in section 3.1. For low light intensities it is directly proportional to the latter. For higher intensities its slope decreases and goes to zero at return rates of 1 for very high intensities.

Fig. 8 shows mean calibration values as a function of the return rate measured by MTLRS-1 in two different tests. The calibration values shown in the upper panel of the figure are the system state averages from Fig. 7. In the lower panel data from a signal strength test in Matera are presented. During this test the light intensity was varied with ND-filters. One data point corresponds to one ND-filter setting. The ranging time for these data points varied from 30 minutes for very low intensities to 3 minutes for high intensities. The data point on the left hand side represents 100 range measurements, the data point on the right 1600.

A careful analysis of both data sets shown in Fig. 8 could not reveal a stongly significant tendency. There is a weak indication for decreasing calibration values with increasing return rates. However, it must be less than 30 ps between 0% and 30% return rate, where MTLRS is normally operated.

Fig. 9 shows the results of the MTLRS-2 signal strength test in Matera. Mean calibration values are plotted as a function of the ND-filter setting attenuating the transmitted laser light by factors of 10^{-10} to $10^{-12.5}$. All mean calibration values are within less than 50 ps of each other for light intensity variations over 2½ orders of magnitude.

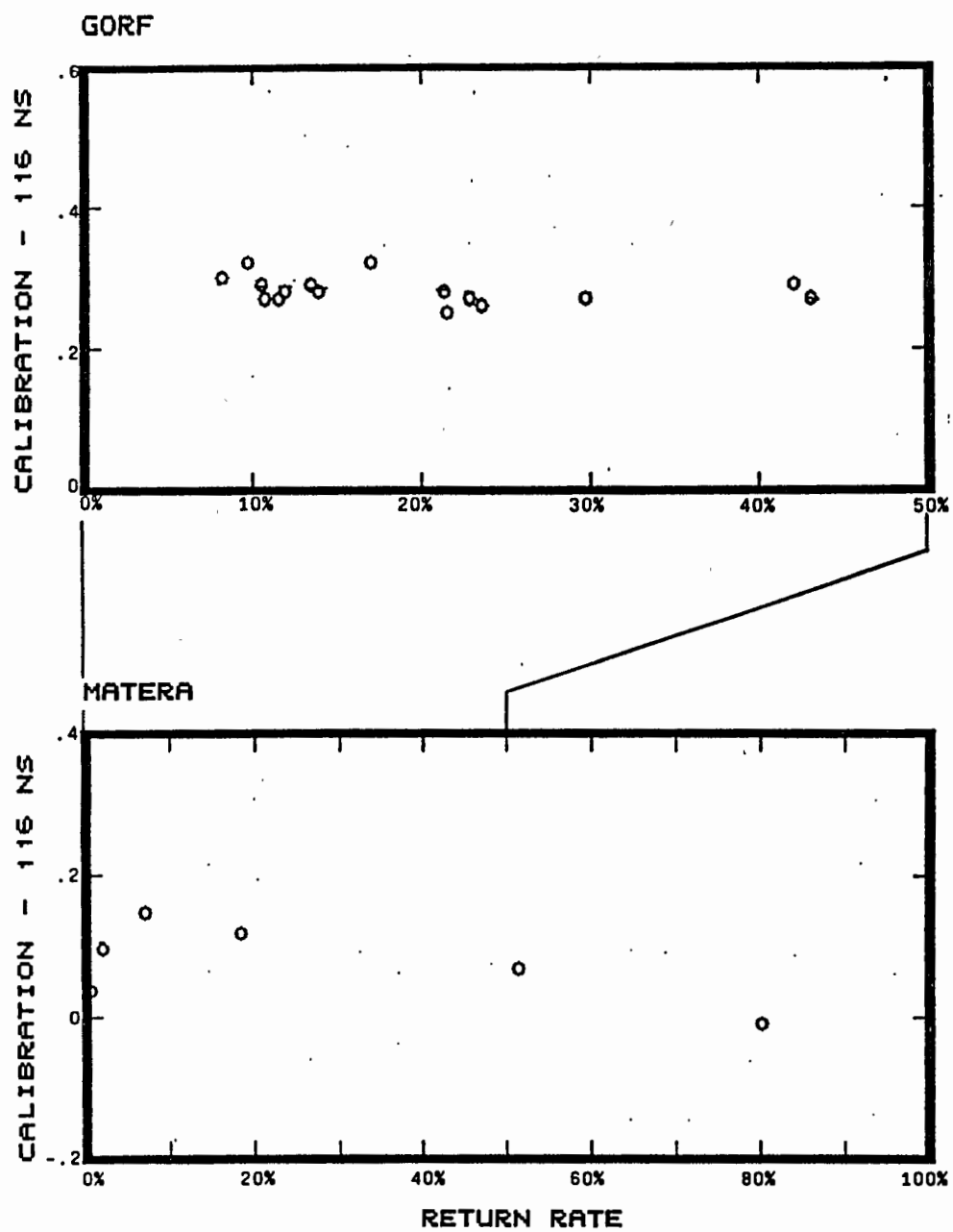


Fig. 8: Calibration constants for MTLRS-1 versus return rate.

MTLRS-2: SIGNAL STRENGTH TEST

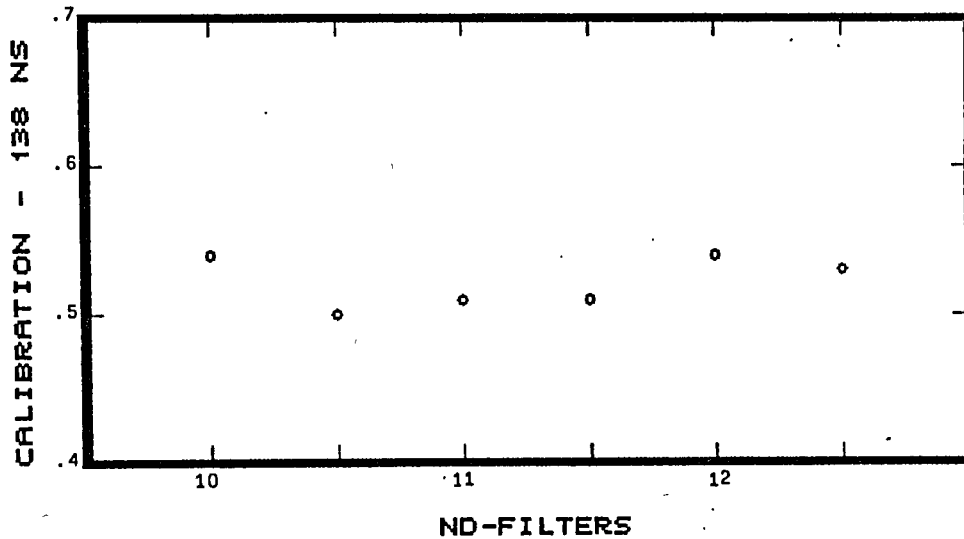


Fig. 9: Calibration constant for MTLRS-2 versus ND-filter setting.

4. Summary and Conclusions

Data from five different ground tests have been presented from at least one MTLR-System. Mean calibration RMS values were always found to be well below 1 cm which is in excellent agreement with the system specifications. No significant bias of the system could be identified.

During the Matera collocation the mean pre- minus post-calibration values for MTLRS-1 and MTLRS-2 were .8 and 1 cm, also within the system specifications but slightly above the RMS of the mean calibration values discussed in this paper. This probably could indicate that there are not yet identified noise sources either in the system hardware or in the operation procedures which can be eliminated. In order to do this we plan to continue and to complete the tests described here. We will try to clarify still open questions concerning for instance temperature effects, intensity dependent biases, wave front distortion, or PMT power supply stability.

Acknowledgements: We would like to thank L. Amberg, G. Blenski, W. Etling, U. Hessels, R. Motz, I. Nowak, N. Rodenburg, and D. Samson who spent many hours to discuss, to prepare and finally to do the described tests. Without their help this paper would not have been possible.

References

- 1 Wilson, P., and H. Visser, Development of the Modular Transportabel Laser Ranging System, Fifth International Workshop on Laser Ranging Instrumentation, Royal Greenwich Observatory, Herstmonceux, UK, Sept. 10 - 14, 1984

ZERO RANGE REALTIME CALIBRATION

J.D. Rayner, S.R. Bowman, C.O. Alley
Department of Physics and Astronomy
University of Maryland
College Park, MD 20742

Telephone (301) 454 34 05
Telex 908787

F.M. Yang
Shanghai Observatory Academia Sinica
Shanghai - China -

ABSTRACT

A real time feedback calibration system is described in which the range to a mirror mounted within .5mm of the elevation axis of the transmitting telescope is measured for each outgoing laser pulse.

In a general feedback calibration system a small portion of the outgoing laser pulse is fed back into the stop detector and its delay relative to the start pulse is measured by the timing electronics. One of the primary motivations for using feedback calibration is that some stations are unable to range to terrestrial calibration targets. There are, however, many other advantages to such a system. First it simplifies the ranging operations since the calibration is done automatically during the ranging session. Secondly, it eliminates the need for a surveyed calibration target, which is particularly advantageous in the case of mobile stations. Also, as we begin to talk of millimeter accuracies survey errors and target stability will become greater problems introducing errors at the centimeter level. At the millimeter level correcting for atmospheric delays in the calibration path which is close to ground and subject to temperature gradients and other local effects will also introduce errors.

In going from an external calibration target to an internal feedback calibration path you trade the surveying problem for one of measuring internal telescope delays. While trying to solve this problem we were reminded of a technique reported by John Degnan (1) at the last Workshop. Tom Zagwodzki and his coworkers installed an open corner with its vertex on the elevation axis of the telescope, to return some of the outgoing laser pulse to the receiving photomultiplier where it was used to start the timing electronics. This is a very elegant solution to the calibration problem since the ranging calibration is now zero. Unfortunately this scheme did not work as well in practice as it did in theory and was, at least temporarily, dropped by the Goddard group. This technique is not directly applicable at the single photoelectron level, since we would have to run the start pulse at the multi-photoelectron level in order to get a reliable start for each shot. The start and stop energies would then be different introducing a energy dependent calibration shift. By using a separate start detector optimized for fast response and low jitter we can remove start jitter from the system error budget. At the present time we are using a bulk GaAs Austin switch with a 20ps rise time as our start detector. It monitors the output of the laser oscillator and thus should provide a start pulse which is independent of laser energy. Since the start and stop channels are independent we must measure the the difference in their delays which we accomplish by timing the return from a small mirror placed at the elevation axis of the telescope. This gives us all the the advantages of a feedback calibration and some additional advantages specific to the zero range configuration of the feedback path. Since the feedback path exactly measures the delay to the reference point for the telescope there is no need for a separate measurement of the internal telescope delay. In fact, any angle dependent telescope delays will automatically be mapped out in the course of ranging, since the telescope delay is measured for each shot. In short, this system automatically measures virtually all calibration corrections without operator intervention.

There are several requirements imposed by the implementation of such a system. The most fundamental requirement is that the same telescope be used as transmitter and receiver, with the transmitted beam filling the telescope aperture. Next, there must be an attenuated path through the transmit/receive switch to allow a small portion of the feedback laser pulse to hit the stop detector. In addition the detector must be immune to the electrical noise associated with the laser firing. Finally, the timing electronics must be able to measure the very short calibration delay and still be able to measure the full range.

Since there is a good fit between these requirements and our system it was easy for us to implement a zero range calibration system. I will describe those features of our system which affect the feedback calibration. We have mounted a small mirror on a micrometer translation stage attached to the side of the telescope tube. By adjusting the micrometer the front surface of the mirror can be made to coincide with the elevation axis of the telescope. This can be checked by moving the telescope in elevation while viewing the mirror through a small telescope. Then if a point on the surface of the mirror seems to remain fixed it is on the elevation axis. Using this technique we were able to position the mirror to within .5 mm of the elevation axis. We use a passive polarization sensitive transmit/receive switch(2). This means that there is a feedback path from the telescope to the detector at all times. The detector is blocked when the laser fires by a rotating vane. We have modified this vane by cutting a hole in it which is then blocked by a ND 13 filter which attenuates the feedback laser pulse to the singles level. The detector is a solid state Geiger mode diode(3) which puts out a five volt pulse for a single photon input and thus is virtually immune to the electrical noise from the laser firing. Finally, for timing we use a four stop event timer with the start pulse being measured by the first stop and the calibration pulse measured by the second stop. This is one weakness of the system since the offset between the first and second stops of the event timer must be separately calibrated. For the present this calibration is limited to an accuracy of about 50 ps.

We have just started working with this system and there will undoubtedly be changes, particularly in the area of event timer calibration. Our preliminary studies suggest that this should be a viable method for automatically calibrating ranging systems at the millimeter level.

REFERENCES

1. T. W. Zagwodski, J. F. McGarry, J. J. Degnan, R.S. Chabot, J. G. Lessner, and J. B. Abshire, "Experimental Large Aperture Satellite Laser Ranging System", Proceedings of the Fifth International Workshop on Laser Ranging Instrumentation, pg.178.

2. S. R. Bowman et al , "Analysis and Performance of a Passive Polarization Telescope Coupling Switch for Lunar Laser Ranging", these Proceedings.
3. S. R. Bowman et al, "The Use of Geiger Avalanche Photodiodes for Precise Laser Ranging at Very Low Light Levels; An Experimental Evaluation", these Proceedings.

SYSTEM STABILITY USING MODE LOCKED TRAIN

K. Hamal, I. Prochazka
Czech Technical University
Faculty of Nuclear Science and Physical Eng.
Brehova 7, 115 19 Prague - Czechoslovakia -

Telephone 848840
TWX 121254 FJFI C

ABSTRACT

The calibration procedure of the INTERKOSMOS satellite laser ranging station is described. Several system configurations and calibration setups were tested within 1984 to 1986. The satellite ranging and calibration echo signal strength in single PE only. The receiver detector is the main contributor to the system jitter and stability. The jitter and stability performance of the dynode PMT and silicon photodiode HP S5 operating in Geiger mode were compared. Replacing the PMT by the HP S5 photodiode, the ranging jitter dropped from 300 psec down to 100 psec rms and the (pre-post) calibration differences spread dropped from 110 psec down to 26 psec.

System configuration, station Helvan	CALIBRATION CONFIGURATIONS TESTED
<p>LASER Nd YAG+2HG, mode locked by ML51 dye train of 2-3 pulses, FWHM 30psec</p> <p>START - PD+tunnel diode switch by M.Cech /1985/ - optical threshold switch /1986/</p> <p>COUNTER - HPS368 /1983-1985/ - HPS3708 /1986/</p> <p>DETECTOR - dynode stage PMT RCA31834A, +15°C, spot diam. 2mm + two HP 120MHz amplifiers</p> <p>DISCRIMINATOR c.f. type, ORTEC 934A</p> <p>SIGNAL STRENGTH single PE echoes only guaranteed by low (echo/lasing) ratio for both calibration and satellite ranging</p>	<p>TARGETS :</p> <p>INTERNAL - pass composed of flat Ag mirrors+diff. screen</p> <p>EXTERNAL 100 METERS OR 500 METERS - corner cube - diffuse flat - mirror flat</p> <p>* The 100 meters target perpendicularity was maintained within 1 milliradian</p> <p>LASER OUTPUT BEAM DIVERGENCE</p> <ul style="list-style-type: none"> - minimal/collimated beam (30 arcsec) - standard for satellite ranging (1-2arcmin) - focus on the external target <p>* In each configuration at least 10 series of calibration runs, 200 echoes each, were completed</p> <p>* The best results were obtained for configuration : BEAM FOCUSSED ON EXTERNAL 100m DIFFUSE TARGET</p>

K. Hanal, I. Prochazka
System stability using mode locked train

1

K. Hanal, I. Prochazka
System stability using mode locked train

2

PRE-POS CALIBRATION DIFFERENCE, SYSTEM STABILITY	SYSTEM STABILITY / SUMMARY																																																
<p>DETECTOR USED - HPSS Silicon photodiode in Geiger mode</p> <p>CALIBRATIONS - 200 single PE echoes each - 10 to 50 minutes between consequent runs</p> <p>SINGLE SHOT 80 - 140 psec RMS</p> <table border="1" style="margin-left: auto; margin-right: auto;"> <tr> <td>PRE-POST CALIBRATION</td> <td>MEAN</td> <td>-2 psec</td> </tr> <tr> <td></td> <td>SIGMA</td> <td>26 psec</td> </tr> </table>	PRE-POST CALIBRATION	MEAN	-2 psec		SIGMA	26 psec	<table border="1"> <thead> <tr> <th>JITTER BUDGET (psec)</th> <th>1983-85</th> <th>1986</th> </tr> </thead> <tbody> <tr> <td>Laser pulse FWHM</td> <td>30</td> <td>30</td> </tr> <tr> <td>Ranging counter HPS368</td> <td>) 100</td> <td></td> </tr> <tr> <td>HPS3708</td> <td></td> <td>35</td> </tr> <tr> <td>Start detector/discriminator</td> <td>) 150</td> <td>30</td> </tr> <tr> <td>PMT /dynode/ RCA31834A</td> <td>298</td> <td>298</td> </tr> <tr> <td>Diode /HPSS in Geiger mode/</td> <td></td> <td>98</td> </tr> <tr> <td colspan="3">RESULTING (psec)</td> </tr> <tr> <td>(PMT)</td> <td>520</td> <td>300</td> </tr> <tr> <td>(Diode)</td> <td></td> <td>100</td> </tr> <tr> <td colspan="3">SYSTEM STABILITY (psec)</td> </tr> <tr> <td></td> <td>1983-85</td> <td>1986</td> </tr> <tr> <td>PMT (dynode) based receiver</td> <td>150</td> <td>118</td> </tr> <tr> <td>Diode based receiver</td> <td></td> <td>26</td> </tr> </tbody> </table>	JITTER BUDGET (psec)	1983-85	1986	Laser pulse FWHM	30	30	Ranging counter HPS368) 100		HPS3708		35	Start detector/discriminator) 150	30	PMT /dynode/ RCA31834A	298	298	Diode /HPSS in Geiger mode/		98	RESULTING (psec)			(PMT)	520	300	(Diode)		100	SYSTEM STABILITY (psec)				1983-85	1986	PMT (dynode) based receiver	150	118	Diode based receiver		26
PRE-POST CALIBRATION	MEAN	-2 psec																																															
	SIGMA	26 psec																																															
JITTER BUDGET (psec)	1983-85	1986																																															
Laser pulse FWHM	30	30																																															
Ranging counter HPS368) 100																																																
HPS3708		35																																															
Start detector/discriminator) 150	30																																															
PMT /dynode/ RCA31834A	298	298																																															
Diode /HPSS in Geiger mode/		98																																															
RESULTING (psec)																																																	
(PMT)	520	300																																															
(Diode)		100																																															
SYSTEM STABILITY (psec)																																																	
	1983-85	1986																																															
PMT (dynode) based receiver	150	118																																															
Diode based receiver		26																																															

K. Hanal, I. Prochazka
System stability using mode locked train

3

K. Hanal, I. Prochazka
System stability using mode locked train

4

SATELLITE LASER RANGING ERRORS

L. Jiyu
Wuhan Technical University of
Surveying and Mapping
23 LO-Yu Road, Wuhan
The People's Republic of China

ABSTRACT

Satellite laser ranging systems are used effectively to determine earthcrustal dynamic parameters. The accuracy and reliability of SLR products are of extraordinary importance for an appearance of new scientific information. This paper has discussed all potential SLR errors and their magnitude, and given some recommendations for decrease, such as how to take meteorological data, how to approximate optimal calibration, how to control transit time jitter.

Satellite Laser Ranging Errors

by Liu Jiuyu

Wuhan Technical University of Surveying and Mapping
23 Loyal Road, Wuhan, The People's Republic of China

ABSTRACT: Satellite laser ranging systems are used effectively to determine earthcrustal dynamic parameters. The accuracy and reliability of SLR products are of extraordinary importance for an appearance of new scientific information. This paper has discussed all potential SLR errors and their magnitude, and given some recommendations for decrease, such as how to take meteorological data, how to approximate optimal calibration, how to control transit time jitter.

ZUSAMMENFASSUNG: Um dynamische Parameter der Erdkruste zu messen, werden die Laserentfernungsmeßsysteme zu künstlichen Satelliten benutzt. Die Genauigkeit und Zuverlässigkeit der Ergebnisse der Laserentfernungsmessung besitzt außerordentliche Wichtigkeit für neue wissenschaftliche Erkenntnisse. Der Artikel hat alle potentiellen Fehler der Laserentfernungsmessung und ihren Größen diskutiert und zeigt einige Vorschläge, z. B. wie bessere meteorologische Daten zu gewinnen sind, wie ein optimale Kalibration durchzuführen ist und wie der Jitter zu verbessern ist.

Fixed and highly mobile satellite laser ranging systems, which located at 40 stations distributed in 19 countries, have been ranging to satellites for the Crustal Dynamics Research Program (acronym CDRP), Part of NASA's Geodynamics Program. In order to execute the CDRP a lot of fund have to be expended, for example, expending approximately \$ 2.8 million in FY 1986 [Edelson, 1985]. The accuracy and reliability of the products are of extraordinary importance for being able to provide valuable and exciting new scientific information on geodynamics. On the basis of unstable ranging products would scientists be able to make the reliable conclusions which, for example, will indicate that the rates of motion of the larger

tectonic plates are within 1 cm/yr? Therefore, it is very necessary to find out all potential source of SLR errors and to search out some methods for eliminating, at least decreasing them.

There have been some effective efforts to improve SLR accuracies, such as making use of pulsewidths as short as 30 picoseconds, micro-channel plate photomultipliers, zero-delay configuration and two-color laser. When a greater improvement is expected for SLR accuracies it will be very useful to systematically investigate all potential errors for SLR. This paper will try to achieve this purpose.

1. SLR Error Expression

It is known that a distance between a ground station and the satellite specially equipped with retroreflectors (laser satellite), D measured by SLR systems can be written as

$$D = \frac{C_0}{2n} \frac{N}{f} + d_0 \quad (1)$$

Where, C_0 = velocity of light in a vacuum;

n = effective refractive index on the laser pulse path;

N = number of a timing clock pulses recorded by a time interval unit (TIU);

f = clock frequency of the TIU;

d_0 = additional constant, including two portions: one is an equivalent length caused by a difference between the electro-optical centre and the mechanical centre of the SLR system, being simplified into system constant; another is a correction resulting from that the effective reflecting points of retroreflectors have to be reduced to the center -of- mass of the laser satellite, equaling 25.8 cm for LAGEOS, 7.5 cm for STARLETTE.

From the above distance equation the following error expression for SLR has been derived [Liu, 1985]:

$$M_D^2 = \left[\left(\frac{M_{C_0}}{C_0} \right)^2 + \left(\frac{M_n}{n} \right)^2 + \left(\frac{M_f}{f} \right)^2 + \left(\frac{M_N}{N} \right)^2 \right] \cdot D^2 + M_{d_0}^2 \quad (2)$$

Where, M = errors whose subscripts depend on the foregoing respective marks.

On the basis of the above expression we shall discuss all errors emerging from SLR as detailing as possible and give some recommendations for decreasing them.

2. Index Error, M_n

The Marini and Murray (MM) formula has been used to calculate atmospheric refraction corrections for SLR [Sylvania, 1974, Bufton, 1978, Tapley, et al, 1982]. The MM formula based on that of atmospheric refractive index in consideration of an elevation angle, site latitude and site altitude [Marini and Murray, 1973]. The surface level measurements of atmospheric pressure, temperature and relative humidity are required when using the MM formula [Bufton, 1978]. However, to the best of writer's knowledge some operators for SLR systems have taken the meteorological data only at one surface point near the earth surface. The height of the point is often lower than that of a transmitted and received telescope of SLR system, achieving several meters lower at the fixed station. How can these readings represent the meteorological data along the laser pulse path in an atmospheric layer? On the other hand, they have always taken one time for the meteorological data while observing one satellite pass, and reading in only ranging start. In general one satellite pass has to last in several decade minutes for LAGEOS. In such long time interval the meteorological data can not keep to the same values at all. When using the same data to calculate the overall refraction corrections, how can the ranging products escape the error effect due to not matching meteorological data? In this case there is a natural difference between the start and end ranging products of one satellite pass due to the only incoordinate refraction correction.

It was pointed out that atmospheric refraction corrections have achieved accuracies within a few cm at 20° elevation when only taking the meteorological data at the ranging site [Abshire and Gardner, 1984]. If taking in consideration of the above two man-made errors the correction accuracies have to be reduced again. When refractive indices calculated contain the error of $\pm 2 \times 10^{-8}$ the

distance error, M_{Dn} will achieve ± 2.4 cm for the atmospheric layer of 1200 km. If the difference between the temperatures is equal to only $\pm 0.5^\circ$ C the distance error will achieve ± 0.53 mm/km for a ground laser ranging under the condition of $P = 760$ mmHg, $-20 \leq t \leq +40^\circ$ C. In order to escape the man-made errors the following recommendations appear as being useful:

- the meteorological instruments have to be settled at least as high as the transmitted and received telescopes of SLR systems;
- the meteorological readings for each satellite pass should be made with a few times, for example, taking them in the start, mid and end of each satellite pass. We, of course, would better make use of an interpolation of the meteorological data at the weather stations of the region near a ranging station;
- the psychrometer and barometer have to be checked to send them to a meteorological bureau for a few times per year. For example, when the drift of the zero point of a barometer equals within only ± 2 mmHg the distance error due to this will achieve ± 0.76 mm/km for a ground laser ranging.

Applications of two-color laser ranging technique can omit not only the exact measurements of the meteorological data, but also improve the accuracy to one order of magnitude for measured distances [Liu, 1984]. When making use of the two-color technique for SLR we must not consider atmospheric refraction corrections. In recent years a few scholars have been investigating two-color laser applications in SLR systems and getting desirous progress [Abshire and Gardner, 1984, Mastrocinque, 1985]. However, pulsed two-color SLR systems require some advanced equipments, such as mode-locked multiple frequency lasers, streak camera receivers and atmospheric delay measurements with an accuracy of 0.5 cm or better. This restricts its wide applications at once.

It must be pointed out that the path curvature correction is less than 1 cm when the zenith angles do not exceed only 70 degrees. If the zenith angles are greater than ones, the path curvature corrections have to be taken into consideration. For example, when the zenith angle is equal to 74 degrees it is greater than 1.5 cm [see Fig. 1, Sylvania., 1974]. To neglect the 1.5 cm correction is equivalent to introduce the same as error.

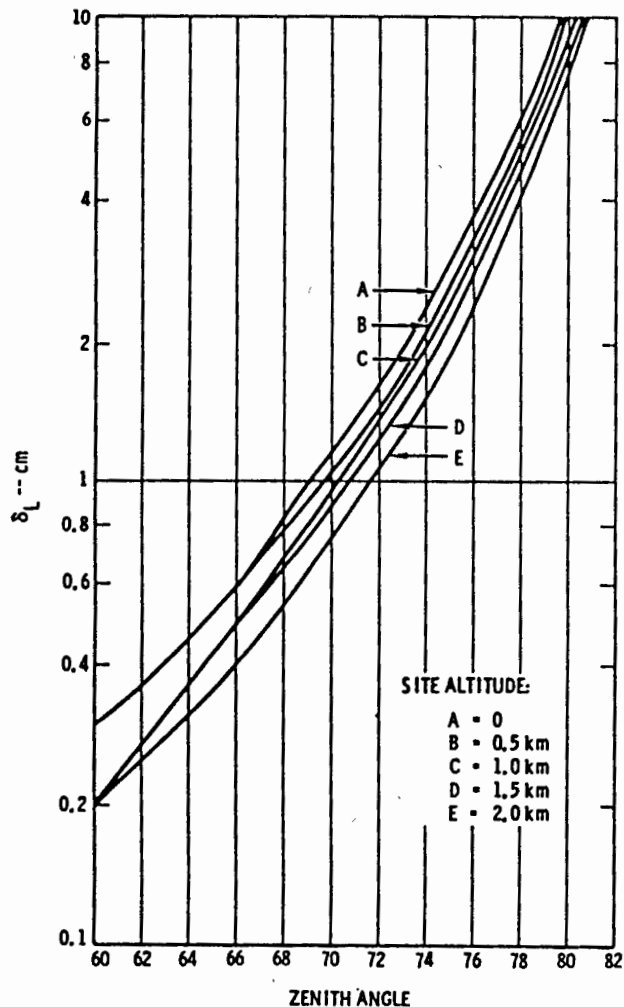


Figure 1 = Path Curvature Correction, from Sylvania

3. Velocity Error, M_{co}

The velocity of light, in a vacuum used for calculation of the foregoing distance, D was obtained by means of measurements at a field or laboratory, beginning at the year of 1676 by Roemer. The recently precise value (299792458 m/s) was also measured to make use of the laser metrology. The latter can only provide an accurate measurement, but not escape any error to influence the velocity value of light in a vacuum. It is known that there is an error for measurements all the time, but it will be different to have its size. Therefore, the following velocity value of light in a vacuum proposed by IUGG in August 1975 is very right:

$$C_0 = 299792458 \pm 1.2 \text{ m/s}$$

It is very necessary that the error of ± 1.2 m/s will be considered for laser ranging far off several thousand kilometers, even far off about 380 thousand kilometers, that is

$$\frac{M_{co}}{C_0} = \pm 4 \times 10^{-9}$$

For example, when only taking the elevation angles from 70° to 15° for LAGEOS the correspondent distances are equal to 6000 km to 9000 km. In this case, even if assuming all other sources of error are zero, the distance error, M_{DCo} produced only by the velocity error, ± 1.2 m/sec will achieve ± 2.4 cm to ± 3.6 cm. If the measured error of the velocity of light in a vacuum were to be decreased from ± 1.2 m/sec to at least ± 0.12 m/sec, the M_{DCo} would be able to be neglected. Except this the only velocity error, M_{DCo} makes the real accuracy can not achieve ± 1 cm for SLR. If we do not employ $C_0 = 299792458 \pm 1.2$ m/sec, but other values for the velocity of light in a vacuum, such as $C_0 = 299792.5 \pm 0.4$ km/sec, the velocity error will be much greater than that. This is very worthy to be considered.

4. Frequency Error, M_f

On the basis of the analyses to materials desirable discriminators have to match with an ideal time interval unit. For example, under the condition of using a constant fraction discriminator (CFD) the measurement accuracy for flight time depends essentially on the TIU. If an advanced event timer is used to measure the flight time, t_d the following expression can be given:

$$t_d = N_0 T_0 + t_1 - t_2 \tag{3}$$

Where, N_0 = number of period of the clock pulse train;

T_0 = period of the clock pulse train;

t_1 = front part for the time interpolation;

t_2 = additive part for the time interpolation.

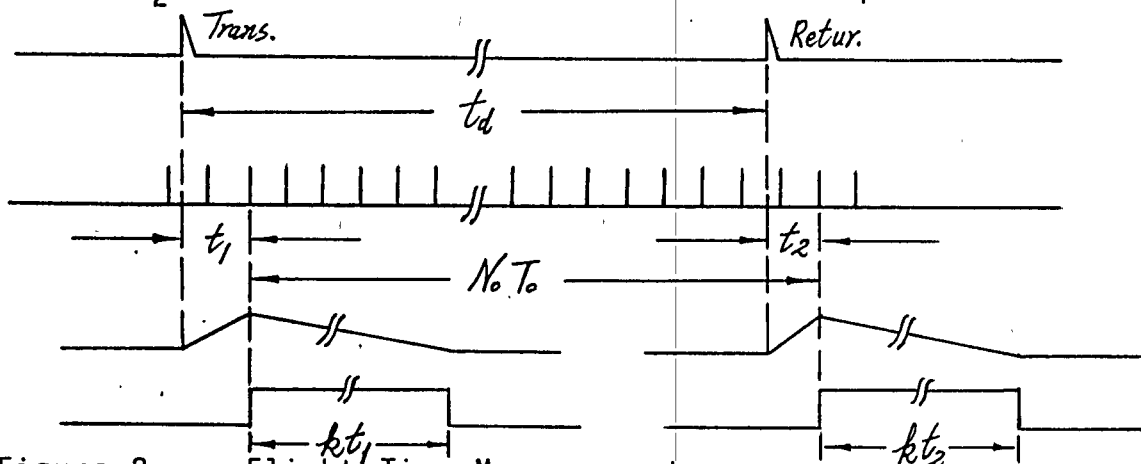


Figure 2 = Flight Time Measurement

When we select $T_o/T_r = k$, where T_r is the desired timing resolution, the following widths of the interpolating pulses are measured:

$$kt_1 = N_1 T_o, \quad kt_2 = N_2 T_o$$

Therefore, the flight time can be written as

$$\begin{aligned} t_d &= (N_o + \frac{N_1}{k} - \frac{N_2}{k}) T_o \\ &= (kN_o + N_1 - N_2) \frac{1}{kf} \end{aligned} \quad (4)$$

Where, f = clock frequency of the event timer;

k = stretching coefficient of the event timer;

N_1 = period number of the clock pulse for the front part;

N_2 = period number of the clock pulse for the additive part.

From the above equation the following error expression for the measured flight time can be acquired:

$$M_{td} = \pm (kN_o + N_1 - N_2) \frac{M_f}{kf^2} = \pm \frac{M_f}{f} t_d \quad (5a)$$

or written as

$$M_{Df} = \pm \frac{M_f}{f} D \quad (5b)$$

If $M_f/f < \pm 1 \times 10^{-9}$, the distance error, M_{Df} which varies as the measured distances to the satellite is not greater than ± 1 cm for the foregoing distance range.

5. Period Error, M_N

The period error consists of a resolution error, pulsewidth error, wavefront error, fluctuation error and timing error. If the resolution of the event timer is equal to 66.7 psec, its equivalent distance resolution will equal 1 cm. In this case the SLR system can only measure the distances for how many times of 1 cm, but not the distance portions within 1 cm. The time interval unit used by SAO

has a resolution of 0.1 nsec [1.5 cm, Pearlman, 1983]. The lower the distance resolution is, the greater the resolution error gets. In a word the resolution error is produced by the timer resolution which cannot be enough small.

The pulsewidth error results from that the energy of a laser pulse is not centralizing in a moment, but distributing in a shorter interval. For example, the pulse of 5 to 7 joules generated by the ruby laser system has the FWHM of 25 nsec for early SAO SLR system [Pearlman, et al, 1978]. Nd:YAG lasers with modelockers can generate light pulses as short as 30 psec [Puell, 1982, Degnan, 1985]. When the laser pulses impinge on a photocathode the conversion from a light pulse to an electronic pulse has to be distorted due to some disturbance. The pulsewidth error, M_W is of a random ranging one which varies as the laser pulse width and the number of received photoelectrons [Degnan, 1985]. It can be written as

$$M_W = \frac{k_p \tau_p}{\sqrt{N_r}} \tag{6}$$

Where, τ_p = FWHM of a laser pulse;

N_r = number of received photoelectrons;

k_p = coefficient depending on different detection.

An external pulse slicer, which consists of a Pockels cell and is situated between crossed polarizers, was used early in order to constrict the laser pulse width from 20 nsec to about 4.5 nsec [Degnan, 1985]. Due to its lower efficiency the cavity dumped Nd:YAG laser was substituted for it rapidly. At present modelocked Nd:YAG lasers are mostly used to obtain a shorter and single mode laser. It has been seen from the ranging results that the accuracies increased to at least 50 % after the pulse width was reduced from 25 nsec to 6 nsec by means of a pulse chopper in the SAO SLR systems [Tapley, et al, 1982].

The wavefront error is caused by the wavefront distortion of a transmitted and returned laser beam. It is known that individual radiation modes which are possessed of different spatial and temporal property, build up at their own rates in Q-switched lasers. When they appear out of the laser cavity these different spatial modes

will have different far field patterns. The latter is defined as the wavefront distortion of the transmitted beam. When the distorted wavefront beam is used to measure the distances to a laser satellite the satellite-borne individual retroreflectors will catch different wavefronts. The returned signal received by SLR systems is an ensemble of reflections from all those retroreflectors facing in the general direction of the ranging station. When the distortion returned signal is used to stop the operation of TIU this will have to produce a ranging error, so - called wavefront error. The latter measured by SAO has shown peak to peak change of 4,5 cm to 7.0 cm [Pearlman, 1983].

At present modelocked Nd:YAG or Nd:YAP lasers are used in the most modern SLR systems. The lasers operate in the fundamental TEM₀₀ mode. The latter produces the smallest beam divergence, the highest power density, and, hence, the highest brightness. Furthermore, the radial intensity profile is uniform and uniphase [Koechner, 1976]. This makes the laser beam transmitted by modelocked Nd:YAG lasers does not exhibit the wavefront distortion. The experiment data on the ground baseline have also demonstrated that the performance of modelocked lasers is far superior to that of other laser types [Degnan and Zagwodzki, 1982].

The fluctuation error is produced by the strength fluctuation of a returned laser pulse from the satellite-borne retroreflectors far off several thousand kilometers. The strength fluctuation makes the output signals from PMT become ones with a randomly varying amplitude. When the latter drives a discriminator, such as fixed threshold, rise time compensated and hybrids one, the varying signal amplitudes will produce time biases on the order of half the input pulse width. Even if using a constant fraction discriminator with a compensation circuitry for the varying signal amplitudes the strength fluctuation can not be compensated wholly due to the rapidly varying atmospheric. It will be seen from the experimental data that when changing input pulse amplitudes from 0.1 voltages to 4 voltages the time walk due to this will be equal to + 3 cm to -2 cm for ORTEC 934 CFD currently used in the NASA MOBLAS network [Degnan, et al, 1984]. The analogous experiment by SAO indicated that the average fluctuation error has achieved $\pm 2,2$ cm, the maximum ± 4.5 cm [Pearlman, 1983].

According to the experience of McDonald Observatory there will not be any significant signal strength effect to the calibration and satellite data when the SLR system operates indeed in the single photoelectron domain. However, it is necessary to monitor hard the operation. When there are significant multi-photoelectron events this will result in a high dynamic range in the returned signal strength [Ricklefs, et al, 1985].

Currently single-stop TIU's are used in almost all operatin SLR systems to measure the flight time. When an incoming noise exceeds the stop discriminator threshold it will be easy to produce pseudo-measurements for this sort of TIU. The timing error does not imply the pseudo-measurements at all, but the effects from the TIU own proterty which can not be as good as possible. It consists of an interpolated and triggered error. In order to measure precisely the flight time an interpolation counts are used in TIU (see Fig.2). For example, the interpolated error results fròm that the stretching coefficient, k has not been calibrated to the nominal value. When the stretching coefficient offset incompatible with the nominal value achieves ± 0.5 the interpolated error is equal to 67 psec. The interpolated error resulting from a nonlinear spreading to the smaller components, $t_1 t_2$ can achieve ± 60 psec for 15 MHz event timer [Guan, et al, 1982]. The interpolated error for HP 5360 A Time Interval Counter is ± 1 nsec from 0° C to 50° C [HP, 1975].

The triggered error of TIU includes both an input trigger circuit error and error due to noise on input signal. It is known that the start and stop input signals are typically DC-coupled in TIU used by SLR systems. Any noise can superimpose on the baseline of the start or stop signals. This has to result in the triggered error. Therefore the advanced HP 5370A TIC with a 20 psec time resolution can only achieve the time measuring accuracy of 100 psec [Deghan, 1985].

6. Constant Error, M_{do}

The constant error contains a transit error, calibration error, sync error and satellite error. The transit error results from the transit time jitter for the photoelectrons from the photocathode to the anode in PMT. The transit time jitter is produced essentially by the following factors:

- the fluctuation of the photocurrent transmitted by the photocathode due to a strong scintillation of the returned laser from Satellite-borne retroreflectors;
- the variance of the position and size of the light spot illuminating on the photocathode;
- the unstability of DC power supply voltage for PMT.

For example, the transit time jitter varied with DC voltage between a pair electrodes has been given [Liu, 1983]:

$$M_{te} = \frac{M_u}{2U} \sqrt{\frac{2md^2}{eu}} \quad (7)$$

Where, m = electron mass, $m = 9 \times 10^{-28}$ grams;

e = electron charge, $e = 4.8 \times 10^{-10}$ statcoulombs;

u = DC voltage between a pair electrodes in statvolt;

d = distance interval between a pair electrodes in centimeter.

When there are nine dynodes in the PMT the overall transit time is equal to 18.8 nsec under the condition of $d = 0.7$ cm, $u = 155$ V. If the voltage change rate of DC power supply for the PMT, M_u/U equals ± 0.019 the overall transit time jitter will achieve ± 180 psec (± 2.7 cm). If $M_u/U = \pm 0.002$ the jitter will be equal to ± 19 psec (± 3 mm). It will be seen from this that a strictly regulating circuitry has to be used for the DC power supply to the PMT, so as to decrease the transit time jitter.

The experiment results measured by E. Bergstand to RCA 1P21 PMT indicated that the transit time difference between an illuminating centre and eccentric point on the photocathode with ± 3 mm is equal to 1.9 nsec (28.5 cm). It will be seen from this that a position stability of the illuminating point has to be required strictly for the photocathode. The variance with time can not be permitted during ranging.

It is will be known that in an illuminating region on the photocathode the photoelectrons from the respective transmitting points are not synced due to the photoeffect feature. Therefore the transit time is a statistical average for the photoelectrons. If the size of the illuminating spot on the photocathode varies as time, the average will be changed with it, so as to result in the transit time jitter.

The transit time jitter for microchannel plate photomultipliers (MCP/PMT) is much smaller than that for dynode chain PMT's. Experiment data have shown that the one sigma transit time jitter for an ungated ITT F4128 MCP/PMT was equal to about two centimeters for single photoelectron inputs, but one for the Amperex 2233B PMT achieved ten centimeters [Degnan, et al, 1984]. There is also faster impulse response for MCP/PMT'S. It will be seen from these that it is desirable to use MCP/PMT in SLR systems.

The calibration error varies as different calibration. It is the purpose of SLR calibration to control the change of the system constant which is produced by the jitter of an internal circuitry delay. When signals in SLR system are transferring from one circuit to other circuit it is necessary to spend a certain time. The spent time in circuitries is defined as the internal delay. Its value can be not only calculated on the basis of the circuitry parameters, but also determined by means of ground baselines whose lengths were measured precisely. If the system constant should not vary there would not be any error for corrected ranging data with one. In fact the system constant is of changing due to that of the internal delay. The latter of the start pulse gotten through the start channel can not compensate that of the stop pulse gotten through the stop channel. The system constant contains the difference between the internal delay of the start and stop pulse. The optimal calibration is defined as being able to eliminate the jitter influence. However, in practice there is any difficulty to achieve this purpose. For example, it can be demonstrated with the following experience [Mangin, 1982]:

On June 17, 1981: cal. = 199.0 nsec.

On September 16, 1981:

- Single round trip: cal. = 198.7 nsec,
- Double round trip: cal. = 198.5 nsec,
- Silverberg method: cal. = 198.7 nsec
- Internal target: cal. = 199.1 nsec.

According to the above calibration results we can calculate that one sigma is equal to ± 0.219 nsec (± 3.3 cm), and know:

- the results are varying with the different calibration method;
- there are the different results for the variant time.

Experience by SAO has also indicated the typical values for the jitter range' from ± 0.15 nsec to ± 0.20 nsec ($\pm 2 - \pm 3$ cm), not including PMT; when including PMT from ± 0.2 nsec to ± 0.3 nsec ($\pm 3 - \pm 4.5$ cm) [Pearlman, et al, 1982].

It will be known from the above experience data that the greater delay jitter has to be taken enough notice for precisely ranging. In order to approximate the optimal calibration a few SLR systems have employed some internal calibration, such as the feedback calibration of TLRS ranging system [Silverberg, 1982], the double calibration of MTLRS mobile system [Wilson, 1982] and the zerodelay system of Goddard new experimental facility [Degnan, 1985]. In writer's opinion there will be a much smaller jitter due to each other compensation for the start and stop delay when the start and stop pulse emerge in common from one channel circuitry based on a common PMT. If the SLR systems with the internal calibration were to make use of one common channel circuitry they would be able to approximate the optimal calibration mostly.

When making use of ground baselines for the SLR calibration the baseline length has to be measured precisely. For example, when baselines are measured to use AGA Geodimeter 8, due to its standard diviation of $\pm (5 \text{ mm} + 1 \times 10^{-6} D)$ the measured error for 5 km baseline will achieve ± 1 cm. If microwave distance measuring instruments

are used to measure the 5 km baseline the measured accuracy of ± 1 cm will be unable to be achieved at all. For example, when using MRA-5 Tellurometer the measured accuracy will only achieve ± 2.5 cm. The low measured accuracy for ground baselines will become into a limitation for the calibration accuracy except using still more precise baselines. In performing the SLR calibration the meteorological data must be taken for the calibration refraction correction. We would better take them on two end points of the ground baseline whose length is equal to several kilometers, so as to improve the calibration accuracy.

When the momentary time arriving at the satellite for the laser pulse can not be exactly reduced to UTC the following sync error will be produced [Liu, 1985]:

$$M_s = -V_s M_t \cos\alpha \quad (8)$$

Where, V_s = movement velocity of the satellite in the space,

M_t = ranging moment error in respect to UTC,

α = Satellite elevation.

It was pointed out that the best synchronization results have an RMS of a half microsecond, and the worst synchronization results have been a four microsecond RMS [Oaks, et al, 1982]. It was known that $V_s = 5698$ m/sec for LAGEOS; $V_s = 7400$ m/sec for STARLETTE [Mastrocinque, 1985]. If taking $M_t = \pm 4 \mu s$, $\alpha = 15^\circ$, we will know $M_{SL} = \pm 2.2$ cm for LAGEOS, $M_{SS} = \pm 2.9$ cm for STARLETTE. Assuming $M_t = \pm 7 \mu s$, we will obtain $M_{SL} = \pm 3.8$ cm, $M_{SS} = \pm 5.0$ cm. If using $M_t = \pm 0.5 \mu s$, we will get $M_{SL} = \pm 3$ mm, $M_{SS} = \pm 4$ mm. It will be seen from these calculated sync errors that there will be greater sync errors for both a high and low satellite when the moment error, $M_t \geq \pm 4 \mu s$ and the elevation is smaller. Therefore, an exact time synchronization has to be performed in order to reduce the sync error. It is better to use a Time Transfer Receiver (TTR) operating with the NAVSTAR Global Positioning System (GPS). Its time synchronization accuracy is expected to achieve a RMS of less than 50 nsec [Oaks, et al, 1982]. GPS TTR's were started to synchronize the time for some SLR systems, such as the mobile MTLRS system in Winter 1985.

The satellite error is caused by a deviation from the satellite center-of-mass (SCM) correction and a coherent fading effect. The satelliteborne retroreflectors are distributed on each laser satellite crust. The effective reflection points depending on a centroid of the incoming laser pulse have to be reduced to the satellite center-of-mass. For LAGEOS the SCM correction is theoretically equal to 258 mm. However, the SCM correction varies with a function of incidence angle, laser pulsewidth, detection means and receiver impulse response. The experimental data have shown that the SCM correction was changed from 245.7 mm to 253.8 mm when the laser pulsewidth was equal to 1 nsec to 61 psec. The SCM correction for centroid detection was 249 mm with a standard deviation of 1.7 mm [Degnan, 1985]. For gravity gradient satellites the incidence angle, ϑ between the laser beam and the axis of symmetry of the satellite can be approximately expressed [Carpenter, 1978]:

$$\vartheta = \arctan \frac{\cos \alpha}{\sin \alpha + \frac{D}{R}} \quad (9)$$

Where, D = distance between a ground station and laser satellite;
R = earth's radius.

It will be known from the above mention that the satellite error has to be produced due to the different pulsewidth, detection means and incidence angle. On the other hand, there is the so-called coherent fading effect for the returned beam. The latter is an ensemble of reflections from all those retroreflectors facing in the general direction of the observation station. Due to superimposing from the individual returned signals each other this results in a coherent interference for corresponding electric fields in the receiver. The coherent fading effect will cause a random timing error with a standard deviation of 77 psec [1.15 cm, Degnan, 1985].

7. Conclusions

From what has been said above, we know that the real accuracy for SLR can not achieve ± 1 cm proposed by them at all, but only a few centimeters for the executed experiments. SLR errors can be divided into two types:

- condition errors caused by exterior conditions in laser ranging,
- instrumentation errors caused by the properties which are not enough good for SLR systems,

and summarized in the following table:

Satellite laser ranging errors	condition errors	velocity error resulting from the measurement error for velocity of light in a vacuum; index error resulting from inaccurate meteorological data; satellite error resulting from the inaccurate satellite center-of-mass correction and coherent fading effect; sync error resulting from an inexact clock synchronization; calibration error resulting from the inexact measurement for the system constant;
	instrumentation errors	frequency error resulting from the difference between the nominal and real value of a clock frequency; resolution error resulting from the counter resolution which can not be enough small; timing error resulting from the counter property which of itself can not be as good as possible; fluctuation error resulting from the strength fluctuation of a returned laser pulse; pulsewidth error resulting from that the energy of a transmitted laser pulse is not centralizing in a moment; wavefront error resulting from the wavefront distortions of a transmitted and returned laser beam; transit error resulting from the transit time jitter for the photoelectrons from the photocathode to the anode in a PMT.

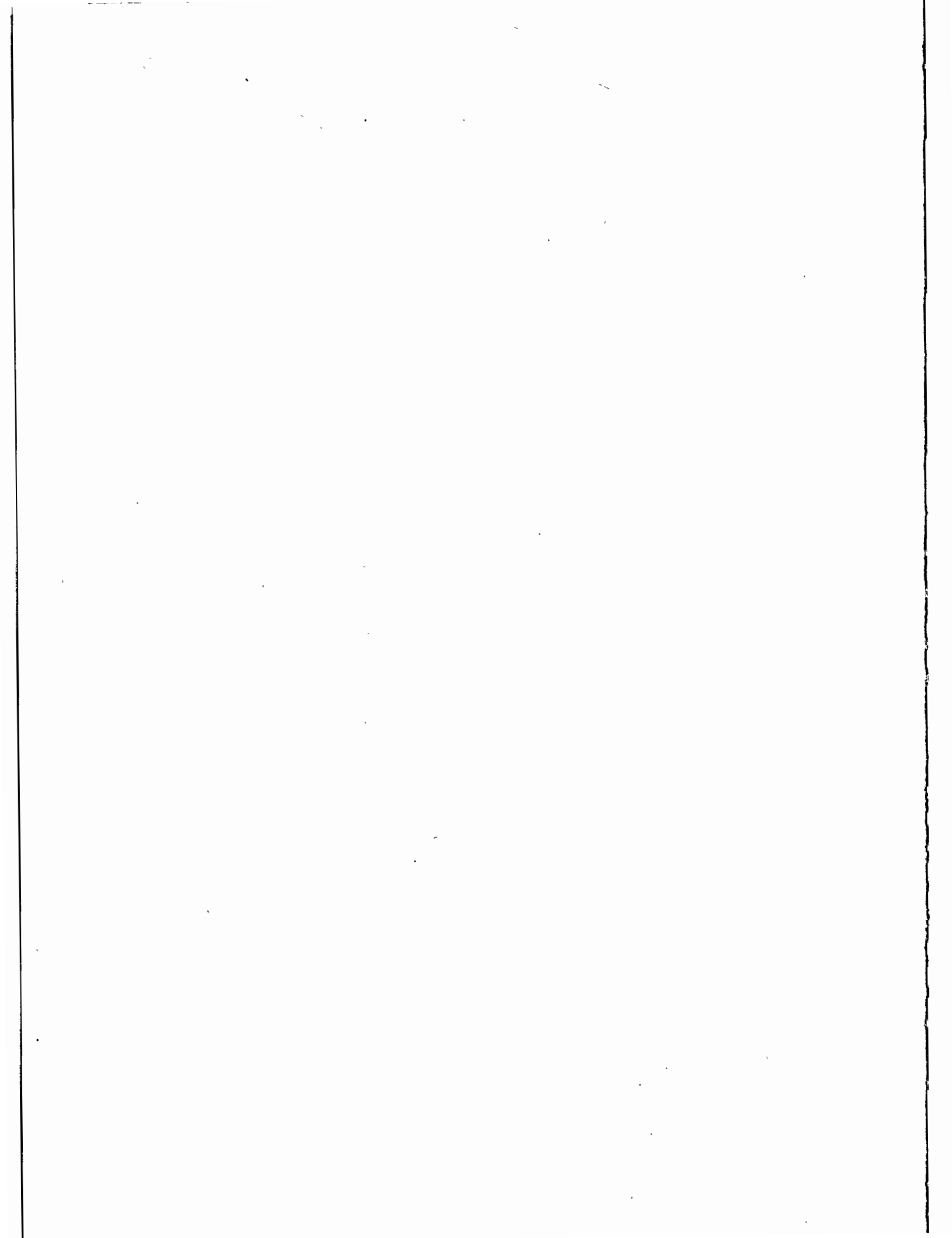
8. Acknowledgments

This paper was written during studying at the Satellite Observation Station Wettzell. The writer would like to express his hearty gratitude to Dr. R. Höpfl for often providing some references and many beneficial discussions, to Mr. W. Schlüter for his help.

References

- [1] B.I. Edelson, Dear Colleague letter
Space Science and Applications Notice, NASA, April 12, 1985
- [2] Liu Jiyu, Will Satellite Laser Ranging Measurements Be Able
to Achieve 1-cm Real Accuracy?
Second International Conference on Trends in Quantum Electro-
nics, Bucharest, September 2-6, 1985
- [3] GTE Sylvania, Proposal for Satellite Ranging system
24 May 1974
- [4] J.L. Bufton, Review of Atmospheric Correction for Laser
Ranging Data
Third International Workshop on Laser Ranging Instrumentation..
Lagonissi. May 23-27.1978
- [5] B.D. Tapley. et al. A Critical Analysis of Satellite Laser
Ranging Data
Proceedings of the Fourth International Workshop on Laser
Ranging Instrumentation, Published by the Geodetic Institute,
University of Bonn, 1982, pp. 523-567
- [6] J.W. Marini and C.W. Murray, Correction of Laser Range Tracking
Data for Atmospheric Refraction at Elevations above 10 Degrees
GSFC Report X-591-73-351, Nov. 1973
- [7] J.B. Abshire and C.S. Gordner, Atmospheric Refractivity Correc-
tions in Satellite Laser Ranging
IEEE Transactions on Geoscience and Remote Sensing September 1984
- [8] Liu Jiyu, Some Recommendations for Improving Two-color Distances
The Canadian Surveyor, Vol. 38, No. 4 Winter 1984, pp.295-298
- [9] G. Mastrocinque, Feasibility of Satellite Tracking with a Dual-
wavelength Laser Ranging System
ESA Journal, 1985, Vol. 9, pp. 273-286
- [10] M.R. Pearlman, Status of the SAO Laser Ranging Systems
CSTG Bulletin, No. 5, march 10, 1983, pp. 66-73
- [11] M.R. Pearlman, et al, The Smithsonian Astrophysical Observa-
tory Satellite Ranging Hardware
Third International Workshop on Laser Ranging Instrumentaltion,
Lagonissi, May 23-27, 1978
- [12] H. Puell, Subnanosecond Laser System for Satellite Ranging
Proceedings of the Fourth International Workshop on Laser
Ranging Instrumentation, published by the Geodetic Institute,
University of Bonn, 1982, pp. 277-284
- [13] J.J. Degnan, Satellite Laser Ranging: Current Status and
Future Prospects
IEEE Transactions on Geoscience and Remote Sensing,
Vol. GE-23, No.4, July, 1985, pp. 398-413
- [14] W. Koechner, Solid-state Laser Engineering
Springer-Verlag, Berlin, 1976, p. 195

- [15] J.J. Degnan, T.W. Zagwodzki, A Comparative Study of Several Transmitter Types for Precise Laser Ranging
Proceedings of the Fourth International Workshop on Laser Ranging Instrumentation, Published by the Geodetic Institute, University of Bonn, 1982, pp. 241-250
- [16] J.J. Degnan, et al, Satellite Laser Ranging Experiments with an Upgraded MOBLAS Station
The Fifth International Workshop on Laser Ranging Instrumentation held at the Royal Greenwich Observatory East Sussex, England, September 10-14, 1984
- [17] R.L. Ricklefs, P.J. Shelus, R.J. Eanes and J.R. Wiant, MLRS System Characterization
September 19, 1985
- [18] Guan Zhenhua, et al, JLJ-2 High Resolution Counter for Laser Ranging Systems, 1982 (in Chinese)
- [19] Hewlett Packard (HP), Operating and Service Manual, Computing Counter 5360A and Input Module 5365A
October 1975
- [20] Liu JiYu, Accuracy Judgement on EDM equipments (in Chinese)
Bulletin of Surveying and Mapping, No. 3, June 1983, pp. 29-35
- [21] J.F. Mangin, The Laser and the Calibration of the CERGA Lunar Ranging System
Proceedings of the Fourth International Workshop on Laser Ranging Instrumentation, Published by the Geodetic Institute, University of Bonn, 1982, pp. 313-322
- [23] E.C. Silverberg, The Feedback Calibration of the TLRS Ranging System
Proceedings of the Fourth International Workshop on Laser Ranging Instrumentation, Published by the Geodetic Institute, University of Bonn, 1982, pp. 331-337
- [24] P. Wilson, The German/DUTCH Mobile Ranging System
Proceedings of the Fourth International Workshop on Laser Ranging Instrumentation, Published by the Geodetic Institute, University of Bonn, 1982, pp. 468-483
- [25] O.J. Oaks, et al, GPS Time Transfer Receiver for the NASA Transportable Laser Ranging Network
Proceedings of the Fourth International Workshop on Laser Ranging Instrumentation, Published by the Geodetic Institute, University of Bonn, 1982, pp. 338-375
- [26] L. Carpenter, Goddard Laser Tracking Data
Third International Workshop on Laser Ranging, Lagonissi, Greece, may 23-27, 1978



SOME CURRENT ISSUES ON LASER COLLOCATIONS

M.R. Pearlman
Smithsonian Institution
Astrophysical Observatory
Cambridge, MA 02138

Telephone (617) 495 7481
Telex 921428 SATELLITE CAM

ABSTRACT

Collocation experiments are being conducted to isolate and study systematic errors in laser ranging systems. Proper use of the unique collocation configuration requires that these experiments be allowed to focus on effects that would be difficult to find in single system ground and readiness tests. This requires that (1) the systems be fully tested and field ready prior to collocation and (2) sufficient time and resources be allocated for proper test and analysis. A brief review of recent collocation requirements and experience is presented along with current issues and shortcomings.

INTRODUCTION

Laser collocations allow us to isolate and study the systematic errors in laser ranging machines. To the extent that the error sources are independent from one machine to another, systematic effects appear as offsets in short arc analyses between the collocated systems. The unique geometry of machines in close proximity permits comparative analysis without corruption from modelling errors such as atmospheric refraction, spacecraft center of mass, and spacecraft orbit. To obtain full value from the collocation, each participating system must be operated in a fully independent manner, thereby simulating conditions and performance that would be anticipated from stations operating on their own at remote locations. The more the systems have in common, the less rigorous is the test.

Even though it is not the intent, collocations have traditionally provided a full test of entire ranging operations from predictions, through hardware and procedures, to final data analysis. This is both good news and bad: A full stress test exposes all of the weak points in the system, but using the collocation configuration to find very mundane problems is a waste of very limited resources.

NATURE OF COLLOCATION RESULTS

Historically, collocations have revealed three kinds of results:

- (1) **INCIPIENT PERFORMANCE LIMITATIONS** which refer to limitations in capability imposed by the characteristics of the ranging system in its current configuration, limitations which would be difficult to find with the existing single station ground tests.
- (2) **CHARACTERIZATION EFFECTS** which refer to limitations which should have been observed and measured with single system ground tests.
- (3) **FAILURES.**

Incipient performance limitations are system shortcomings which may be very elusive and frustrating, but discovery represents experiment success; something unexpected and possibly new was discovered. In the past, effects such as wavefront variations, signal strength variations, variations with equipment temperature and azimuth dependence were discovered, and in most cases procedures were then added to the standard ground tests to include these effects.

Characterization effects are effects that we have seen before, effects for which ground based tests already exist

within the standard test procedures. Problems in this category usually arise because preliminary ground tests and engineering tests have not been properly conducted and/or analyzed.

Failures are those things that inhibit us from measuring the system performance. These are items that should have been detectable with single station preliminary testing: Failure of the equipment, improper use of operating procedures, and failure of the data processing and/or support systems.

There may be some philosophical dispute over the boundary between categories, but the basic tenet should be that a collocation is a unique event and should be allowed to focus on effects that are difficult or impossible to find with single station testing.

PREREQUISITES

To insure that we get the most value during collocation experiments, we should insist on the following prerequisites:

- Both systems should be working at a satisfactory level in terms of target acquisition, data yield, range noise, etc.
- Both systems should be working independently including: timing, software, meteorological equipment data preprocessing, etc.
- Both systems should have completed and "passed" the specified ground tests (including system characterization)
- Fully tested comparison software should be available
- A management plan with schedules, responsibilities, data flow, and anticipated system performance should have been developed.

GROUND TESTS

The ground tests and the related data analysis have been specified in detail in previous sessions of the Workshop (see Pearlman 1984) and in the Collocation Plans prepared by NASA/Bendix for measurements at GORF. These tests have included:

1. Multiple Ground Target Tests (MINICO) in which several ranging sequences are taken sequentially off of two or more ground targets at different ranges and azimuths to verify reproducibility, system linearity, and mount eccentricity model.

2. Stability tests in which ranging sequences are taken off of a single ground target for one to two hours to examine temporal stability of the system over a time period consistent with a full LAGEOS tracking sequence.
3. Wavefront tests in which a corner cube map is made to measure the laser wavefront spatial variations.
4. Signal strength tests in which extended target calibrations are taken over the full dynamic range of the ranging instrument to measure and characterize the variation in system calibration.
5. Specialized engineering tests (as necessary) including the measurement of changes in system delay with (1) PMT voltage, (2) position of return within the range gate, (3) stop channel (in multistop system), etc.

The data set for a collocation test consists of more than just simultaneous satellite ranging data. It should include the information, data and results from all of the preliminary activities, ground calibrations, and post analysis. Without this, proper interpretation of collocation results is not possible.

SATELLITE TRACKING REQUIREMENTS

The satellite data requirements for the collocation experiments conducted by NASA are based on the following:

- ° Adequate data volume and coverage to disclose systematic effects on LAGEOS
- ° Evaluation of performance on daytime tracking on LAGEOS
- ° Evaluation of performance on low orbiting satellites

Proper engineering evaluation of a laser system requires a data set sufficient not only in data volume (enough passes with simultaneous data), but also sufficient sky coverage to observe azimuth and elevation dependent errors, adequate temporal coverage to achieve the needed sky coverage and to test system reliability, and adequate operation under daytime conditions.

The requirements for satellite tracking by NASA have been specified as follows:

1. Twenty simultaneous passes on LAGEOS with:

- Data spaced over 30 minutes per pass
 - A minimum of seven two-minute overlapping normal points per pass
 - Five passes in daylight
 - Two of the passes in each sky quadrant
 - Two passes in each of the ascending and descending equatorial modes
2. Two simultaneous passes on Starlette or BE-C
- A minimum of three simultaneous normal points per pass

DATA ANALYSIS

Collocation satellite data are analyzed at several levels. The first examination is made on a single station basis and includes:

- Calibration RMS
- Calibration stability
- Pre/Post calibration shift
- Satellite data RMS
- Satellite normal point RMS
- Residual signatures to orbital solutions

At the next level, the data for the collocated systems are compared using short arc solutions to investigate effects such as:

- Mean offset
- Drift and temperal variations
- Range dependence
- Elevation and azimuth dependence
- Signal strength variations
- Diurnal variations

- Variation with system calibration
- System changes
- Temperature variations

RECENT EXPERIENCE AND ISSUES

Some of the recent collocation experiences are tabulated in Table 1. Analysis is still underway on several of the experiments, so that results since early 1985 are still preliminary. For this summary, the offset value is expressed simply as the mean difference between the systems over the full data set, paying no additional recognition to residual signatures or the actual nature of the systematic biases. As noted above, however, these signatures are a fundamental key to system performance and their close scrutiny is an essential part of any collocation evaluation. Specific experiments will be discussed by others in this session.

A tabulation of problems encountered during collocation experiments is shown in Table 2. The difficulties fall basically into two categories: (1) The ranging machines and/or their supporting systems were not ready for collocation, or (2) the machines did not stay long enough to acquire a sufficient set of data or to allow proper engineering scrutiny. We are historically behind schedule in development, construction, deployment, etc., and as such, the preliminary phases to collocation have in almost every case been compromised.

Many laser systems have participated in collocation experiments, but in most if not all cases, the collocations have been inadequate. In some cases, the machines have not really functioned. Less than half of the tests provided twenty passes of data, and even in these cases some of the passes were inadequate for proper analysis, due to insufficient data volume, insufficient coverage, and/or changes that were made during the tests that precluded test continuity. The greatest void in data acquisition, however, has probably been the lack of daylight ranging.

The maintenance of configuration control in hardware, software and procedures has been a traditional problem. In principle, the systems should be operated in a fixed, independent manner. Almost without exception, however, we have succumbed to temptation to adjust, repair, and modify. Unfortunately, there is never enough time to start the collocation test over again, and we end up with discontinuous data sets that are hard to relate.

Many problems have surfaced that relate to data processing. This, of course, becomes more prevalent as more

systems built and operated by different groups are collocated (although it has been experienced in collocations with only NASA systems). Inconsistent use of models (refraction, spacecraft center-of-mass, calibration correction, etc.) and differences in data manipulation and screening have recently required attention. One of the most notorious problems is probably that of ground surveys: to calibration targets and over the interstation vector. Ground surveys, although a routine process, must be done very carefully and analyzed properly. Surveys must be repeated on a regular basis to insure the results and to detect any local movements. More than once, ground motions or unstable calibration target structures have compromised ranging results. The ground target is in most cases the basis of our entire measurement program, yet it is often the weakest link.

Speed of data processing has been a perpetual headache. As noted earlier, analyses of experiments taken over a year ago are still underway. The lasers leave the collocation, and may take data for a year or more before we fully understand the performance characteristics. At times, even when there are indications of anomalous behavior, we do not apply the manpower and time to pursue the evidence in a timely manner. As a result, problems surface later at an even less opportune time.

Proper interpretation of the collocation results relies on the conduct of complete preliminary ground tests, analyses of this data, and timely availability of the results. This information is critical to the understanding of machine performance and may play a crucial role in proper data reduction. A recent example is system delay variation with signal strength. In those systems where the effect is pronounced, algorithms based on calibration data could have a very significant effect on satellite results. Yet, if the data is not readily available, we see serious degradation in system performance and have no opportunity to apply proper data corrections.

CONCLUSIONS

The difficulties experienced in past collocations, and improvements seen in some of the recent tests, reiterates again that collocations must be as carefully managed as any other activity making use of scarce resources. Every collocation requires a detailed plan encompassing everything from the readiness of support systems through the management of the data flow and analysis. Compromises have not served us well. The "Rush to Collocation" and the "Rush to Deploy from Collocation" have been very costly to us. In the future, every effort must be made to use collocations more effectively to study the fundamental limitations of the systems rather than merely

cleaning up the routine problems that we just did not have time to examine before.

Reference:

Pearlman, M.R., "Laser System Characterization", Proceedings of the Fifth International Workshop on Laser Ranging Instrumentation, Herstmonceux Castle, September 1984, published by Geodetic Institute, University of Bonn, Bonn, Federal Republic of Germany 1985.

RECENT COLLOCATION EXPERIENCE

<u>DATES</u>	<u>COMPARISON</u>	<u>LOCATION</u>	<u>NO PASSES</u>	<u>OFFSET</u>
7/81	MOB7- STALAS	GORF	12	3-4cm
9/81 - 1/82	HOLLAS - MOB1	HALEAKALA	45	<1 cm
9/81 - 10/81	MOB4 - MOB7	GORF	4	7 cm
7/82 - 10/82	MOB6 - MOB7	GORF	27	1-2 cm
7/82 - 8/82	MTLRS - TLRS1	McDONALD	23	6 cm
9/82 - 11/82	MTLRS - TLRS2	GORF	27	<1 cm
5/83 - 6/83	MOB4 - MOB7	GORF	13	1 cm
7/83 - 8/83	LTRS1 - MOB8	QUINCY	15	2-3 cm
10/83	TLRS1 - MOB4	MT. PEAK	7	6 cm
4/84 - 5/84	MTLRS1 - KOOLAS	KOOTWIJK	2	-
9/84 - 10/84	TLRS1 - MOB8	QUINCY	43	2-3 cm
11/84	MTLRS2 - WETLAS	WETTZELL	5	-
5/85 - 8/85	MTLRS1 - MOB7	GORF	13	1-2 cm
10/85 - 1/86	MTLRS1 - MTLRS2 - MATLAS	MATERA	13-36	1-2 cm

TABLE 1

FAILURES

- ° SYSTEMS NOT READY
 - INADEQUATE SHAKE-OUT ON SATELLITES
 - INADEQUATE GROUND TESTING

- ° INSUFFICIENT DATA SET
 - NOT ENOUGH ACCEPTABLE PASSES
 - LIMITED SKY COVERAGE/DISTRIBUTION
 - LITTLE OR NO DAYLIGHT DATA
 - INADEQUATE TEMPORAL COVERAGE (30 DAYS)

- ° LACK OF CONFIGURATION CONTROL
 - HARDWARE
 - SOFTWARE
 - PROCEDURES

- ° LACK OF PREPARATION FOR PROCESSING
 - INCONSISTENT USE OF MODELS
 - INCONSISTENT DATA MANIPULATION
 - INCONSISTENT DATA SCREENING
 - INCORRECT SURVEY DATA
 - SLOW DATA PROCESSING

- ° LACK OF AVAILABILITY OF ENGINEERING DATA
 - GROUND TEST RESULTS

- ° SURVEY PROBLEMS
 - CALIBRATION TARGET SURVEY
 - CALIBRATION TARGET STABILITY
 - INTERSTATION VECTOR SURVEY

MANAGEMENT OF THE LASER RANGING SYSTEMS COLOCATION

A. Cenci
Telespazio S.p.A.
Via A. Bergamini, 50
00158 - Rome Italie

Telephone (39) 6 4987407
Telex 610654 TSPZROI

ABSTRACT

The colocation testing for satellite laser ranging systems provides a unique opportunity to test the ranging capabilities and to identify possible sources of systematic errors.

Being the colocation experiment strongly influenced by many unforeseeable aspects, like atmospheric conditions, systems failures, logistic problems and so on, the management of the experiment has to be carefully organized in order to reduce any other possible sources of problems as well as to optimize the operational and analysis activities.

This paper concentrates on various aspects of the colocation management, starting from the identification of the major requirements to be satisfied prior the beginning of the colocation, like site requirements, systems errors characterization, definition of tasks and responsibilities,...

The main procedures and tests to be performed during the colocation period are also discussed, with particular emphasis to the ground test procedures and supporting information data set.

Further possible sources of errors to be carefully investigated, concerning data handling and processing, are discussed too in a section dedicated to the Software Benchmarking.

Finally, a general overview of the colocation data analyses is given.

This paper refers in particular to the procedures and criteria adopted during the colocation experiment recently performed at Matera between the MTLRSI, MTLRS2 and MATLAS systems (January-March 1986).

MANAGEMENT OF THE LASER RANGING SYSTEM COLOCATION

INTRODUCTION

The laser ranging stations differ from each other in several aspects: characteristics of the laser, mount system, receiving electronics, optics, timing system, software capability, operating procedures, etc.

Any of these aspects can map into systematic errors in measurements.

The colocation testing is the only reliable method to identify laser system problems comparing two or more stations, isolating station dependent systematic errors from other major sources of errors, like atmosphere, orbit determination, station location, etc.

Being the colocation testing strongly influenced by many unpredictable aspects, like atmospheric condition, systems and logistic problems etc., the management of the experiment has to be carefully organized in order to reduce any other possible sources of problems, as well as to optimize the operational and analysis activities.

A real time supervision during the colocation period is also necessary together with a joint cooperation between all the involved groups.

This paper presents the requirements and procedures to perform the colocation testing, with particular reference to the procedures and criteria adopted during the colocation experiment performed at Matera with the MTLRS1, MTLRS2 and MATLAS systems.

Writing this paper, reference was made in particular to the standard colocation plan of the Bendix Field Engineering Corporation (ref. [2], [3]) and the 1986 Matera Colocation Plan (ref. [1]).

The report is divided into five sections: the first section summarizes the various prerequisites to be satisfied prior the beginning of the colocation.

The second section analyzes the procedures and tests to be performed during the colocation.

Section 3, is dedicated to the benchmarking of the processing software.

In section 4 an overview of the analysis procedures is given.

The last section gives a summary of the colocation reports.

An overview table is also given for each section.

1. COLOCATION PREREQUISITES

1.1. COLOCATION SCHEDULE

Particular attention has to be given to the choice of the colocation period, in relation with weather conditions and satellite visibility, in particular if second generation stations, which have only night time tracking capability, are involved.

The colocation test period must be long enough to meet the colocation data set requirements for the analysis of both short and long term biases (see sect. 2.2.). Distribution of data over at least one month is in general required.

1.2. ON SITE FACILITIES

1.2.1. Power Supply

The requirements for the electrical power are in general not critical, being at least one of the collocating stations connected to the commercial power.

In any cases, if power requirements are not largely satisfied, interactions between the systems are possible during laser firing, mainly if high energy lasers are involved. In this case, independant sources from power generators are requested.

1.2.2. Communications

The basic communication systems needed at the site are:

- telephone line: for general communication and quick-look transmission (to access MARK III data network);
- telex line: for information exchange and quick-look transmission;
- mail/carrier: express mail or carrier is necessary to maximize the full-rate data timeliness. Complete data flow tests are strongly advised before the colocation starts, in order to evaluate the real possibilities;
- on site: an internal phone line between the collocating stations should be installed in order to allow the crews to communicate each other during tracking or tests as well as for meteo measurements exchange, time comparison, emergency and so on.

1.3. COLOCATION SITE REQUIREMENTS

The main requirements for the colocation site are summarized in the following:

- re-inforced concrete slabs are required for mobile systems to accommodate for a leveled and stable support for the mounts. SLR universal NASA pads are recommended. The reference markers must be carefully isolated from the pad and extended sufficiently into the subsurface for maximum stability [4];
- the collocating stations should be positioned as close as possible, to reduce errors in local survey measurements and geometrical data analysis (60 meters or less is recommended);
- a reference marker network with a typical side length of 100 to 200 meters around the site is strongly advised;
- appropriate electrical ground network has to be installed around and under stations locations. In case of risk for excessive storm conditions, proper tie-downs are also required;
- at least three ground targets at different azimuth and distances (typically 500 to 2000 meters) should be available (corner cube reflectors and/or billboards depending on type of stations), to allow terrestrial ranging tests.

1.4. SITE SURVEY

One of the most frequently experienced source of systematic errors in colocation data analysis concerns the survey of the relative station positions and critical calibration ranges (reference markers and calibration target).

Errors on survey directly map into relative station biases, so that absolute accuracy better than 0.5 cm is required.

Accurate local survey, including pads and reference markers measurements, must be performed prior the beginning and directly after the completion of the colocation period.

Connection to the national geodetic network is also advised, although it does not impact directly the colocation experiment.

A report of the pre-survey results must be distributed to all involved analysis groups prior the first colocation data is available, as reported in sect. 5.2.

Being the survey one of the most critical pre-requisites to be satisfied for the colocation, particular attention is necessary for:

- calibration of instruments;
- measurement procedure;
- data reduction;
- error control.

Details about the above topics are given in ref. [5] and [6].

1.5. SYSTEMS CHARACTERIZATION

One of the objectives of the colocation experiment is to verify and compare the performances of the laser stations.

A complete characterization of each system is therefore required prior the colocation in terms of definition of system performance and estimation of errors budget.

With reference to the model proposed by M. Pearlman at the 5th International Workshop in Laser Ranging Instrumentation (ref. [7]), the system characterization must include at least the following items:

RANGING MACHINE ERRORS

Systematic:

- Spatial Variations (Wavefront distorsion, cube map);
- Temporal Variations (Pre-post calibration shift, long term system delay variations);
- Signal Strength Variations (unmodelled variations of system delay with signal strength);
- Calibration Path (survey, meteo - if applicable -).

Statistical noise:

- Single Shot Precision (day/night; high/low satellite);
- Calibration S.S. Precision (day/night; high/low satellite).

TIMING ERRORS

- Broadcast Monitoring (timekeeping accuracy).

MODELLING

- Data Aggregation (Normal points model accuracy, Normal Points precision/data availability);
- Atmospheric Correction (Model Accuracy, Meteo measurements accuracy).

The overall error budget should specify the relevant time period or periods for each component (pass, day, month, etc.).

The statistical means of characterizing each component must be also specified (one-sigma, peak to peak, etc.).

In order to verify the above characteristics during the colocation phase, adequate hardware and software configurations and operational procedures should be prepared prior the beginning of the experiment (see also sect. 2.6.).

1.6. MANAGEMENT AND RESPONSIBILITIES

The management of the colocation experiment needs to be organized prior the beginning of the experiment as much in detail as possible in close cooperation with all the participating groups.

All the tasks and responsibilities have to be clarified not only at high level but also at crew level which directly impacts the colocation results.

Fig. 1 shows the block diagram of the management structure which has been adopted during the Matera colocation.

The tasks performed by the various members are summarized inside the blocks.

A management on site is needed to coordinate the crews and the colocation activities.

Depending on the involved personnel and systems, different responsibilities may be attributed to the colocation manager who operates in any case in close cooperation with the stations managers under the supervision of the operational manager of the campaign.

One of the most critical areas to be handled by the colocation manager concerns the supporting information collection and exchange and the reporting.

In fact, difficulties and confusion may be experienced in colocation analysis due to missing or incomplete supporting information.

A strict control of hardware and software configurations during the colocation period is also required.

Any forced change in systems or procedures must be adequately documented.

2. COLOCATION PROCEDURES

2.1. OPERATIONAL SCHEDULING

The scheduling of the operational activities include:

- organization of the crews (shifts);
- pass scheduling;
- test scheduling;
- data and information exchange.

The definition of the acquirable passes depends on operational staff availability and organization.

Due to the particular kind of the experiment, a flexible organization is in general preferable, to reduce the effects of forced unactivity periods (due to weather, failures, etc.).

An a priori scheduling is in any case necessary together with the definition of priority criteria for both acquisition and off line activities (e.g. minimum culmination, daytime or nighttime passes, etc.) depending on forecasts and kinds of involved systems.

The requested colocation data set (see sect. 2.2.) is also considered in this context. All the requested ground test are scheduled too, following the assigned priority, as well the frequency of the data and information exchange (pass, daily, weekly, etc.).

2.2. SATELLITE RANGING

The raw satellite data set required during the colocation consists of the following:

- 1) All raw satellite data taken during the colocation period, including both simultaneous and non-simultaneous passes.
- 2) Each system should have observed a minimum of 20 LAGEOS passes with any other system spaced over a period of at least 30 days. Depending on the analysis method used the 20 passes should have either a minimum of seven consecutive overlapping two minute normal points (geometric analysis) or four consecutive two-minute normal points in three groups at the ascending, highest elevation and descending side of the pass (dynamic analysis).
- 3) these 20 passes should include a minimum of five daytime simultaneously tracked LAGEOS passes responding to the same normal point overlap criteria (if applicable).
- 4) These 20 passes must include a minimum of two simultaneously tracked LAGEOS passes in each sky quadrant and a minimum of two passes in both the ascending and descending equatorial nodes.
- 5) A minimum of two simultaneously tracked STARLETTE passes to confirm low satellite tracking capability. Each pass must contain a minimum of three 2 min normal points (if applicable).

The possibility to satisfy the above minimum data set requirements must be a priori verified in relation with the colocation schedule (ref. sect. 1.1.).

2.3. SYSTEM DELAY CALIBRATIONS

All tracking calibration data taken during the colocation must be included in the data set.

Particular attention needs to be given to the system delay variations in both short (pre-post calibration shift) and long period.

A real time analysis on this area is useful to identify system problems as well as to detect anomalous atmospheric effects along the calibration path, in case of using calibrations with external target, which directly map into systematic errors.

One interesting example is visible in fig. 2.1, where the behaviour of the calibration system delay and pre-post shift relative to the Matera colocation is shown.

Some anomalous system delay values were observed for both MATLAS and MTLRS2 systems. In the case of MATLAS, being this fact due to atmospheric effects of the external calibration path, station biases up to 10 cm have been detected on final data analysis. The jumps of the MTLRS2 system delay, due to internal system variation, did not affect on the contrary the final data, being present also during satellite ranging.

2.4. EPOCH TIMING

The philosophy which has been followed during the Matera colocation in definition of colocation procedures and criteria was to remove any possible source of a priori known errors.

Under this philosophy the system clock closure between the three systems was measured (generally on daily basis) with 100 nS accuracy and maintained to 500 nS level.

The effort to maintain time closure to less than half microsecond appears to be not fully justified being the epoch resolution in the archiving data formats actually limited to one microsecond.

In case of using Rubidium standards or in case that better time keeping accuracy be approached, comparisons made on pass-by-pass basis are necessary.

If closure within 0.5 microsecond with respect to the reference scale (USNO, BIH) is also maintained (this represents also a colocation test), both Full Rate and Quick Look data do not need in general time corrections, unless the epoch resolution be increased to accomodate the subcentimeter accuracy.

Being the colocation a unique opportunity to compare and test the entire system configuration, the comparison of different methods of synchronization is important too. In the case of Matera difference up to 0.3 microsecond between LORAN-C and GPS have been found, mainly due to the accuracy of the LORAN-C Master station offset. The storing of all timing intercomparison measurements allows also to verify and compare the system clocks stability.

A summary of timing closure informations should be included in the final colocation report.

2.5. METEOROLOGICAL DATA

Meteorological data closure between the collocating systems should be established and maintained at least to the following tolerance:

- Pressure: +0.5 mBar;
- Temperature: +5 degrees for satellite ranging,
+1 to 3 degrees C for terrestrial ranging, depending on the distance,
- Humidity: +30%.

In case of terrestrial ranging, averaging of temperature and pressure measurements taken along the target path is necessary (a variation of 1 degree in temperature introduces an error in range of about 1 mm per km).

For satellite ranging the most critical point concerns the pressure measurements.

In the case of Matera collocation, for example, a difference of about 0.8 mBar was found between the MATLAS and MTLRSI barometers, which also represents about the difference between the Bendix and IFAG standards (used to calibrate the instruments).

In order to remove any known source of relative error bias, readings from a unique pressure reference (MATLAS) were therefore used on data.

In case that a unique set of meteo instruments is used by all collocating stations, comparison between the various instruments must be also done and stored.

It is also to point out that an accuracy in the pressure readings (and relative closure) better than 0.5 mBar appears to be actually not fully significant because:

- archiving data format resolution is limited to 1 mBar;
- meteo reading are (in general) recorded only once per pass, so that changing conditions during the pass are not taken into account (variations up to 1 mB and 3 degrees have been observed during Lageos passes).

Upgradings of systems capability and data formats appear therefore necessary to accomodate subcentimeter accuracy.

A summary of the meteo closure informations should be included in the final collocation report.

2.6. GROUND TESTS

A minimum set of ground tests to be performed during the collocation period in order to evaluate system performance or to explore performance problems is described in the following.

Further investigation appear to be necessary to make the full ground test data available to all involved groups (formats and procedures need to be decided).

2.6.1. Terrestrial Targets Ranging

This test consists of a minimum of five daytime and five nighttime range series of a significant number of returns (depending on systems), over at least 3 minutes period, with the calibration data, each taken on at least three range targets at significantly different azimuth and distance.

Ranging must be done simultaneously by all the colocating systems to reduce unmodelled atmospheric effects.

The ranging conditions, e.g. return energy, should be similar to the satellite ranging.

This data can be used to confirm range bias deduced from satellite data and/or verify and compare terrestrial ranging capability.

2.6.2. Stability Test

It consists of at least two one-hour ranging on internal and/or external target to evaluate:

- range RMS stability;
- range drift;
- return energy stability.

Analysis of the pre-post calibrations data can be also used to verify the system stability ([7] , [8]).

2.6.3. Signal Strength Variation Test

It consists of ranging on internal and/or external target over the full dynamic range of the receiving system.

This is obtained performing various set of range series with a significant number of returns, changing for each set the ND optical filter in the transmitting or receiving section.

The RMS and mean variations from all set of data allow to evaluate the unmodelled variations of system delay with signal strength (arising because the performance of

devices within the systems including PMTs are amplitude and/or pulse width dependent) [7], [8].

2.6.4. Wavefront Map Test

It consists of mapping the wavefront variations by ranging on an external cube reflector several range series, at different azimuth and elevation angles (with adequate steps depending on beam divergence) in order to cover the entire laser beam.

The evaluation of the return energy variations and range variations give the map of the beam shape and the spatial wavefront distortion respectively (two tests must be done separately to remove signal strength dependence from wavefront distortion).

The measurement sets are taken in random order with return to the central reference position to check for temporal drift [7], [8].

This test is particularly important for systems with high energy laser pulses (duration over 500 ps FWHM) because the effect of spatial distortion has been experienced to be in general no more than 10% of the pulse duration.

2.6.5. PMT Test

It consists of producing a smooth systematic change in system delay as a function of PMT voltage.

This test is mandatory in case that change in PMT voltage is used to manage the received pulse to maintain the receiver system in the linear region.

2.7. QUICK LOOK DATA FLOW

The Quick-Look data are normally transmitted from the stations to the data processing centers on daily basis using telex or Mark III line.

To accommodate for a more reliable quick data analysis, the quick-look data set was expanded to 200 points per pass during the Matera collocation.

Quick Look data from all collocating stations were also collected and merged on site, after calibration corrections, in order to perform the polynomial fit analysis and a preliminary collocation data analysis (data were reformatted and processed in Telespazio, Rome; see also sect. 3.2.).

The Quick Look data flow during the Matera collocation is shown in fig. 2.2.

It has to be noted that in case of maintaining timing closure within tolerance, the quick look informations are only limited by the 0.1 nanosec. resolution in range, so that quick look analysis accuracy is expected to be comparable with that of the full-rate analysis (depending also on accuracy of the pre-post calibrations).

2.8. FULL RATE DATA FLOW

As mentioned in sect. 1.2. the timeliness of the Full Rate data flow must be optimized depending on:

- express mail/carrier availability;
- site location;
- involved pre-processing groups (number and locations);
- involved analysis centers (number and locations).

Full Rate data transmission should be in any case done at least on weekly basis.

Fig. 2.2 shows also the Full Rate data flow for the Matera colocation.

Copy of Full Rate data from MTLRS1 and MTLRS2 were also directly sent to DUT and IFAG respectively (on weekly basis) for analysis and benchmarking.

It has to be noted that several groups were involved in both pre-processing and data analysis, during the Matera colocation, so that the best timeliness for the complete full rate data flow was in general about three weeks.

The Full Rate data set and exchange procedures may also differ between the groups depending on:

- data formats (system format/standard; binary/ASCII; etc.);
- data support (9 tracks magnetic tape/Linc tape/floppy disk; etc.);
- Full Rate informations.

All the above differences may introduce difficulties in data processing and benchmarking (see sect. 3).

2.9. SUPPORTING INFORMATION

One of the major sources of confusion and delay in data analysis effort, experienced in the past colocation experiments, concerns the supporting information collection and exchange.

One of the criteria adopted during the Matera Colocation was to issue a weekly report on which the principal information to support both system performance evaluation and data analysis were summarized.

A summary of these informations, collected from each stations on daily basis, is shown in Fig. 2.3.

All tests and analysis results, not included in this form, were added as off-line activities as well as any crew comments and problem description (the Polyfit analysis section reported the results of an independent polynomial fit analysis performed on site by Telespazio using Quick Look data).

A final operational updated report, on which all the supporting information are summarized, should be issued at the end of the experiment and distributed to all participating groups (see sect. 5.).

Any additional supporting information generated on site, like tracking log, on site detailed analysis output, non-recorded test data, detailed crew comments etc., should be included in Full Rate data shipments.

3. SOFTWARE BENCHMARKING

The colocation experiment offers a unique opportunity not only to compare the performance of the hardware systems, but also to detect differences in the on site station and data control software and in the models and procedures for data preprocessing and analysis.

In our experience, a "Benchmarking" and comparison of the above software appeared as important as the system hardware comparison, in particular considering the subcentimeter accuracy being now approached in laser measurements.

3.1. SYSTEMS SOFTWARE COMPARISON

The on site software capabilities are in general dedicated to:

- system orientation;
- raw orbit propagation;
- satellite tracking;
- real time data acquisition;
- post-pass processing (raw data);
- Quick Look data generation;
- system delay calibration (raw data);
- data formatting;
- off line tests and procedures.

Although many different techniques are used, depending on hardware configurations, some common output and procedure can be verified and compared, like the following:

- Quick Look and Full Rate data formats;
- Quick Look data sampling criteria;
- Pre-Post calibrations evaluation;
- Pre-Post calibrations editing criteria;
- Raw data screening procedure;
- Full Rate data editing criteria;
- Timing and Meteo data handling;
- Modeled system delay corrections (PMT, attenuator delay).

For example, during the Matera Colocation, some differences (at centimeter level) on Quick Look system delay evaluation between MTLRS1 and MTLRS2 systems have been found, although the two system configurations were basically identical.

Different procedures and editing criteria have also been experienced concerning data screening (in both raw manual pre-screening and post fit editing).

In case that identical hardware configuration systems are involved, the interchangeability of the system software needs to be previously tested.

The same set of real or simulated data should be processed by all systems to verify and check the mentioned results and output.

In case of different systems, it may be useful to make available some software and procedures to convert data formats and maximize the compatibility between the collocating systems, to accomodate for pre-processing benchmarking and data analysis.

3.2. PRE-PROCESSING BENCHMARKING

We can divide the data pre-processing phase in the following sections (basically):

- Modelling of system delay variations;
- Pre-Post system delay calibrations;
- Timing corrections (reference to standard scales);
- Satellite time correction;
- Center of mass correction;
- Atmospheric refraction correction;
- Data re-formatting (if requested);
- Normal points generation (if requested).

The above procedures are in general not all performed by the same centers and, generally, data from different stations are processed by different centers.

To benchmark the pre-processing software, appropriate procedures must be therefore adopted each time depending on:

- systems;

- pre-processing centers;
- data formats;
- data supports;
- data availability;

and so on.

In general the philosophy should be to compare a same set of raw data after pre-processing made by different groups, looking at the pre-processed data sets in terms of:

- timing and pre-processing indicators;
- epoch differences;
- range differences;
- correction values.

Analysis can be made in terms of:

- single observation differences;
- pass-by-pass statistics (single pass average, RMS, Peak to Peak of the differences);
- global statistics (mean and RMS of the differences over all passes in data set).

The above informations may be useful to individuate the cause of eventual discrepancies (for example a constant range bias through a single pass may be attributed to differences in pre-post mean system delay evaluation).

Fig. 3 shows the two data processing flows adopted during the Matera Colocation to perform the Telespazio Analysis.

In the flow B the Full Rate data were pre-processed separately by DUT, IFAG and Bendix for MTLRS2, MTLRS1 and MATLAS respectively (part of MTLRS1 and MTLRS2 pre-processing was made by Bendix).

Data distributed by GLTN have been used for colocation analysis using GEODYN without any pre-processing option.

A independent analysis was performed using data collected directly on site (flow A in fig. 3.1) and pre-processed in terms of:

- Center of mass correction (GEODYN);
- Satellite time correction;
- Atmospheric propagation (GEODYN);
- System delay calibration.

The results of the comparisons between the two pre-processed data set in addition with a separate benchmarking performed jointly by DUT and IFAG on MTLRS1 and MTLRS2 data, pointed out some discrepancies (at centimeter level); the subsequent analysis pointed out some critical points of general interest:

- Data truncation or roundoff in the Full Rate (e.g; epochs) and Quick Look formats introduce errors of several millimeters. Sequential corrections in separate processor and/or at separate centers may worsen the problem.
- Pre-processing parameters should be carefully verified (e.g. laser wavelength).
- Data flags and applied corrections should be verified (some confusion on sign of applied corrections was experienced).
- The atmospheric refraction correction models should be periodically verified to accomodate their evaluation.
- Different screening and editing criteria may influence significantly the pre-processing (in term of pre-post system delay evaluation).

The last point is particularly important for low rate firing laser systems, for which a limited number of points from pre and post calibrations is available (at relatively high noise level).

For example, comparisons between Bendix and Telespazio pre-processing on MATLAS data showed bias differences up to 1 cm (occasionally 2 cm) on single passes (the differences averaged to zero over several passes), to be mainly attributed to different editing criteria on pre-post calibration data (ref. [10]).

A further point to be investigate concerns the normal points generation.

Due to different procedures and criteria adopted by the various centers to generate normal points (and consequently different bin widths and reference epochs), comparison can be made in general only looking at the results obtained after geometrical and/or dynamical analysis, using the same data set span from different normal point sources.

Tab. 3.1 summarizes the principal sources of preprocessing differences.

3.3. DATA ANALYSIS BENCHMARKING

Since several different groups are independently working at the analysis of data, the Matera Colocation experiment provided a unique opportunity of benchmarking the pre-processing and processing software and the method of analysis.

Besides of the global analysis approach (geometrical or dynamical) several differences in procedures and criteria have been experienced as well as consequent not negligible systematic effects on final results.

The various possible differences are summarized in tab. 3.2.

The effects on the final results caused by these different approaches are difficult to evaluate a priori, depending on data quality and quantity and on systematic effects in data distribution.

For example, differences up to 0.5 cm were found on final mean relative station biases for MATLAS using 2.5 or 3 sigma rejection criteria (up to 2 cm bias differences were found on single pass mean residuals) on Matera colocation data (ref. [10]).

About the same amount of discrepancy has been found using Full Rate data or sampled Full Rate data (every 5 seconds).

In order to accommodate the subcentimeter level accuracy, being now approached, we can therefore observe that:

- Comparison of the results from different groups appears to be fully significant only if the software used for data analysis are compared by means of a detailed benchmarking procedure.
- Aggregation of the results appear to be fully significant only in case of compatibility of all or part of the analysis approach criteria, in particular concerning data set and screening/editing procedures.
- In general, the colocation analysis (as well other data analysis) appears to be fully significant only if a detailed characterization of the adopted procedures is in addition given.

4. COLOCATION DATA ANALYSIS

4.1. ON SITE ANALYSIS

The analysis normally performed on site, having interest for colocation purpose, should include the following:

- Post pass analysis of the residuals (versus predicted orbit);
- Polynomial fit (applied to residuals and/or range);
- Data screening and editing;
- Pass statistics (duration, number of returns, sky coverage, etc.);
- Range bias determination (referred to predicted orbit);
- Time bias determination (referred to predicted orbit);
- RMS noise determination (after polynomial fitting);
- Ground test analysis (raw);
- System delay evaluation (pre-post calibration, modelling).

4.2. SATELLITE DATA ANALYSIS

Two general approaches are recognized in colocation analysis:

- Geometrical approach; basically the POLYQUICK analysis performed by Bendix (polynomial fit techniques);

- Dynamical approach; based on Orbit Determination Techniques (GEODYN, UTOPIA, etc.) including:
 - multi-short arc analysis,
 - long arc analysis,
 - long arc analysis and polynomial fit.

In both cases the following tests and relative plots can be performed:

- Mean range bias;
- Range bias drift;
- Range bias versus range;
- Range bias versus elevation;
- Range bias versus azimuth;
- Long term mean range bias stability;
- Diurnal effect;
- Range bias correlation with applied system delay.

Details on Dynamical approach analysis are given in ref. [9].

4.3. GROUND TEST ANALYSIS

Detailed ground test analysis may require additional software capabilities not available on site.

In general the analysis relative to colocation ground tests include:

- Terrestrial Ranging : similar procedures applied on satellite post-pass processing, including pre-post calibrations.
- Stability test : data binning and statistical estimation (RMS, Peak-to-Peak averaging).
- Signal strength variations : data binning and statistical estimation.
- Wavefront map test : additional software/hardware configuration is required to accommodate the beam mapping (in automatic way).

All ground test analysis should include appropriate graphics facilities like:

- targets ranging residuals (or relative differences) versus time;
- statistical ranging parameters versus time;
- statistical ranging parameters versus signal strength;
- beam map plot.

4.4. ENGINEERING ANALYSIS

Detailed data processing and additional investigation are necessary if the bias get out of the expected tolerance or problems arise.

In this case detailed system oriented engineering analysis is requested.

A detailed knowledge of the hardware/software configuration, as well as a complete access to the station logs and operational archives and procedures is necessary.

This kind of analysis may be therefore fruitfully performed only by or in close cooperation with the system operational teams and analysis centers.

Appropriate procedures should be jointly investigated each time depending on the type of problems.

5. COLOCATION REPORTS AND DOCUMENTATION

Tab. 5.1 shows a summary of the colocation reports.

This report plan has been adopted for the Matera colocation following also the past colocation experiences.

5.1. COLOCATION PLAN

A pre-colocation document, to be jointly issued by all participating groups, defines all the experiments requisites and activities, including:

- colocation prerequisites;
- colocation procedures;
- analysis procedures;
- responsibilities;
- results and reporting.

5.2. SITE SURVEY REPORT

As discussed in sect. 1.3, a technical report of the site survey should be distributed prior the beginning of the colocation and updated after its completion with the results of the post-colocation survey.

The report should include the following:

- Site description;
- Geodetic information;
- Equipment description and calibrations;
- Survey measurements procedures;
- Astronomical determinations;
- Data processing;
- Summary of results (colocation vectors and error budget);
- Pad measurements;
- Target measurements;
- Eccentricity vectors.

5.3. OPERATIONAL REPORTS

As discussed in 2.9., the weekly reports as well as the final operational report should include:

- timing information;
- meteo information;
- statistics of the satellites passes;
- on site analysis;
- ground test preliminary results;
- off line activities;
- crew commentary.

5.4. ANALYSIS REPORTS

Intermediate analysis results should be interchanged between all the involved analysis centers as soon as the first batch of data has been received and analyzed.

Results to be exchanged include:

- Pass identification;
- Station identification;
- Reference station identification;
- Number of points (accepted/rejected);
- RMS of fit;
- Estimated station relative range bias.

A brief description of analysis techniques and criteria adopted is also requested.

A final detailed individual analysis report should be issued as soon as the complete analysis and final results are available.

A final review of the results should be jointly performed by all participating groups.

5.5. FINAL REPORT

A final colocation report, including both operational (supporting information) and analysis activities is jointly issue by all participating groups.

The analysis results consist of data and data graphs which describe the performance of the colocating systems and best reflect the results of the colocation test.

This information are supplemented by comments and data provided by all participation groups.

The final report should include:

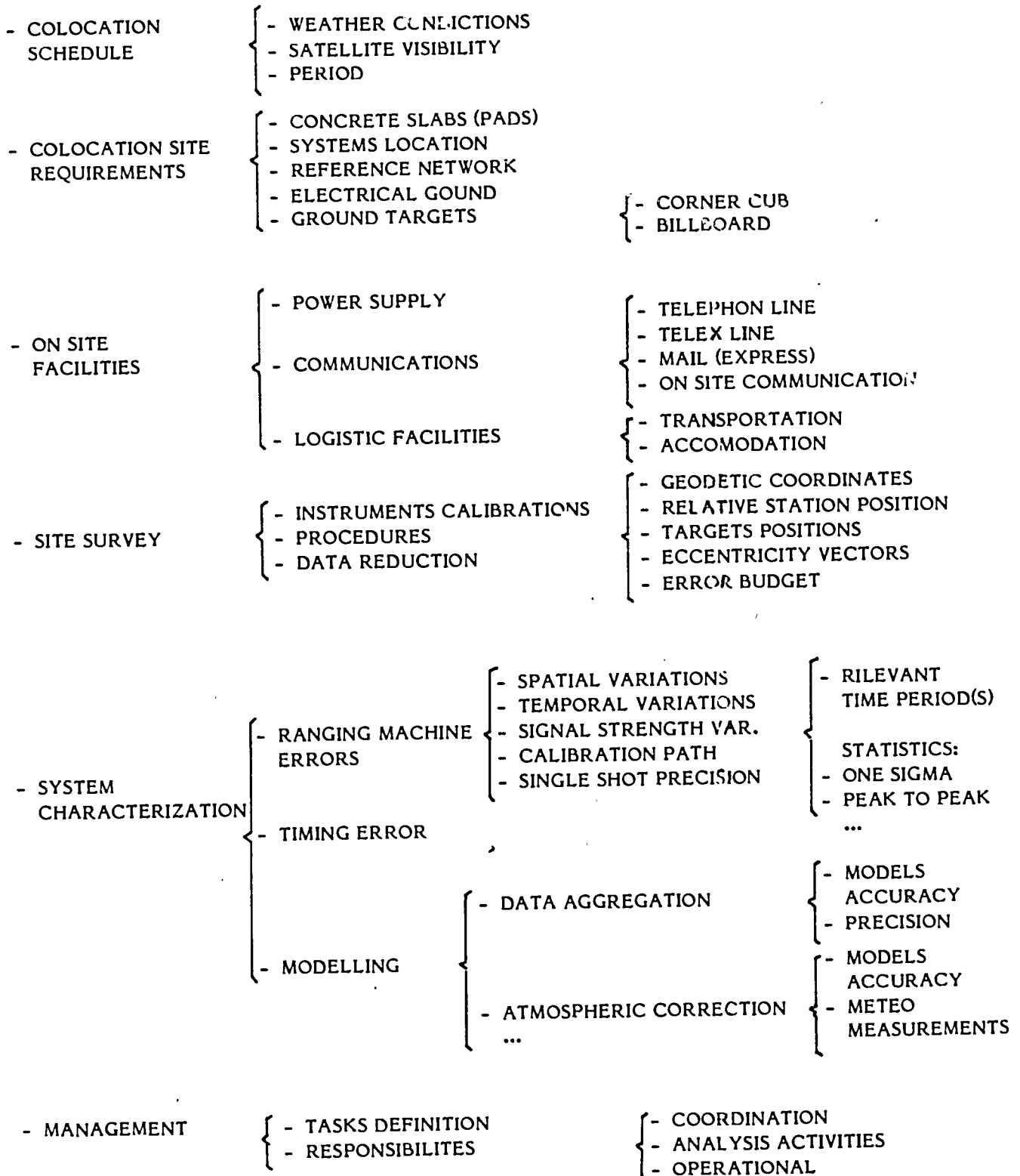
- laser systems description;
- site description;
- site survey (separate report);
- data acquisition statistic;
- description of ground tests;
- verification of epoch timing;
- verification of meteorological data;
- Quick Look data flow;
- Full Rate data flow;
- supporting information data flow;
- software benchmarking;
- analysis group reports;
- comments and conclusions.

REFERENCES

- [1] Dr. B. H. W. van Gelder
"The 1986 Matera Colocaiton Plan for MATLAS, MTLRS1 and MTLRS2"
January 1986 - Delft University of Technology (based on B.F.E.C. standard colocation analysis plan)
- [2] D. R. Edge
"Colocation Test Plan for the Laser Ranging Systems TLRS-3 and MOBLAS-7"
January 1985 - Bendix Field Engineering Corp.
- [3] Bendix Field Engineering Corp.
"MTLRS1 and MOBLAS-7 Colocation Analysis Plan"
May 1985
- [4] E. Vermaat
"Site Selection for MTLRS, Release 84.2.1"
September 1983 - Delft University of Technology
- [5] A. Cenci, D. van Loon
"Survey of the Matera Laser Station Site"
release January 1986, release May 1986 - Telespazio
- [6] D. van Loon
"On the Eccentricity Vectors for Colocation Purpose"
September 1986 - Delft University of Technology; presented at the 6th IWLRI, Juan Les Pines
- [7] M. Pearlman
"Laser System Characterization"
September 1984 - presented at the 5th IWLRI, Herstmonceux
- [8] A. Cenci
"Matera Laser System Characterization"
February 1985 - Telespazio
- [9] A. Caporali
"Colocation Data Analysis: Dynamical Approach"
September 1986 - Università di Padova; presented at the 6th IWLRI, Juan Les Pines
- [10] A. Cenci, M. Fermi
"Matera Colocation Analysis"
May 1986 (preliminary) - presented at the 2nd WEGENER/MEDLAS Conference, Dyonisos

TAB. 1

COLOCATION PREREQUISITES OVERVIEW



TAB. 2

COLOCATION PROCEDURES OVERVIEW

- OPERATIONAL SCHEDULING
 - CREW ORGANIZATION
 - PASS SCHEDULING
 - TEST SCHEDULING
 - DATA AND INFORMATION

- SATELLITE RANGING
 - RAW DATA SET
 - SIMULTANEOUS PASSES
 - SKY COVERAGE
 - SATELLITES

- SYSTEM DELAY CALIBRATIONS
 - CALIBRATION DATA SET
 - REAL TIME ANALYSIS

- EPOCH TIMING
 - TIME REFERENCES
 - LOCAL
 - REMOTE
 - TIME CLOSURE
 - GPS
 - LORAN-C
 - TV-SYNC
 - CLOCK TRIP

- METEOROLOGICAL DATA
 - METEO MEASUREMENTS
 - METEO CLOSURE

- GROUND TESTS
 - TERRESTRIAL TARGET RANGING
 - STABILITY TEST
 - SIGNAL STRENGTH VARIATIONS
 - WAVEFRONT DISTORSION
 - PMT TEST

- DATA MANAGEMENT
 - QUICK LOOK DATA FLOW
 - FULL RATE DATA FLOW
 - DATA ROUTE
 - TIMELINESS
 - FORMATS
 - SUPPORTING INFORMATION
 - WEATHER CONDITIONS
 - PASSES STATISTIC
 - POST PASS ANALYSIS
 - TARGETS RANGING
 - TIMING COMPARISON
 - OFF LINE ACTIVITIES
 - COMMENTARY
 - ...

PREPROCESSING BENCHMARKING

DATA ANALYSIS BENCHMARKING

TIMING	{ reference scale satellite time	{ TRUNCATION / ROUND OFF
SYSTEM DELAY CORRECTION		{ TRUNCATION / ROUND OFF MODELS EDITING CRITERIA
CENTER OF MASS CORRECTION		
ATMOSPHERIC REFRACTION CORR.		{ TRUNCATION / ROUND OFF MODELS PARAMETERS : wavelength meteo data ...
DATA FORMATTING		{ INFORMATION FLAGS APPLIED CORRECTIONS ...
NORMAL POINTS GENERATION		{ TRUNCATION / ROUND OFF MODELS EDITING CRITERIA ...

GEOMETRICAL
{ POLYQUICK }

DYNAMICAL
{ GEODYN
UTOPIA
... }

PASS ACCEPTANCE	{ GLOBAL COMMON	{ OVERLAPPED OBS. FULL OBSERVATIONS
PASS EDITING	{ DURATION N° OBSERV. 2 TO 4 SIGMA REJ. (to mean range bias) ...	
DATA SOURCE	{ QUICK-LOOK FULL-RATE	
DATA COMPRESSION	{ NORMAL POINTS SAMPLED NONE	
DATA FITTING	{ GLOBAL SINGLE PASS	{ MULTI-STATION SINGLE-STATION
DATA EDITING	{ GLOBAL SINGLE PASS	{ 2 TO 4 SIGMA REJ.

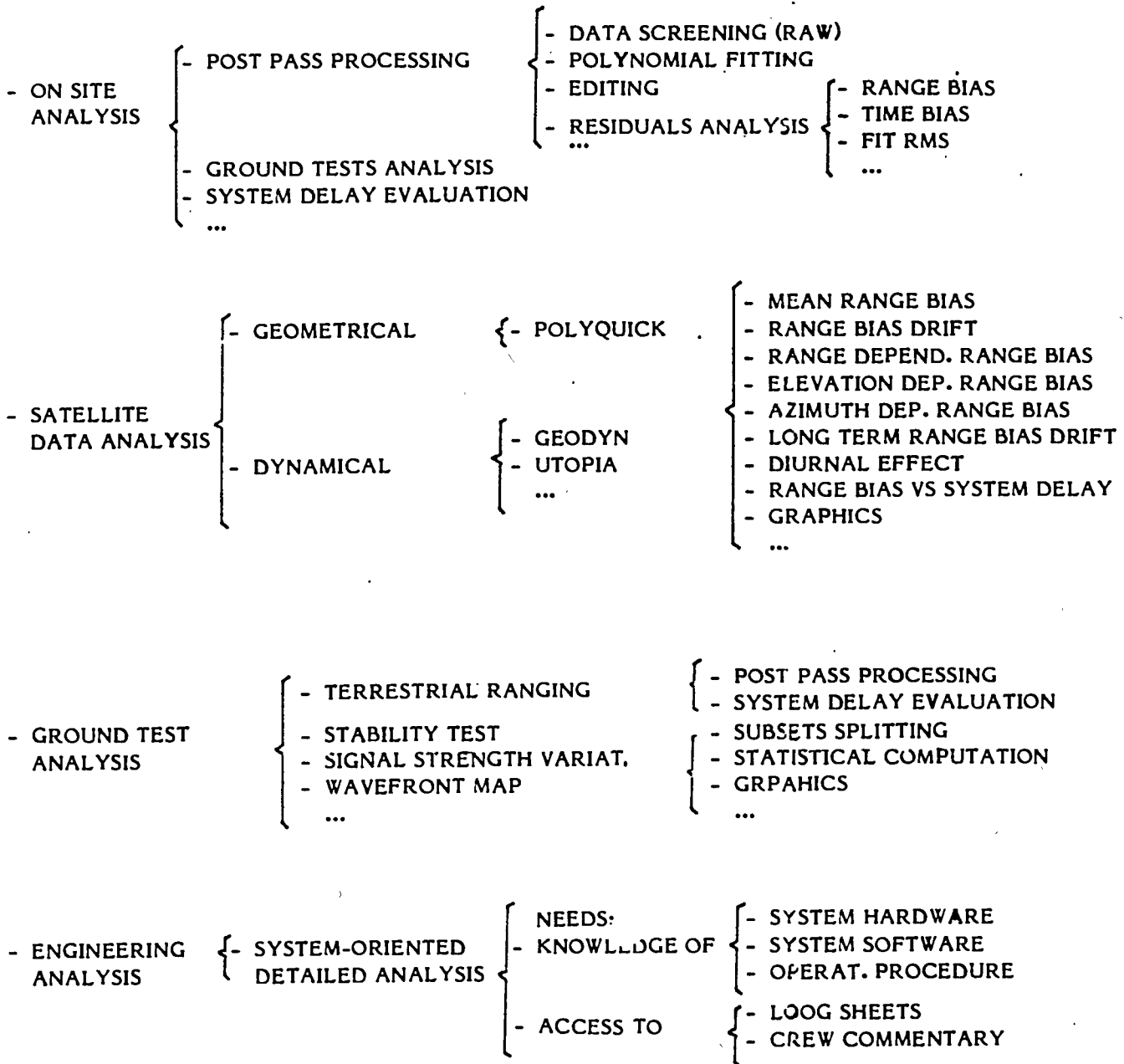
Tab. 3.1

Overview of the principal sources
of differences in Data Processing

Tab. 3.2

TAB. 4

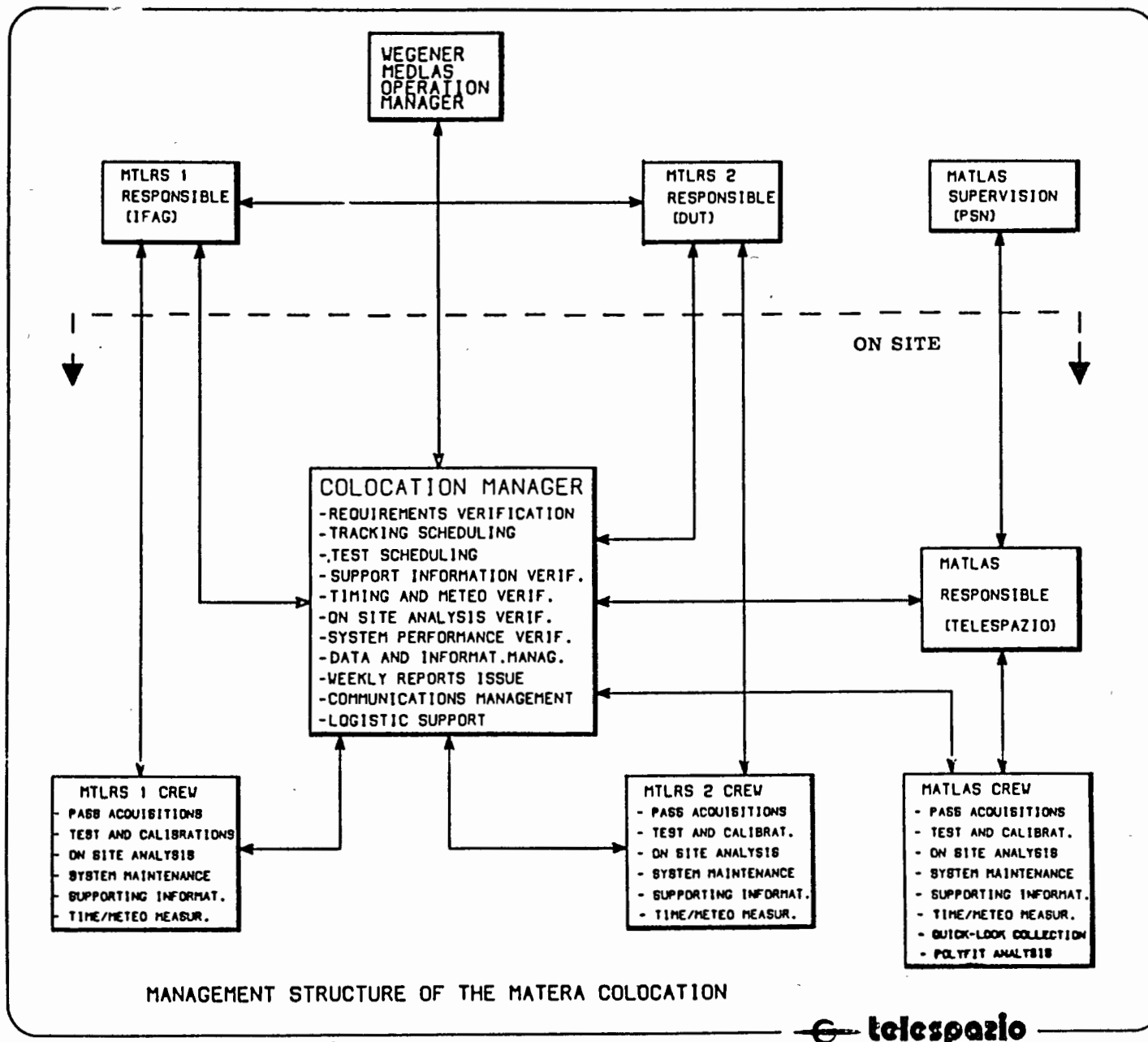
COLOCATION DATA ANALYSIS OVERVIEW



TAB. 5

COLOCATION REPORTS SUMMARY

<u>DOCUMENT</u>	<u>SCHEDULING</u>	<u>CONTENTS</u>	<u>DISTRIBUTION</u>
- COLOCATION PLANE	BEFORE COLOCATION	COLOCATION MANAGEMENT	ALL PARTICIPATING GROUPS
- SITE SURVEY	BEFORE COLOCATION	SURVEY OF THE COLOCATION SITE (TO BE UPDATED AFTER POST-SURVEY)	ALL INVOLVED GROUPS
- DAILY OPERATIONAL	DAILY	SUPPORTING INFORM. ON SITE ANALYSIS. ...	ON SITE MANAGEMENT
- WEEKLY OPERATIONAL	WEEKLY	SUPPORTING INFORM. ON SITE ANALYSIS ...	ALL PRE-PROCESSING AND ANALYSIS CENTERS
- FINAL OPERATIONAL	N.A.	FINAL UPDATED OPERATIONAL REPORT (TO BE INCLUDED IN FINAL REPORT)	ALL INVOLVED GROUPS
- INTERMEDIATE ANALYSIS	AS SOON AS AVAILABLE	INTERMEDIATE ANALYSIS RESULTS	INTERCHANGED BETWEEN ALL ANALYSIS CENTER
- INDIVIDUAL ANALYSIS	N.A.	FINAL RESULTS FROM EACH GROUPS	COMMITTEE
- FINAL ANALYSIS	N.A.	FINAL AGGREGATED RESULTS (TO BE INCLUDED IN FINAL REPORT)	ALL INVOLVED GROUPS
- FINAL REPORT	N.A.	FINAL COLOCATION REPORT (OPERATIONAL AND ANALYSIS) PREPARED JOINTLY BY ALL COMMITTED GROUPS	SCIENTIFIC COMMUNITY



MANAGEMENT STRUCTURE OF THE MATERA COLOCATION



Fig. 1

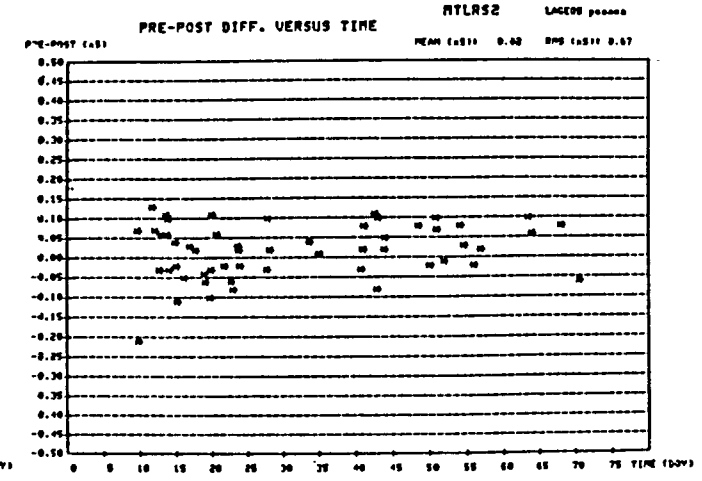
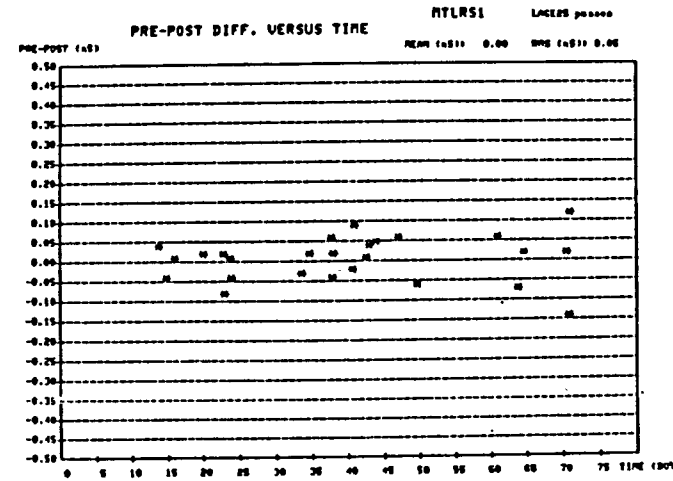
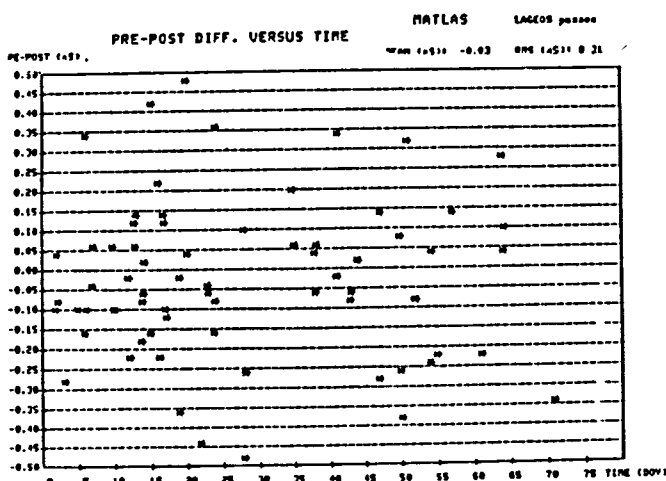
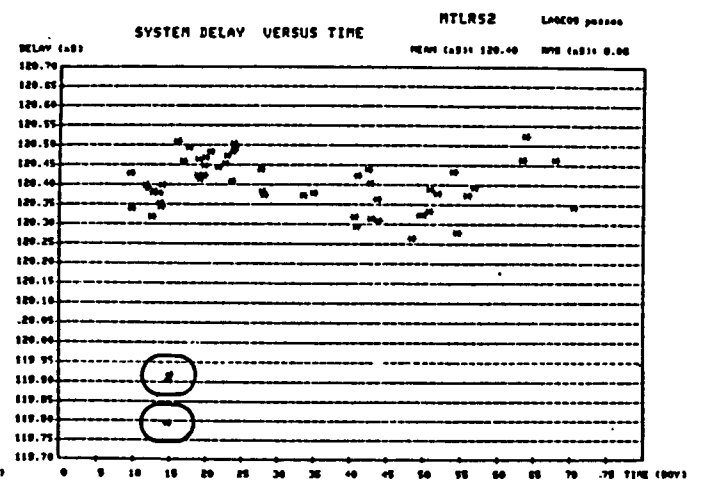
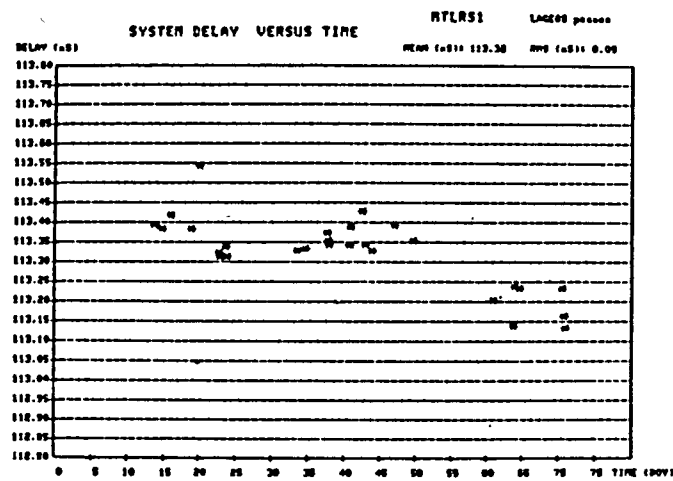
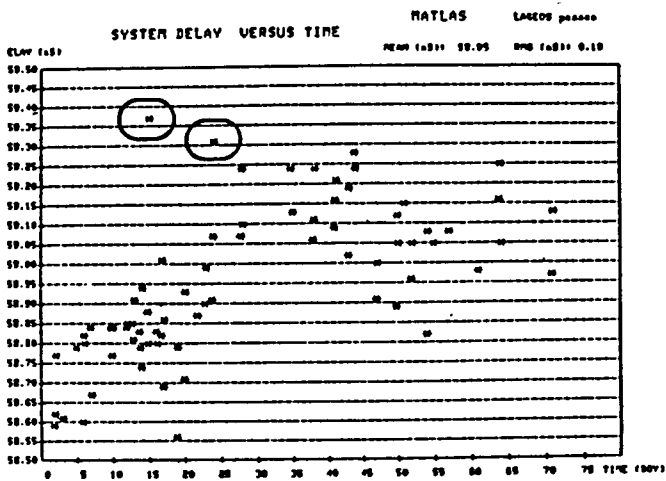


Fig. 2.1

System delay calibrations during the Matera Colocation

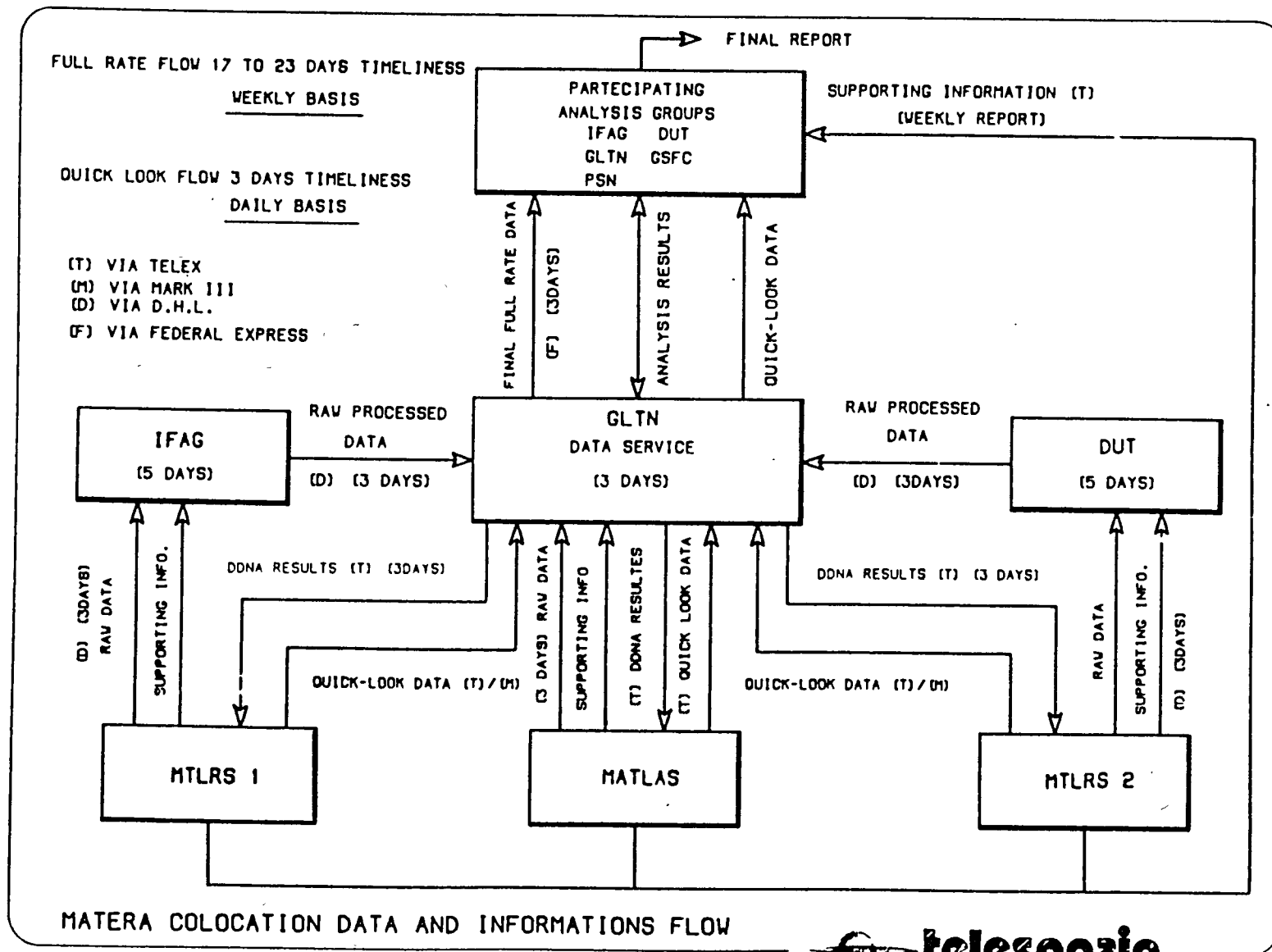


Fig. 2.2

- MATERA CO-LOCATION -

- WEEKLY REPORT FROM TO 1986 -

- WEATHER CONDITIONS -

DAY	TEMP (DEG)	PRES (MBAR)	HUM (%)	WIND (KM/H)	CLOUD	FOG	RAIN
-----	-----	-----	-----	-----	-----	-----	-----

STATION 7541 MTLRS2

- PASSES INFORMATION -

PASSES	LAGEOS	STARLETTE
- A PRIORI ACQUIRABLE		
- ACQUIRED		
- NOT ACQUIRED (DUE TO WEATHER)		
- NOT ACQUIRED (DUE TO PROBLEMS)		

- OBSERVED PASSES INFORMATION -

STAT NAME	SAT NAM	START EPOCH YYMMDD HHMM	END HHMM	TOT OBS	VALID OBS	RANGE BIAS(m)	TIME BIAS(mS)	FIT RMS(m)
-----	-----	-----	-----	-----	-----	-----	-----	-----

- POLYFIT ANALYSIS -

STAT NAME	SAT NAM	START EPOCH YYMMDD HHMM	END HHMM	TOT OBS	NO REJECTION		2.5 SIGMA REJECTION	
					VALID OBS	FIT RMS(L)	VALID OBS	FIT RMS(M)
-----	-----	-----	-----	-----	-----	-----	-----	-----

- TERRESTRIAL TARGETS RANGING -

DAY/TIME	TARGET	RANGE AVER(NS)	RANGE RMS(NS)	TEMP (DEG)	PRES (MBAR)	HUM (%)	PRE (NS)	POST (NS)
-----	-----	-----	-----	-----	-----	-----	-----	-----

- TIMING DATA -

DAY	TIME	UTC(MTL2)- UTC(GPS) (NSEC) SV	TIME	UTC(MTL2)- UTC(USNO) (NSEC)	TIME	UTC(MTL2)- UTC(MATL) (NSEC)
-----	-----	-----	-----	-----	-----	-----

- OFF LINE ACTIVITIES -

- REMARKS -

Fig. 2.3

An example of weekly Report

MATERA CO-LOCATION

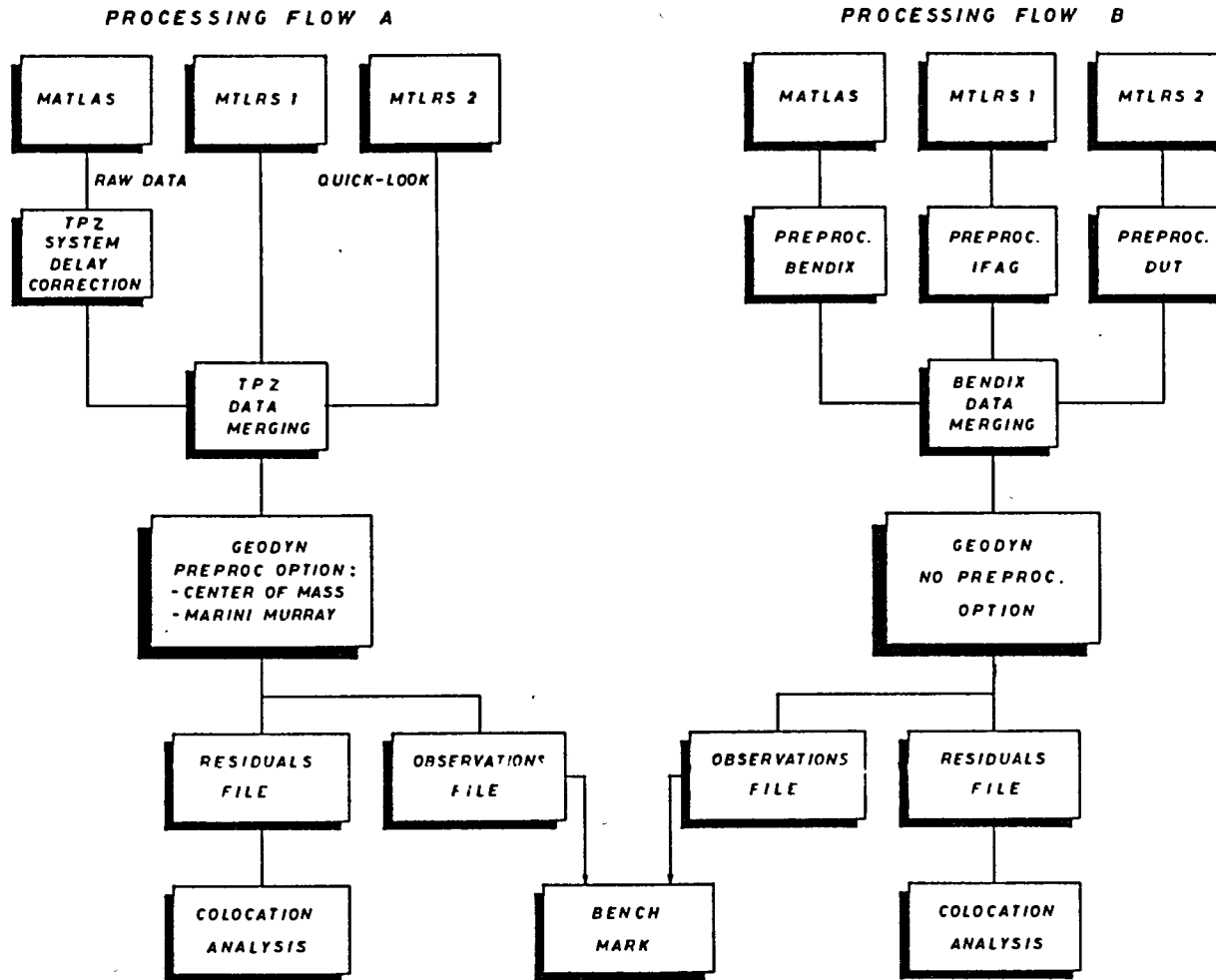


Fig. 3

An example of Analysis and Benchmark Processing

ECCENTRICITY VECTORS FOR COLOCATION PURPOSES

D.L.F. Van Loon
Delft University of Technology
Observatory for satellite Geodesy
P.O. Box 581
7300 An Apeldoorn - The Netherlands

Telephone 32 5769 341
TWX 36442 SATKO NL

ABSTRACT

Colocation testing is accepted as the only reliable method to determine systematic differences between operational laser ranging systems. To enable a direct comparison between two such systems the eccentricity vector between the reference points of the concerning instruments has to be determined. The current satellite laser ranging systems perform observations at the centimeter and even sub-centimeter level. Consequently the connecting eccentricity vector has to be determined with similar or higher accuracy.

In practice the determination passes in two steps :

- determination of the eccentricity vector between the prime markers on the respective pads, provided by a first order geodetic survey, and
- determination of the eccentricity vector between the reference point of the instrument and the prime marker, based on known instrumental parameters, eventually supplemented either with a typical instrumental establishing procedure or with other necessary geodetic measurements.

To identify systematic differences in laser ranging systems different observation techniques are applied viz : range measurements to terrestrial targets and range measurements to satellites.

Dependent on the observation technique and the analysis procedure the final eccentricity vector has to be given either in a local or in a global reference frame.

1. Introduction.

In planning of establishing a geodetic network using similar or even different types of Satellite Laser Ranging (SLA) stations, both stationary and transportable, a calibration of the concerning instruments is to be considered as necessary before going into the field.

Since third generation laser systems have a single shot precision of some centimeters, the colocation testing procedure seems to be the only reliable method to recognize systematic ranging differences between such instruments.

A direct comparison of both satellite ranging observations and terrestrial target ranging observations taken by the individual stations during simultaneous tracking offers the opportunity to evaluate laser ranging performance at the centimeter and subcentimeter level.

Different analysis methods are applied for the evaluation of colocation data, whereby the relative position of the involved instruments (the eccentricity vector) anyhow has to be determined. MERIT guidelines for geodetic survey [MERIT,83] recommend a precision better than 5 millimeter.

The determination of the eccentricity vector (fig.1.1) between the reference points of the instruments passes in practice in two separate steps:

1. between the prime markers at the respective pads (Section 3),
 2. between the reference point of the instrument and the prime marker at the pad (Section 4),
- both with their specific requirements.

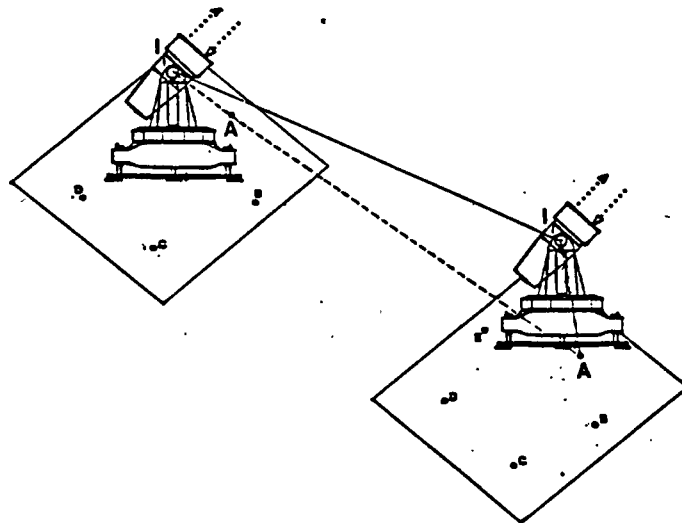
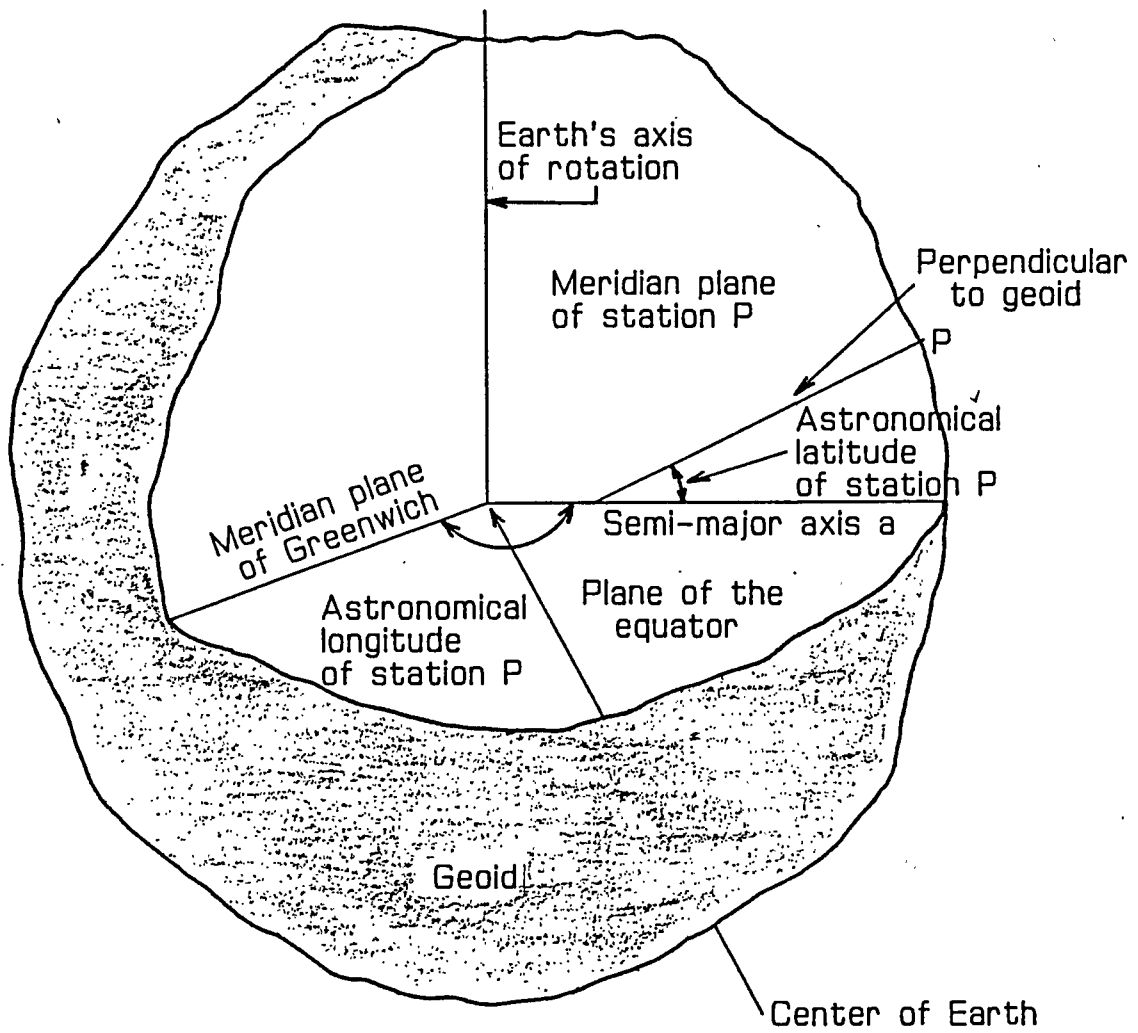


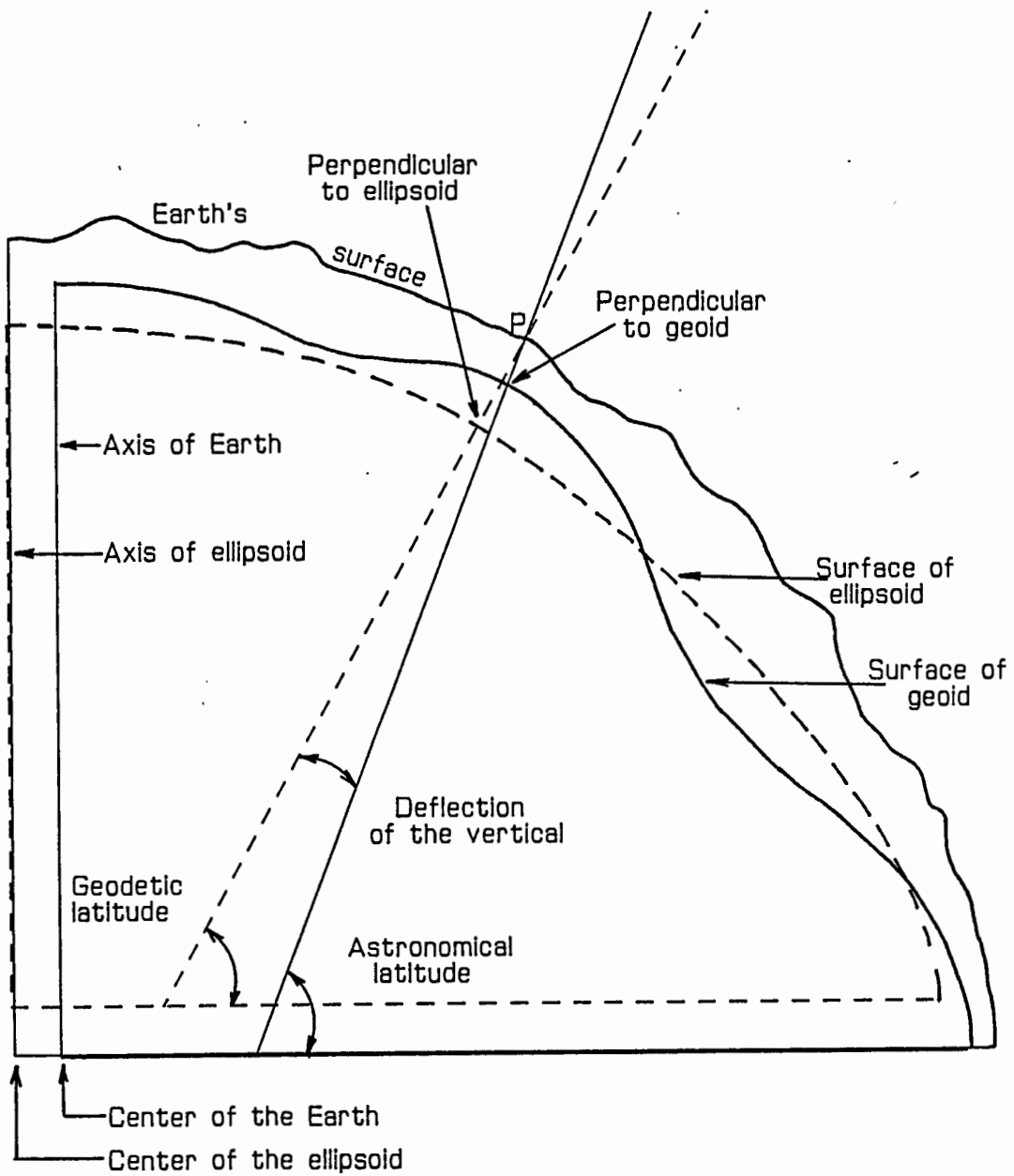
fig.1.1 Eccentricity vector between two SLA systems.

I refers to the reference point of the instrument, while A refers to the prime marker at the pad.



ASTRONOMICAL COORDINATES

fig.2.1



DEFLECTION OF THE VERTICAL
AT STATION P

2. Reference frames.

2.1 Introduction.

Satellite ranging observations and terrestrial target ranging observations are performed by astrometric instruments, whose orientation are referred to the directions of the local plumbline and the astronomical north. A direct comparison between the range observations emphasizes a determination of the eccentricity vector in a reference frame of an orientation, referred to the same directions.

2.2 Station coordinates.

The station position itself is on the surface of the earth defined relative to the Greenwich meridian and the equatorial plane.

As mentioned previously the observations are made with reference to the local plumbline at the station of observation P (fig.2.1 and fig.2.2).

The astronomical latitude is referred to the normal of the geoid and does not coincide exactly with the direction of the plumbline at station P and needs therefore a standard correction of

$$\Delta\phi'' = -0.000171 h \sin 2\phi \quad (2.1)$$

where ϕ is the latitude and h the geoid height at P. In general this correction can be neglected.

The longitude of station P is the angle between the meridian plane of station P and the Greenwich meridian plane.

Astronomical determinations refer to an instantaneous axis and to the equator, and by a motion of the earth relative to the axis of rotation, reduction to a common or mean position of the pole is then required.

2.3 Transformations.

Dependent on the analysis method and using either ranges to satellites or ranges to terrestrial targets, the eccentricity vector is required either in a local reference frame whose axes are referred to the local vertical and astronomical north or in a global reference frame whose axes are referred to the instantaneous pole and the Greenwich meridian. It is to recommend to follow the MERIT Guidelines [MERIT,83] defining the offsets DX, DY, DZ in a coordinate system defined by the FK-4 Fundamental Star Catalog and referred to the pole and origin of longitude using polar coordinates and time information published by the Bureau International de l'Heure.

Transformation results into the following formulas:

$$(\underline{X}^2) = R_3(\gamma) \cdot (\underline{X}^1) \quad (2.2)$$

$$(\underline{X}^3) = R_3(-\Lambda) \cdot R_2(90 + \emptyset) \cdot (\underline{X}^2) \quad (2.3)$$

where (\underline{X}^1) is the eccentricity vector in an arbitrary local system, referred to the local vertical,

(\underline{X}^2) is the eccentricity vector in a local system oriented to the astronomical north direction and referred to the local vertical,

(\underline{X}^3) is the eccentricity vector in the global system oriented to the pole and Greenwich meridian,

γ is the rotation angle in the horizontal plane in order to orient the system with respect to the astronomical north direction,

\emptyset, Λ are respectively astronomical latitude and longitude.

3. Eccentricity vector between the prime markers.

3.1 Introduction.

Determination of the eccentricity vector between the prime markers at the respective pads has to be performed by a first order geodetic survey.

Mutual distances and 3-dimensional geometry of the collocating stations affect the accuracy to be required.

3.2 Survey equipment.

Table 3.1 summarizes geodetic survey equipment that has to be available in general. Section 2 mentioned already the rotation parameters to be determined, but also for setting-up the local network distance, angle and height difference measurements have to be made.

Besides this list is completed with information of precision, use and purpose of each individual instrument.

<u>EQUIPMENT</u>	<u>PRECISION</u>	<u>TO USE FOR MEASUREMENTS OF</u>
measuring tape	20 ppm)
invar tape	2 ppm) 1. distances
EDM instruments	2 mm + 2 ppm)
theodolite	1-4 mdegrees	2. horizontal angles 3. vertical angles
leveling instrument	2 ppm	4. height differences
clock and stopwatch	0.1 sec.	5. hourangle of sun or stars
<u>PURPOSE:</u>		
1.) + 2.) + 3.)	Determination of vector in an arbitrary local reference frame	
4.)	To measure direct height differences	
2.) + 5.)	Determination of astronomical azimuth	
3.) or 4.) + 5.)	Determination of astronomical latitude and longitude	

Table 3.1. Summary of equipment and its purpose.

3.3 Survey reconnaissance.

3.3.1 Influence of distance and vertical angle measurements on the vertical component of a local coordinate system.

The influence of distance and vertical angle measurements on the vertical component can simply be derived, assuming without correlation:

$$\sigma_H = \sqrt{HD^2 \cdot \sigma_\alpha^2 + \frac{H^2}{HD^2 + H^2} \cdot \sigma_D^2} \quad (3.1)$$

where σ_α is the precision in the vertical angle measurements,
 σ_D is the precision in the distance measurements,
 HD is the estimated horizontal distance,
 H is the estimated height difference,
 σ_H is the expected precision in the vertical component.

HD(m)	H(m)	σ_H (mm)
20	0-8	1.6
30	0-8	1.8
40	0-8	2.2
50	0-8	2.7
60	0-8	3.2
70	0-8	3.7

Table 3.2 Expected precision in H: (σ_H).
 Assumed precisions: $\sigma_D = 3$ mm, $\sigma_\alpha = 0.003$ degr.

Table 3.2 gives an example for the Matera station and it should be noted that if a maximum tolerance of 3 mm is accepted and if the horizontal distances are larger than 50 m, it is to be preferred to measure the vertical component direct with a leveling instrument instead of calculating it from distance and vertical angle measurements.

3.3.2 Influence of astronomical observations.

An astronomical azimuth determination in order to rotate an arbitrary local system to a local system referred to the astronomical north direction, causes a maximum error in the horizontal vector components, simply expressed as

$$e = \frac{HD \cdot \sigma_A}{206.265} \quad (3.2)$$

where e is the maximum error in the horizontal components (in mm),
 and $\frac{HD}{\sigma_A}$ is the horizontal distance between the stations (m),
 σ_A is the estimated precision in the astronomical azimuth determination (arcsec.).

The influence of the astronomical latitude and longitude determination on the vector components can be derived from (2.1) and (2.2).

However for practical reasons it is to be preferred to ascertain a maximum tolerance in the individual vector components and then to consider the highest precision of determination of latitude and longitude to require after their successive rotations.

$$\sigma_{\phi_1}'' = \frac{e \cdot 206.265}{-\cos \Lambda \cdot \cos \phi \cdot DX + \cos \Lambda \cdot \sin \phi \cdot DZ} \quad (3.3)$$

$$\sigma_{\phi_2}'' = \frac{e \cdot 206.265}{-\sin \Lambda \cdot \cos \phi \cdot DX + \sin \Lambda \cdot \sin \phi \cdot DZ} \quad (3.4)$$

$$\sigma_{\phi_3}'' = \frac{e \cdot 206.265}{-\sin \phi \cdot DX - \cos \phi \cdot DZ} \quad (3.5)$$

$$\sigma_{\Lambda_1}'' = \frac{e \cdot 206.265}{\sin \Lambda \cdot \sin \phi \cdot DX + \sin \Lambda \cdot \cos \phi \cdot DZ - \cos \Lambda \cdot DY} \quad (3.6)$$

$$\sigma_{\Lambda_2}'' = \frac{e \cdot 206.265}{-\cos \Lambda \cdot \sin \phi \cdot DX + \cos \Lambda \cdot \cos \phi \cdot DZ + \sin \Lambda \cdot DY} \quad (3.7)$$

where $\sigma_{\phi_1}, \sigma_{\phi_2}, \sigma_{\phi_3}$ is the precision in the required latitude,
 $\sigma_{\Lambda_1}, \sigma_{\Lambda_2}$ is the precision in the required longitude,
 DX, DY, DZ are the coordinate differences between the stations (in m),
 e is the maximum error in the individual components of the coordinate system (in mm),
 ϕ, Λ are resp. latitude and longitude.

STATION	DX (m)	DY (m)	DZ (m)	HD (m)	e (mm)	σ_A (arcsec.)	σ_ϕ	σ_Λ
7939	0	0	0					
7540	-17.3	-31.7	-7.2	36.9	3	17	37	24
					1	6	12	8
7541	-33.7	-33.6	-7.5	48.2	3	12	22	17
					1	4	7	5

Table 3.3 Requirements for the determination of the astronomical rotations at the Matera Station. Latitude = 40.6 degr. Longitude = 16.7 degr.
 DX) approximate differences in resp. east,
 DY) north and up vector components
 DZ)
 HD approximate horizontal distance
 e max. tolerance in the vector components after rotation
 σ_A) max. acceptable error in resp. the
 σ_ϕ) astronomical azimuth, latitude and
 σ_Λ) longitude determination.

Table 3.3 shows a survey reconnaissance with respect to the astronomical parameters, i.c. the Matera site as an example.

If we accept a maximum error of 3 mm in the separate vector components, the determination of resp. azimuth, latitude and longitude must be performed with a precision better than 12, 17 and 22 arcseconds.

Obviously in this case we may not use the geodetic latitude and longitude as rotation parameters, because we know from geoid maps [BRENECKE et al,1983] that the deflection of the vertical (fig.2.2) at the Matera site is more than 30 arcseconds.

3.3.3 Final measurements and results.

After a thorough reconnaissance and selection of the right survey equipment and after the geodetic survey has been performed, the final results of the network, successively in an arbitrary local coordinate system, a local coordinate system oriented to astronomical north direction and a global coordinate system, have to be tested properly on the precision and reliability anyhow.

<u>DETERMINATION OF:</u>	<u>USED EQUIPMENT</u>	<u>RMS</u>
eccentricity vector in the arbitrary local reference frame	EDM and theodolite (KERN)	3 mm
astronomical azimuth	KERN theodolite and clock/stopwatch	11 arcsec.
astronomical latitude	MTLAS-1 and MTLAS-2	5 arcsec.
astronomical longitude	MTLAS-1 and MTLAS-2	5 arcsec.

Table 3.4 Some results at the Matera site.

Table 3.4 shows the tested final results for the Matera site as an example [CENCI et al,1986].

4. Eccentricity vector between the reference point of the instrument and the prime marker.

Determination of the eccentricity vector between the reference point of the instrument and the prime marker at the pad can be performed by an establishing procedure dependent on the specific characteristics of the instrument.

The precise reference point of each instrument must be identified thoroughly e.g. the intersection of azimuth and elevation axes. It is important that the observed ranges to both satellites and terrestrial targets are also referred to this precise reference point.

Usually the offset of an auxiliary reference point to the prime marker is determined, while the offset of the precise reference point to this auxiliary point is reconstructed from the design.

To seek for a determination procedure of the separate offsets is strongly recommended, where especially a regular calibration of the instrumental offset parameters is certainly included.

A reliable determination procedure of this eccentricity vector is applied with the MTLRS [VERMAAT et al, 1983 and VERMAAT, 1984].

Because the eccentricity vector between the reference points of the instruments is required with a precision better than 5 mm, and while in general the precision in the determination of the eccentricity vector between the prime markers will be in the order of 3 mm, consequently the precision of the eccentricity vector between the reference point of the instrument and the prime marker must be then guaranteed with a precision better than 2 mm.

5. Conclusions and recommendations.

Prior to the definitive construction of the pads at a colocation site, their relative location has to be settled on basis of geodetic requirements such as geometry, mutual distances and height differences.

The first order geodetic survey has to be performed with great care and with the proper geodetic instruments. The final results have to be tested on precision and reliability. A pre and post geodetic survey is to recommend.

A critical part of the determination of the final eccentricity vector is the determination of the offset of the precise reference point to the prime marker, that often seems to be neglected. A regular calibration, eventually verified with a geodetic survey is not abundant and to seek for a well defined determination procedure with testing possibilities on precision and reliability, is highly recommended, certainly in case of transportable systems.

References

Vermaat, E. and B.H.W. van Gelder, 1983. "On the eccentricity of MTLRS." Delft University of Technology, Reports of the Department of Geodesy, Mathematical and Physical Geodesy, No. 83.4.

Vermaat, E. "Establishing ground ties with MTLRS.", Proceedings of the fifth international workshop on laser ranging instrumentation, Herstmonceux Castle, United Kingdom, 1984 page 47.

MERIT/COTES JOINT WORKING GROUPS. "Merit campaign : connection of reference frames - implementation plan -." Bureau International de l'Heure, Paris, France, 1983.

Cenci, A. and D.L.F. van Loon, 1986. "Survey of the Matera laser station site." Telespazio S.p.A., Rome, Italy.

Schanzle, A.F., "Lectures on orbit determination and trajectory analysis." EG and G, Washington analytical services center, Inc., USA.

Mueller, I.I., 1968. "Spherical and practical astronomy as applied to geodesy." Frederick Ungar Publishing Co., New York, USA.

Brennecke, J., D. Leigemann, E. Reinhart and W. Torge, W. Weber, H.-G. Wenzel, 1983. "An european astro-gravimetric geoid.", Reihe D, heft nr. 269, Deutsche Geodaetische Kommission, Frankfurt a.M., FRG.

POLYQUICK COLLOCATION ANALYSIS

V. Husson, D. Edge
Bendix Field Engineering Corporation,
Columbia, Maryland - U.S.A. -

Telephone (301) 344 5013
TWX 197700 GLTN

ABSTRACT

POLYQUICK is a purely mathematical collocation analysis system that has been used as a key analysis tool of collocated laser data for the last five (5) years. POLYQUICK geometrically corrects the ranges from the standard system to the test system using measured or computed angles. The range error introduced in the geometric correction is dependent on the closeness of the two systems and the standard system angle accuracy. The range error is less than 1 cm if the two systems are within 60 meters of each other and if the standard system angles are accurate to 0.01 degrees

Only collocated simultaneous passes are analyzed. A least squares polynomial is fit through the standard system geometrically corrected range on a pass-by-pass basis. The polynomial generated for each pass is then used to analyze the test system data and to generate residual statistics for both stations for every simultaneous pass. Time batched normal points are created from the polynomial fit for each system for each collocated pass. These normal points are then differenced if there is an acceptable amount of data from each station in that time interval. The normal point differences then are stored for every collocated pass so that the aggregate collocation data set can be analyzed for every bias test contained in the collocation analysis plan. These bias tests have revealed systematic biases when there is an adequate number of healthy simultaneous LAGEOS passes taken over an extended period of time.

POLYQUICK COLLOCATION ANALYSIS CONCEPTS

- * MATHEMATICAL TECHNIQUES
- * SIMULTANEOUS COLLOCATION SATELLITE RANGING OBSERVATIONS
- * SATELLITE ANGLE DATA FROM ONE STATION
- * STATION SURVEY GEOMETRY
- * GEOMETRIC RANGE TRANSLATION
- * POLYNOMIAL DATA FIT TO REFERENCE STATION
- * COMPARISON OF OBSERVATION RESIDUALS
- * EVALUATION OF PASS AND AGGREGATE DATA SET STATISTICS

POLYQUICK COLLOCATION ANALYSIS SYSTEM

INPUTS

Merged Collocation
Satellite Ranging
Observations With
Supporting Angles

Survey Data For
The Collocating
Stations

PROCESS

Geometric Range Translation
Simultaneous Data Selection
Polynomial Fit
Normal Point Computation
Observations and Normal Point
Residual Computations
Comparison Statistics Computations

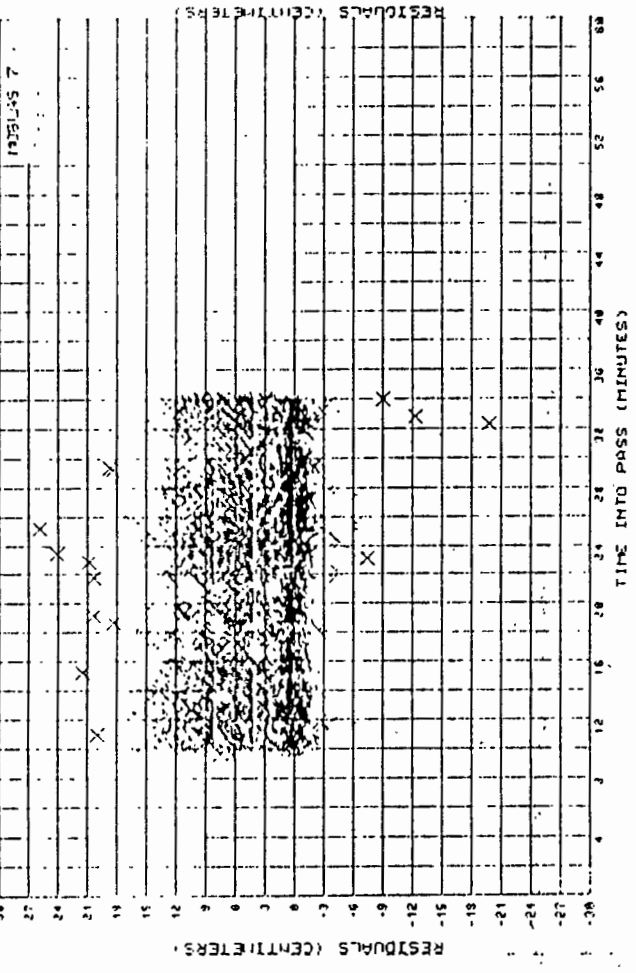
OUTPUTS

Plots
Histograms
Statistics
Data

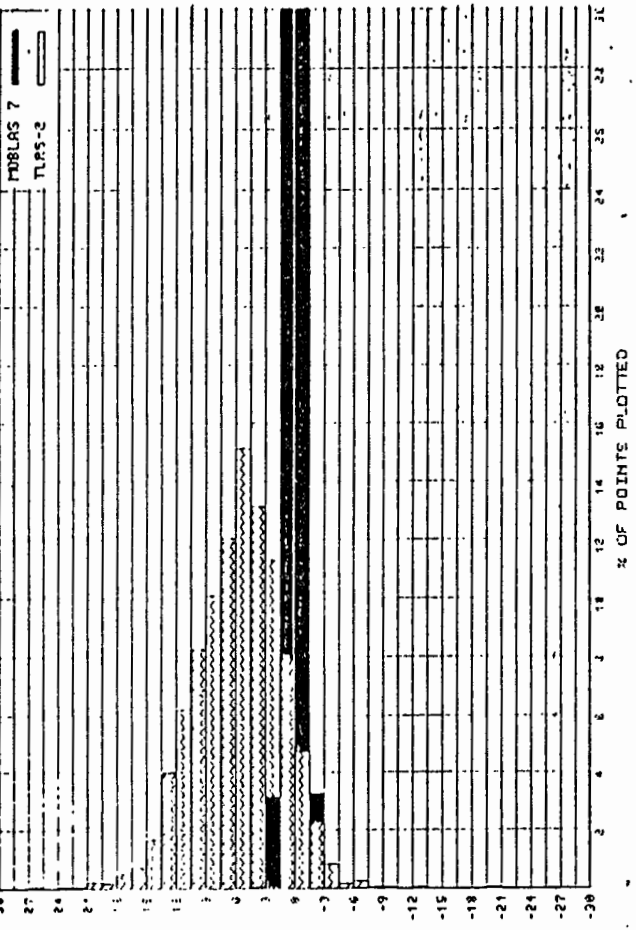
PERFORMANCE EVALUATION

Pass Analysis
Aggregate Data Set Analysis

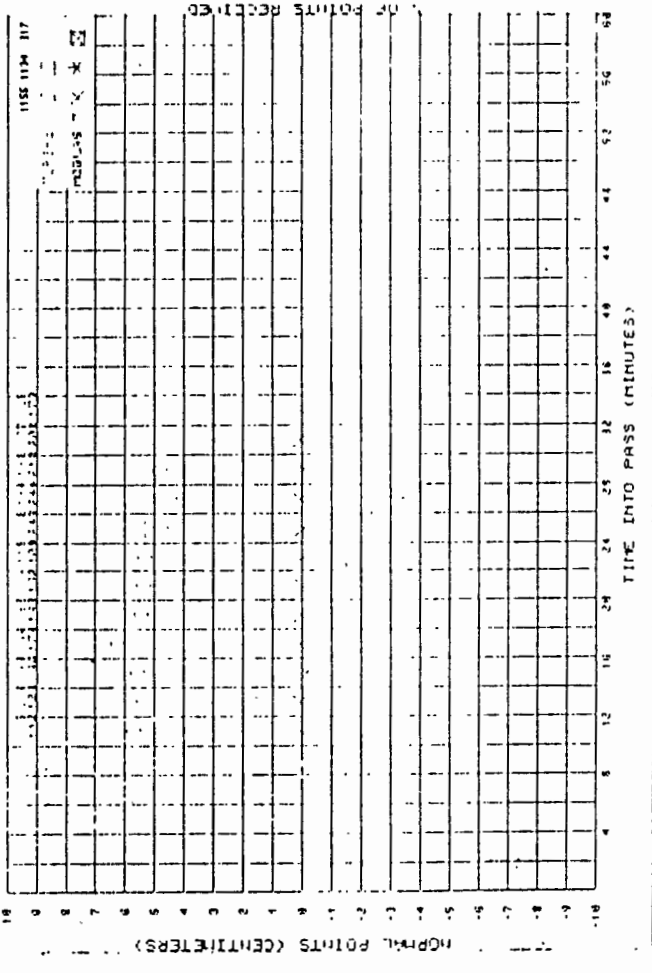
LAGEOS
8/30/88 - 9:16



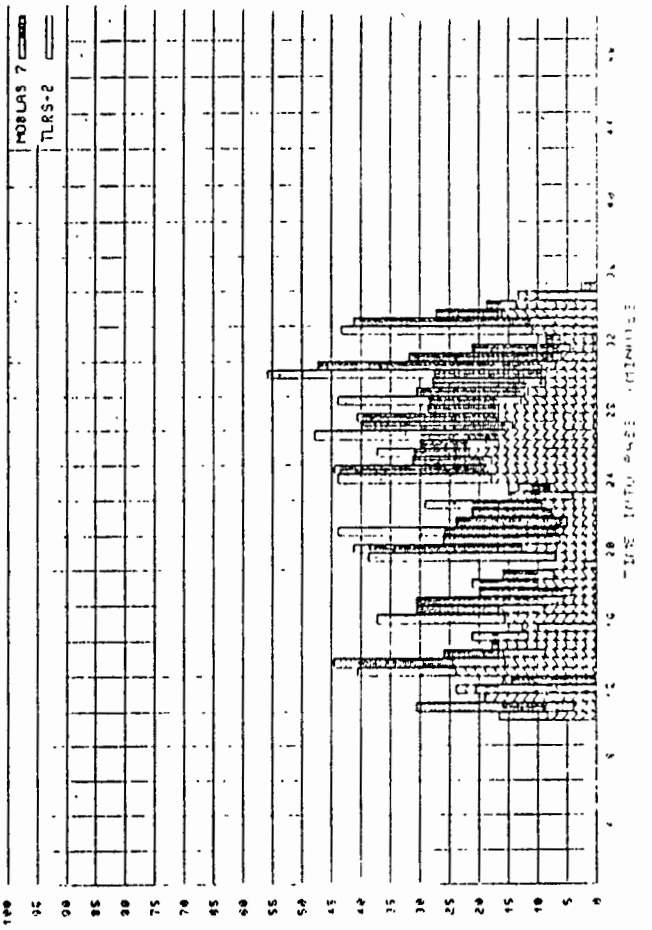
LAGEOS
8/30/88 - 9:16



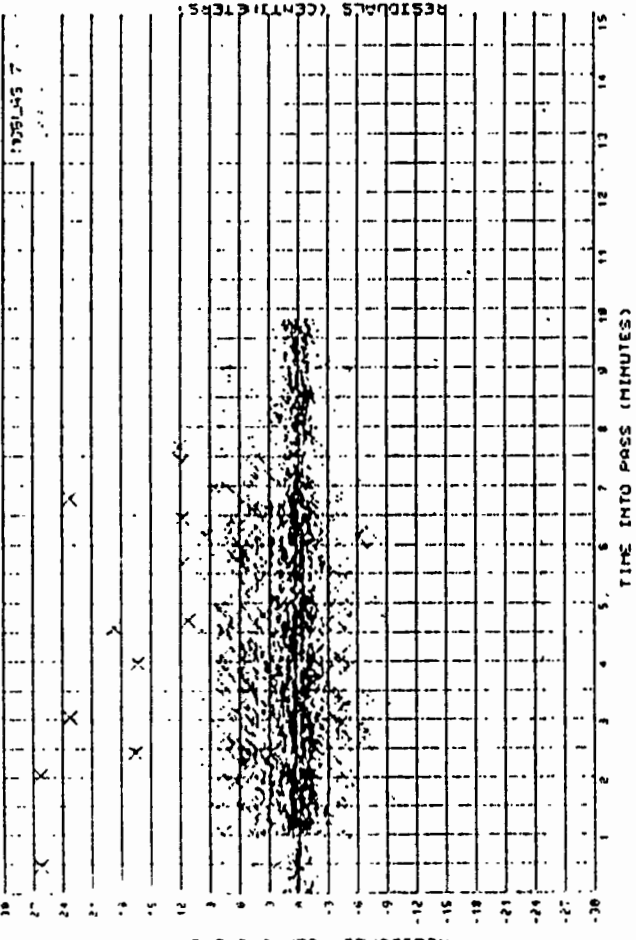
LAGEOS
8/30/88 - 9:16



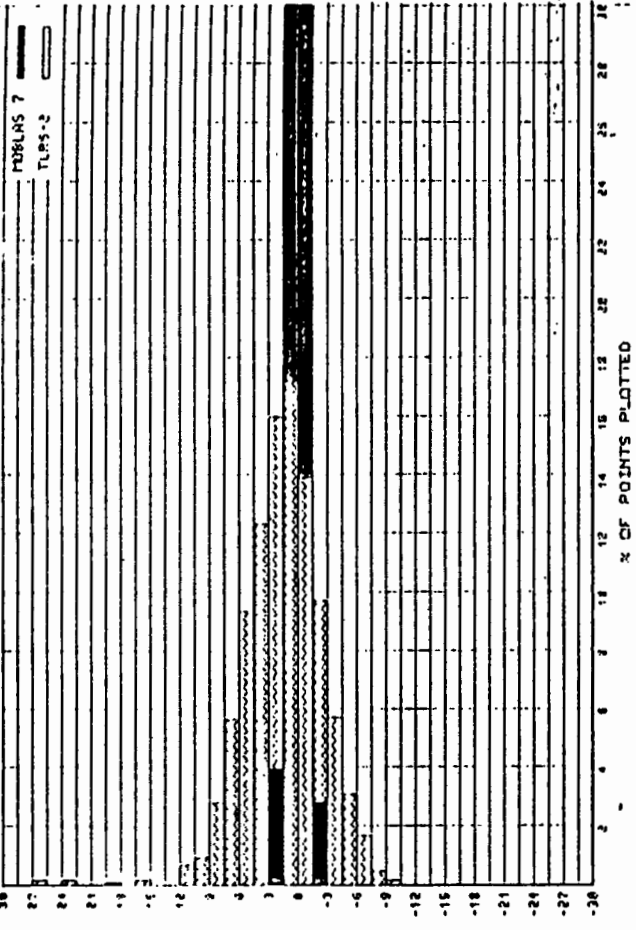
LAGEOS
8/30/88 - 9:16



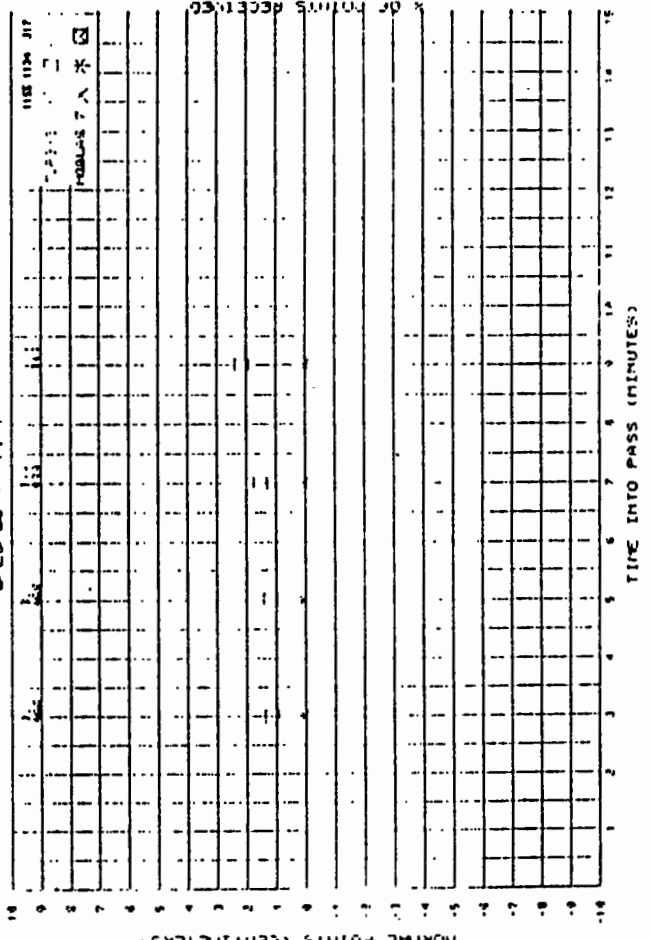
STARLETTE
8-26-88 - 7: 7



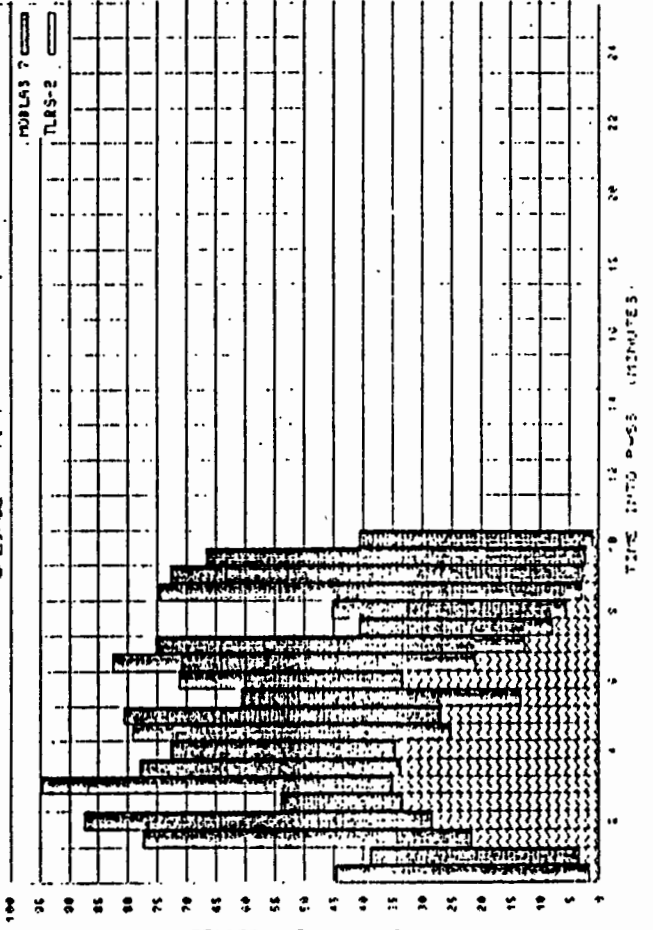
STARLETTE
8-26-88 - 7: 7



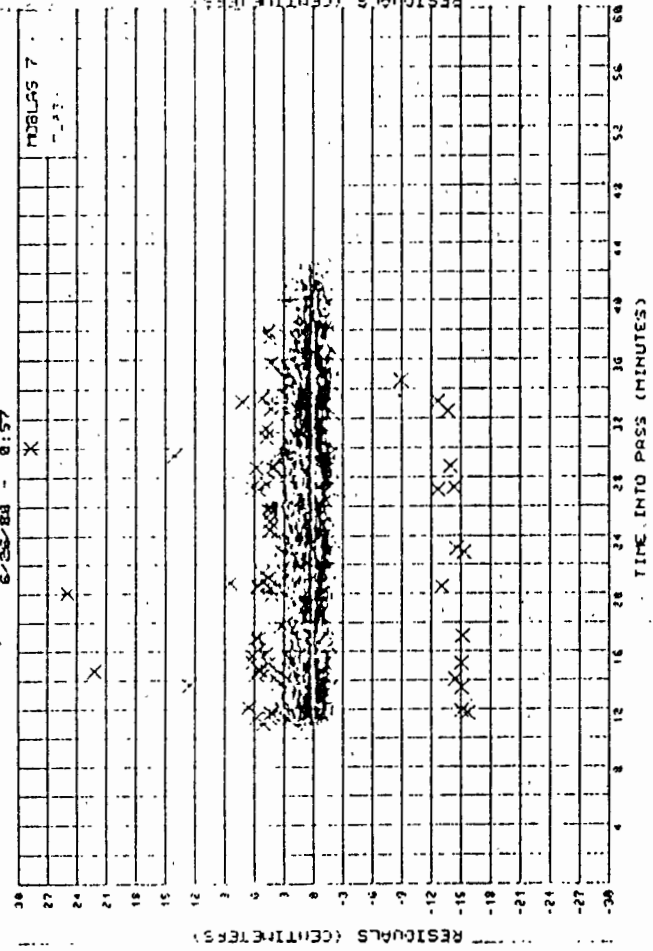
STARLETTE
8-26-88 - 7: 7



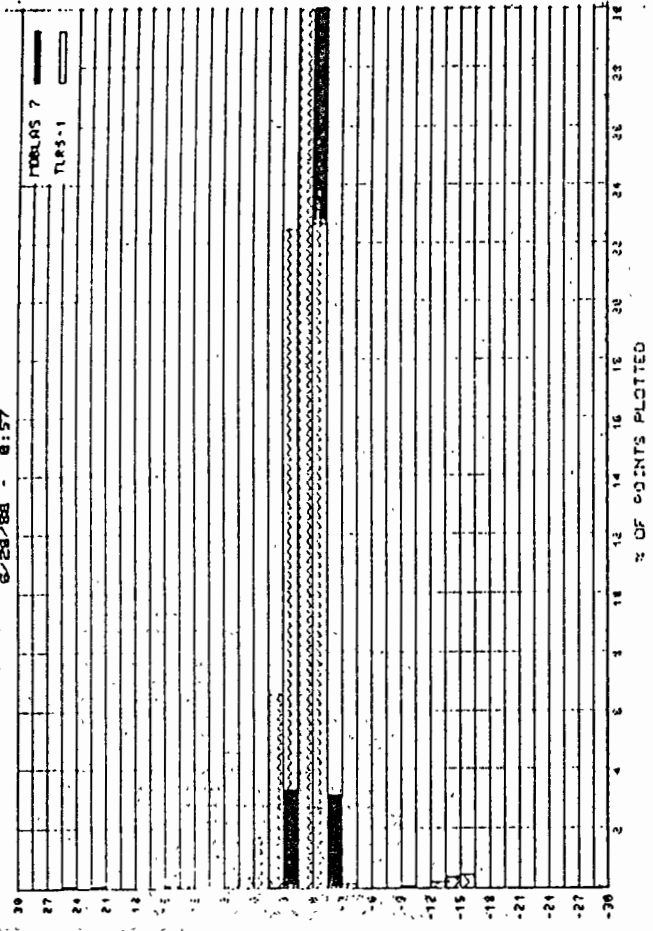
STARLETTE
8-26-88 - 7: 7



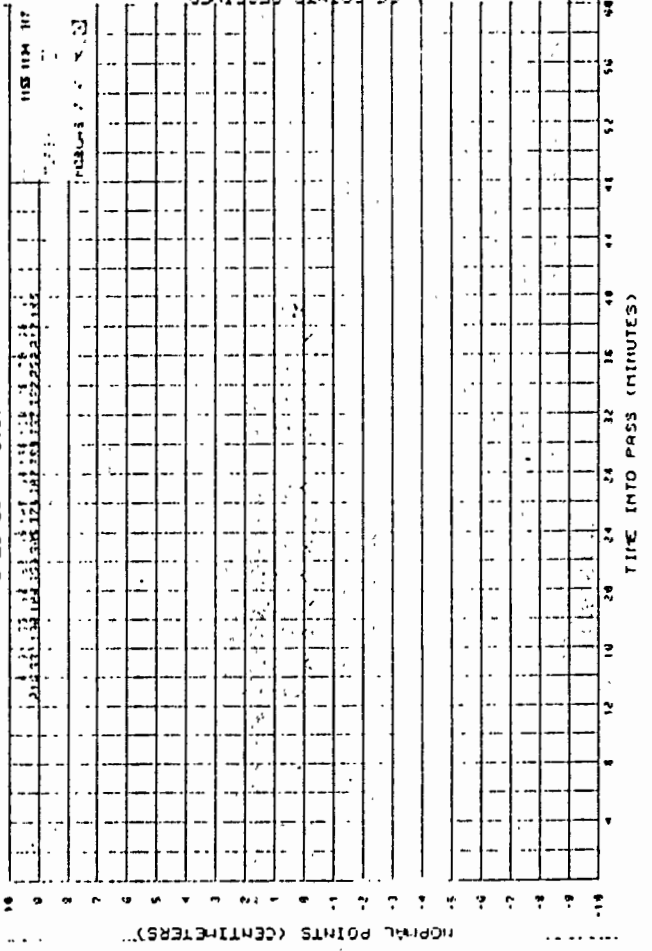
LAGEOS
6-26-86 - 0:57



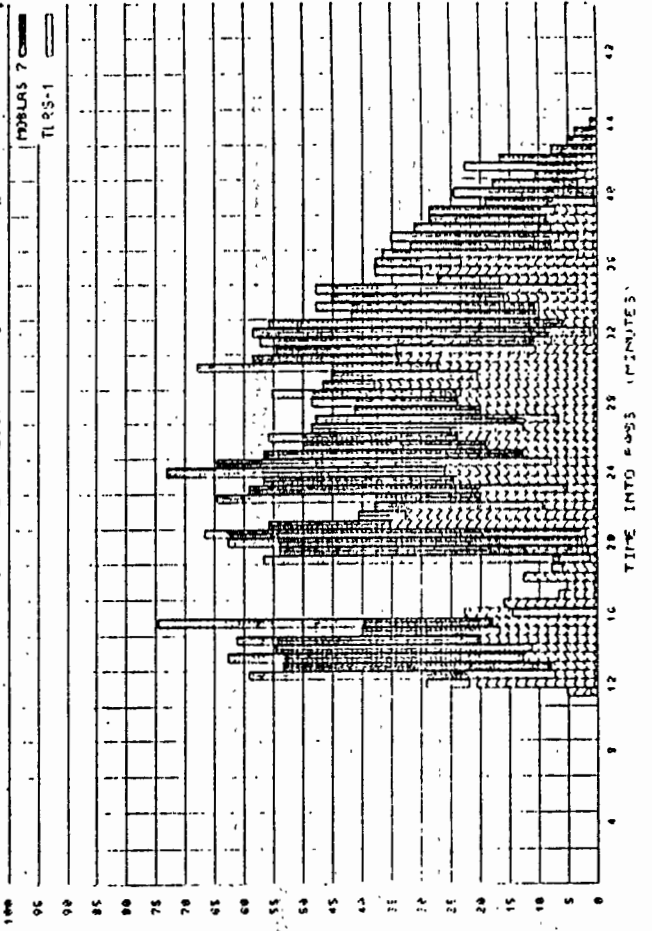
LAGEOS
6-26-86 - 0:57



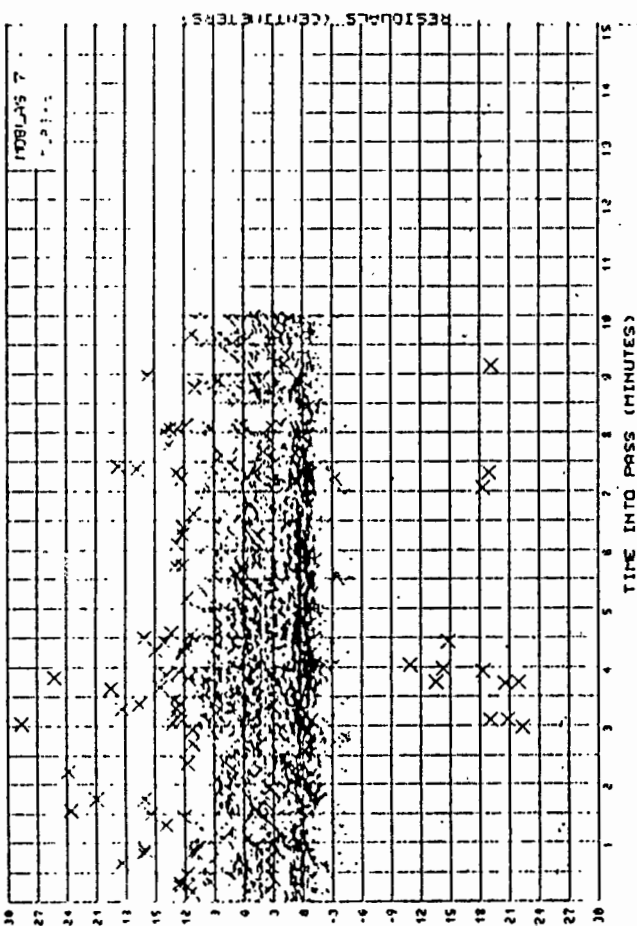
LAGEOS
6-26-86 - 0:57



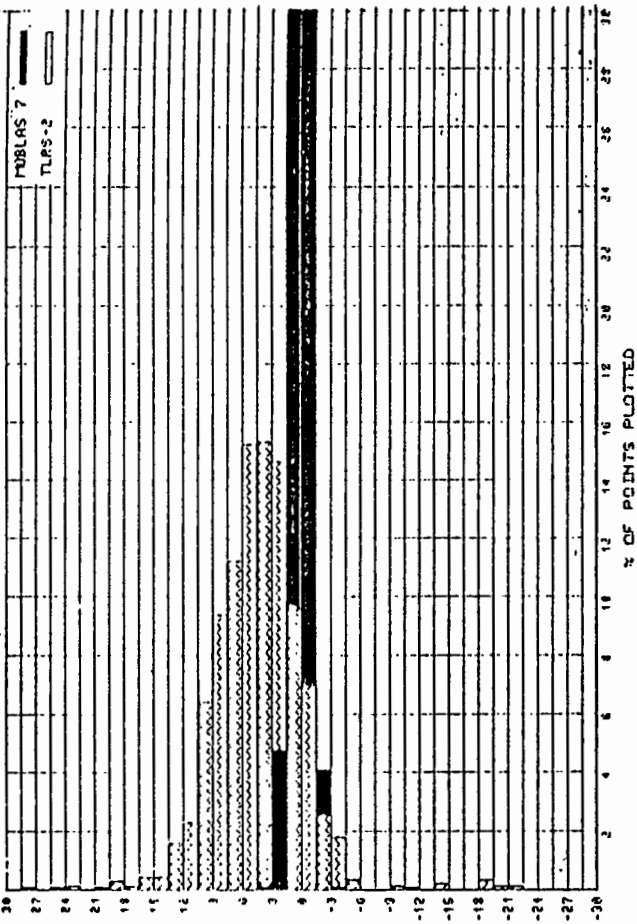
LAGEOS
6-26-86 - 0:57



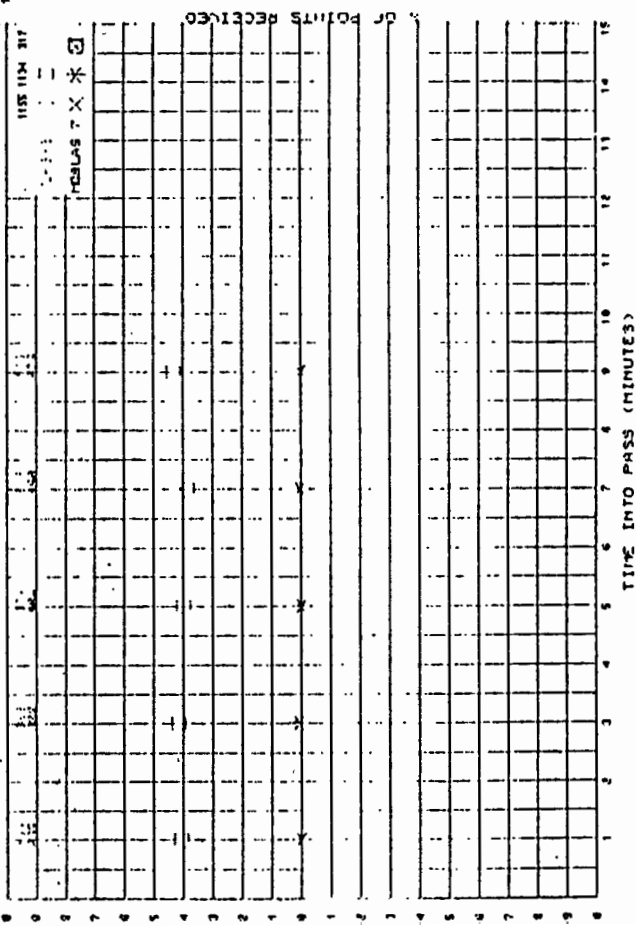
STARLETTE
8-29-88 - 8:18



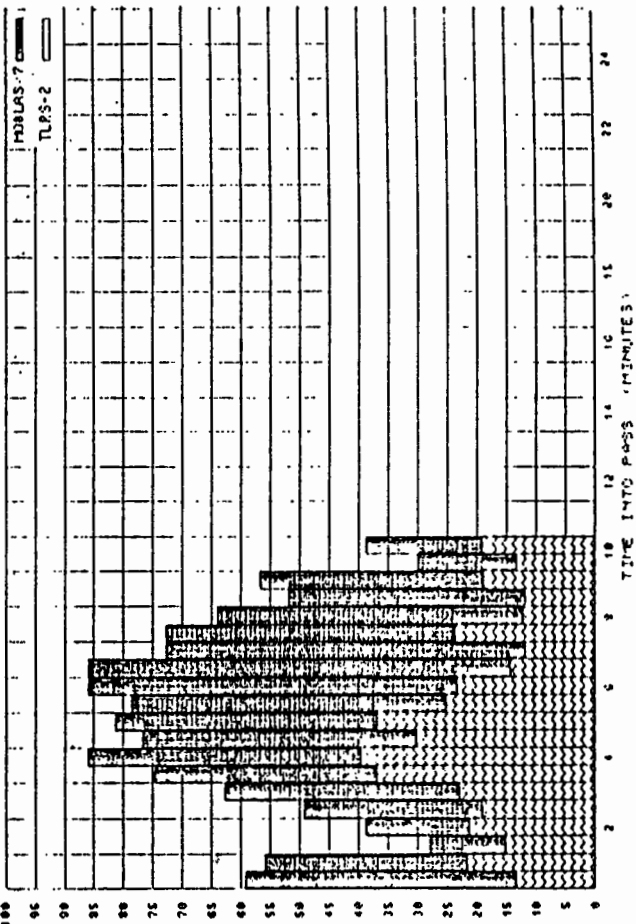
STARLETTE
8-29-88 - 8:18



STARLETTE
8-29-88 - 8:18

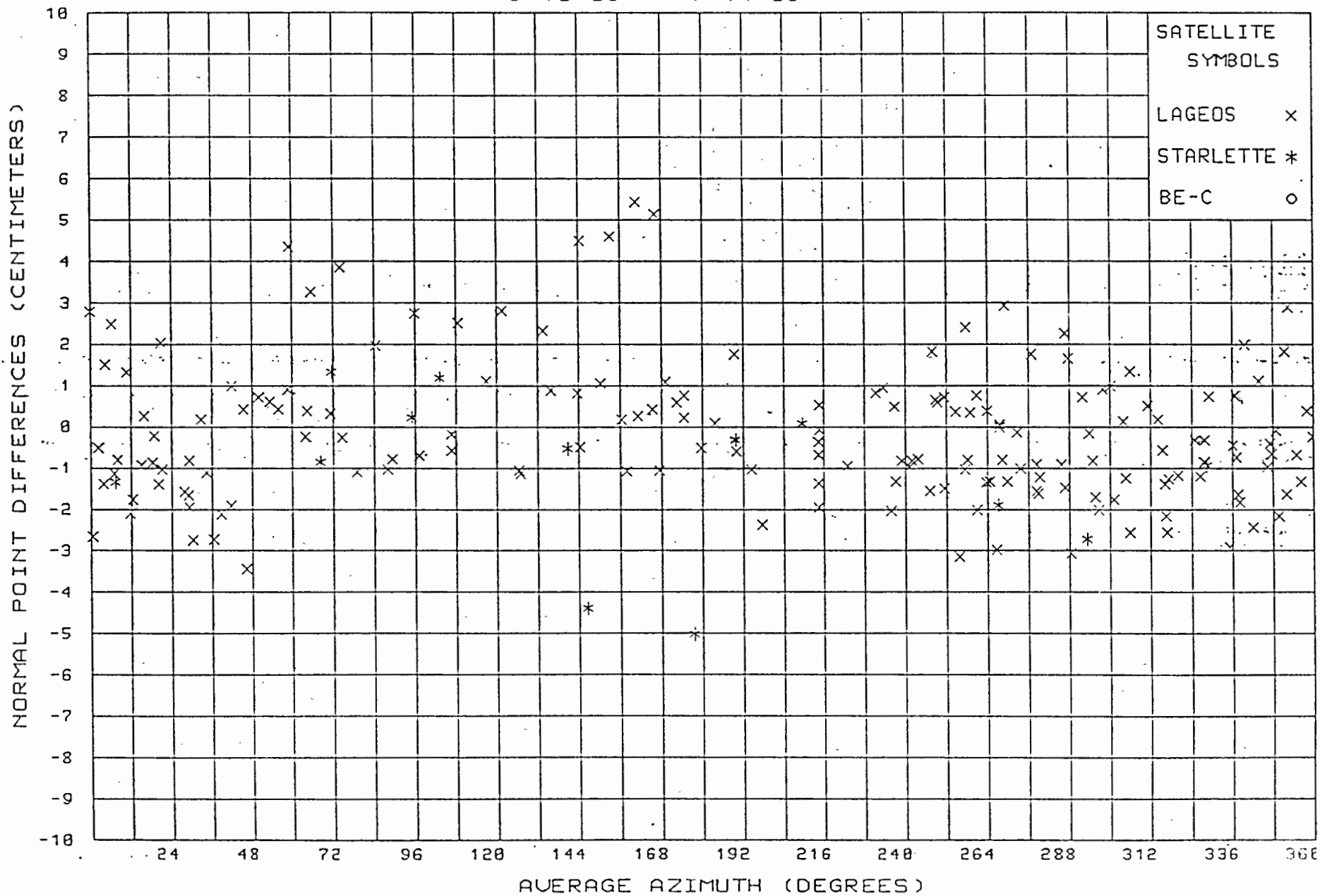


STARLETTE
8-29-88 - 8:18

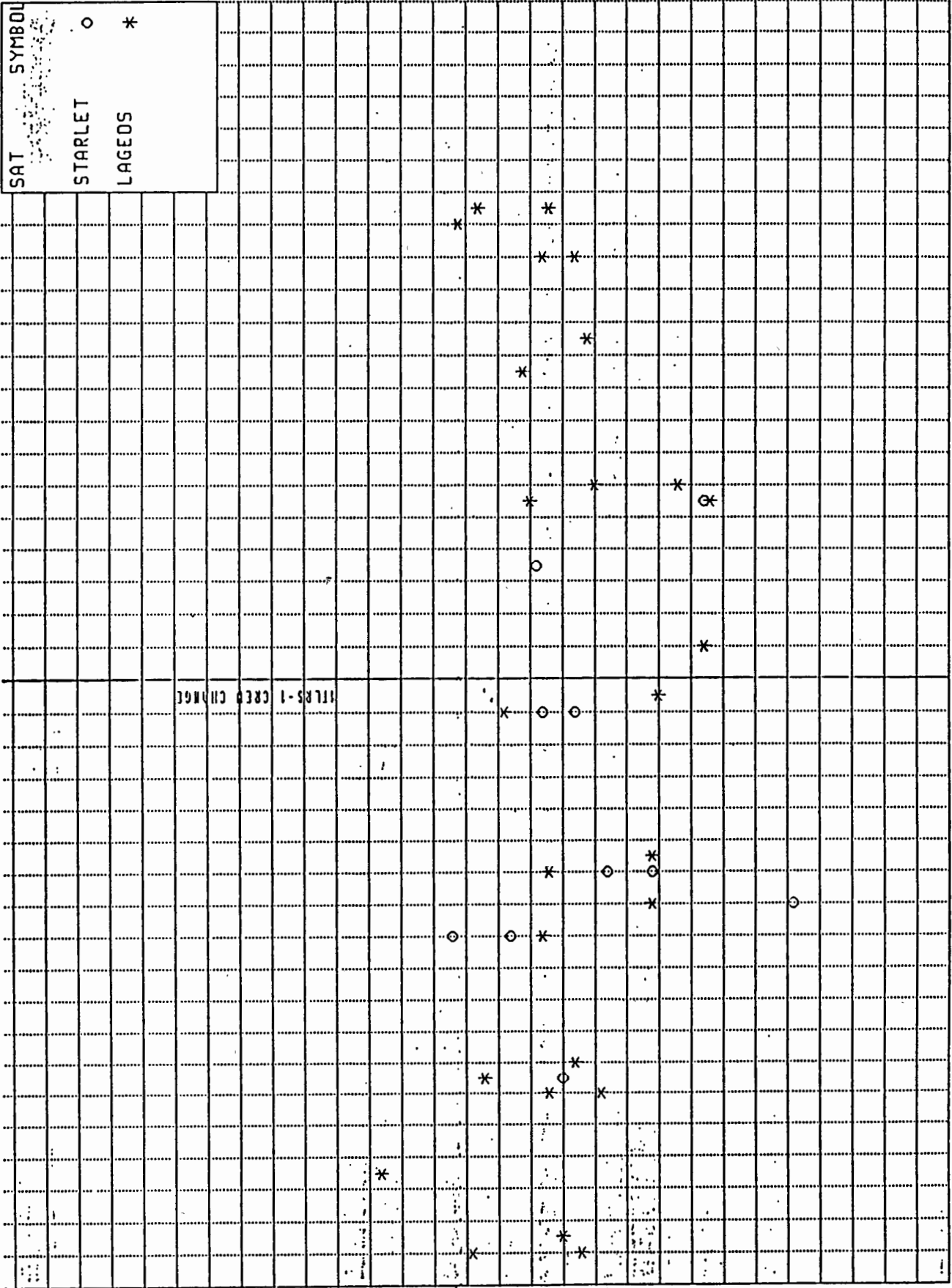


LAGEOS - STARLETTE

5/10/85 - 7/14/85



SAT	SYMBOL
STARLET	○
LAGEOS	*



RANGE BIAS VS DAY OF YEAR

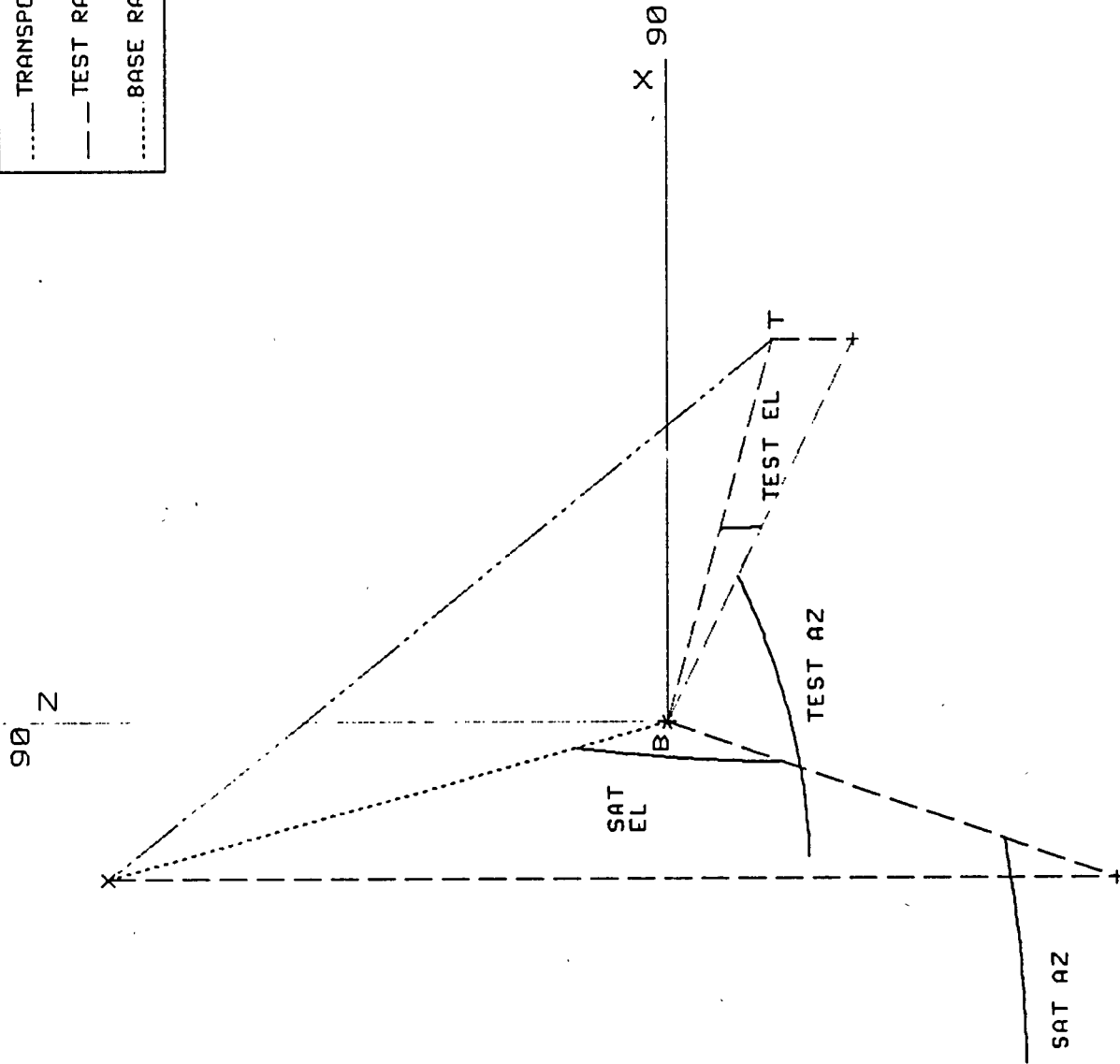
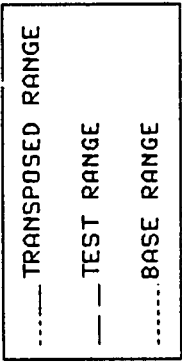
DAY

MAY 10 - JULY 14 1985

Polyquick Development History

1981	Polyquick prototype
1981-82	GEODYN benchmarking, GEODYN output plots, early collocation support
1983	Normal point analysis added to identify sub-pass bias structure
1983-84	Enhanced fitting procedures, improved statistical techniques
1984-85	Aggregate data set analysis, special bias tests
1986	Expanded graphics, Collocation Analysis Package (CAP) developed paralleling GEODYN update changes

POLYQUICK GEOMETRY



EL ==> ELEVATION ANGLE FROM THE BASE STATION

AZ ==> AZIMUTH ANGLE FROM THE BASE STATION

RANGE ==> MEASURED RANGE FROM THE BASE STATION

X_s, Y_s, Z_s ==> THE X, Y, Z COMPONENTS OF THE SATELLITE FROM THE BASE STATION

X_t, Y_t, Z_t ==> THE X, Y, Z COMPONENTS OF THE TEST STATION FROM THE BASE STATION

$$\begin{aligned} X_s &= \text{RANGE} * \cos(\text{EL}) * \sin(\text{AZ}) \\ Y_s &= \text{RANGE} * \cos(\text{EL}) * \cos(\text{AZ}) \\ Z_s &= \text{RANGE} * \sin(\text{EL}) \end{aligned}$$

$$\begin{aligned} X_t &= \text{RANGE} * \cos(\text{EL}) * \sin(\text{AZ}) \\ Y_t &= \text{RANGE} * \cos(\text{EL}) * \cos(\text{AZ}) \\ Z_t &= \text{RANGE} * \sin(\text{EL}) \end{aligned}$$

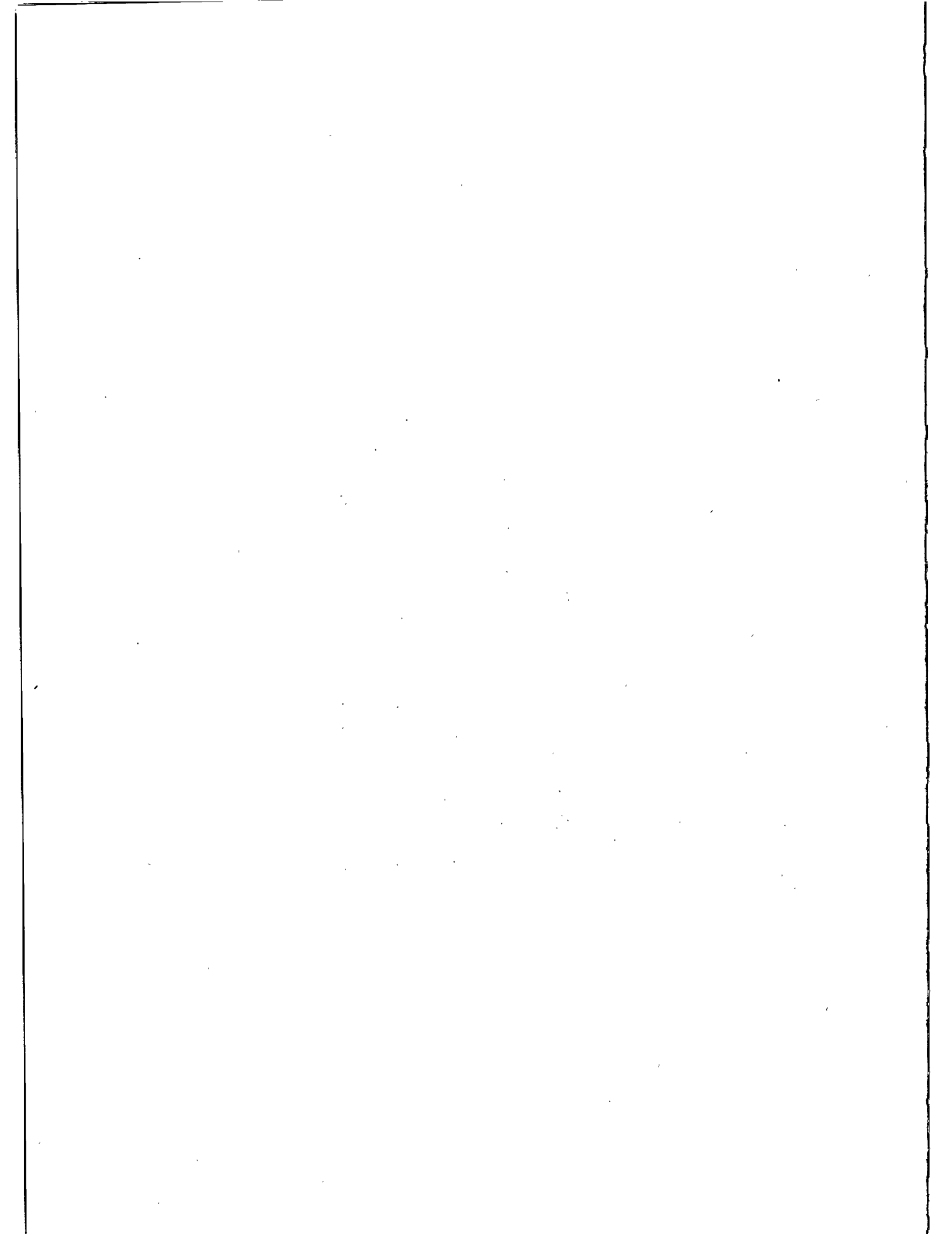
NEW RANGE =

$$\sqrt{(X_s - X_t)^2 + (Y_s - Y_t)^2 + (Z_s - Z_t)^2}$$

POLYQUICK COLLOCATION ANALYSIS SYSTEM

SUMMARY

- * ACCURATE
- * EFFICIENT
- * COMPLIMENTS ORBIT DETERMINATION TECHNIQUES
- * COMPREHENSIVE COLLOCATION ANALYSIS INFORMATION
- * MULTIPLE APPLICATIONS
- * PRIMARY TOOL FOR GLTN COLLOCATION ANALYSIS
- * SUPPORTS LASER RANGING ACCURACY IMPROVEMENTS



COLOCATION DATA ANALYSIS : DYNAMICAL APPROACH

A. Caporali
Dipartimento di Fisica Galileo Galilei
Universita di Padova
Via F. Marzolo 8
I - 35131 Padova - Italie -

Telephone (39) 49 844 278
Telex 430308 DFGGPD I

ABSTRACT

Colocation experiments of satellite laser ranging systems have proved to be much more interesting than simply a "precampaign calibration". They, in fact, permit the intrinsic precision of different ranging systems to be compared and exploited in depth. They also provide a unique source of information both to the engineer, and to the scientist.

The data analysis is the process which creates such body of information. Although virtually every group has its own technique of analysis, these can - in a broad sense - be classified within one of two different approaches : one is geometric, the other is dynamic, in the sense that a nominal ephemeris is used to filter the bulk of the curvature in the ranging data and to produce residuals.

We discuss here the basic features of the dynamic approach, in particular :

- data selection
- generation of nominal ephemeris and residuals
- criteria of editing and their impact on the results
- computation and analysis of ranging biases and calibration constants.

1. Introduction

All laser stations of the international laser tracking network differ from each other in several aspects. The characteristics of the laser oscillator, the mount, the receiving electronics, optics, timing system make each tracking station a unique instrument. And even in those cases, like the German and Dutch stations MTLRS1 and MTLRS2, where the stations are nominally identical, different procedures for calibration and satellite tracking can produce non negligible effects in the measurements.

Because any of these differences can map into systematic errors in the baseline, it is crucial for a successful campaign to dedicate sufficient time for an exhaustive calibration experiment.

This need has been recognized by NASA and the European Organizations participating in the WEGENER Consortium. In the past, colocation experiments have been done both in the United States and Europe.

From April to May, 1984 the German mobile system MTLRS1 was colocated at the Kootwijk Observatory with the fixed laser KOOLAS (Van Gelder and Blumer, 1985, Noomen, Ambrosius and Wakker, 1985). In November 1984 MTLRS1 was colocated at Wettzell with the fixed installation (Hauck and Lelgemann, 1985). In March and April 1985 MTLRS1 and 2 joined in Wettzell for a three-system colocation experiment (Hauck, van Gelder et al., 1985).

From May to July 1985 the NASA station MOB LAS7 and the German station MTLRS1 were colocated at Greenbelt, Maryland, with the objective to intercompare tracking technology and techniques of data analysis, and to transfer the Crustal Dynamics Project Laser standard to Europe (Kolenkiewicz, 1986). The data from this experiment have been analyzed by three groups, NASA, Bendix and IFAG, and their findings extensively documented (Husson 1986; Hessels et al. 1985, Kolenkiewicz et al. 1985, Hauck, Herzberger et al. 1985).

Finally, at the beginning of the Wegener MEDLAS 1986 Campaign, MTLRS1 and MTLRS2 were extensively colocated at Matera, before leaving for remote sites in the East Mediterranean Region. Table 1 summarizes these experiments and permits to appreciate how this type of experiment has evolved. A more complete list of colocation experiments is given by Pearlman (1986).

2. Dynamical Approach to the Analysis of Colocation Experiments.

2.1 Range bias, time bias and calibration constant.

It is common practice to call "range bias" and "time bias" the mean translations in space and time respectively by which the actual observed path of data differs from the path computed using a nominal ephemeris. These biases are computed by fitting the residuals r relative to predictions to a curve

$$\Delta r(t) = r_b + \dot{r}(t) t_b$$

where r_b and t_b are the range and time biases, and \dot{r} is the range rate. The time and range biases quantify how "early or late", or "off" an ephemeris is in predicting a pass over a station, and should not be confused with system biases of the ranging equipment, for which we reserve the word of "calibration constants".

If two stations are colocated, relative timing and position errors are negligible and one might expect that an ephemeris is range-and time-biased for the same amount relative to each station. This is not exactly true, as it can be seen with the following example. Given two colocated stations, compute for all passes, common and not, the range bias and time bias. Now select the range bias and time bias relative to the common passes, and note that these biases have been computed - for a given pass - using time intervals which, in general, do not exactly overlap.

Because the ephemeris is not "tailored" on a specific pass, the least squares estimated values of the range and time biases will depend on the tracked portion of the pass. Consequently, it is reasonable to expect that if two stations do not track the same portion of the pass, different estimates of range bias and time bias may result.

Only if the ephemeris happens to fit a pass with random residuals (as for multi-single pass methods, see next section) then the time bias is zero and the range bias is constant and independent of overlap.

Figures 1 and 2 have been obtained with a non tailored ephemeris for the Matera experiment (full rate data). They give the differences in range bias and time bias as a function of overlap time. They indicate that the longer the overlap, the higher is the probability that the relative range bias and time bias approaches zero.

Note that differences of several centimeters exist even for maximum overlap (45 min.). This is due to the use of unevenly spaced, full rate data, with noise of variable frequency added by the numerical differentiation of ranges to produce range-rates.

Our conclusion is that pass comparison should be safely limited to the simultaneous portion, unless one is very confident on the randomness of the residuals produced by the adopted ephemeris.

2.2 Dynamical Computations of the Calibration Constant.

The methods of analysis so far used differ in two important aspects: one is the criteria for data selection, the other is the computational technique. The Matera experiment shows an unprecedented variety of options (tab. 2). There is clearly considerable space for subjective decisions which may have non negligible impact on the final results.

The computational methods are summarized in tab. 3. They imply that there exist two basic methods of computing the relative calibration constant between two ranging systems: one is to consider the range bias as a "solve for" parameter in a multi-single pass" (see below) least squares adjustment. The other is to define the calibration constant as a mean difference - for each pass - between pairs of residuals referred to a same smooth curve (ephemeris, polynomial or both).

Concerning the first method we note, with reference to tab. 2, that by multi-single pass method it is meant a least squares fit to data of a single pass, done simultaneously for several passes. The "solve for" parameters consist of a subset of the orbital parameters chosen so that the resulting normal equations are non degenerate, and perhaps a range and time bias for each station, to accommodate for model inaccuracies. The difference in range bias is interpreted as an estimate of the calibration constant for the pass, provided the post-fit residuals are random.

Concerning the second method, the subtraction of a best fitting, smooth curve from the residuals to the predicted ephemeris removes the effect of the predicted ephemeris being not tailored on the actual data. In the Telespazio approach, the polynomial fit is done three times: first with station A residuals, and station B residuals downweighted; second, with the roles of A and B interchanged; third, residuals of A and B fitted altogether to a polynomial. The pair of time series

of residuals resulting from each fit is plotted together. The "full rate residuals" are replaced by means at common epochs, for sake of easier comparison. The three means of the polynomial residuals are finally averaged to produce, for the given pass, the estimated calibration constant.

Again the all procedure should produce random time series. It some time happens that this is not the case, due to real relative random walks of one system relative to the other, or to numerical unstabilities of the filtering procedures. Having different types of approaches available should permit to separate numerical unstabilities from system unstabilities.

Fig. 3 gives an example of residual plots obtained for the same pass by IFAG and Telespazio, during the Matera Colocation Experiment. IFAG used a "multi-single arc technique" and estimated by least squares the range bias of the ephemeris relative to each station simultaneously with an along track, radial, inclination and node correction. Telespazio instead subtracted from the orbital residuals a best fitting polynomial and computed the mean of the post-fit residual differences.

The agreement between the two methods is evident. The largest difference between the calibration constants is 1.4 cm (MATLAS-MTLRS2) and is most probably due to different criteria for data selection and editing, rather than to the computational technique.

2.3 Data Selection

The number of data present in a data set varies considerably from station to station and, for a given station, from pass to pass. Aggregating data into normal points permits a more uniform data distribution. The aggregation process is non trivial, especially if the data rate is low (e.g. Quick Look normal points, or normal points from second generation stations). A normal point made of 10 data differs from one of 11 data by 1.5 cm if the additional data point is off, relative to the mean of the other ten data points, by 15 cm (the typical noise level r.m.s. of a second generation station).

An alternate option successfully tested at Telespazio during the Matera experiment was to sample the data 1 point every 5 seconds and compare the results obtained with the full-rate data. Table 4 summarizes the results of this test.

It is interesting to note the effect of different criteria of editing of outliers: whenever MATLAS data are

used, the 3σ editing criterion in place of 2.5σ produces a shift of the calibration constant of 5mm in the negative direction.

This implies the existence of non random data aggregations, but fortunately the effect is small, especially if compared with the nominal noise level of this station.

3. Conclusion

To evaluate systematic differences between two collocated laser systems, all proposed methods of analysis are probably equally viable. It is very likely that different results, when they occur, are due to different criteria for data selection more than the computational approach itself.

Software benchmarking has proven to be a very valuable tool of comparison of procedures (A. Cenci, 1986). To separate the issue of editing from that of computational technique, a simulated data set could be generated for two collocated stations with known-but not to the analysts-relative calibration constants. No data point can be edited out. Then, the same range bias ought to be recovered by all methods of analysis. A successful benchmarking of this type between a GEODYN based algorithm and a kinematic algorithm based on POLIQUICK (Edge, 1986) has been reported by Kolenkiewickz (1986). Hopefully the same experiment is repeated for the remaining algorithms.

Whether or not this experiment is done, the evidence so far is that collocation periods of several months are very advisable, if the body of data is to be sufficiently complete.

Acknowledgment. I thank Alberto Cenci for several discussion on a first draft of the manuscript.
This work is supported by Piano Spaziale Nazionale, Consiglio Nazionale delle Ricerche.

References

- Cenci, A.: Management of the Laser Ranging Systems Colocation. Proc. of the 6th. International Workshop on Laser Ranging Instrumentation, Antibes, Sept. 22-26 1986 (this volume).
- Edge, D. : this volume.
- Hauck, H., Herzberger and P. Wilson: The Results of the Colocation Experiment MOBLAS7 - MTLRS1. IFAG Intern. Report, 1985.
- Hauck, H., van Gelder B.H.W., van Loon, D.L.F., Vermaat, E. and Blumer, B.M.H.: Co-locating MTLRS1 and MTLRS2 with the stationary Wettzell Laser Ranging System. AGU Spring Meeting, Baltimore Md: May 27-31 1985.
- Hauck, H. and Lelgemann, D.: A Comparison between MTLRS1 and the Stationary Laser System in Wettzell. Crustal Dynamics Working Meeting , NASA GSFC March 19-20 1985
- Hessel, U., Junginger, H., Etling, W., Nowak, I. : Stabilität und Winkelabhängigkeit der Kalibrations Konstante bei MTLRS1. IFAG Intern. Report, 1985.
- Husson, V.S.: MTLRS1 and MOBLAS7 Colocation Report. Bendix Field Engineering Corporation, 1986.
- Kolenkiewickz, R., Husson V.S., Dunn P.J. , Martin C.F., Poullose, S., Abresh, M.: Recent Lageos Satellite Laser Ranging Colocation Analysis. AGU Fall Meeting Dec. 12 1985, S. Francisco, Ca.
- Kolenkiewickz, R.: The MTLRS1 and MOBLAS7 Colocation. Crustal Dynamics Principal Investigator Meeting. Jet Propulsion Laboratory, March 26 1986.
- Kolenkiewickz, R.: this volume.
- Noonen, R., Ambrosius, B.A.C. and Wakker, K.F.: Results of a Colocation Experiment Between MTLRS1 and the fixed Kootwijk Laser,. Crustal Dynamics Working Meeting, NASA GSFC March 19-20 1985.
- Pearlman, M.: this volume.
- Van Gelder, B.H.W. and Blumer, B.M.H.: Co-location of KOOLAS and MTLRS1 at the Kootwijk Observatory using raw laser range data to LAGEOS. Crustal Dynamics Working Meeting, NASA GSFC March 19-20 1985.

	Kootwijk	Wetzell	Wetzell	Gorf	Matera
OD	April-May '84	November '84	March '85	May-July '85	Jan-March '86
TEM	M1,K	M1,W	M1,M2,W	M1,M7	MO, M1, M2
ULTANEOUS SES	8	4	3 M1, M2, W 5 M1, W 3 M2, W 4 M1, M2	32	11 MO, M1, M2 24 MO, M1, 39 MO, M2 14 M1, M2
A: CK LOOK MAL POINTS	X	X	X X	X X	(see tab.2)
GE BIAS(mm)	M1-K<-100 DUT/A M1-K:-35(+) DUT/G	M1-W 260	M1-M2 -6 -13 W-M1/2 -1 -58 M1-M2 +15 on target	M1-M7: -5 -20 (BFEC) -3 (IFAG)	(see tab.2)
ALYSIS GROUP	DUT/A DUT/G	IFAG	DUT/G IFAG	BFEC NASA GSFC IFAG	TPZ-UP IFAG UT-CSR NASA-GSFC BFEC, DUT/G

e: M1= MTLRS1; M2=MTLRS2; K=KOOTLAS; W=WETLAS; M7=MOBLAS7; MO=MATLAS
after relative height adjustment

le 1 Some Recent Colocation Experiments Involving European Laser Systems

DATA SOURCE	ORBITAL FILTER RESIDUALS GENERATIONS	DATA EDITING	NORMAL POINTS	ACCEPTANCE CRITERIA	RESULTS (mm)	
UP	MO Full Rate MI, M2 QL, Full Rate	Long arc adjust- ment; polynomial fit to GEODYN residuals	tailored 2.5 and 3 sigma/single pass	5 min. Normal residuals	Simultaneous tracking of common pass (5 min. minimum)	MO-M1 -5 MO-M2 -10 MI-M2 -5
		Multi-single pass adjustment	3 sigma/single pass	2 min.	Common pass	MO-M1 -7±20 MO-M2 +7±41 MO-M2 +8±10
		Single pass Polyn. with geom. correc- tions	3 sigma/single pass	2 min.	Simultaneous tracking of common pass	MO-M1 -38±19 MO-M2 -21±17 M1-M2 -4± 9
G		Multi-single pass adjustment	3.5 sigma/single pass		Common pass	MO-M1 -18±23 MO-M2 0±31 M1-M2 -20±20
		Multi-single arc adjustment	2.7 sigma/global	1 min.	Normal points at common epoch	MO-M1 -9± 70 MO-M2 -11±74 M1-M2 -14±33
SR		Multi-single pass adjustment polyn. fit	3.5 sigma/single pass	2 min.	Simultaneous tracking of common pass	MO-M1 MO-M2 TBD M1-M2

Figure 2: geometric and dynamic approaches to the analysis of the Matera Collocation data.

- Multi single pass techniques:

- * Pass-by-pass least square estimate of a subset of orbital parameters and, for each station, of a range bias and time bias.

- * Calibration constant of the pass defined as difference of range biases for that pass.

- Long arc and polynomial fit:

- * "Coarse" filtering of the orbit using long arc techniques:

- * Pass-by-pass "fine tuning" of long arc residuals using polynomial techniques

- * Calibration constant for the pass as mean of residual differences after polynomial fit.

- Multi-arc technique:

- * Ephemeris generated using normal points from global network

- * Orbital residuals of normal points of colocated stations at the same epoch are differenced

- * Calibration constant computed as mean of simultaneous residuals.

Table 3: Methods of computation of the calibration constant.

TELESPAZIO-University of Padova Analysis of Matera Colocation Data

STATISTICS OF RESIDUAL DIFFERENCES (cm)

DATA SET: Full rate data from Bendix MT2MAT8

	N. of passes	FULL RATE DATA		1/5 SEC. SAMPLING	
		2.5 σ EDIT	3 σ EDIT	2.5 σ EDIT	3 σ EDIT
MATLAS - MTLRSI	17	-0.1 \pm 2.5	0.3 \pm 2.7	-0.6 \pm 2.4	-0.3 \pm 2.8
MATLAS - MTLRS2	36	0.0 \pm 1.9	0.5 \pm 2.0	-0.4 \pm 2.3	0.2 \pm 2.3
MTLRSI - MTLRS2	13	-0.3 \pm 1.4	-0.3 \pm 1.6	0.0 \pm 1.6	0.3 \pm 1.6

Note: Only passes with more than 5 min overlapping time and more than 30 observations are considered.

Passes on Jan. 16 01:51 and Jan. 24 23:51 are not used in MATLAS-MTLRS2 final average

Numbers after indicate the passby pass rms of the differences and are not divided by the square root of the number of passes.

Table 4: effect of different criteria of editing on final results.

Delta T-Bias vs. overlap (usec)

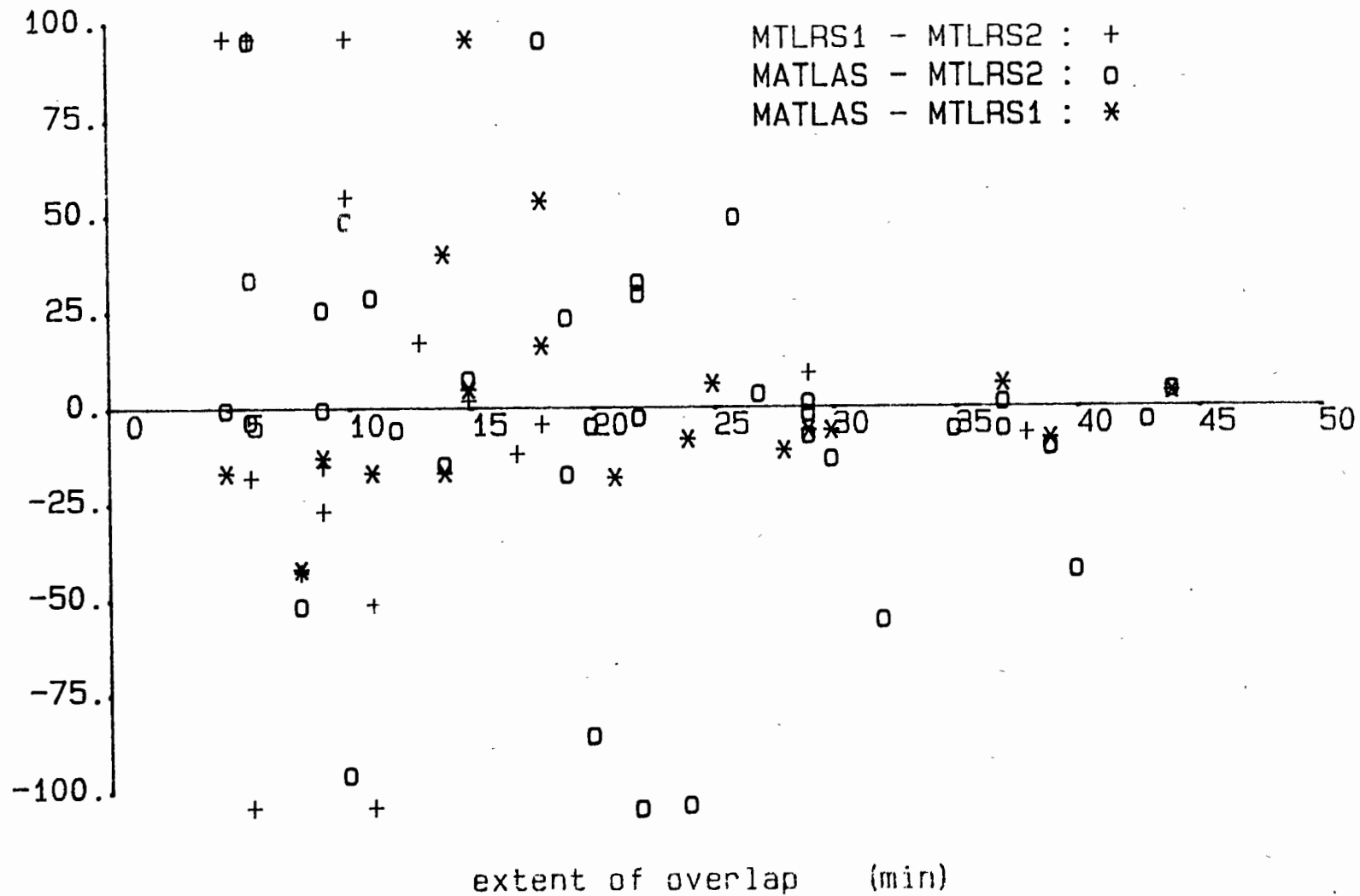


Fig. I: differences of time biases of common passes computed relative to the same reference ephemeris, as a function of interval of simultaneous tracking.

Delta R-Bias vs. overlap (mm.)

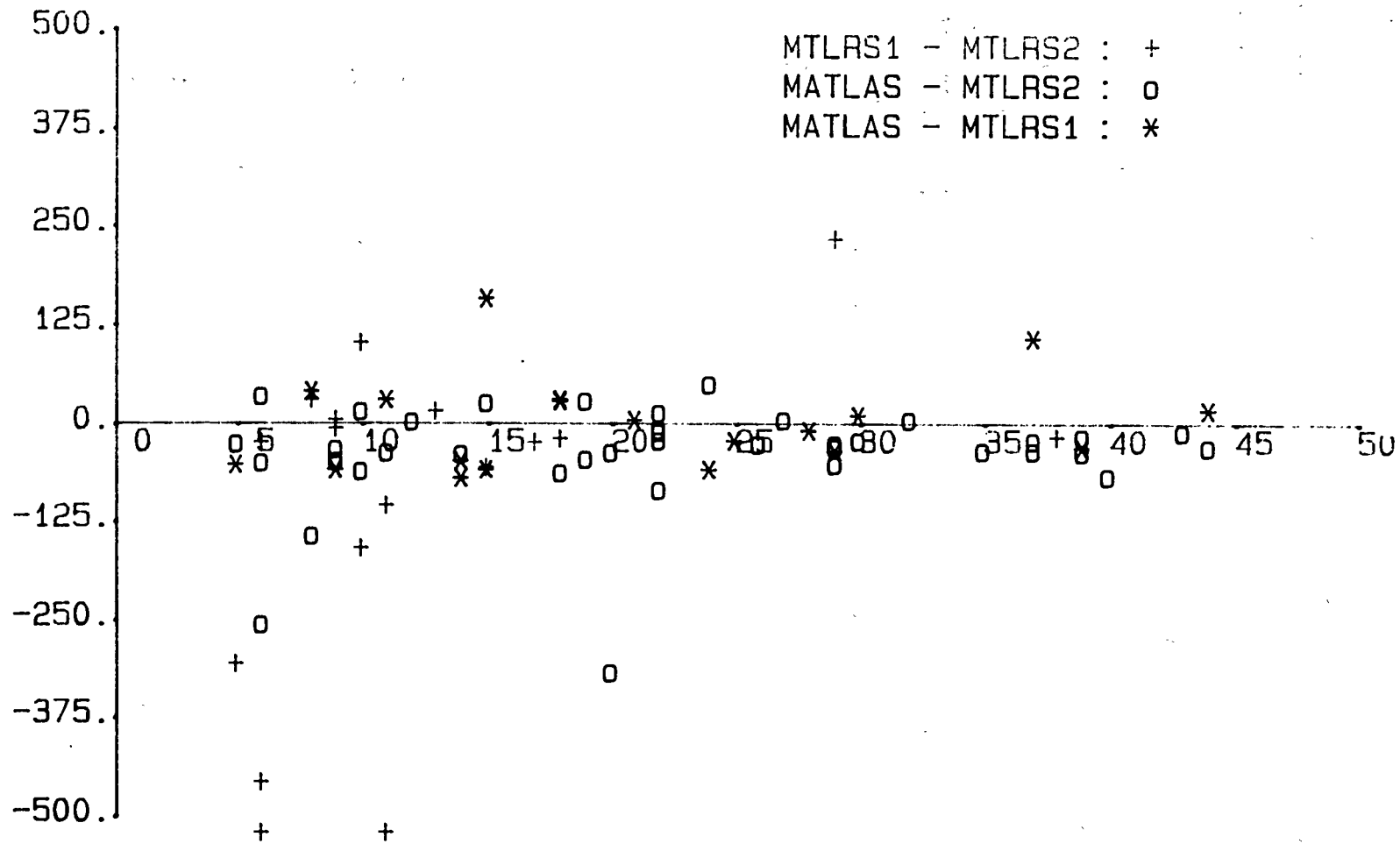


Figure 2: same as fig. I, for the range bias differences.

***** PLOT DER VERDESSERUNGEN *****

EPOCHE ANFANG: 8601483842 ENDE: 8621500154
2.2.72

SCALE = 7.198 METER.
INTERVALL = 0.204 METER.

orbit residuals
of pass 8601483842
after adjusting the
orbit

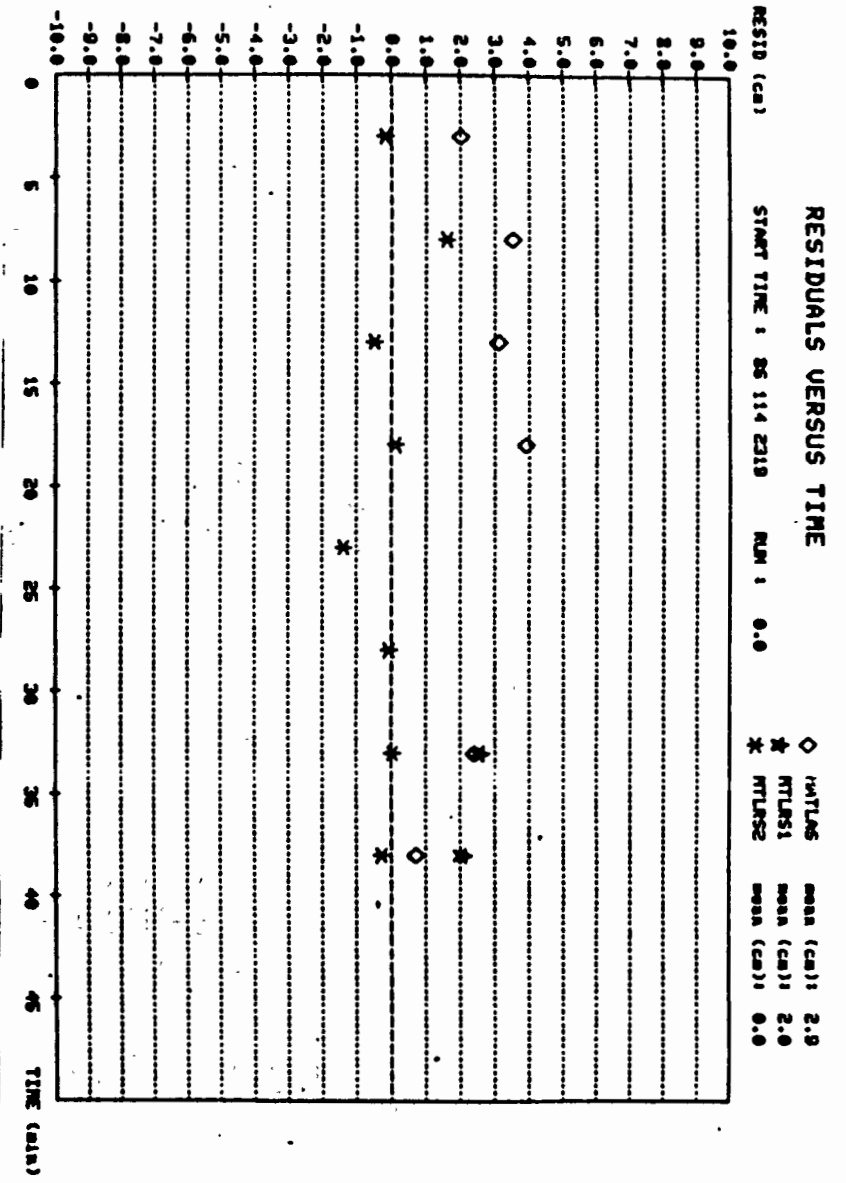
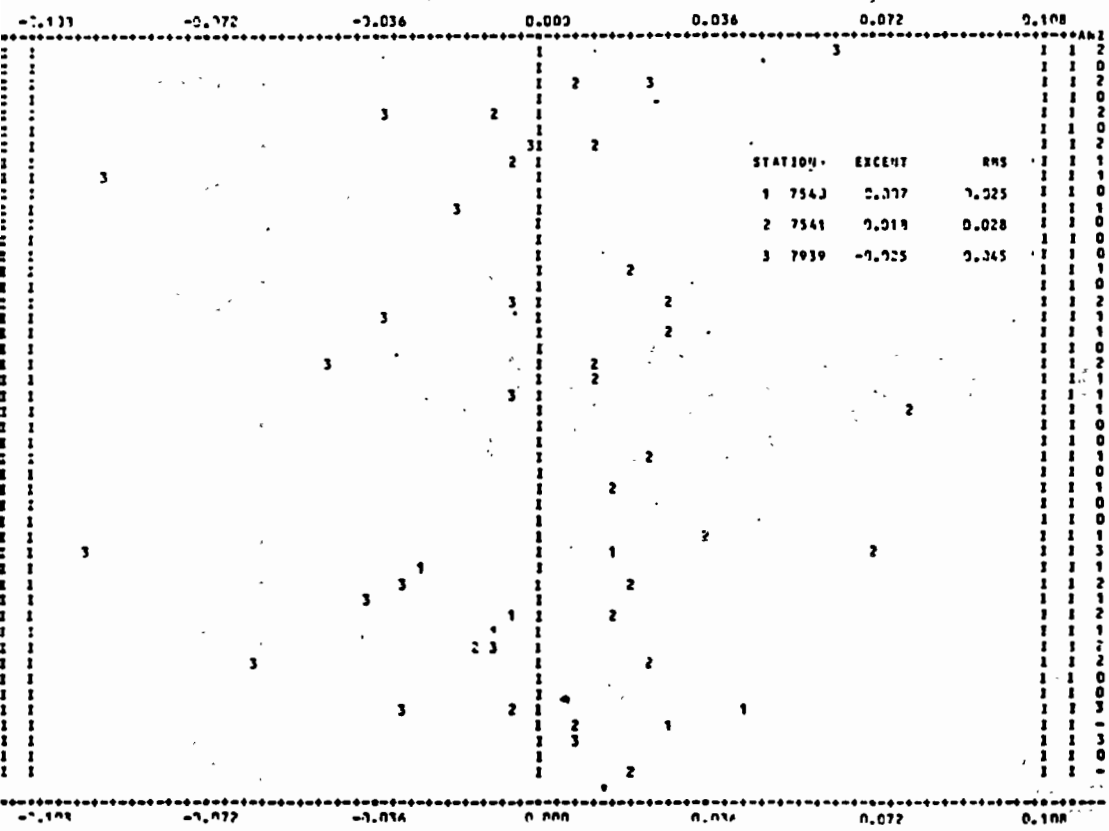


FIG.3 · Same pass analyzed by Telespazio and IFAG

GEODYN COLLOCATION ANALYSIS AND ITS COMPARISON
WITH POLYQUICK

R. Kolenkiewicz
Nasa Goddard Space Flight Center
Greenbelt, Maryland 20771 - USA -

Telephone (301) 286 5373
TWX 710828 9716

Van S. Husson
Bendix Field Engineering Corp.
Columbia, Maryland

Ch. Martin
EG&G Washington Analytical Services Center Inc.
Lanham, Maryland

S. Poulouse, M. Abresch, K. Doyle
RMS Technologies Inc.
Landover, Maryland

ABSTRACT

GEODYN is a precision orbit determination program used by NASA at Goddard Space Flight Center (GSFC) for analysis of data collected from lasers ranging to the LAGEOS satellite. This program is also used as a means of comparing satellite laser ranging systems. This process, known as collocation analysis, consists of placing two satellite laser ranging systems side by side, at a known orientation to each other, tracking the same target satellite, and comparing the range data obtained. As an aid in the analysis of these data, additional software has been developed by NASA. This software uses the GEODYN produced laser range residuals as input. An additional program developed for NASA by the Bendix Field Engineering Corporation is called POLYQUICK. This program performs collocation analysis by fitting polynomials to satellite laser ranging data. In addition to using the ranging data, POLYQUICK must also use the angular (azimuth and elevation) data obtained from one of the laser systems being compared. The advantage of the POLYQUICK over the GEODYN approach is that the analysis is independent of orbit integration and hence can be performed more rapidly. This disadvantage is that the lasers being compared must be in close proximity of each other (approximately 50 m) in order to produce accurate results. To assess the collocation software and analysis approaches, both collocation programs were utilized at GSFC for a collocation between the MTLRS-1 laser from the Federal Republic of Germany and the MOBLAS-7 laser belonging to NASA. For a typical collocation pass (6/27/85 at 04/00 hr.) containing 15 two minute overlap normal points between MTLRS-1 and MOBLAS-7, the maximum difference between GEODYN and POLYQUICK is 0.4 cm with an rms of the 15 points of 0.16 cm. For the entire pass GEODYN indicates MOBLAS-7 is measuring long relative to MTLRS-1 by 1.47 cm, and POLYQUICK indicates 1.58 cm. For a group of 13 LAGEOS passes tracked during the summer of 1985 the rms difference in pass results obtained by GEODYN and POLYQUICK amounted to 0.15 cm. Details of the GEODYN collocation analysis program and its comparison with the POLYQUICK results will be described.

INTRODUCTION

An objective of the NASA Crustal Dynamics Program is to obtain Satellite Laser Ranging (SLR) data from the Laser Geodynamics Satellite (LAGEOS). In order to achieve this goal new laser systems must be developed and compared to each other. This process of comparison is called collocation. As an aid in the analysis of these data, new computer software has been developed by NASA. This software uses laser range residuals produced by GEODYN, the precision orbit determination computer program used by NASA at GSFC. A second piece of software, called POLYQUICK, designed to do a similar task was created for NASA by the Bendix Field Engineering Corporation. Each of these programs has its place in the analysis of laser collocation data as will be described in this paper. The purpose of this paper is to compare the GEODYN analysis with the POLYQUICK analysis during a collocation.

GEODYN ANALYSIS

In order to assess the collocation software and analysis of GEODYN and POLYQUICK, both programs were used to reduce data from a recent collocation held at GSFC. The collocation selected was for the MTLRS-1 laser from the Federal Republic of Germany and the MOBLAS-7 laser belonging to NASA. This collocation was held between May and July of 1985. A typical collocation pass (6/27/85 at 04:00 hr. GMT) will be looked at in detail in order to describe the GEODYN analysis. A precision GEODYN orbit, approximately 50 minutes in duration, was fit solely through the MOBLAS-7 data with the MTLRS-1 data weighted out (not contributing) to the solution. Figure 1 shows the range residuals as a function of time for the MOBLAS-7 laser for the converged orbit. Since MOBLAS-7 is a 2.5 cm. rms system, and a three sigma editing criterion will be used, only residuals within 7.5 cm. of the orbit are used in the analysis. This amounts to using 9553 of the total 11063 points taken during this pass. Figure 2 is similar plot for the MTLRS-1 range residuals. MTLRS-1 is a 5.5 cm. rms system and a three sigma editing (16.5 cm.) is used. Therefore 3236 of the total 4423 MTLRS-1 points are retained for the analysis. The elapsed time zero in Figures 1 and 2 corresponds to 04:00 hours GMT on June 27, 1985. Beginning with this epoch time, two minute time intervals (or bins) are selected during the orbit. For each time interval the number of range residuals, the mean, the rms (sigma), and the standard deviation of the mean (sigma divided by the number of points) are computed and given the time tag for the center of the bin (the odd minute). Results for the MOBLAS-7 residuals are given in the first 5 columns of Table 1. Corresponding results for the MTLRS-1 residuals are given in columns 6 through 9. The number of points necessary in a two minute bin for each of the lasers is an option that can be set by the analyst. In this case a two minute mean point would not be considered as a part of the analysis unless it consisted of at least 300 residuals from MOBLAS-7 and 30 residuals from MTLRS-1 (indicated by an asterisk in Table 1). Differences of the means MTLRS-1 minus MOBLAS-7 (columns 7 minus 3) are given in column 10. The standard deviation of these differences is given in column 11.

For example the fifth row in Table 1 indicates an elapsed time of 9.00 minutes (04:09 hr. GMT) which corresponds to the middle of the two minute bin beginning at 04:08 and ending at 04:10 hr. GMT. There were 489 laser range residuals within ± 7.5 cm. of the computed orbit during this time period. The mean of these residuals is 0.16 cm. with an rms of 1.97 cm. which when divided by the square root of the number of points yields a standard deviation of this mean of 0.09 cm. Correspondingly there were 136 points for MTLRS-1 within ± 16.5 cm. of the orbit having a mean of -0.50 cm., an rms of 5.84 cm. and a standard deviation of 0.50 cm. The difference of the means MTLRS-1 minus MOBLAS-7 is -0.66 cm. with a standard deviation of the difference of 0.51 cm.

Figure 3 is a plot of the two minute values with associated one sigma error bars for MOBLAS-7 and MTLRS-1. These are the points in Table 1 columns 3 and 5 for MOBLAS-7 and columns 7 and 9 for MTLRS-1 which are to be considered in the solution. Note that there are 15 pairs of points sharing the same two minute bin which can be differenced.

Figure 4 is a plot of the two minute mean range differences between MTLRS-1 and MOB LAS-7. These are columns 10 and 11 of Table 1. For this set of points the weighted mean (\bar{X}), the weighted standard deviation of the mean (β) and the weighted standard deviation about the mean (ϕ), as defined below, are calculated in Table 1 and shown on Figure 4.

For a population, x_i , with uncertainties, σ_i , the weighted mean is defined as

$$\bar{X} = \frac{\sum_{i=1}^n w_i x_i}{\sum_{i=1}^n w_i}$$

where

$$w_i = \frac{1}{\sigma_i^2}$$

The weighted standard deviation of the mean, β , is given by:

$$\beta = \left[\frac{1}{\sum_{i=1}^n w_i} \right]^{\frac{1}{2}}$$

and the weighted standard deviation about the mean (absolute variance) ϕ , is:

$$\phi = \left[\frac{\sum_{i=1}^n w_i x_i^2}{\sum_{i=1}^n w_i} - \bar{X}^2 \right]^{\frac{1}{2}}$$

Figure 4 indicates the ultimate goal of the GEODYN collocation analysis for two laser systems. It indicates how well the lasers are measuring the range to the satellite and indicates the systematic trends during the pass. The results indicate that the weighted mean difference between MTLRS-1 and MOB LAS-7 is -1.47 cm. or that for this pass the MTLRS-1 is measuring short by 1.47 cm. relative to the MOB LAS-7 measurement. In addition to this bias there are systematic jumps of 1 to 2 centimeters during the measurement period. An indication of this scatter is the relatively large value of 0.84 cm. for the standard deviation about the mean. Systematic differences of this nature must be understood and corrected in order for laser systems to achieve the current goal of less than a centimeter.

GEODYN AND POLYQUICK COMPARISON

The POLYQUICK computer program (*Husson and Edge*, this issue) was used to analyze the same collocation data (6/27/85 at 04:00 hr. GMT) previously analyzed by GEODYN. Rather than using a precision orbit as its basis, POLYQUICK uses the data in the form of laser range residuals and azimuth and elevation angles together with polynomials to compare the MOBLAS-7 and MTLRS-1 laser systems. Basically this consists of transforming the laser range results from one of the collocation lasers to the second, fitting polynomials to both data sets, and taking a difference. In the POLYQUICK analysis an effort was made to use similar parameters to those used in the GEODYN analysis. This consisted of the bin size, number of points selected for each laser in the bin and common statistics. Figure 5 shows the comparison between GEODYN and POLYQUICK for the test case. The top plot is for the 15 point difference between MTLRS-1 minus MOBLAS-7 with the GEODYN results, except for the error bars repeated, and the POLYQUICK results shown for comparison. The greatest difference between any of the 15 points shown is 0.4 cm. The bottom plot is the difference (POLYQUICK minus GEODYN) where the rms difference for this pass of data is 0.16 cm. GEODYN and POLYQUICK are also in good agreement as far as the weighted mean differences for the entire pass are concerned. Where the GEODYN analysis predicts MTLRS-1 is measuring short by 1.47 cm. relative to MOBLAS-7, the POLYQUICK analysis predicts a value of 1.58 cm., or a difference of 0.11 cm. This result is just one of 13 LAGEOS passes analyzed by GEODYN and POLYQUICK during the MOBLAS-7 and MTLRS-1 collocation. The remaining results are given in Table 2. In Table 2 the date of the pass, the time of the pass, and the weighted mean difference (MTLRS-1 minus MOBLAS-7) for GEODYN and POLYQUICK as well as their differences are tabulated. The largest difference between GEODYN and POLYQUICK for a given collocation pass is 0.28 cm. and the rms difference for the 13 collocated passes is 0.15 cm. As far as the collocation between MOBLAS-7 and MTLRS-1 is concerned MTLRS-1 is measuring short relative to MOBLAS-7 by 1.80 cm. (GEODYN) or 1.76 cm. (POLYQUICK).

SUMMARY

GEODYN and POLYQUICK analyses are currently being used by NASA at GSFC for collocation analysis of satellite laser ranging systems. GEODYN uses precision orbit determination and POLYQUICK uses polynomial fits to obtain laser range residuals, from two laser systems, which can then be differenced in order to compare the ability of the systems to measure the same range distance. GEODYN requires more computer time than POLYQUICK to obtain the final result, in all other respects GEODYN is the superior method for collocation analysis. In the GEODYN analysis only ranges are required whereas POLYQUICK requires azimuth and elevation angles for its analysis. As the laser systems' accuracy increases, the polynomial approach may prove unable to achieve the precise measurements required for collocation. In addition the accuracy of the POLYQUICK results deteriorates as the distance between the collocated lasers increases, with studies indicating distances in excess of 50 meters to be prohibitive. GEODYN has the ability to dynamically solve for a relative station position (navigate) from a group of collocation passes and thus discover survey errors; this is more cumbersome to accomplish with POLYQUICK. For the current laser ranging systems undergoing collocation, the above analysis indicates that either the GEODYN or POLYQUICK approach yields comparable results. POLYQUICK should be used in conjunction with other engineering analysis on a real time basis to insure rapid turn around of the data in order to correct problems in a more timely manner.

REFERENCES

Husson, V. S., and D. R. Edge, POLYQUICK collation analysis, Sixth International Workshop on Laser Ranging Instrumentation, Antibes, France, Sept. 1986, this issue.

MOBLAS-7
LAGEOS
6/27/85 04:00

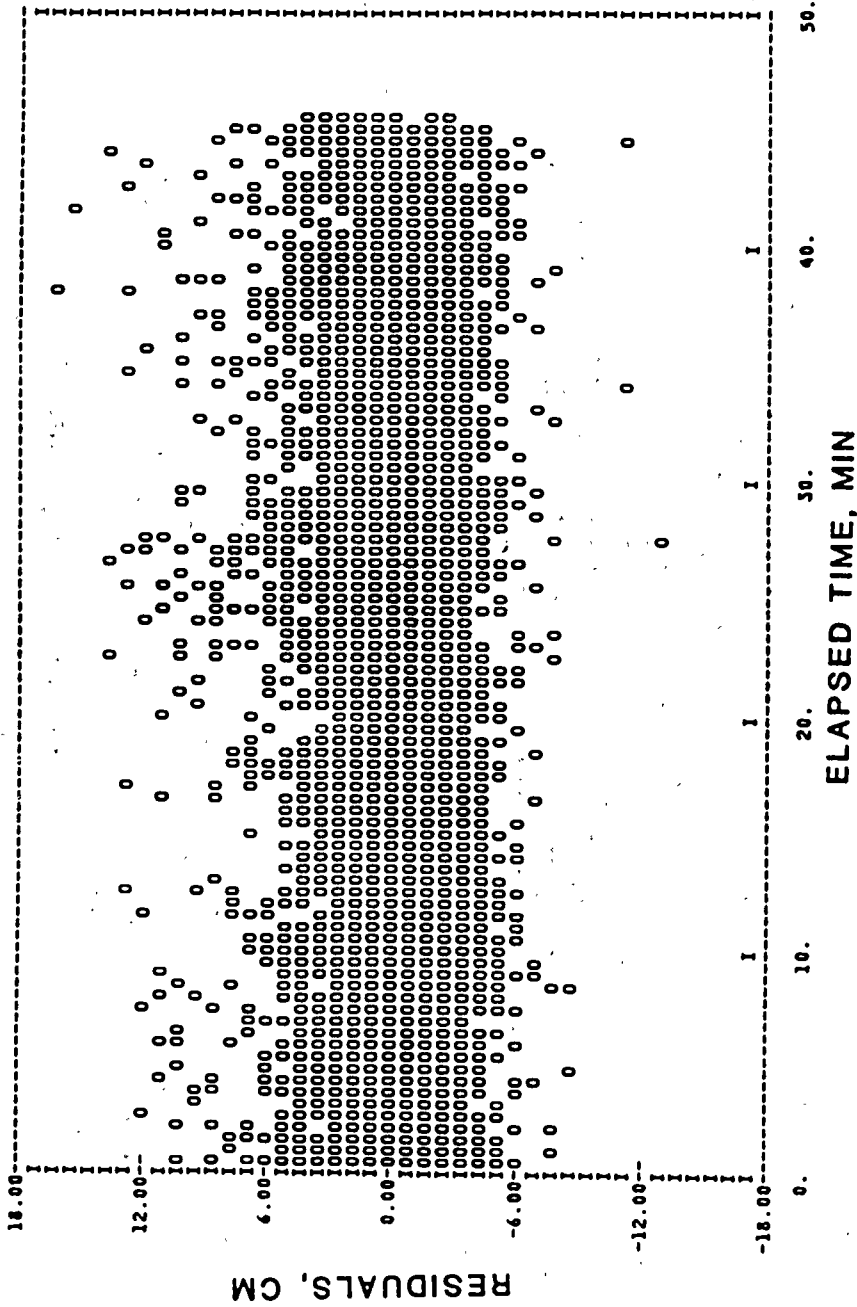


FIGURE 1 MOBLAS-7 range residuals as a function of time.

MTLRS-1
LAGEOS
6/27/86 04:00

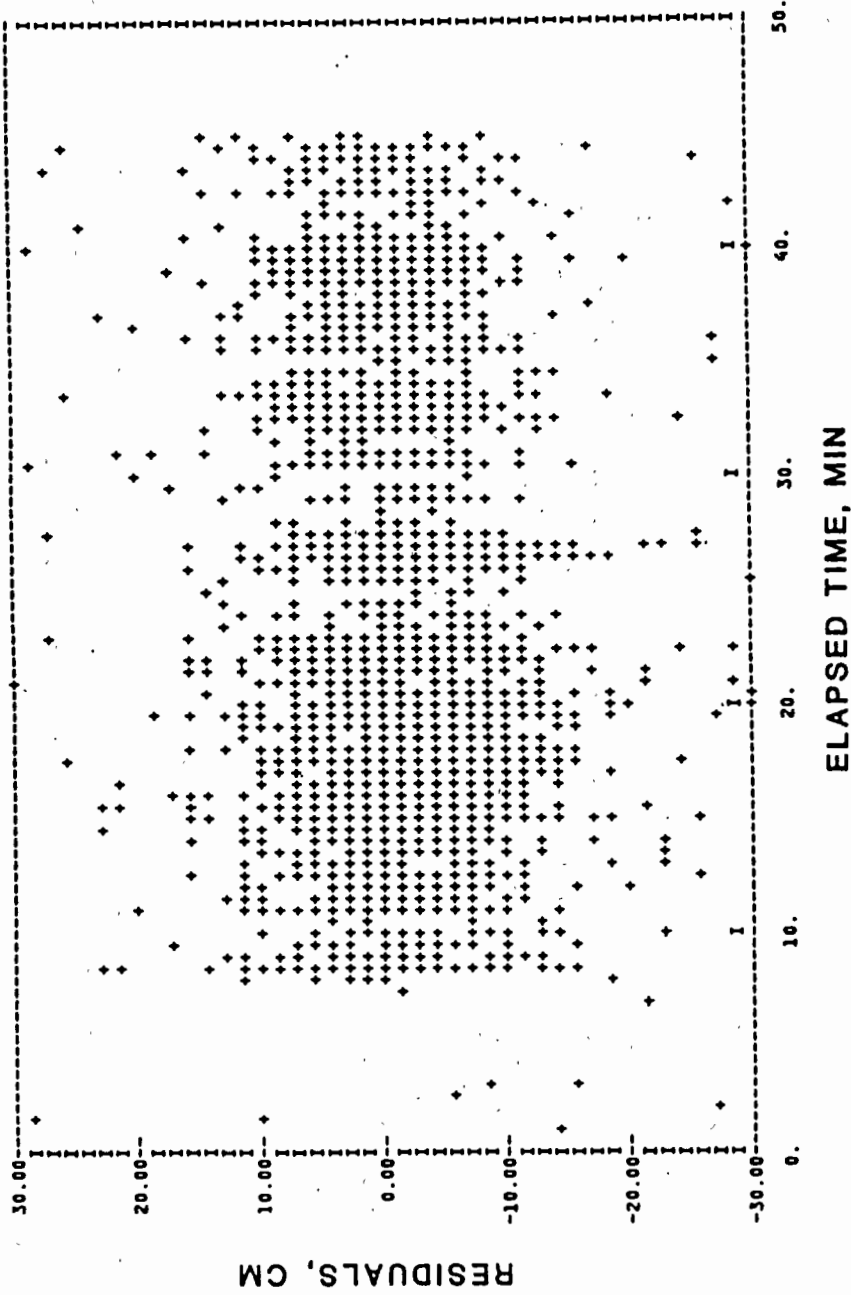


FIGURE 2 MTLRS-1 range residuals as a function of time.

LAGEOS 6/27/85 04:00

MOBLAS-7

MTLRS-1

MTLRS-1
MINUS
MOBLAS-7

ELAPSED TIME	NO. OF POINTS	MEAN CM	SIGMA	STD. DEV. OF MEAN	NO. OF POINTS	MEAN CM	SIGMA	STD. DEV. OF MEAN	DIFF OF THE MEANS	STD. DEV. OF DIFF.
1.00	258 *	-0.10*	2.32*	0.14*	0 *	0.00*	0.00*	0.00*	0.00*	0.14*
3.00	382	-0.11	2.24	0.11	0 *	0.00*	0.00*	0.00*	0.00*	0.11*
5.00	427	0.13	2.15	0.10	0 *	0.00*	0.00*	0.00*	0.00*	0.10*
7.00	502	0.14	2.00	0.09	7 *	3.06*	3.88*	1.47*	0.00*	1.47*
9.00	489	0.16	1.97	0.09	136	-0.50	5.84	0.50	-0.66	0.51
11.00	492	0.01	2.01	0.09	110	-0.55	5.95	0.57	-0.56	0.57
13.00	505	-0.07	1.84	0.08	159	-0.90	5.73	0.45	-0.83	0.46
15.00	482	-0.06	1.76	0.08	318	-0.97	5.41	0.30	-0.92	0.31
17.00	469	0.11	2.03	0.09	378	-2.51	5.09	0.26	-2.63	0.28
19.00	484	-0.02	1.80	0.08	436	-2.48	5.57	0.27	-2.47	0.28
21.00	462	-0.06	2.04	0.09	244	-2.47	5.36	0.34	-2.41	0.36
23.00	463	-0.09	1.95	0.09	182	-1.68	5.34	0.40	-1.59	0.41
25.00	268 *	0.26*	2.26*	0.14*	91	0.04	5.32	0.56	0.00*	0.57*
27.00	205 *	0.57*	2.72*	0.19*	239	-2.49	5.28	0.34	0.00*	0.39*
29.00	485	-0.18	2.19	0.10	34	-0.81	5.33	0.91	-0.63	0.92
31.00	511	-0.11	1.91	0.08	116	-0.68	5.32	0.49	-0.57	0.50
33.00	500	0.08	1.94	0.09	207	-0.41	5.13	0.36	-0.48	0.37
35.00	501	0.19	1.91	0.09	98	-0.85	5.67	0.57	-1.04	0.58
37.00	424	0.28	2.29	0.11	128	-0.88	4.47	0.40	-1.16	0.41
39.00	468	0.10	2.09	0.10	170	-0.66	4.96	0.38	-0.76	0.39
41.00	341	-0.30	2.25	0.12	48	-0.75	5.77	0.83	-0.45	0.84
43.00	274 *	0.11*	2.55*	0.15*	90	0.13	5.29	0.56	0.00*	0.58*
45.00	161 *	0.10*	2.59*	0.20*	45	0.56	6.08	0.91	0.00*	0.93*

MTD. MEAN = -1.47
STD OF MEAN = 0.10
STD ABOUT MEAN = 0.84

NO. OF ITERATIONS = 4

TABLE 1 Two minute interval analysis of residuals.

LAGEOS 6/27/85 04:00

ONE SIGMA ERROR BARS

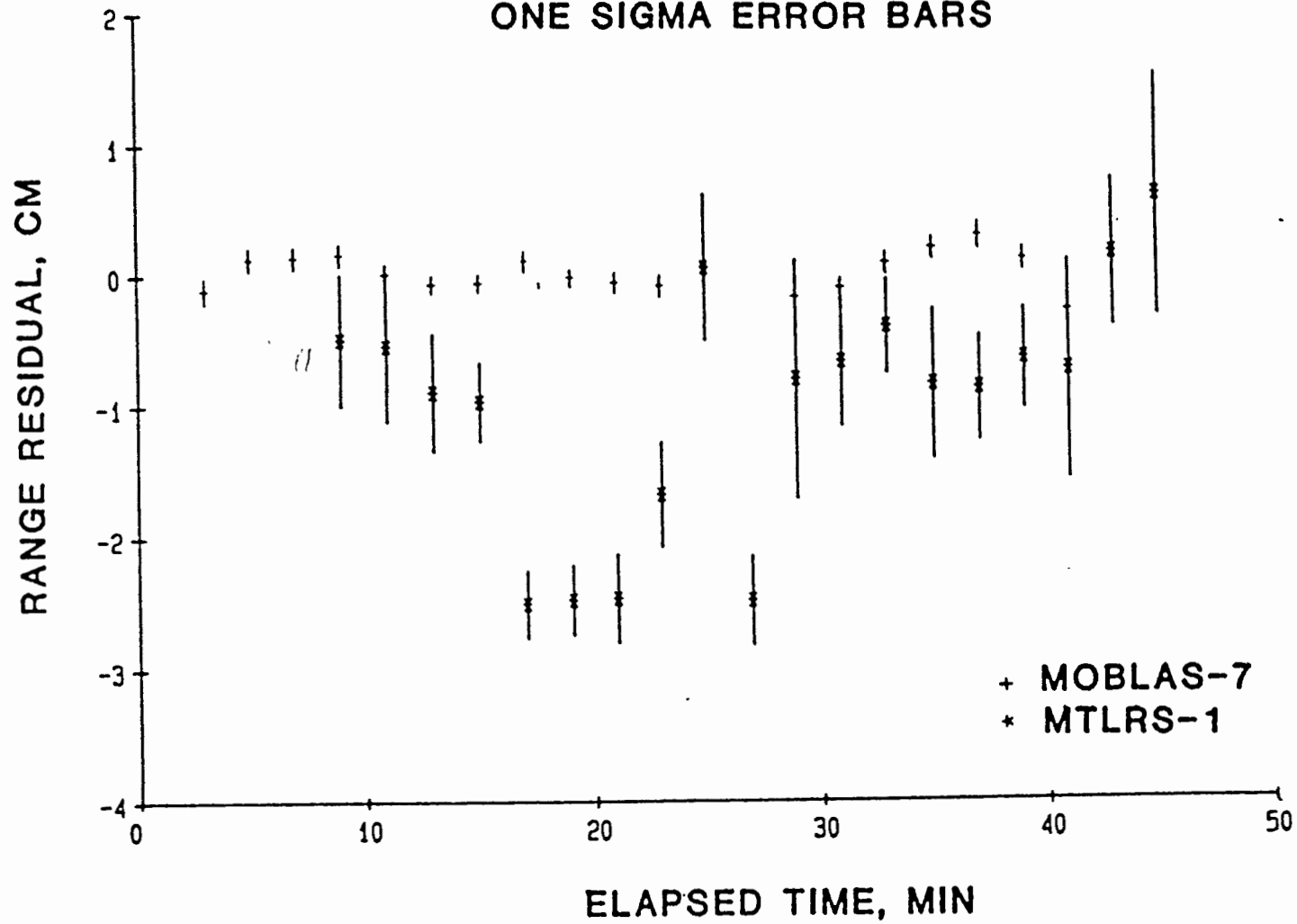


FIGURE 3 Two minute mean range residuals.

LAGEOS 6/27/85 04:00

ONE SIGMA ERROR BARS

x MTLRS-1 MINUS MOBLAS-7

$\bar{X} = -1.47, \beta = 0.10, \phi = 0.84$

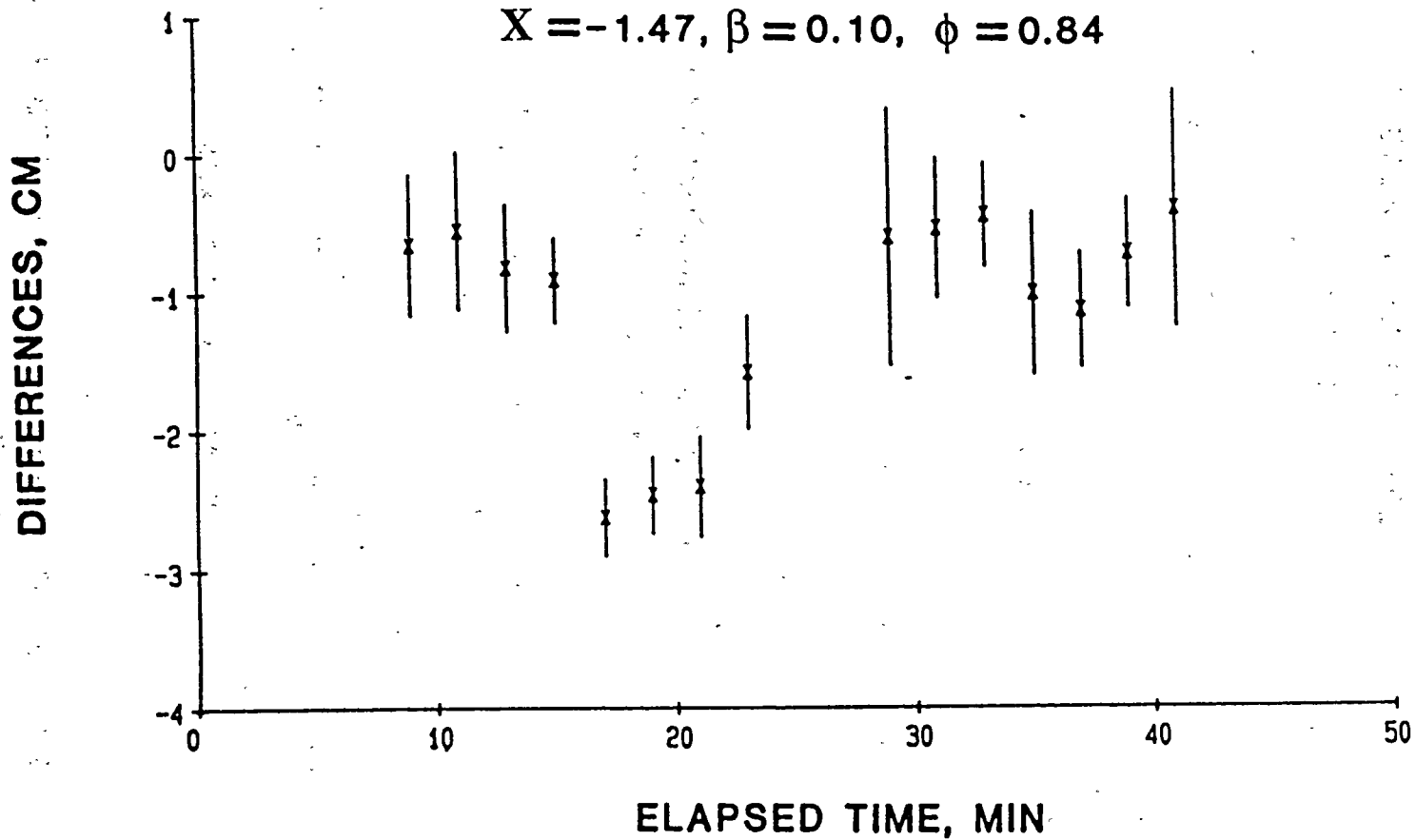


FIGURE 4. Two minute mean range residual differences.

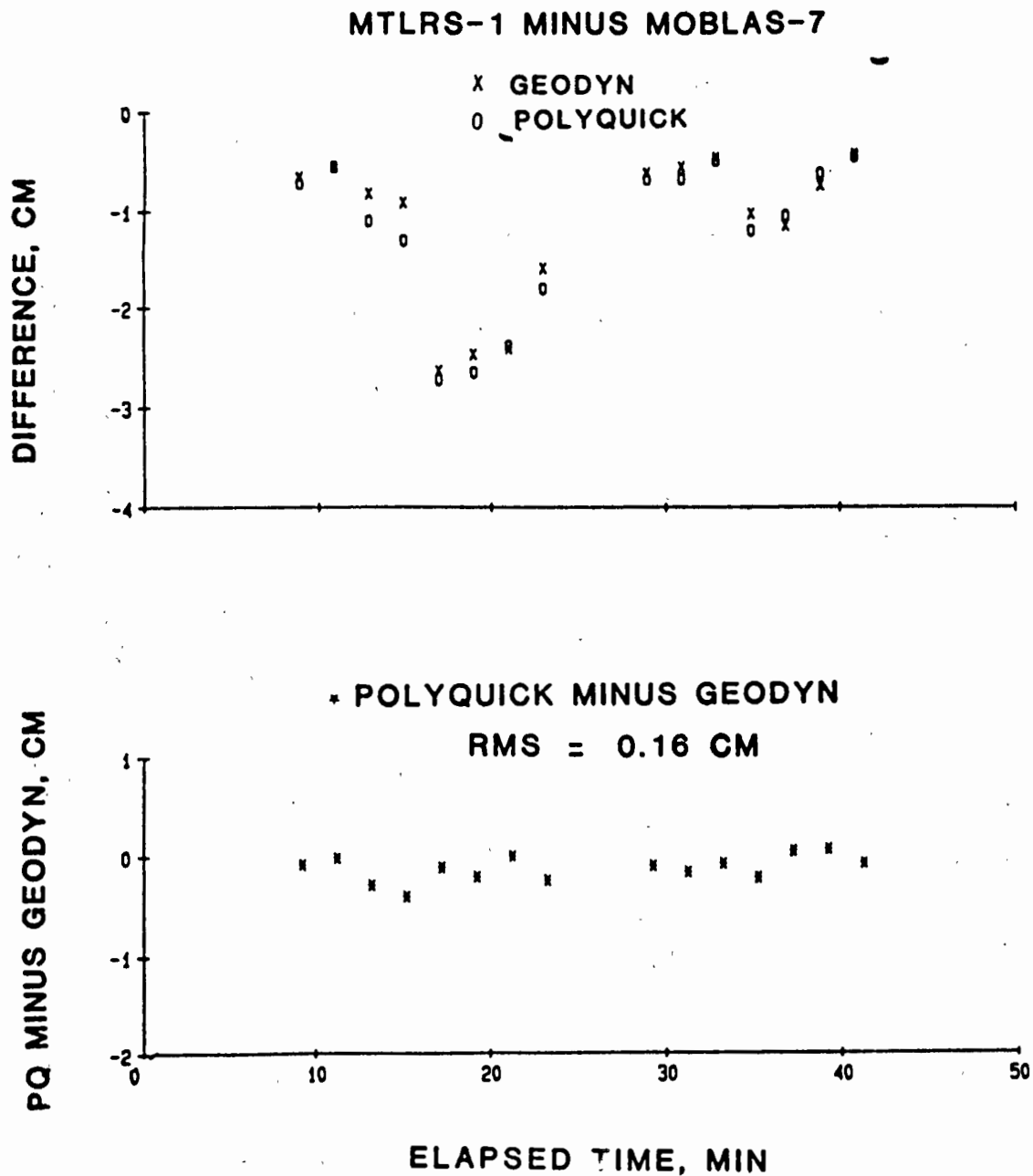


FIGURE 5 Comparison between GEODYN and POLYQUICK for LAGEOS 6/27/85.

DATE IN 1985	TIME, GMT	WEIGHTED MEAN DIFFERENCE MTLRS-1 MINUS MOBLAS-7, CM		POLYQUICK MINUS GEODYN, CM
		GEODYN	POLYQUICK	
5/10	0934	-1.65 ± 0.20	-1.44 ± 0.20	0.21
5/15	0612	1.55 ± 0.14	1.42 ± 0.14	-0.13
5/20	0628	-1.93 ± 0.12	-1.96 ± 0.12	-0.03
5/21	0838	0.05 ± 0.15	0.06 ± 0.15	0.01
5/30	0704	-0.95 ± 0.10	-0.96 ± 0.10	-0.01
6/03	0848	-1.39 ± 0.14	-1.12 ± 0.14	0.27
6/14	0738	-2.58 ± 0.11	-2.60 ± 0.11	-0.02
6/17	0704	-3.76 ± 0.10	-3.56 ± 0.10	0.20
6/26	0520	-3.41 ± 0.18	-3.28 ± 0.18	0.13
6/27	0400	-1.47 ± 0.10	-1.58 ± 0.10	-0.11
6/27	0732	-3.10 ± 0.10	-3.08 ± 0.10	0.02
7/04	0838	-0.66 ± 0.30	-0.51 ± 0.30	0.15
7/14	0530	-0.08 ± 0.20	0.20 ± 0.20	0.28
WEIGHTED MEAN = -1.80			-1.76	rms = 0.15
STD OF MEAN = 0.04			0.04	
STD ABOUT MEAN = 1.42			1.38	

TABLE 2 Comparison between GEODYN and POLYQUICK for the MOBLAS-7 and MTLRS-1 collocation.

Year	Population	Area	Population	Area
1900	1,000,000	100,000	1,000,000	100,000
1910	1,200,000	120,000	1,200,000	120,000
1920	1,400,000	140,000	1,400,000	140,000
1930	1,600,000	160,000	1,600,000	160,000
1940	1,800,000	180,000	1,800,000	180,000
1950	2,000,000	200,000	2,000,000	200,000
1960	2,200,000	220,000	2,200,000	220,000
1970	2,400,000	240,000	2,400,000	240,000
1980	2,600,000	260,000	2,600,000	260,000
1990	2,800,000	280,000	2,800,000	280,000
2000	3,000,000	300,000	3,000,000	300,000

The following table shows the population and area of the United States from 1900 to 2000. The population is shown in millions and the area is shown in thousands of square miles. The population has increased from 1 million in 1900 to 3 million in 2000. The area has increased from 100,000 thousand square miles in 1900 to 300,000 thousand square miles in 2000.

REAL TIME, ON SITE EARTH ORIENTATION PARAMETER
GENERATION AT THE MLRS USING LUNAR LASER RANGING
DATA

P.J. Shelus, R.L. Ricklefs
McDonald Observatory and Department of Astronomy
University of Texas at Austin
Austin, Texas 78712-1083 - USA -

Telephone (512) 471 3339
TWX 910874 1351

ABSTRACT

For more than a year, earth rotation parameters (i.e, UT-0) have been computed on site, in real-time at the McDonald Observatory Laser Ranging Station (MLRS) using lunar observations to the Apollo 15 corner retroreflector. These parameters have then been immediately electronically transmitted, via the General Electric Company Mark III network, to the U.S. Naval Observatory for eventual use in their earth orientation prediction services. In this paper we shall briefly discuss the recent history of this endeavor, the hardware and software components which compose this system, the observational strategy which is being employed, and the results which have been obtained so far. Because of the unique nature of the lunar laser ranging data type, which allows this rather straightforward real-time, on-site earth rotation computation to be made, and because of the common software which exists at all of the lunar capable laser ranging stations, it is hoped that within a year or so all of the LLR stations will be able to provide similar services for earth orientation results.

This research is being supported by the National Aeronautics and Space Administration under Contract NAS5-29404 and Grant NAG5-754 to McDonald Observatory and the University of Texas at Austin from the Goddard Space Flight Center in Greenbelt, Maryland.

Introduction

The securing of precise Earth orientation information has long been the one of the major goals of laser ranging observations to Earth orbiting targets (see, for example, Bender et al, 1973 or Mulholland, 1980). Although much successful work has been performed at various analysis centers over the past ten years in securing these results, spurred by such international projects as EROLD and MERIT (see, for example, Langley et al, 1981 or Dickey and Williams, 1983), the presence of powerful mini- and micro-computers on-site at modern ranging stations, coupled with the long period modeling accuracies now available, make it possible for one to consider the computation of these data products in a near-real-time environment on-site at the laser ranging stations themselves. At the McDonald Observatory Laser Ranging Station (MLRS), located near Fort Davis, Texas, we have been producing such results, using lunar laser ranging observations, since early 1985. This paper describes the techniques which are being applied and the results which have so far been obtained.

Techniques

The basic equation for dynamical parameter improvement used in most lunar laser ranging analysis is the following:

$$\tau_o - \tau_c = \sum_{i=1}^n \frac{\partial \tau}{\partial \kappa_i} (\kappa_i - \kappa_c) \quad (1)$$

where τ_o and τ_c are the observed and calculated ranges (i.e., time delays), respectively, and the κ_i are parameters associated with whatever model is currently being used. Since it is convenient to deal with changes in the Earth's orientation as changes in the longitude, λ , and the latitude, ϕ , of the observing station, we can re-write equation 1 explicitly as (see, for example, Stolz and Larden, 1977 or Shelus et al, 1981):

$$\tau_o - \tau_c = \frac{\partial \tau}{\partial \lambda} (\lambda - \lambda_o) + \frac{\partial \tau}{\partial \phi} (\phi - \phi_o) + C. \quad (2)$$

For our purposes, it has been assumed that all short period terms having amplitudes of 1 cm or more, other than those dealing with the orientation of the earth, have been eliminated in the modeling and that, since we shall be averaging data over no more than a few days, all longer period terms can be assumed to be constant. We feel that this is certainly a reasonable assumption for the lunar system.

Of course, the major requirement for the production of real-time earth orientation information on-site (in addition to the capability of making the observations themselves) is the availability of a convenient and precise lunar range prediction system. The transfer of such a system to the MLRS was accomplished some two years ago when we succeeded in reproducing MIT lunar range prediction results at the 20-30 psec level. We are presently working to attain the same levels of accuracy with the JPL lunar model predictions.

The obtaining of earth orientation parameters from MLRS lunar laser ranging observations can be summarized as follows. With the completion of a lunar "run", using various interactive graphics tools, the lunar data set is statistically filtered and mathematically compressed to form a single normal point. When several such normal points have been formed within a pre-defined interval of time (usually 24-48 hours), an earth orientation solution is performed using the residual and partial derivative values appropriate to equation 2 above. At the present time, only observations to the Apollo 15 (Hadley) retroreflector are used and only a longitude, i.e., UT-0, solution is made. We consider an earth orientation reduction to be "prime" if it is obtained using data within a single lunar transit and with an hour angle spread of at least 3 hours. Under any other circumstances, the reduction is considered to be "non-prime". Results are inspected on-site for potential problems and, if they prove to be satisfactory, are placed onto the General Electric Company Mark III system for general distribution. Under normal circumstances, the total time, from the beginning of the observing sequences for a "prime" data set to Earth orientation parameter transmittal, encompasses an interval of less than 18 hours.

Results

Since February, 1985 there have been some 38 UT0 points produced at the MLRS in this real-time environment. Of these, 8 are considered "prime". Comparisons of our "quick-look" results with "full-rate" results obtained by X X Newhall at JPL (Figure 1), those obtained by the BIH (Figure 2), and those obtained by our own after-the-fact Earth orientation reduction system in Austin (Figure 3) have been quite satisfactory. For the JPL comparisons, it was necessary to convert the "standard" $UT0_R - UTC$ values to $UT0 - UTC$ by re-introducing the short period zonal tide terms (see Yoder et al, 1981). For the BIH comparisons, $UT0 - UTC$ values at McDonald Observatory were inferred from the BIH final values for x, y, and $UT1 - UTC$, interpolated to the time of the MLRS $UT0$ point..

Although our early results seem to be somewhat off the mark, as our procedures mature and our experience improves, quite a good agreement is being obtained with the more recent data. To re-iterate, and as a caveat to prospective users, it is quite important to realize that this is essentially a "quick-look" procedure. Since we deal in a real-time environment, our results can sometimes be contaminated by data which proves to be poor, under later analysis. Further, we do no fitting of the data for other parameter improvement, as is done in the regular after-the-fact, full-rate data environment. In spite of these shortcomings, we feel that our product is a good one and can serve many of the "quick-look" needs of the Earth orientation community.

As a final comment, it must be stated that the biggest difficulty with which we are being presently confronted is a severe paucity of Earth orientation results using this lunar technique. At the MLRS, the station has been working flawlessly; the data gaps are completely a product of the environment. It is hoped that most of this type of problem can be solved by a move of the MLRS from its present "saddle-site" to one at the top of a near-by mountain. On the positive side, in our processing of lunar laser ranging data from the Haleakala site, we are attempting to apply the self-same MLRS data reduction techniques to compute Earth orientation parameters from Hawaii data. In addition, we are also interested in the sharing of this software with other stations, which have equipment that is capable of making similar types of reductions on-site, and are encouraging them to undertake similar "quick-look" types of analyses to obtain additional earth orientation results.

Acknowledgements

The authors cannot too strongly acknowledge and thank Robert W. King at MIT for his invaluable aid in the implementation of the MIT lunar range prediction package at the MLRS.

Additional computer equipment, which provides the capability of simultaneous data gathering and data reduction at the MLRS, has been secured, in part, through funding provided by Dennis D. McCarthy of the U. S. Naval Observatory. Many thanks also go to Nelson Zarate, who produced large parts of the original version of the Earth orientation analysis routines, and to Janice Storm, who runs the present software system so productively at the MLRS. Finally, we acknowledge that this research is being supported at McDonald Observatory and the University of Texas at Austin by National Aeronautics and Space Administration Contract NAS5-29404 and Grant NAG5-754 out of Goddard Space Flight Center, Technical Officers Mr. Robert L. Appler and Dr. Gilbert D. Mead, respectively.

References

- Bender, P.L., Currie, D.G., Dicke, R.H., Eckhardt, D.H., Faller, J.E., Kaula, W.M., Mulholland, J.D., Plotkin, H.H., Poultney, S.K., Silverberg, E.C., Wilkinson, D.T., Williams, J.G., and Alley, C.O. 1973, "The Lunar Laser Ranging Experiment", *Science*, **182**, 229-238.
- Dickey, J.O. and Williams, J.G. 1983, "Earth Rotation from Lunar Laser Ranging", *Astron. Astrophys. Suppl. Ser.*, **54**, 519-540.
- Langley, R.B., King, R.W., and Shapiro, I.I. 1981, "Earth Rotation from Lunar Laser Ranging", *J. Geophys. Res.*, **86**, 11913-11918.
- Mulholland, J.D. 1980, "Scientific Achievement from Ten Years of Lunar Laser Ranging", *Rev. of Geophy. and Sp. Phys.*, **18**, 549-564.
- Shelus, P.J., Zarate, N.R., and Eanes, R.J. 1981, "Earth Rotation from a Simultaneous Reduction of LLR and LAGEOS Laser Ranging Data", *Proceedings of the 63rd Coll. of the IAU*, O. Calame, ed., D. Reidel, 31-40.
- Stolz, A. and Larden, D. 1977, "Accuracy Obtainable for Universal Time and Polar Motion During the EROLD Campaign", *Scientific Applications of Lunar Laser Ranging*, J.D. Mulholland, ed., D. Reidel, 37-50.
- Yoder, C.F., Williams, J.G., Parke, M.E., and Dickey, J.O. 1981, "Short Period Tidal Variations of Earth Rotation", *Ann. des Geophy.*, **37**, 213.

Figure 1. MLRS Earth Orientation Parameters

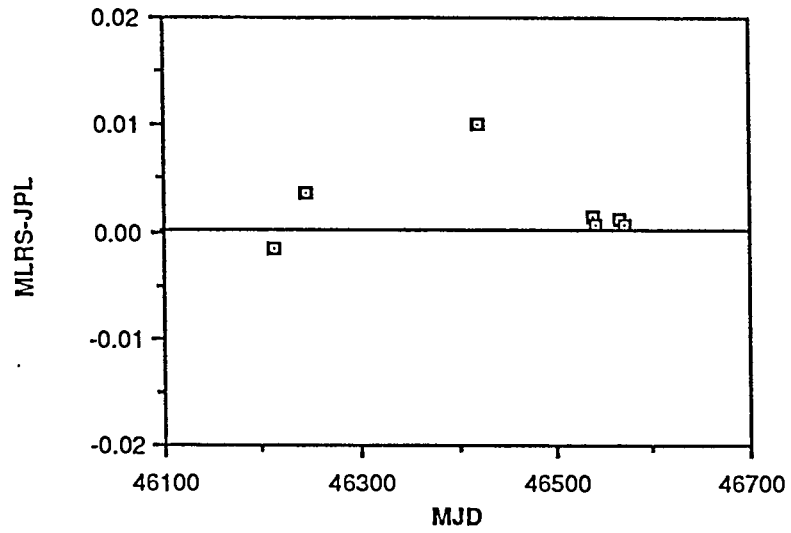


Figure 2. MLRS Earth Orientation Parameters

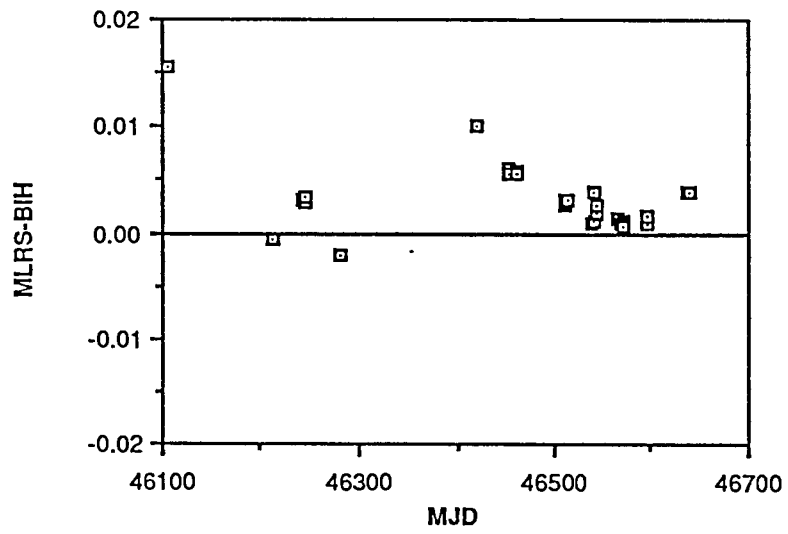
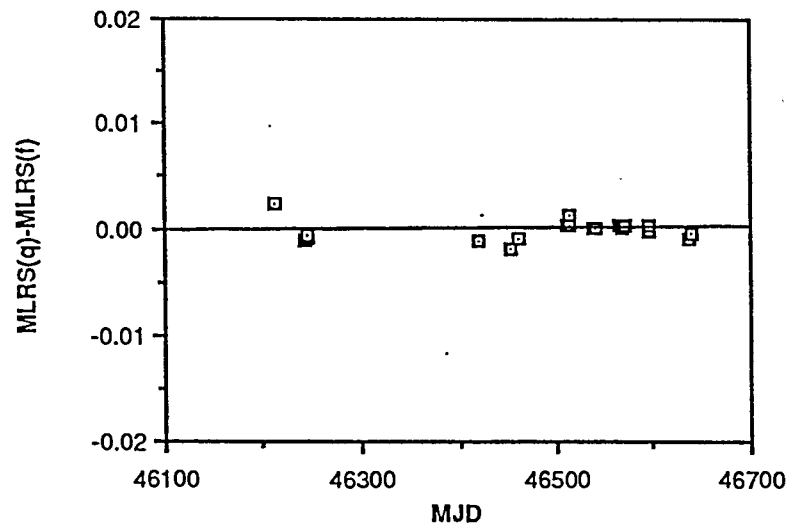
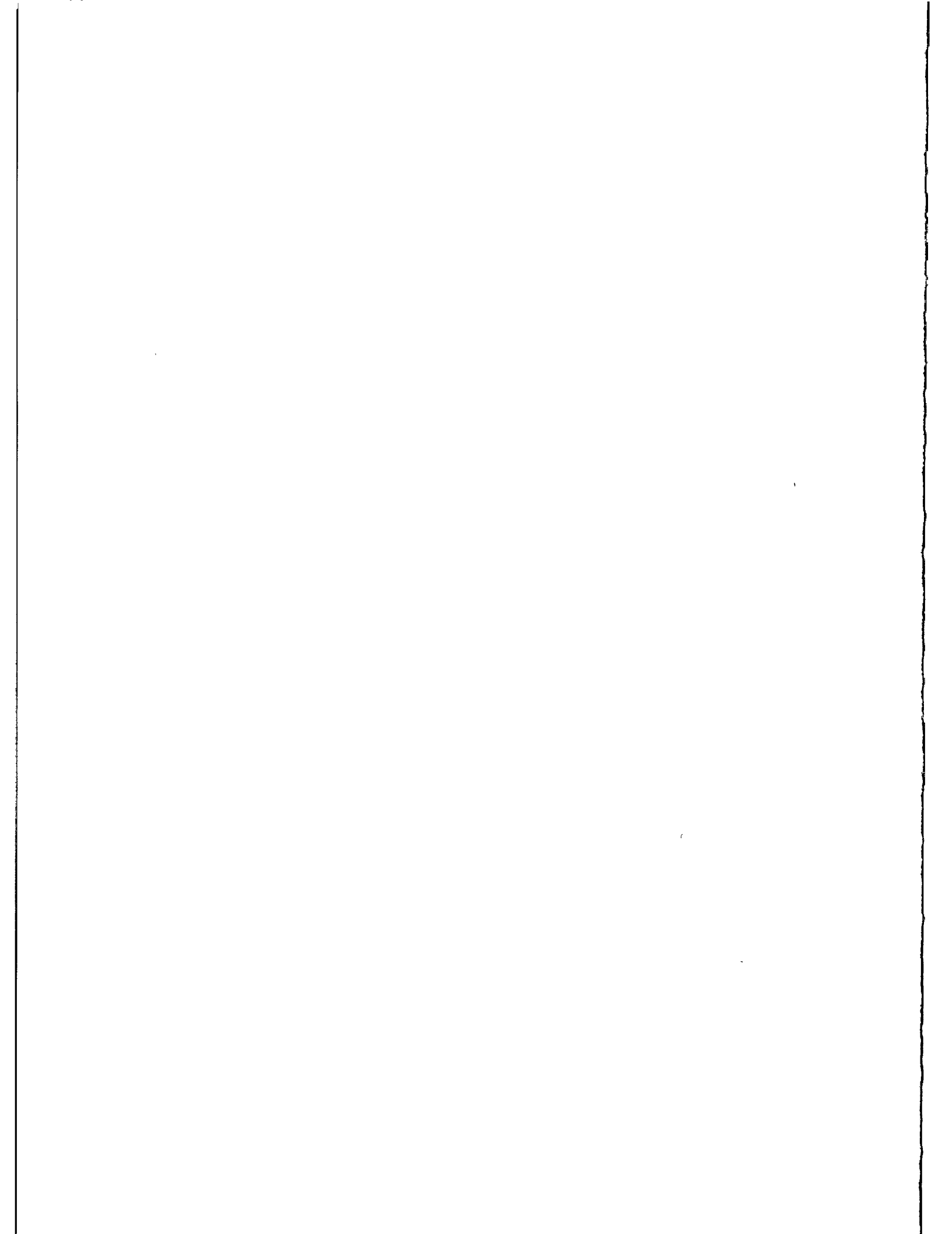


Figure 3. MLRS Earth Orientation Parameters





A NOTE ON THE USE OF THE CSR LAGEOS EPHEMERIDES

G.M. Appleby, A.T. Sinclair
Royal Greenwich Observatory
Herstmonceux Castle
Hailsham
East Sussex BN27 1RP - England -

Telephone (0323) 833171
Telex 87451

ABSTRACT

Using the predicted state vectors of the satellite LAGEOS supplied by the Center for Space Research, Texas University, to form local predictions, the UK Satellite Laser Ranging System at the Royal Greenwich Observatory routinely obtains very precise range observations of the satellite both during the day and at night. This note describes our method of improving extrapolated quantities implicit in the predictions, such that remaining prediction errors are of the order of only 5m in range. We further obtain approximate values of UT1-UTC during periods when several passes have been observed within a short time interval.

A NOTE ON THE USE OF THE CSR LAGEOS EPHEMERIDES

G.M. Appleby and A.T. Sinclair
Royal Greenwich Observatory
Herstmonceux Castle
Hailsham
East Sussex BN27 1RP
England

Telephone (0323) 833171
Telex 87451

Summary. Using the predicted state vectors of the satellite LAGEOS supplied by the Center for Space Research, Texas University, to form local predictions, the UK Satellite Laser Ranging System at the Royal Greenwich Observatory routinely obtains very precise range observations of the satellite, both during the day and at night. This note describes our method of improving extrapolated quantities implicit in the predictions, such that remaining prediction errors are of the order of only 5m in range. We further obtain approximate values of UT1-UTC during periods when several passes have been observed within a short time interval.

1. Introduction

The principal target for the SLR operations being carried out at the Royal Greenwich Observatory, Herstmonceux, is the Laser Geodynamic Satellite, LAGEOS. In order to predict accurately the position of the satellite at any time we depend upon the set of daily state vectors supplied by the Center for Space Research at Texas University (CSR). These vectors are used as starting values for an integration of the satellite's equations of motion to yield its expected position at any given time. The integration uses a simplified force model, and so the optimum accuracy of the integration over 1 day would be a few metres. However, as the orbit is predicted ahead for many months, the real errors are considerably greater. The principal errors are an along-track displacement of the satellite, and an error due to the assumed value of UT1-UTC. This note describes our use of these predictions with particular reference to the determination of the along-track error from our range measurements and the correction of the assumed values of UT1-UTC implicit in the starting values, in order to improve the accuracy of the predictions to about 5 metres. We further derive some near-realtime values of UT1-UTC from our range measurements.

2. The accuracy of the CSR predictions

The CSR predictions for Lageos are issued for up to 18 months ahead, so inevitably they have increasing errors towards the end of their span. The major source of error is the uncertain drag-like acceleration affecting Lageos, which leads to an along-track positional error. This acceleration is generally modelled very well by CSR, the remaining error being only 600 m in along-track position (equivalent to a time bias of 100 ms) at the end of ephemeris 19. This would cause a maximum effect at the start or end of a pass on the two-way range of 500 m or 1700 ns. Such an error would cause serious problems for day-time ranging with a narrow range gate, but fortunately the time bias varies slowly, and the current value can be determined as part of the pre-processing of the range data obtained in each Lageos pass (Appleby and Sinclair, 1985). The time bias is determined as a correction to the orbital mean anomaly of the satellite, and this is converted to a time bias by dividing by the mean motion.

The second most significant source of error in the CSR predictions is caused by errors in the extrapolated values of UT1 used by CSR in referring their predictions to the Greenwich meridian. The coordinate system of the CSR state vectors is nominally the true equator of date and the Greenwich meridian, but as is shown in Figure 1, the CSR x-axis will differ from the Greenwich meridian by $1.00273 \Delta UT1$, where $\Delta UT1$ is the error in the extrapolated value of UT1, and where we are measuring angles in time units. The typical magnitude of the error $\Delta UT1$ is about 100 ms, which was the value half-way through ephemeris 19. The simplest way to use the CSR predictions is to ignore this error, and treat the predictions as if they were referred to the Greenwich meridian. For a north-south pass of Lageos this had little effect on range, but for an east-west pass it changes the two-way range at the start or end of a pass by 80 m or 260 ns.

The variation of range through an east-west pass caused by an error in UT1(extrap) is very similar to that caused by a time bias, such that an error of 100 ms in UT1 (extrap) has virtually the same effect on range for an east-west pass as a time bias of 15 ms. Hence if the effect of the error in UT1(extrap) is not corrected in the predictions, the value of the time bias determined from east-west passes will be corrupted by the order of 15 ms, while from north-south passes the correct value of the time bias will be obtained.

For a ranging system using a narrow range gate of the order of 100 ns, and particularly during day-time ranging, this variation of the value determined for the time bias according to the pass direction is very inconvenient, since the typical error in time bias of 15 ms can cause two-way range residuals for a subsequent pass of 80 m or 260 ns. Hence at RGO the error in UT1(extrap) is corrected during the computation of predictions.

Further it is expected that this unpredictable error in UT1(extrap) may well be the dominant effect in future Lageos ephemerides, as the model representing the drag forces on the satellite inevitably improves. We comment in passing that the velocities given in the CSR state vectors are, for historical reasons, referred to the reference frame rotating with the Earth, and have to be converted to an inertial frame before performing the numerical integration. This is done in the CSR program IRVINT. It is also carried out in the equivalent RGO program ORBIT, which uses a reference frame defined by the true equator of date and X axis which is displaced from the mean equinox of date by $1.00273 \Delta UT1$. This reference

frame error has negligible effect on the calculation of the forces acting on the satellite, and hence in the derived predicted position. For subsequent calculation of topocentric position, the satellite coordinates are again referred to the CSR reference frame.

3. Application of corrections to UT1(extrap)

In order to minimise the pass-dependent effect on the determination of the time bias we need a close approximation to the error of UT1(extrap) to be used in computing predictions. The extrapolated values of UT1-UTC used by the CSR to generate the predictions are available in a file along with the state vectors on the magnetic tapes distributed by CSR. Thus for a given pass we compute

$$\Delta UT1 = (UT1-UTC)_{CSR} - (UT1-UTC)_{BIH}$$

where we have obtained $(UT1-UTC)_{BIH}$ by short extrapolation from the most recent values of the BIH rapid service. We then reduce the longitude of the station by $1.00273 \Delta UT1$ (in time measure), thus effectively removing the small rotation about the z-axis between the satellite and terrestrial reference systems. This will improve the accuracy of the predictions, and a solution for or time-bias will be free from corruption by $\Delta UT1$, regardless of orientation of the pass. With the removal of the reference system error in this way, and using recently-determined values of the time bias, we find we can predict the range to the satellite to an accuracy of about 5m, or 30ns in 2-way time-of-flight. The plot shown as Figure 2 gives the derived time bias values for the duration of CSR ephemeris 19. The small scatter of values about the fitted smooth curve shows the effectiveness of the above method. The small size of the time bias, even near the end of the ephemeris, shows how well the CSR drag model has predicted the accelerations experienced by Lageos.

4. Estimation of UT1-UTC from the observations

Based on the above analysis it is clear that any small errors in our short-term extrapolation of $(UT1-UTC)_{BIH}$ should become apparent as small differences in the determined value of the time bias according to pass direction. In particular if we observe several passes in a day, we may use the N-S or S-N passes to derive a current, uncorrupted, value for the time bias. This value may then be assumed when reducing an E-W pass and the observations used to derive a correction to our assumed value of UT1-UTC.

In practice we use the observed ranges from 2 or more passes in a given day in a simultaneous solution for time bias, correction to our assumed $(UT1-UTC)$ and correction to the geodetic latitude of the SLR instrument. The latitude correction allows for small errors in our short-term extrapolated values of the coordinates of the pole. Strictly we should only determine UT0-UTC from one observing station, but we find that our extrapolation of the coordinates of the pole from the rapid service results are usually in error by no more than ± 0.005 in x_p and y_p . Then for the coordinates of Herstmonceux ($\lambda \approx 0^\circ$, $\phi \approx 51^\circ$),

$$\begin{aligned} \delta UT1 &= 0.005 \tan \phi \\ &= 0.4 \text{ms} \end{aligned}$$

is the corruption to UT1-UTC due to the error in the extrapolated x_p and y_p . This error is within the probable error of the derived values of $(UT1-UTC)$ by our approximate method. The results of some determinations of

UT1-UTC are given in Figure 3, where the values are compared to the raw UT1-UTC results taken from BIH Circular D.

5. Conclusion.

We have described our use of the University of Texas Lageos ephemerides to generate predictions in order to obtain laser range measurements. We have shown that given the best available estimated values of UT1-UTC we can effectively remove the errors in the extrapolated values of UT1-UTC implicit in the satellite reference system. We can then use our range measurements to derive uncorrupted estimates of orbital along track error which can be used to improve subsequent predictions such that the prediction errors are less than 5 metres. We further find that we can obtain approximate values of UT1-UTC from our observations on days when several passes of Lageos have been observed, the accuracy of these estimates depending upon how well the long-term behaviour of the node of the orbit has been modelled in the CSR ephemerides.

Reference: Appleby, G.M. and Sinclair, A.T. 1985.
SLR Technical Note No.5.
Data Processing and Preliminary Analysis Software for the UK
Satellite Laser Ranging Facility.

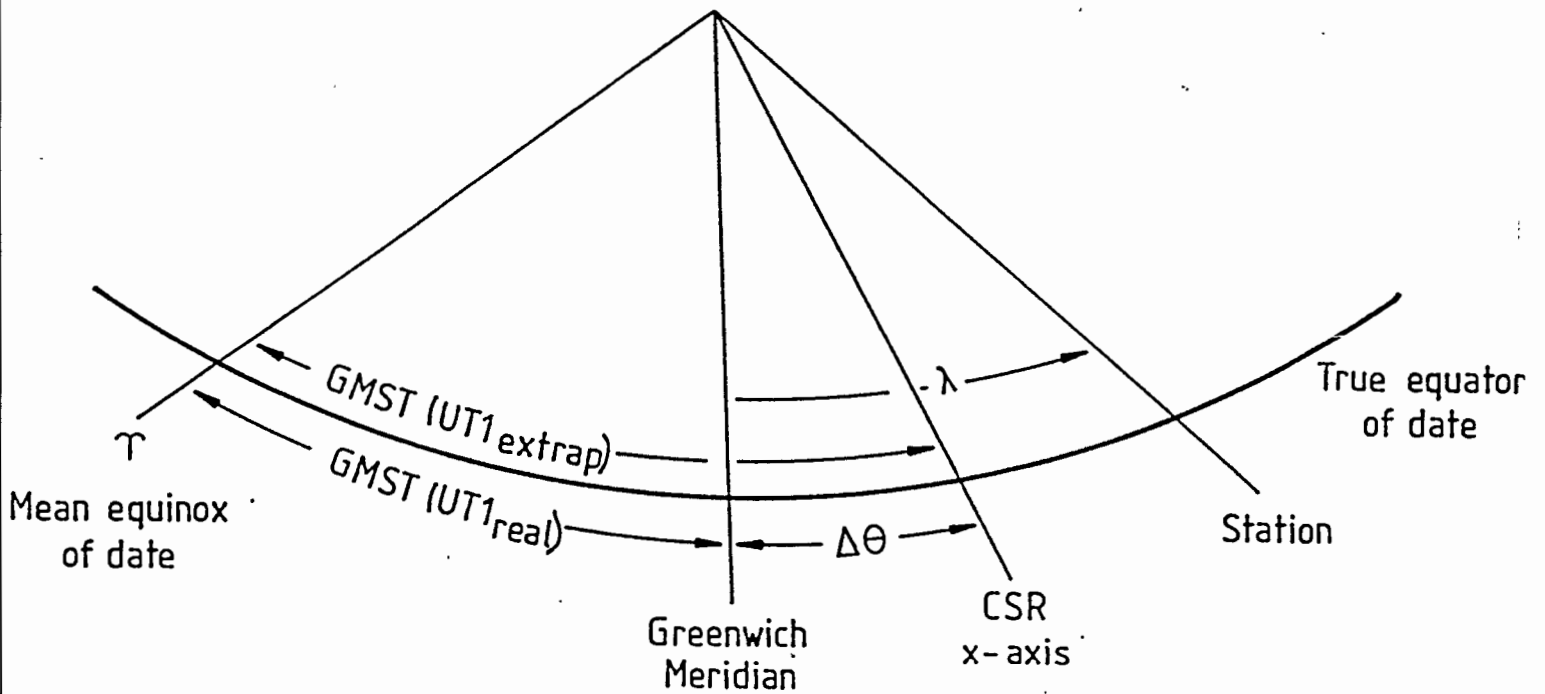


Figure 1. The location of the CSR x-axis relative to the Greenwich Meridian.

$$\Delta\theta = 1.00273 \cdot \Delta UT1 \quad (\text{in time units}),$$

where $\Delta UT1 = UT1(\text{extrap}) - UT1(\text{real})$.

The longitude of a station should be reduced by $\Delta\theta$ in order to refer it to the CSR x-axis.

REAL TIME UT0 DETERMINATION AT CERGA LLR STATION

Ch. Veillet, D. Feraudy, J. Pham-Van
CERGA
Avenue Copernic
06130 Grasse - France -

Telephone 93 36 58 49
Telex 470865 F

ABSTRACT

UT0 determinations based on single night LLR data are presented. They use Pole coordinate predictions from BIH. Comparisons are made with final values by CERGA and JPL. The available software can be used at the end of an observing session in order to allow close real-time UT determination.

1/ Introduction

A great advantage of the LLR technique is to be able to provide a quite accurate UT0 value in close real time, for instance at the end of an observing night. In fact, the three Earth Rotation parameters can be determined from LLR if various stations give data at the same time. Unfortunately, such a situation occurs rarely and only single station (CERGA) UT0 determinations will be presented here.

2/ CERGA data and UT0 determination

Table 1 shows the number of UT0 determinations made in 1985 with the LLR data from the various stations, together with the corresponding number of nights and the mean standard deviation. A UT0 value can be obtained from data on a single lunar reflector and a single night as long as the hour angle coverage is large enough. As the CERGA station is able to range more than one reflector on a single night, there are more UT0 values than observing nights for this site.

Stations	UT values	nights	msd (ms)
McDonald 2.7m	12	12	.6
MLRS	6	5	.3
Haleakala	29	28	.3
CERGA	118	67	.7

Table 1 - Statistics on UT determinations from LLR for 1985

3/ Single night process

Three examples are shown using two different nights and two reflectors. The first night is one of the longest never obtained at CERGA. It covers more than 10 hours. Fig 1 shows the residuals (observed-calculated) determined on the station computer from the prediction software (based on DE121/LLB13 JPL ephemeris) and the predicted ERP from BIH. These residuals are fitted in order to extract the UT information. The found value for $UT0 - UTC$ is given on the figure and compared with CERGA and JPL a posteriori determinations using Circular D BIH Pole coordinates. For such a night on Appolo XV, the error on $UT0 - UTC$ is small, mainly due to the very long hour angle coverage. Even with a few data, as on Fig. 2 (Lunakhod 2 on the same night), this error is small for the same reason.

As the last observing session (Fig. 3) is much shorter, the uncertainty on $UT0 - UTC$ is much larger. However, the "real-time" value is very close to the final one. The error on UT due to the fact that "real-time" determinations are made with predicted Pole coordinates is small: X and Y are easy to predict with a quite good accuracy.

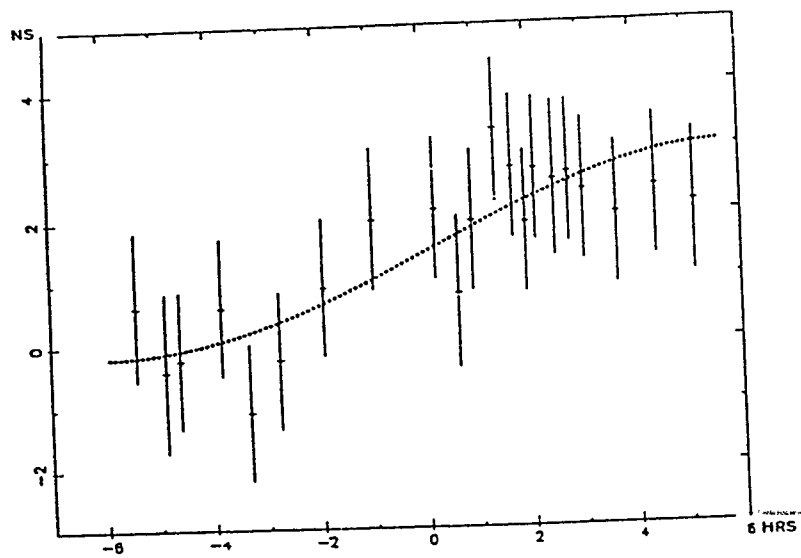
4/ Conclusion

The software used for these "real-time" UT determinations is available at the station and can be run at the end of an observing session. The agreement between them and the "final" values is quite good and shows that LLR "real time" UT can significantly contribute to accurate short term UT predictions.

CERGA + BIH prediction
 UTOR - UTC = .53166

CERGA + Cir. D
 UTOR - UTC = .53176 (16)

JPL + Cir. D
 UTOR - UTC = .53198 (14)



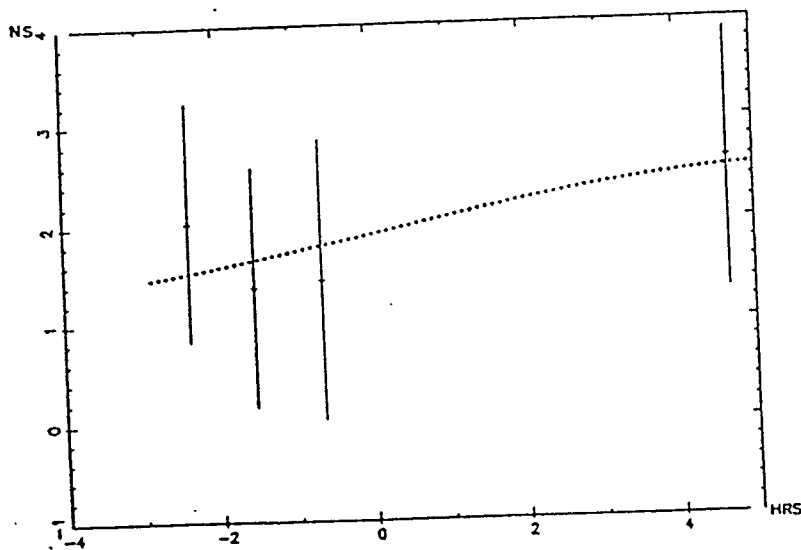
CERGA - Apollo XV - 6/Sep/1985

Fig. 1 - Residuals of range measurements (+) over one night relative to hour angle.
 Dashed curve shows the fit used for UT determination

CERGA + BIH prediction
 UTOR - UTC = .53183

CERGA + Cir. D
 UTOR - UTC = .53132 (43)

JPL + Cir. D
 UTOR - UTC = .53154 (41)



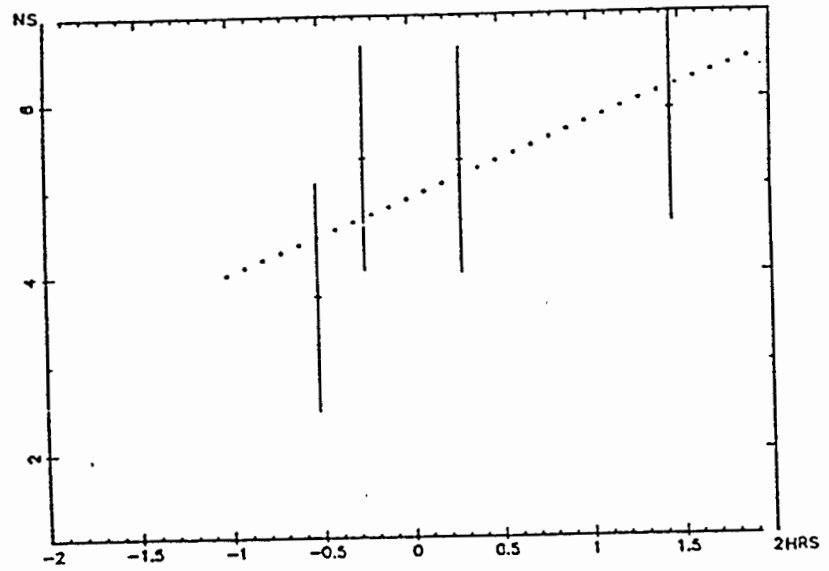
CERGA - Lunakhod 2 - 6/Sep/1985

Fig. 2 - Residuals of range measurements (+) over one night relative to hour angle.
 Dashed curve shows the fit used for UT determination

CERGA + BIH prediction
 UTOR - UTC = .54075

 CERGA + Cir. D
 UTOR - UTC = .54060 (133)

 JPL + Cir. D
 UTOR - UTC = .54117 (125)



CERGA - Apollo XV - 28/Aug/1985

Fig. 3 - Residuals of range measurements (+) over one night relative to hour angle.
 Dashed curve shows the fit used for UT determination

Derived UT1-UTC compared with BIH raw values

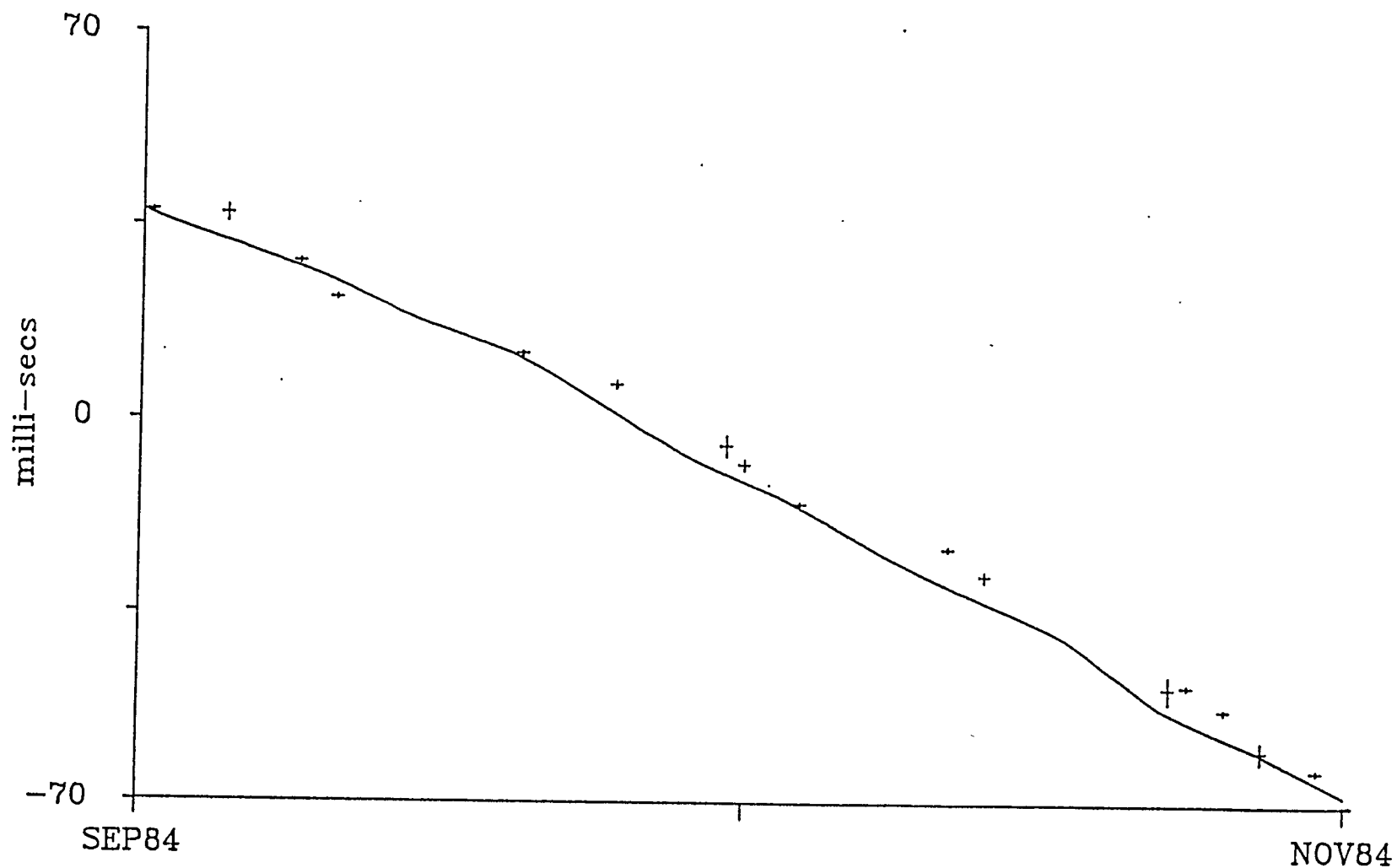


Figure 3. Values of UT1-UTC derived by combining Lageos range observations from 2 or more passes on a given day. The values are shown with 1-sigma error bars, and the full line has been drawn through 5-day raw values of UT1-UTC taken from BIH Circular D.

Observed Time Bias (ms)

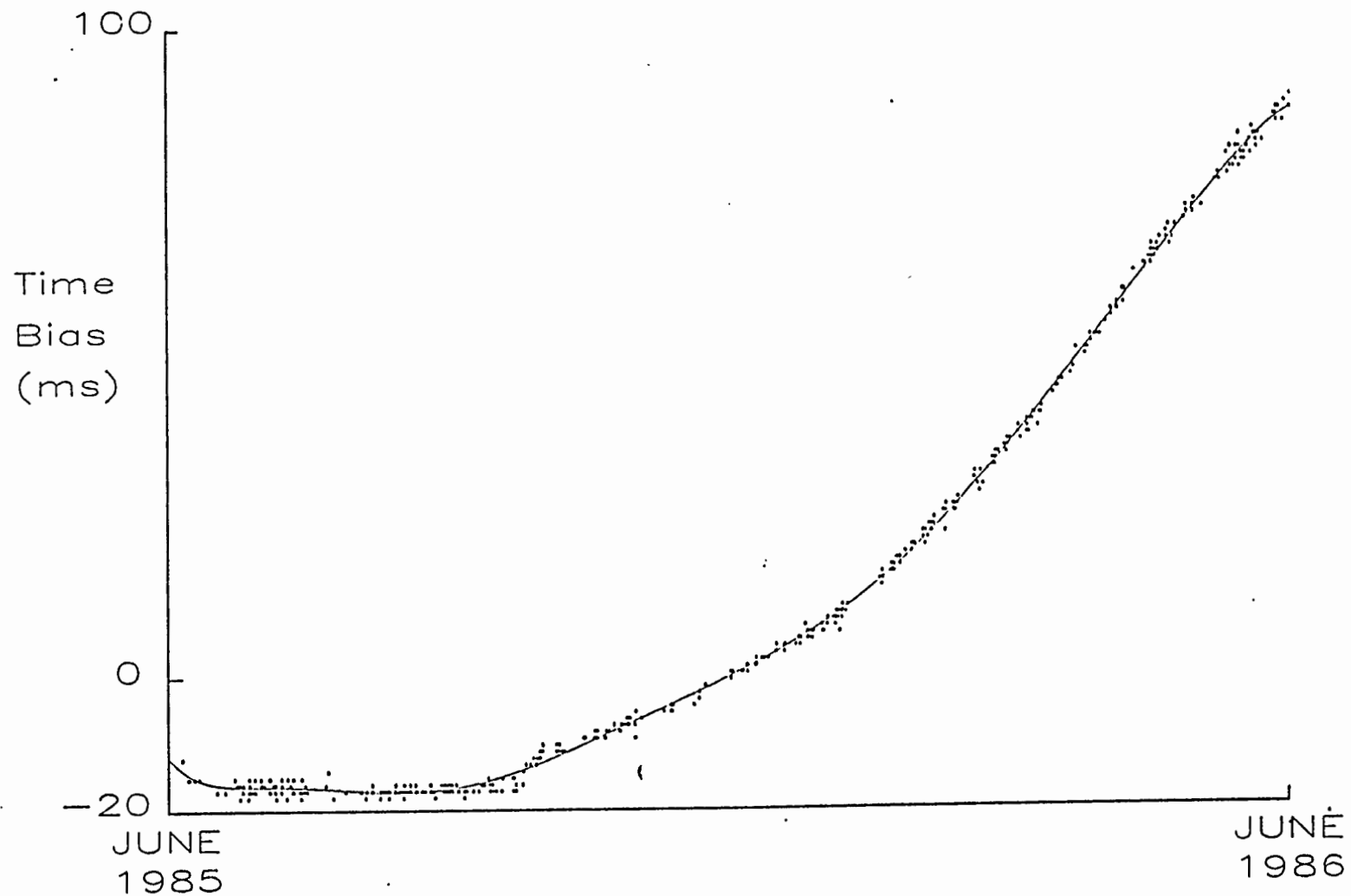


Figure 2. Determinations of Lageos orbital time bias.

Each point gives the time bias value in milliseconds as derived from observations of a single pass. The formal standard errors of the determinations are about 0.1ms. The full line shows a fitted high order polynomial.

A SIMPLE SOFTWARE SCHEDULING TOOL FOR EFFICIENT OBSERVING
OPERATIONS AT A LUNAR/LAGEOS LASER RANGING STATION

P.J. Shelus
McDonald Observatory and Department of Astronomy
University of Texas at Austin
Austin, Texas 78712-1083 - USA -

Telephone (512) 471 3339
TWX 9108741351

ABSTRACT

Once a laser ranging station has crossed the threshold from implementation and development to routine observing, one of the major problems of station operation (aside from preventive maintenance, repairs and upgrades) concerns the efficient scheduling of observing manpower, especially when several different targets are to be regularly observed. This paper describes a simple yet powerful tool which we have developed over the years to aid us in efficient observing crew scheduling for a mix of lunar and LAGEOS operations at the McDonald Laser Ranging Station (MLRS), which is located near Fort Davis, Texas. With a single glance, one can scan the graphical output from this software tool to see lunar and LAGEOS observational opportunities at the MLRS with such items as the visibility times of the moon and LAGEOS, the rising and setting times of the sun, moon, and LAGEOS, the maximum elevation and duration of all visible LAGEOS passes, as well as the lunar phase, age, maximum elevation, and declination during lunar visibility. With this graphical information at one's fingertips, it is then a simple procedure to manually schedule observing crews to take maximum advantage of mutual target visibilities and/or to accommodate whatever station and personnel constraints may be active. This tool has been created using Microsoft_r FORTRAN and is presently running on an Apple_r Macintoshtm computer. Only very slight revisions would need to be made to accommodate the specific locations of other ranging stations and, since the compiler used is a full implementation of FORTRAN 77, few (if any) changes would need to be made for transporting the code to other computers.

This research is being supported by the National Aeronautics and Space Administration under Contract NAS5-29404 to McDonald Observatory and the University of Texas at Austin from the Goddard Space Flight Center in Greenbelt, Maryland.

Introduction

The uses of laser ranging data in the astronomical and geodynamical sciences is now well established. In order to take maximum advantage of whatever resources are available to these scientific endeavors, it is imperative that all possible efficiencies be brought to bear in all phases of data gathering, reduction, and analysis. In a part-time project over the past several years we have put together and implemented a very simple software tool at McDonald Observatory which allows us to manually schedule our observing crews with a minimum of effort while preserving the opportunity for full man-power utilization and maximum target coverage. Our initial task had been made somewhat more difficult due to our responsibilities to both the lunar and the LAGEOS user communities.

On first glance, as one examines the output of this software tool, one might be tempted to comment that the exercise has been a trivial one since the results obtained are so well known and so readily available from so many sources. And we are quick to agree, except for the fact that it is not only the results of the computations which are important, it is also the ease and the convenience with which those computations can be performed and the manner in which those results can be presented. Our purpose was to bring together, in a single, easy to understand graphical display, many of the relevant parameters of solar, lunar, and LAGEOS visibility at the location of a particular laser ranging facility, thereby allowing for the simple and efficient scheduling of observing operations.

Program Description

The nucleus of this software tool is a LAGEOS visibility package which had been assembled by Richard J. Eanes, of the Department of Aerospace Engineering and Center for Space Research at the University of Texas at Austin, to be run on a CDC Cyber computer in simple batch mode. Using nominal elements for the orbit of LAGEOS, such parameters as rise and set times, rise and set point angles, and maximum elevation angles were produced for any input station location and range of dates. With the later inclusion of general mathematical expansions for the orbits of the sun and the moon, also produced were the positions of both the sun and the moon at LAGEOS rise and set times as well as at the time of maximum LAGEOS elevation. The results of these computations could be presented in columnar form on a standard line-printer.

The additions to this program, which were provided by the present author, were several-fold. The logic of the program was altered to compute approximate solar and lunar rise and set times in addition to those of LAGEOS. Added to the program were algorithms to provide the approximate lunar age, phase, and declination at maximum lunar elevation, as well as a day-of-the-week algorithm. The changes which were most extensive (and the most helpful, however) were those which dealt with the printed output. Finally, the entire program was modified to be run, in interactive mode, on a personal, desk-top micro-computer (an Apple® Macintosh™). As a bonus, and specific to the Macintosh™ environment, is the ability to create special symbols for the standard printer output (especially useful for providing lunar phase information) and the ability to use other standard Macintosh™ software, like Microsoft® Word and MacDraw™, for greater readability and to actually manually incorporate scheduling information in the final output.

Output Products

Figure 1 gives a sample of actual program results. The standard output text file shown has been processed by Microsoft® Word to provide for font selection, page alignment, and the

setting of margins and page breaks. Program output is generally printed using an Apple LaserWriter, but excellent results are obtained using any Macintosh™ compatible dot-matrix printer. In the example, for the ten day interval, September 1-10, 1986, one sees complete time-lines which illustrate the visibility of the sun, the moon, and LAGEOS at the MLRS, together with other information vital for crew scheduling.

The very top line on the page gives the month and the year, followed by three lines delineating three appropriate time scales, i.e., Central Daylight Time, Universal Time, and Central Standard Time. Each daily time line is identified by the day-of-the-week, i.e., S, M, T, W, T, F, S and the calendar day-of-the-month at the extreme left. Hour marks are given by vertical bars, "|", and tick marks delineate 12-minute intervals. A sun symbol, "☼", appears when the sun is above the horizon as seen from the MLRS. Just above the sun-line is the moon-line. A changing lunar symbol, denoting the moon's phase (new, "☾"; waxing crescent, "☾"; 1st quarter, "☽"; waxing gibbous, "☾"; full, "☽"; waning gibbous, "☾"; 3rd quarter, "☾"; waning crescent, "☾"), appears when the moon is above 20° elevation as seen from the MLRS. The approximate lunar declination and age at maximum lunar elevation appear at the extreme right end of the moon-line. The LAGEOS time-line is just below the sun-line with a LAGEOS symbol, "☾", appearing when LAGEOS is above 20° elevation as seen from the MLRS. The two digit number, appearing just to the right of each set of LAGEOS symbols, denotes the approximate maximum elevation at MLRS for that particular LAGEOS pass.

Figure 2 illustrates the results which were obtained by manually inserting scheduling information onto the basic time-lines, using the commercial software product MacDraw™ (a simple and convenient process). Scheduling for this particular illustration has assumed a two-crew operation; one to follow the moon, the other to follow LAGEOS. Each crew takes the other target to be a target of opportunity, when applicable. The large open rectangles represent the suggested lunar crew coverage; the small open rectangles (within the large open rectangles) represent the LAGEOS passes which should be accessible to the lunar crew as a target of opportunity. The large filled rectangles represent the suggested LAGEOS crew coverage. It is especially important to again note that the scheduling part of this software tool is not automatic; it is accomplished manually by a human scheduler after the software tool has done its work in producing the various time-lines.

Conclusions

Although simple in concept (but a little tougher in the original implementation) this software tool now proves to be invaluable to us for the quick and easy scheduling of MLRS laser ranging operations. Listing 1 depicts the actual FORTRAN code now in use. This code can be made available in Apple® Macintosh™ 3 1/2-inch disk format; upon request, for individuals who might wish to implement it on their own systems. Note that station coordinates and local time modifications would need to be made in order to incorporate the system at other installations.

Without too much difficulty the code for this tool can be modified to run with almost any FORTRAN-capable system. As proof of this fact, we have already ported this code (with only very minor changes) for running on an IBM® PC/AT™ (see Figure 3 for sample output). Although this version does not have access to the special lunar phase characters which are available with the Apple® Macintosh™ version, nor is it as yet amenable to the convenient manual insertion of specific crew scheduling information via a MacDraw type of software interface, the output is quite satisfactory and eminently useful. The output shown in Figure 3 was printed on an Apple Laser Writer after the original test file was ported to a VAX 11/780. Very satisfactory results are also obtained by using a standard dot-matrix printer. This IBM®

PC/AT™ version should also be available, on request, to interested users in appropriate machine-readable form in the very near future.

Acknowledgements

I cannot too strongly acknowledge and thank Richard J. Eanes of the University of Texas Department of Aerospace Engineering and Center for Space Research and the work which he had performed on the original LAGEOS visibility package. Many thanks also go to Jerry Wiant, Randy Ricklefs, Windy Williams, and Robert Gonzalez (all associated with MLRS laser ranging operations at McDonald Observatory) for all of their inputs, which have made this tool so much more valuable to our operations. This research is being supported at McDonald Observatory and the University of Texas at Austin by National Aeronautics and Space Administration Contract NAS5-29404 out of Goddard Space Flight Center, Robert L. Appler, Technical Officer.


```

PROGRAM PASFRE
C
C...PROGRAM TO PREDICT THE TIMES OF SATELLITE PASSES AND THE
C LOCATION OF THE SUN AND MOON DURING THE PASSES
C
C...PROGRAMMED BY: RICHARD JAMES, CENTER FOR SPACE RESEARCH,
C DEPT. OF AEROSPACE ENG. AND ENG. MECHANICS,
C UNIVERSITY OF TEXAS AT AUSTIN
C
C...VERSION OF 13 JUN 83
C
C...Amended by Peter J. Shelus to MacFortran Capability for MLRS crew
C scheduling.
C...April, 1985
C

```

```

DOUBLE PRECISION JD, JDP
DOUBLE PRECISION XMJD, XMJDF, XMJD1, XMJD2, DO, D
REAL LUN, LUNMAG, LUNAL, LUNEL, LUNRO, LUNST, LUNLON,
1 LUNLAT
logical deprin1, deprin2
real sunup1, sunup2, lunup1, lunup2, lagup1, lagup2
integer dayid
character*1 idow, moonsym, axel(2), idays(7)
character*4 sun, sun, lag, up, dn
character lunin(121), sunin(121), lagin(122)
DATA idays /'M', 'T', 'F', 'S', 'S', 'M', 'T'/
DATA deprin1/.FALSE./, deprin2/.FALSE./
DATA sun/'moon'/, sun/'sun' /, lag/'lago'/, up/'up' /, dn/'down'/
DIMENSION LUN(3), STALUN(3)
DIMENSION SUN(3), SAT(3)
DIMENSION STASAT(3), STASUN(3), STA(2), IMDY1(5), IMDY2(5)
DIMENSION IMDY3(5), IMDY4(5), IMDY5(5)
DATA ELAST /-99999./, NPT /0/
DATA TRASS /0/
DATA DTMIN /12./, XMJDF /46247.25/
DATA ELMIN /20./
DATA SUNLIM /5./
DATA RE /6378137./, FINV /298.255/
C...McDonald Observatory, Fort Davis, Texas
DATA STAL, STALON, STALAT /1963.344, 255.984083795, 20.676976609/
DATA STA(1) /0./
DATA IMAX / 9999999999999 /, DAYMAX / 10. /
DATA RAD /0.0174532925199433/
DATA DEG /57.295779513082 /
DATA PI /3.14159265358979/
DATA TMOPI /6.2831853071796/
DATA CLITE /299792458./
C
C...SATELLITE EPHEMERIS
DATA DO /2442905.5/
C XMO, XMI ARE EPOCH VALUES RATES (DEG/DAY) FOR TRUE OF DATE NODE
C XLO, XLI ARE FOR ANG OF LATITUDE (PERT+MEAN)
C XMO, XMI ARE FOR TRUE OF DATE PERIAPSE
C XMO, XMI ARE FOR MEAN ANOMALY
C NOTE: PERIODIC PERTURBATIONS ON PERIAPSE AND MEAN ANOMALY CAN
C BE SEVERAL DEGREES, BUT IN ANG OF LATITUDE THEY ARE AROUND
C TENTHS OF DEGREES.
C...JD=2442905.5
DATA XMO, XMI / 29.5672, 0.34256/
DATA XLO, XLI /223.195, 2298.9763/
DATA XMO, XMI /259.235, -0.2126/
DATA XMO, XMI /223.860, 2299.1889/
DATA XINCL /109.845/
DATA ECC / 0.0046 /
DATA ASAT /12.2726/
C

```

```

C-----
C This is a temporary 'read & write' test patch!
C
OPEN (UNIT=2, FILE='CALENDAR')
REWIND 2
11 call covers (jmo, jmo, iyr, XMJDF, DAYMAX, deprin2)
if (deprin2) then
OPEN (UNIT=3, FILE='EAMES.OUT')
REWIND 3
endif
dayid=1
hmoon=0.0
maxelct=3
DTDAY = DTMIN/1440.
CALL SHADMO
C
C...CONVERT ANGLES TO RADIANS
XMO = XMO*PI/180
XMI = XMI*PI/180
XLO = XLO*PI/180
XLI = XLI*PI/180
XMO = XMO*PI/180
XMI = XMI*PI/180
XINCL = XINCL*PI/180
COSI = COS(XINCL)
SINI = SIN(XINCL)
CLTST = COS(STALAT*PI/180)
SLTST = SIN(STALAT*PI/180)
CLNST = COS(STALON*PI/180)
SLNST = SIN(STALON*PI/180)
IF (STA(1).NE.0.) GO TO 5
FLAT = 1./FINV
ESQUAR = FLAT*(2.-FLAT)
XMS = RE/SQRT(1.-ESQUAR*SLTST**2)
XNPR = XMS + STALAT
STA(1) = XNPR*CLTST*CLNST
STA(2) = XNPR*CLTST*SLNST
STA(3) = (XNPR-ESQUAR*XMS)*SLTST
5 CONTINUE
C
C...DATE LOOP
call time (itzero)
I = 0
10 I = I + 1
IF (I.GT.IMAX) GO TO 20
C...DATES BY SEARCH AT DTMIN (MINUTES) SPACING FROM XMJDF
DELDAY = (I-1)*DTDAY
IF (DELDAY.GT. DAYMAX) GO TO 20
XMJD = XMJDF + DBLE(DELDAY)
C
C...COMPUTE TOPOCENTRIC SATELLITE AND SUN VECTORS
JD = XMJD + 2400000.500
D = JD - DO
C
C...GREENWICH HOUR ANGLE, OR SIDEREAL TIME AT 0 DEG LONG.
TRETAG = RAOC(JD, TRETAD)
COSTE = COS(TRETAG)
SINTB = SIN(TRETAG)
C
C...SATELLITE COORDS IN TRUE OF DATE SYSTEM
XM = XMO + XMI*D
XL = XLO + XLI*D

```

```

XM = AMOD(XM, TMOPI)
XL = AMOD(XL, TMOPI)
XM = AMOD(XM, TMOPI)
IF (XM.LT.0.) XM = XM + TMOPI
IF (XL.LT.0.) XL = XL + TMOPI
IF (XM.LT.0.) XM = XM + TMOPI
XL = XL + 2.*ECC*SIN(XM)
COSM = COS(XM)
SINM = SIN(XM)
SLAM = SIN(XL)
CLAM = COS(XL)
SATMAG = (1. - ECC*COS(XM))*ASAT
SAT(1) = (COSM*CLAM - SINM*COSI*SLAM)*SATMAG
SAT(2) = (SINM*CLAM + COSM*COSI*SLAM)*SATMAG
SAT(3) = (SINI*SLAM)*SATMAG
C
C...ROTATE ABOUT X AXIS TO GET (PSUEDO)BODY FIXED POSITION
CALL XROT(SAT, COSTE, SINTB)
C
C...GET TOPOCENTRIC SATELLITE POSITION
CALL TOPO(SAT, STA, STASAT, CLTST, SLTST, CLNST, SLNST, SATAT, SATEL,
1 SATRO)
c IF (SATEL.LT.ELMIN) GO TO 10
SATRO = (2.*SATRO/CLITE)*1000.
C
C...GET SATELLITE LATITUDE, LONGITUDE, AND HEIGHT
CALL GTRAK (SAT, SATMAG, RE, ESQUAR, SATST, SATLON, SATLAT)
C
C...GET THE SOLAR AND LUNAR POSITION VECTORS IN THE MEAN OF DATE
C EQUATOR AND EQUINOX SYSTEM.
CALL SUNLUN (JD, SUN, LUN)
SUNMAG = SQRT(SUN(1)**2 + SUN(2)**2 + SUN(3)**2)
LUNMAG = SQRT(LUN(1)**2 + LUN(2)**2 + LUN(3)**2)
C
C...ROTATE ABOUT X TO GET SUN AND MOON IN (PSUEDO)BODY FIXED SYSTEM
C...REMEMBER THIS PROGRAM NEGLECTS NUTATION AND POLAR MOTION
CALL XROT(SUN, COSTE, SINTB)
CALL XROT(LUN, COSTE, SINTB)
C
C...GET SUB-SUN POINT ON THE EARTH
CALL GTRAK (SUN, SUNMAG, RE, ESQUAR, SUNST, SUNLON, SUNLAT)
CALL GTRAK (LUN, LUNMAG, RE, ESQUAR, LUNST, LUNLON, LUNLAT)
C
C...GET TOPOCENTRIC SUN AND MOON COORDINATES
CALL TOPO(SUN, STA, STASUN, CLTST, SLTST, CLNST, SLNST, SUNAL, SUNEL,
1 SUNRO)
CALL TOPO(LUN, STA, STALUN, CLTST, SLTST, CLNST, SLNST, LUNAL, LUNEL,
1 LUNRO)
AGELUN = (LUNLON-SUNLON)*29.330539/360.
IF (AGELUN.LT. 0.) AGELUN = AGELUN + 29.330539
IF (AGELUN<-1.845659.AND.AGELUN>27.684880) moonsym=' '
IF (AGELUN<-1.845659.AND.AGELUN<-5.536976) moonsym=' '
IF (AGELUN<-5.536976.AND.AGELUN<9.228293) moonsym=' '
IF (AGELUN<9.228293.AND.AGELUN<12.919611) moonsym=' '
IF (AGELUN<12.919611.AND.AGELUN<16.610928) moonsym=' '
IF (AGELUN<16.610928.AND.AGELUN<20.302248) moonsym=' '
IF (AGELUN<20.302248.AND.AGELUN<23.993563) moonsym=' '
IF (AGELUN<23.993563.AND.AGELUN<27.684880) moonsym='g'
if (LUNEL>hmoon) then
declun=ASIN(LUN(3)/LUNMAG)*DEG
lunde=INT(declun+0.5)
hmoon=LUNEL
AGELUN = (LUNLON-SUNLON)*29.330539/360.
IF (AGELUN.LT. 0.) AGELUN = AGELUN + 29.330539
lunage=INT(AGELUN+0.5)
endif
c...Monitor rising and setting times of all three objects*****
c...Initialize parameters if this the first time through:
if (I=1) then
lunup2=LUNEL
sunup2=SUNEL
lagup2=SATEL
write(9,1001) LUNEL, SUNEL, SATEL
lunlin(1)=' '
lagin(1)=' '
sunlin(1)=' '
if (LUNEL>ELMIN) lunlin(1)=moonsym
if (SATEL>ELMIN) lagin(1)='0'
idow=idays(mod(idint(XMJD), 7)+1)
1001 format ('LUNEL=',F10.5,'; SUNEL=',F10.5,'; SATEL=',F10.5)
call prepape(jmo, iyr)
else
c...Come here for second time and later returns:
lunup1=lunup2
lunp2=LUNEL
sunup1=sunup2
sunup2=SUNEL
lagup1=lagup2
lagup2=SATEL
if (lunup1<ELMIN.AND.lunup2>ELMIN) write(9,9) I, XMJD, sun, up
if (lunup1>ELMIN.AND.lunup2<ELMIN) write(9,9) I, XMJD, sun, dn
if (sunup1<0.0.AND.sunup2>0.0) write(9,9) I, XMJD, sun, up
if (sunup1>0.0.AND.sunup2<0.0) write(9,9) I, XMJD, sun, dn
if (lagup1<ELMIN.AND.lagup2>ELMIN) write(9,9) I, XMJD, lag, up
if (lagup1>ELMIN.AND.lagup2<ELMIN) then
write(9,9) I, XMJD, lag, dn
maxelag=IFIX(ELMAX*0.5)
call convert(maxelag, axel)
maxelct=1
endif
9 format ('I = ',16,'; XMJD = ',F15.5,'; ',A4,' is ',A4,'.')
k=mod(I,120)
if (k>1) then
lunlin(k)=' '
if (maxelct>2) lagin(k)=' '
sunlin(k)=' '
if (LUNEL>ELMIN) lunlin(k)=moonsym
if (SATEL>ELMIN.AND.maxelct>2) lagin(k)='0'
if (maxelct=1) then
lagin(k)=axel(1)
lagin(k+1)=axel(2)
endif
if (SUNEL>0.0) sunlin(k)='0'
if (mod(k,3)=1) sunlin(k)='|'
elseif (k=0) then
lunlin(120)=' '
if (maxelct>2) lagin(120)=' '
sunlin(120)=' '
if (LUNEL>ELMIN) lunlin(120)=moonsym
if (SATEL>ELMIN.AND.maxelct>2) lagin(120)='0'
if (maxelct=1) then
lagin(120)=axel(1)
lagin(121)=axel(2)
endif
if (SUNEL=0.0) sunlin(120)='0'
if (mod(k,3)=1) sunlin(120)='|'
elseif (k=1) then
lunlin(121)=' '
if (maxelct>2) lagin(121)=' '
sunlin(121)=' '
if (LUNEL>ELMIN) lunlin(121)=moonsym
if (SATEL>ELMIN.AND.maxelct>2) lagin(121)='0'

```

```
laglin(121)=max(1)
laglin(122)=max(2)
else
  laglin(122)=-
endif
if(SUNEL>0.0) sunlin(121)='0'
if(mod(k,5)=1) sunlin(121)='1'
write(2,106) lunlin, lundec, lunage
write(2,108) ldown, dayid, sunlin
write(2,109) laglin
write(2,107)

106 format(5x,121a1,14,'/',12)
107 format(' ')
108 format(a1,13,1x,121a1)
109 format(5x,122a1)
call prtym(itzero,dayid,DAYMAX)
hyscom=0.0
if (dayid=0.OR.dayid=20) then
  call postage
  call prepage(jmo,lyr)
endif
if (dayid=1st(DAYMAX)) then
  call postage
endif
ldown=days(mod(idint(XMJD),7)+1)
dayid=dayid+1
lunlin(1)=' '
laglin(1)=' '
sunlin(1)=' '
if(LUNEL>ELMIN) lunlin(1)=moonsyn
if(SATEL>ELMIN) laglin(1)='0'
if(SUNEL>0.0) sunlin(1)='0'
if(mod(k,5)=1) sunlin(1)='1'
endif
maxelct=maxelct+1
endif
if (SATEL.LT.ELMIN) GO TO 10
C.....
if(deprin) then
c2345678912345678921234567893123456789412345678951234567896123456789712
C...First de-bug print (20 April)
WRITE(9,1)I,DELDAY,SATEL, XMJD,SUNEL,JD,LUNEL,D,THETAG
1 FORMAT('I',16,2X,'DELDAY=',F15.5,' SATEL=',F15.5/
2 13X,'XMJD ',F15.5,' SUNEL=',F15.5/
3 13X,'JD ',F15.5,' LUNEL=',F15.5/
4 13X,'D ',F15.5,' THETAG=',F15.5)
C READ(9,2)CINPOT
2 FORMAT(F10.5)
C...End of first de-bug print (20 April)
endif
C.....
C...CHECK FOR A NEW PASS
IF (ABS(D-DLAST)=1440. .LT. 30.) GO TO 15
IF (NPT.EQ.0) GO TO 30
C
C...PASS COMPLETED, PRINT SUMMARY.
IPASS = IPASS + 1
SUNELA = SUNELA/NPT
AMJDP = AMJDP/NPT
UTP = AMJDP - AINT(AMJDP)
SOLTA = UTP*24. + STALON/15.
SOLTA = ANCD(SOLTA,24.1)
PTIME = (XMJD2-XMJD1)*1440.
IMAXEL = ELMAX + 0.5
if(deprin) then
JDP = DBLE(XMJD1) + 2400000.500
CALL KALDAY(JDP,IMDY1,XSEC1,MONTE1)
JDP = DBLE(XMJD2) + 2400000.500
CALL KALDAY(JDP,IMDY2,XSEC2,MONTE2)
C WRITE(9,320) IPASS, AMJDP, IMDY1(3)-1900, IMDY1(1), IMDY1(2),
C 1 IMDY1(4), IMDY1(5), IMDY2(4), IMDY2(5), PTIME, NPT,
C 2 SUNELA, SOLTA
C 320 FORMAT (/1X,'PASS ',I4,F12.4,2X,3I2,1X,2I2,1X,2I2,F6.2,14,
C 2F10.3)
write(9,310) IMDY1(3)-1900, MONTE1, IMDY1(2), IMDY1(4), IMDY1(5),
1 IMDY2(4), IMDY2(5), AMJDP
C WRITE(1,340) IMDY1(3), IMDY1(1), IMDY1(2), IMDY1(4), IMDY1(5),
C 1 IMDY2(4), IMDY2(5), IMAXEL
C 340 FORMAT (1X,14,13,13,13,13,13,13,13,13,13,13,13,13,13,13,13)
310 FORMAT (/1X,'PASS OF ',12,1X,A3,1X,12,' BEGIN ',12,13,
1 ' END ',12,13,4X,' MID-MJD ',F12.4)
write(9,315) A11, E11, A12, E12
315 FORMAT (3X,'SATELLITE AT AN EL AND AT RISE = ',2F7.2,3X,
1 ' SET = ',2F7.2)
write(9,316) BALUN1, BALUN2, ACELUN
316 FORMAT (3X,'LUNAR HOUR ANGLE AT RISE AND SET = ',2F7.2,
1 2X,' LUNAR AGE = ',F7.2,' DAYS')
write(9,317) SUNELA, SOLTA
317 FORMAT (3X,'SUN ELEVATION = ',F10.3,3X,' LOCAL MEAN ',
1 ' TIME = ',F10.3,' HOURS')
JDP = DBLE(TEMAX) + 2400000.500
CALL KALDAY(JDP,IMDY3,XSEC3,MONTE3)
write(9,600) IMDY3(4), IMDY3(5), ELMAX
600 FORMAT (3X,'TIME OF MAX EL (2H MM) = ',12,13,3X,
1 ' MAX EL = ',F6.2,' DEG')
IF (DLIT2.LT.0.) GO TO 30
JDP = DBLE(DLIT1) + 2400000.500
CALL KALDAY(JDP,IMDY4,XSEC4,MONTE4)
JDP = DBLE(DLIT2) + 2400000.500
CALL KALDAY(JDP,IMDY5,XSEC5,MONTE5)
write(9,601) IMDY4(4), IMDY4(5), IMDY5(4), IMDY5(5)
601 FORMAT (3X,'SATELLITE IS SUNLIT FROM ',12,13,' TO ',
1 12,13)
IF (DBURN.GE.0.) write(9,602)
602 FORMAT (3X,'SATELLITE TOO CLOSE TO SUN AT SOME POINT IN THE',
1 ' PASS',/)
endif
C
C...BEGIN A NEW PASS
30 CONTINUE
NPT = 0
AMJDP = 0
SUNELA = 0.
XMJD1 = XMJD
A11 = SATEL
E11 = SATEL
C BALUN1 = (STALON-LUNLON)/14.492
BALUN1 = (STALON-LUNLON)/15.
IF (BALUN1.LT.-12.) BALUN1 = BALUN1 + 24.
IF (BALUN1.GT.12.) BALUN1 = BALUN1 - 24.
C
C...GET AGE OF MOON AT PASS START.
ACELUN = (LUNLON-SUNLON)*29.530539/360.
IF (ACELUN.LT.0.) ACELUN = ACELUN + 29.530539
ELMAX = 90.
DLIT1 = 999999.
DLIT2 = -999999.
DBURN = -999999.
C
C...NOT A NEW PASS
15 DLAST = D
```

```
A12 = SATEL
E12 = SATEL
C BALUN2 = (STALON-LUNLON)/14.492
BALUN2 = (STALON-LUNLON)/15.
IF (BALUN2.LT.-12.) BALUN2 = BALUN2 + 24.
IF (BALUN2.GT.12.) BALUN2 = BALUN2 - 24.
NPT = NPT + 1
FJD = SNGL(JD)
SUNELA = SUNELA + SUNEL
AMJDP = AMJDP + XMJD
C
C...GET MAX ELEVATION POINT
IF (SATEL.GT.ELMAX) ELMAX = SATEL
IF (SATEL.EQ.ELMAX) TEMAX = XMJD
C
C...SUN AND SATELLITE GEOMETRY
CALL SHADOW(SAT,SATMAC,SUN,SUNMAC,SEFRAC,RSUN,RSUN1,RSUN2)
SATSUM = ACOS(STATAS(1)*STASUN(1) + STASAT(2)*STASUN(2)
1 + STASAT(3)*STASUN(3))*DEG
C
C...FIND INTERVAL DURING WHICH SATELLITE IS SUNLIT
IF (SEFRAC.LT.0.) GO TO 16
IF (XMJD.LT.DLIT1) DLIT1 = XMJD
IF (XMJD.GT.DLIT2) DLIT2 = XMJD
16 CONTINUE
C
C...IS SATELLITE TOO CLOSE TO THE SUN
IF (SATSUM.LT.SUNLIM) DBURN = XMJD
C
C...RECYCLE
GO TO 10
C
C 20 CONTINUE
write(9,101)
101 format('This session is over. However your job is not totally'
1 ' done. The print file now must be properly formatted using'
2 ' WORD. Once you have file CALENDAR in WORD, do the following:'
3 ' 1. choose WIDE in the PAGE SETUP section under FILE;'
4 ' 2. change all the MARGINS to 0.5 (except for GUTTER);'
5 ' 3. under FORMAT, choose the 9-point COURIER font;'
6 ' 4. insert page breaks (SHIFT-ENTER) at the 10 and'
7 ' 20 day calendar lines during each month and at the'
8 ' end of each month.'//
9 ' That's all there is. Press RETURN and then open WORD to begin'
10 ' the re-formatting process.'//
11 ' If you asked for a LAGEOS summary print-out, you'll find it'
12 ' in the file named "LANES.OUT"'
accept lyr
END
subroutine cheknd(answer)
character*1 answer
write(9,101)
1 type(9,102)
101 format('Do you need a LAGEOS summary print-out?')
1 ' (Answer "Y" or "N")'
102 format(' Enter your choice here (followed by a RETURN)---->')
103 format('You typed a ',A1/
1 ' I expected Y or N. Try again')
accept answer
if(answer='Y'.OR.answer='y'.OR.answer='N'.OR.answer='n')return
write(9,103)answer
go to 1
end
subroutine cnvrt(i,c)
character*1 c(2)
if (i>9 .AND. i<100) then
i1=i/10
i2=i-11*i0
c(1)=CHAR(i1+48)
c(2)=CHAR(i2+48)
else
c(1)=' '
c(2)=' '
write(9,101)
101 format('Call to CNVRT with out of range Argument, i =',I6.0.
')
endif
return
end
subroutine prtym(itzero,lday,DAYMAX)
call time(41)
ihrl=int(it/3600.)
ian1=int((it-ihrl*3600.)/60+0.5)
elapsd=REAL(it-itzero)/60.0
togo=elapsd/REAL(lday)*(DAYMAX-REAL(lday))
finished=REAL(it)+togo*60.
ihrl=int(finished/3600.)
ian2=int((finished-ihrl*3600.)/60+0.5)
write(9,101)lday,elapsd,togo,ihrl,ian1,ihrl2,ian2
101 format('Computations for day ',I2,' have just been completed.'/
1 ' Elapsed time : ',F5.1,' minutes.'/
2 ' Est.time to go: ',F5.1,' minutes.'/
3 ' Time right now: ',I2,'.',I2/
4 ' Est.comp.time : ',I2,'.',I2)
return
end
SUBROUTINE SUNLON (TJD, XS, XM)
C
C...GET MEAN OF DATE EQUATOR AND EQUINOX SOLAR AND LUNAR POSITION
C VECTORS FROM BROWNS LUNAR THEORY
C
DOUBLE PRECISION TJD
DIMENSION XS(3), XM(3), ARG(5)
DATA LUNPRE /2/
C
CALL DIANA (TJD, LUNPRE, XM, ARG)
C
C...GET SOLAR ORBIT ELEMENTS
AUS = 1.496E11
ECS = 0.01673104 - 0.1144422E-8*(TJD-2415020.000)
XIS = 0.
CAPOMS = 0.
PERIS = ARG(5)
XMS = ARG(2) - ARG(5)
C
C...CONVERT ORBIT ELEMENTS TO POSITION VECTOR
CALL KEP (AUS, ECS, XIS, PERIS, CAPOMS, XMS, XS)
C
C...ROTATE ECLIPTIC ELEMENTS INTO EQUATORIAL SYSTEM
CALL ECLEQ (XS, TJD)
CALL ECLEQ (XM, TJD)
C
RETURN
END
subroutine convers(imo,jmo,lyr,xmjdf,daymax,deprin2)
double precision xmjdf
character*1 jmo
character*1 answer
logical leap,deprin2
write(9,101)
type(9,102)
accept imo
write(9,103)
```



```

accept iyr
C...Check if "long Zanes-type print-out" is desired
call chetend(answer)
if(answer='Y'.OR.answer='y') deprin2=TRUE.
write(9,105)
101 format('MARS Observing Crew Scheduling Calendar Program'///
1 'Enter the month for which a calendar is desired.'/
2 '(1-Jan, 2-Feb, 3-Mar, ..., 12-Dec) /
3 '(Complete your entry by pressing RETURN)')
102 format('Your choice--> ')
103 format('///
1 'Enter the year for which the calendar is desired.'/
2 '(A 4-digit number is desired, i.e., 1984, 1985, etc)'/
3 '(Complete your entry by pressing RETURN)')
104 format('Your choice--> ')
105 format('///Thank you!///
1'This should take about 30 minutes. Go and have a cup of coffee!')
SELECT CASE (imo)
case (1) jmo='Jan'
case (2) jmo='Feb'
case (3) jmo='Mar'
case (4) jmo='Apr'
case (5) jmo='May'
case (6) jmo='Jun'
case (7) jmo='Jul'
case (8) jmo='Aug'
case (9) jmo='Sep'
case (10) jmo='Oct'
case (11) jmo='Nov'
case (12) jmo='Dec'
END SELECT
leap=.FALSE.
if(mod(iyr,4)=0.AND.mod(iyr,100)NE.0)leap=.TRUE.
if(imo=2.AND.leap)then
daymax=29
elseif(imo=4.AND.NOT.leap)then
daymax=28
elseif(imo=4.OR.imo=6.OR.imo=9.OR.imo=11)then
daymax=30
else
daymax=31
endif
xjdf=367*iyr-7*(iyr+(imo+9)/12)/4-3*((iyr+(imo-9)/7)/100+1)/4
+275*imo/9+1+1721029-2400000.75
write(9,201)xjdf
201 format('///XJDFF =',F9.2)
return
subroutine prepape(jmo,yjr)
character*3 jmo
integer yjr
C...Prepare and print 'month and year' header, then skip a line.
write(2,101)jmo,yjr
write(2,102)
101 format('M,JA,AS,14)
102 format(' ')
C...Print CDT, UT, and CST lines, then skip a line.
call cdline
call utline
call cstline
write(2,103)
C...Return to call routine
return
end
subroutine postape
C...Print CST, UT, and CDT lines.
call cdline
call utline
call cstline
C...Return to call routine
return
end
subroutine cdline
C...Prepare and print 'CDT' line
type(2,103)
do 10 i=2,11
10 type(2,104)i
type(2,105)
do 20 i=1,11
20 type(2,104)i
write(2,106)
103 format(' CDT 1')
104 format(' N')
105 format(' M 1 CDT')
return
end
subroutine utline
C...Prepare and print 'UT' line
type(2,103)
do 10 i=7,23
10 type(2,104)i
do 20 i=4,6
20 type(2,104)i
write(2,105)
103 format(' UT 6')
104 format(' 15')
105 format(' UT')
return
end
subroutine cstline
C...Prepare and print 'CST' line
type(2,103)
do 10 i=1,11
10 type(2,104)i
type(2,105)
do 20 i=1,11
20 type(2,104)i
write(2,106)
103 format(' CST M')
104 format(' 15')
105 format(' N')
106 format(' M CST')
return
end
SUBROUTINE DIANA( DATE, EXACT, XE, ANGLE )
C...COMPUTES GEOCENTRIC COORDINATES OF THE MOON BY ILL
C LUNAR THEORY
C...PRECISION= 2. SEC. OF ARC IN LONGITUDE (WHEN EXACT=4)
C 1. SEC. OF ARC IN LATITUDE (WHEN EXACT=4)

```

```

C...INPUT PARAMETERS
C DATE JULIAN DAY IN EPOCHERIS TIME (DOUBLE PRECISION)
C EXACT INTEGER NUMBER -1,2,3,4 FOR PRECISION
C 4 WILL BE THE MOST ACCURATE
C...OUTPUT PARAMETER
C XE THE POSITION OF THE MOON WITH RESPECT TO ECLIPTIC SYSTEM
DOUBLE PRECISION DATE
DIMENSION XE(3), ANGLE(5), IX(4,1), X(6), IY(4,4), Y(48),
$ IX(4,20), X(20), IX(10), IX(4,10), IX(11), IX(4,13), SERY(61),
$ SERY(48), SERN(10), SERG(13), SERI(30), NG(4), NX(4), NY(4),
$ NX(4), NN(4), ADD(3)
INTEGER SERY, SERY, SERI, SERN, SERG, EXACT
DATA RAD /0.0174532925199433/
DATA PI /3.1415926535897/
DATA TMOP1 /6.2831853071796/
DATA SECRAD /4.8481368110945E-6/
DATA AE /6378137./
C...SUPPLY DATE (JULIAN DATE+DECIMAL OF THE DAY) AND EXACT (1 TO 4)
DATA NX/6,21,39,61/, NY/4,13,23,48/, NN/1,4,10,30/,
$ NN/3,7,10,10/, NG/0,0,2,13/
DATA SERN/78,3,25,15,53,26,32,6,16,40,21,32,54,103,109,
$ 9,70,27,41,14,59,64,39,24,2,71,84,110,78,58,47,77,46,
$ 90,108,32,34,187,60,31,79,85,95,96,116,5,149,17,124,118,
$ 193,129,125,72,83,89,135,69,102,150/
DATA SERY/410,412,398,423,408,481,460,425,456,458,479,397,579,
$ 563,434,414,427,438,456,494,457,436,469,421,400,409,477,
$ 518,509,483,370,511,406,464,544,413,399,444,411,581,516,
$ 432,513,548,549,492,424,550/
DATA SERN/78,789,792,793,795,791,796,790,788,794/
DATA SERG/669,721,737,678,700,717,641,709,642,723,650,
$ 633,733/
DATA SERI/808,809,803,823,807,816,831,836,820,830,893,
$ 859,810,815,825,814,824,822,802,835,837,834,871,860,
$ 849,846,865,842,888,832/
DATA IX/1,0,0,0, 1,0,0,-2, 0,0,0,2, 2,0,0,0, 0,+1,0,0,
$ 0,0,2,0, 2,0,0,-2, 1,1,0,-2, 1,0,0,2, 0,1,0,-2, 1,-1,
$ 0,0,0,0,1, 1,1,0,0, 0,0,2,-2, 1,0,2,0, 1,0,-2,0,
$ 1,0,0,-4, 3,0,0,0, 2,0,0,-2, -1,1,0,-2, 0,1,0,2, 1,0,0,-1,
$ 0,1,0,1,1, -1,0,2, 2,0,0,2, 0,0,0,4, 3,0,0,-2, 2,-1,0,0,
$ 1,0,-2,-2, 2,1,0,-2, 1,0,0,1, 0,2,0,-2, 2,1,0,0, 0,2,0,0,
$ 1,2,0,-2, 1,0,-2,2, 0,0,2,2, 1,1,0,-4, 2,0,2,0, 1,0,0,-3,
$ 1,1,0,2, 2,1,0,-4, 2,-1,0,-2, 1,-2,0,0, 1,-2,0,-2, 0,1,
$ 2,-2, 2,1,0,0, 0,1,0,-4, 2,0,0,-1, 0,1,-2,2,
$ 2,0,-2,0, 1,1,0,2, 2,0,0,-2, 3,0,0,-4, 2,-1,0,2, 1,2,0,0,
$ 1,-1,0,-1, 3,0,0,2, 1,0,2,2, 4,0,0,-2,
DATA IY/1,0,0,0, 1,0,0,-2, 0,0,0,2, 2,0,0,0, 1,0,0,2,
$ 1,1,0,-2, 0,1,0,-2, 2,0,0,-2, -1,1,0,0, 0,1,0,0, 1,1,
$ 0,0,0,0,1, -1,0,2,0, 0,0,2,-2, 3,0,0,0, 1,0,0,-4,
$ 2,0,0,4, 2,1,0,2, -1,0,2, -1,1,0,2, 0,1,0,1, 3,0,
$ 0,-2, 0,2,0,0, 2,0,0,0, 0,0,0,4, 1,0,0,1, 1,1,0,2,
$ 2,-1,0,0, 2,1,0,0, 1,1,0,-4, 1,0,2,-2, 2,1,0,-2, 1,0,
$ 0,4, 0,1,0,-4, 1,2,0,-2, 1,0,0,-3, 0,0,0,3, 4,0,0,0,
$ 1,0,0,-1, -1,0,2,-2, 2,-1,0,2, 3,0,0,2, 2,1,0,-4, -1,
$ 2,0,2, -1,2,0,0, -1,1,0,4, 2,0,0,-1, -1,2,0,-3/
DATA IXI/0,0,1, 1,0,0,-2, 0,0,0,2, 2,0,0,0, 1,0,0,2,
$ 0,1,0,-2, 1,1,0,-2, 1,1,0,0, 0,0,0,1, 1,1,0,0, 1,0,
$ -2,0, 3,0,0,0, 1,0,0,-4, 0,1,0,0, 2,0,0,-4, 0,1,0,2,
$ 2,0,0,-2, 2,0,0,2, 0,0,0,4, 1,-1,0,2, 1,-1,0,-2, 0,1,
$ 0,1, 2,-1,0,0, 3,0,0,-2, 1,0,0,1, 0,0,2,-2, 2,1,0,0,
$ 0,2,0,-2, 1,0,2,-2, 1,1,0,-4/
DATA IYI/0,0,1, 1,0,1,-2, -1,0,1,-2, -2,0,1,0, 0,1,1,
$ -2, -1,0,1,0, 0,-1,1,-2, 1,0,1,-4, 0,0,1,-4, -2,0,1,2/
DATA IG/2,0,0,-2, 1,1,0,-2, -1,1,0,-2, 3,0,0,0, 0,1,0,0,
$ 1,1,0,2, 0,0,0,1, 0,2,0,-2, 0,0,0,2, 1,1,0,-4, 1,0,0,4,
$ 1,0,0,1, -1,1,0,2/
DATA X/2263.6, -4386.5, 2369.9, 769.0, -668.1, -411.6,
$ -211.6, 147.0, 132.0, -163.1, 147.7, -125.2, -109.7,
$ -55.2, -45.1, 39.3, -38.4, 36.1, -30.8, 28.3, -24.4,
$ 18.6, 18.0, 14.6, 14.4, 13.9, -13.2, 9.7, 9.4, -8.6,
$ -8.5, -8.1, -7.6, -7.3, -7.4, -6.4, -5.7, -4.4, -4.0,
$ 3.2, -2.9, -2.7, -2.5, 2.6, 2.5, -2.1, 2.0, 1.9, -1.8,
$ 1.8, -1.4, -1.3, 1.3, 1.2, -1.1, 1.2, -1.1, -1.1, 1.0,
$ -1.0, -0.5/
DATA Y/22609., -4578.1, 2373.4, 768., 192.7, -182.4, -165.,
$ -152.5, -138.8, -127.0, -115.2, -112.8, -85.1, -52.1,
$ 50.6, -38.6, -34.1, -31.7, -25.1, -23.6, 17.9, -16.4,
$ 16.6, 14.78, 14.06, -13.51, -11.75, 11.67, -10.56, -9.66,
$ -9.52, -7.58, 6.8, -6.46, 6.4, -4.01, 3.60, 3.59,
$ 3.37, 3.32, 2.96, -2.34, -2.40, -2.32, -2.27, 2.01, -1.82/
DATA Z/186.5, 34.3, 28.2, 10.2, 3.1, 1.9, 1.3, 1.2, -1.0,
$ -0.9, -0.71, 0.62, 0.60, -0.40, 0.37, -0.30, -0.30, 0.28,
$ 0.26, 0.23, -0.23, 0.15, 0.13, -0.12, -0.11, -0.11, -0.10,
$ 0.09, -0.08, 0.07/
DATA EM/-526.0, 44.3, -30.6, -24.6, -22.6, 20.6, 11.0,
$ -6.0, -3.3, -2.0/
DATA EG/5.7, 2.1, -1.5, -1.3, -1.3, 0.8, -0.7, -0.7, 0.6,
$ -0.5, -0.4, 0.4, -0.4/
IF (EXACT.LT.1) GO TO 20
IF (EXACT.GT.4) GO TO 30
NX=NX (EXACT)
NY=NY (EXACT)
NN=NN (EXACT)
NG=NG (EXACT)
D=DATE-2415020.00
DD=0/1,E4
DD2=DD*DD
DD3=DD*DD*DD
ANGLE(1)=-270.434164E0+13.1763965268E0*D-.0000850E0*DD2
$ +.00000039E0*DD3
ANGLE(2)=-279.696678E0+.9856473354E0*D+.00002267E0*DD2
$ +.00000000E0*DD3
ANGLE(3)=-334.329356E0+1.114040803E0*D-.00077392E0*DD2
$ -.00000026E0*DD3
ANGLE(4)=-239.183275E0-.0529539222E0*D+.0001557E0*DD2
$ +.00000000E0*DD3
ANGLE(5)=-281.220844E0+.0000470684E0*D+.0000339E0*DD2
$ +.00000007E0*DD3
C ANGLE1 IS MEAN LONGITUDE OF MOON AT EPOCH
C ANGLE2 IS MEAN LONGITUDE OF SUN AT EPOCH
C ANGLE3 IS LONGITUDE OF LUNAR PERIGEE AT EPOCH
C ANGLE4 IS LONGITUDE OF ASCENDING NODE AT EPOCH
C ANGLE5 IS LONGITUDE OF SOLAR PERIGEE AT EPOCH
DO 1 I=1,5
J=ANGLE(I)/360.E0
IF (ANGLE(I)-360.*J)*RAD
1 IF (ANGLE(I)-360.*J)*RAD
ADD(1)=-2.*PI*(1.422222E0+.0000153622E0*D)
ADD(2)=-2.*PI*(.48298132E0-.000147269147E0*D+43.E-16*D*D)
ADD(3)=-2.*PI*(.33732431E0-.000010104982E0*D+191.2E-16*D*D)
EEL=ANGLE(1)+SECRAD*(14.27*SIN(ADD(3))+7.26*SIN
$ (ANGLE(4))+.84*SIN(ADD(1)))
C THE 1.9 ARCS/SEC TERM ON ANODE (BELOW) IS COMPUTE WITH
C APPROXIMATE ARGUMENT
ANCOE=ANGLE(4)+SECRAD*(96.*SIN(ANGLE(4))+(15.6+1.9)
$ *SIN(ADD(2)))
C MOON=ANGLE(3)+SECRAD*(-2.10*SIN(ADD(1)))-2.08*SIN
$ (ANODE)+.84*SIN(ADD(2)))
EL=EL-CMOON
ELP=ANGLE(2)-ANGLE(5)
F=EL-ANCOE
DEE=EEL-ANGLE(2)
IF (EL.LT.0.0) EL=-EL, TMOP1

```

```

IF(F.LT.0.0) F=F+TWOFI
IF(DEL.LT.0.0) DEE=DEE+TWOFI
CLONG=EEL
S=F
PAR=3422.7*SECRAD
DO 11 K=1,MX
CLONG=CLONG+X(K)*SECRAD*SIN(IX(1,K)*EL+IX(2,K)*ELP
+IX(3,K)*F+IX(4,K)*DEE)
IF(CLONG.GE.TWOFI) CLONG=CLONG-TWOFI
IF(CLONG.LT.0.0) CLONG=CLONG+TWOFI
DO 12 K=1,MY
S=S+Y(K)*SECRAD*SIN(IY(1,K)*EL+IY(2,K)*ELP
+IY(3,K)*F+IY(4,K)*DEE)
SCREM=(1.-.4664E-3*COS(ANODE)-.754E-4*COS
(ANODE+4.82))*SIN(S)
BETA=(18519.7E0*SCREM-6.2*SIN(3.*S))*SECRAD
DO 13 K=1,MS
FAR=FAR+Z(K)*SECRAD*COS(IZ(1,K)*EL+IZ(2,K)*ELP
+IZ(3,K)*F+IZ(4,K)*DEE)
DO 14 K=1,MW
BETA=BETA+WH(K)*SECRAD*SIN(IN(1,K)*EL+IN(2,K)*ELP
+IN(3,K)*F+IN(4,K)*DEE)
GIC=0
DO 15 K=1,MG
GOC=EG(K)*COS(IG(1,K)*EL+IG(2,K)*ELP+IG(3,K)*F
+IG(4,K)*DEE)
GIC=GIC+GOC
GIC=CLONG+GIC
CONTINUE
BETA=BETA+GIC*SIN(S)
C...COMPUTE THE LUNAR COORDINATES WITH RESPECT TO MEAN
C OF DATE SYSTEM
R=AE/SIN(PAR)
CI=COS(CLONG)
SI=SIN(CLONG)
CD=COS(BETA)
SD=SIN(BETA)
XE(1)=R*CD*CI
XE(2)=R*CD*SI
XE(3)=R*SD
RETURN
20 WRITE(9,25) EXACT
25 FORMAT(IX,'PRECISION INDICATOR, EXACT, NOT IN RANGE AT
$ POINT',I5)
GO TO 40
30 WRITE(9,35) EXACT
35 FORMAT(IX,'PRECISION INDICATOR, EXACT, OUT OF RANGE AT
$ POINT',I5)
40 CLONG=0.0
BETA=0.0
PAR=0.0
RETURN
C... END DIANA
END
SUBROUTINE ECLEQ (X,TJD)
C
C...VERSION #10727
C...AUTHOR: BRIAN CUTBERTSON, U.T. ASTRONOMY/AEROSPACE
C...PURPOSE: TO ROTATE ECLIPTIC CARTESIAN COORDINATES INTO MEAN
EQUATORIAL COORDINATES USED FOR IRV INTEGRATIONS.
C
C DOUBLE PRECISION TJD
C DIMENSION X(3)
C
C...POLYNOMIAL COEFFICIENTS FOR MEAN OBLIQUITY DIVIDED BY 362525*N:
DATA EP0, EP1 /4.0931975520273E-1, 6.2179594501235E-9 /
DATA EP2, EP3 /2.1441068744107E-17, 1.8008716772507E-22 /
C
C...JULIAN DAYS ELAPSED SINCE 1900 JAN 0 DAYS 12 HOURS:
T19001 = TJD - 2415020.000
T19002 = T19001 + T19001
T19003 = T19001 + T19002
C
C...COMPUTE MEAN OBLIQUITY:
EFSM = EP0 - EP1*T19001 - EP2*T19002 + EP3*T19003
SEM = SIN (EFSM)
CEM = COS (EFSM)
C
C...ROTATE FROM ECLIPTIC PLANE TO MEAN EQUATORIAL PLANE:
X2 = X(2)*CEM - X(3)*SEM
X(3) = X(2)*SEM + X(3)*CEM
X(2) = X2
C
C
C...DONE:
RETURN
END
SUBROUTINE KEP (A, EC, I, OMEG, CAMEG, M, X)
C...COMPUTES THE POSITION FROM THE ORBITAL ELEMENTS
C...INPUT PARAMETERS:
OMG THE GRAVITATIONAL PARAMETER
A THE SEMI-MAJOR
EC THE ECCENTRICITY
I THE INCLINATION
OMEG THE ARGUMENT OF PERIGEE
CAMEG THE LONGITUDE OF THE ASCENDING NODE
M THE MEAN ANOMALY
C...NOTE: ALL ANGLES SHOULD BE INPUT IN RADIANS
C...OUTPUT PARAMETERS:
X THE POSITION VECTOR
DIMENSION P(3), X(3)
REAL I,M
DATA TOL/1.E-06/
C...COMPUTE THE SEMI-MINOR AXIS
E2=EC**2.E0
EDIFF=1.0E0-E2
B=A*SQRT(EDIFF)
C...SOLVE KEPLERS EQUATION
E=0
1 SE=SIN(E)
E=M+EC*SE
SE=SIN(E)
CHECK=E-EC*SE-M
IF(ABS(CHECK).GT.TOL) GO TO 1
C...COMPUTE THE MAGNITUDE OF POSITION VECTOR
CE=COS(E)
R=A*(1.0E0-EC*CE)
C...COMPUTE THE TRUE ANOMALY
SF=B*SE/R
CF=A*(CE-EC)/R
F=ATAN2(SF,CF)
C...COMPUTE THE SINE AND COSINE OF THE ARGUMENT OF
PERIGEE +THE TRUE ANOMALY
OMEGA=OMEG+F
CTR=COS(OMEGA)
STR=SIN(OMEGA)

```

```

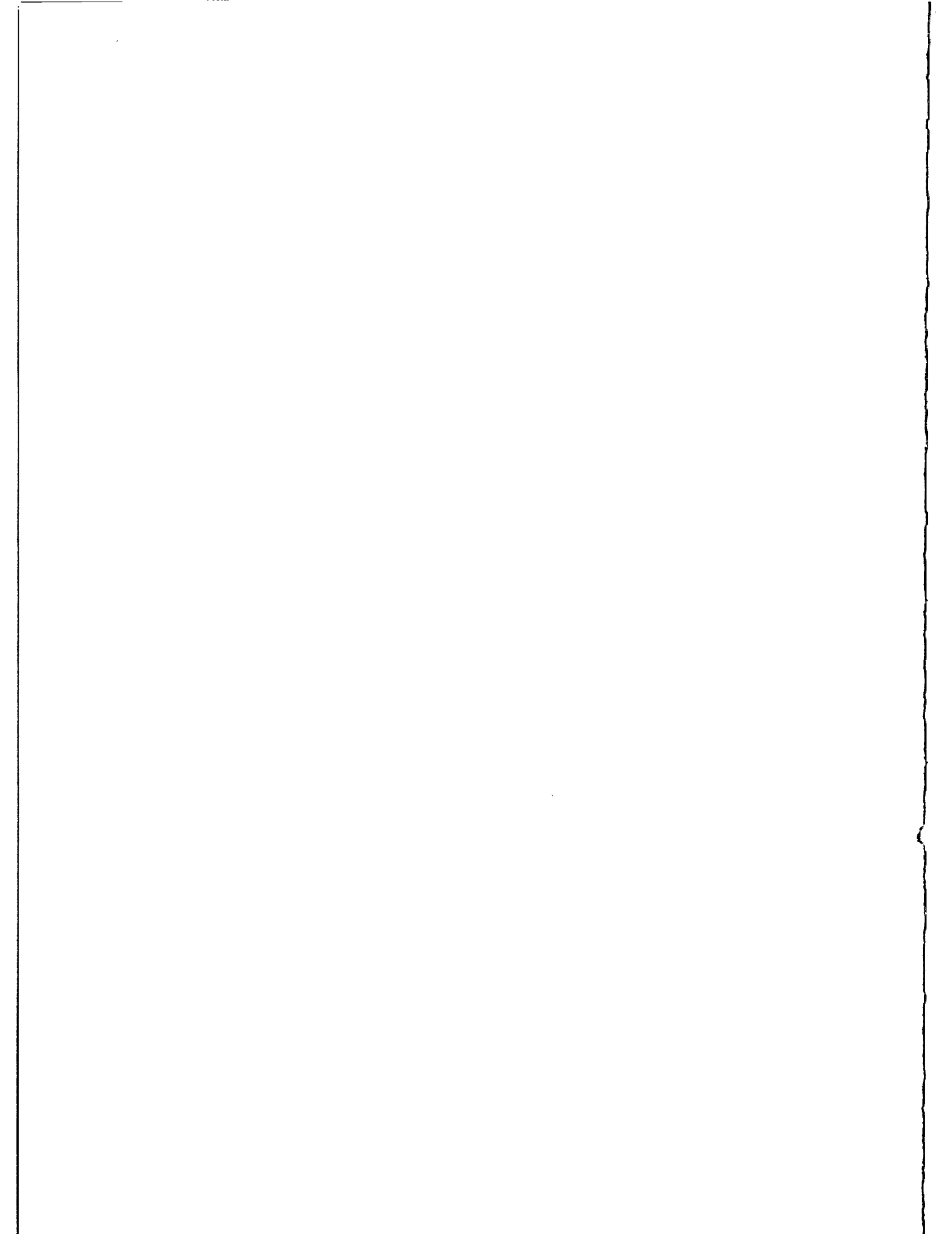
CI=COS(I)
SI=SIN(I)
C...COMPUTE THE SINE AND COSINE OF THE LONGITUDE
C OF THE MOON
COM=COS(CAMEG)
SOM=SIN(CAMEG)
C...COMPUTE THE POSITION VECTOR
P(1)=-COM*CTR-SOM*STR*CI
P(2)=-SOM*CTR+COM*STR*CI
P(3)=-STR*SI
X(1)=P(1)*R
X(2)=P(2)*R
X(3)=P(3)*R
RETURN
C...END KEP
END
SUBROUTINE RROT (X, C, S)
DIMENSION X(3)
T1 = X(1)*C + X(2)*S
X(2) = -X(1)*S + X(2)*C
X(1) = T1
RETURN
END
SUBROUTINE GTRAK (SAT, RSAT, RE, ESQUAR, SATST, SATLON, SATLAT)
DIMENSION SAT(3)
DATA DEG /57.29577 95130 82/
SATLAT = ASIN(SAT(3)/RSAT)
SATLON = ATAN2(SAT(2), SAT(1))
SATST = RSAT - RE
SATLAT = SATLAT*DEG
SATLON = SATLON*DEG
IF (SATLON.LT.0.) SATLON = SATLON + 360.
RETURN
END
SUBROUTINE TOPO (SAT, STA, STASAT, CLAT, SLAT, CLON, SLON, AZI, ELE,
RBO)
DIMENSION SAT(3), STA(3), STASAT(3), T(3)
DATA DEG /57.29577 95130 82/
DO 10 I=1,3
10 STASAT(I) = SAT(I) - STA(I)
T(1) = -STASAT(1)*SLON + STASAT(2)*CLON
T(2) = -STASAT(1)*SLAT*CLON - STASAT(2)*SLAT*SLON + STASAT(3)*CLAT
T(3) = STASAT(1)*CLAT*CLON + STASAT(2)*CLAT*SLON + STASAT(3)*SLAT
RBO = SQRT(T(1)**2 + T(2)**2 + T(3)**2)
DO 20 I=1,3
20 STASAT(I) = T(I)/RBO
ELE = ASIN(STASAT(3))
AZI = ATAN2(STASAT(1), STASAT(2))
ELE = ELE*DEG
AZI = AZI*DEG
IF (AZI.LT.0.) AZI = AZI + 360.
RETURN
END
SUBROUTINE KALDAY (JD, IPTIMES, XSEC, MONTH)
C
C...PROGRAMMED BY JAMES D. MCHILLAN - UNIV. OF TEXAS - 7/23/1973,
C...MODIFIED BY RICHARD EAMES, UT AUSTIN, 26 MARCH 1977
C
C...PURPOSE: TO COMPUTE THE CALENDAR DAY FROM THE JULIAN DATE (JD)
C...INPUT FORMAL PARAMETERS: (ANGLES ARE IN RADIANS)
JD THE JULIAN DATE IN DOUBLE PRECISION
C...OUTPUT FORMAL PARAMETERS
IPTIMES AN INTEGER ARRAY CONTAINING THE MONTH, DAY OF MONTH,
YEAR, HOUR, AND MINUTE IN THAT ORDER
XSEC SECONDS (FLOATING POINT)
MONTHS THREE CHARACTER ROLLERITH (38) NAME OF THE MONTH
C
C DOUBLE PRECISION JD
C DIMENSION IPTIMES(5), MONTHS(12)
C
C DATA MONTHS /31JAN, 31FEB, 31MAR, 31APR, 31MAY, 31JUN,
31JUL, 31AUG, 31SEP, 31OCT, 31NOV, 31DEC /
MONTHS(1)='JAN'
MONTHS(2)='FEB'
MONTHS(3)='MAR'
MONTHS(4)='APR'
MONTHS(5)='MAY'
MONTHS(6)='JUN'
MONTHS(7)='JUL'
MONTHS(8)='AUG'
MONTHS(9)='SEP'
MONTHS(10)='OCT'
MONTHS(11)='NOV'
MONTHS(12)='DEC'
C
C...COMPUTE THE HOUR, MINUTE, AND SECOND.
JDINT = JD
XTIME = AMOD (SINGL(JD-JDINT)*24.0+12.0,24.0)
IPTIMES(4) = XTIME
XTIME = (XTIME-IPTIMES(4)) * 60.0
IPTIMES(5) = XTIME
KSEC = (XTIME-IPTIMES(5)) * 60.0
C
C...COMPUTE THE YEAR, MONTH, AND DAY.
IF (IPTIMES(4).LT.12) JDINT = JDINT + 1
LX = JDINT + 68569
NX = 4 * LX / 146097
LX = LX - (146097*NX+3)/4
IPTIMES(3) = 4000 + (LX+1) / 1461001
LX = LX - 1461*IPTIMES(3)/4 + 31
IPTIMES(1) = 80 * LX / 2447
IPTIMES(2) = LX - 2447*IPTIMES(1)/80
LX = IPTIMES(1) / 11
IPTIMES(1) = IPTIMES(1) + 2 - 12*LX
IPTIMES(3) = 100*(NX-49) + IPTIMES(3) + LX
C
C...SET THE NAME OF THE MONTH
LX = IPTIMES(1)
MONTH = MONTHS(LX)
C
C RETURN
C...END KALDAY
END
SUBROUTINE SHADOW (X, R1, RSOL, RSOL1, FRAC, RSUN, RSUM1, RSUM2)
C
C...PURPOSE: DETERMINE AMOUNT OF SHADOWING USING A CYLINDRICAL OR
CONICAL SHADOW MODEL
C
C...CODED BY: J RIES - UNIVERSITY OF TEXAS - FEB 1980
C
C...REFERENCE: D. BAILEY; SOLAR RADIATION PRESSURE CALCULATIONS IN THE
CLODTH PROGRAM; WOLF RESEARCH AND DEVELOPMENT CORP.
C
C...INPUT FORMAL PARAMETERS:
X X SATELLITE POSITION IN 1950.0 NON-ROTATING COORDINATES
R1 MAGNITUDE OF X
RSOL POSITION OF THE SUN IN 1950.0 NON-ROTATING COORDINATES
RSOL1 MAGNITUDE OF RSOL

```

```

C...OUTPUT FORMAL PARAMETERS:
C   FRAC   FRACTION OF SOLAR RADIATION PRESSURE NOT ECLIPSED
C   RSUM   UNIT VECTOR ALONG SATELLITE TO SUN DIRECTION
C   RSUM1  RECIPROCAL OF SATELLITE-SUN DISTANCE
C   RSUM2  RSUM1 SQUARED
C
C   DIMENSION X(3),RSOL(3),RSUM(3)
C   COMMON /JUNK1 / D, B, R2, Q, RSAP, RSAP2, SUN(3), P(3), U(3), A,
C   .
C   .   AV, AU, COSB, COSDP, COSDU, COSB, SIN1, XI, RP,
C   .   TRTS, TRBTC
C   DATA EARNR/5.0E-8/
CXXXXX
C...DATA STATEMENTS ADDED TO UTOPIA ROUTINE TO MAKE INDEPENDENT OF
C   COMMON BLOCKS CONVAT AND SOLRAD
C
C   DATA PI /3.1415926535898/
C   DATA AEFF, RS, ISRAD /6371000., 6.96E+8, 0/
CXXXXX
C
C   FRAC = 0.0
C
C...COMPUTE THE PROJECTION OF X ON RSOL
C   D = X(1)*RSOL(1) + X(2)*RSOL(2) + X(3)*RSOL(3)
C   IF (D.GT.0.0) GO TO 1
C
C...CHOOSE SHADOW MODEL
C   IF (ISRAD .EQ. 1) GO TO 3
C
C   CYLINDRICAL SHADOW MODEL
C
C...COMPUTE PROJECTION OF X ON PERPENDICULAR TO RSOL
C   R2 = R1**2 - (D/RSOL1)**2
C   IF (R2 .LT. AE2) RETURN
C
C...SATELLITE IS IN FULL SUN; COMPUTE SATELLITE TO SUN VECTOR
C   1 RSUM(1) = RSOL(1) - X(1)
C     RSUM(2) = RSOL(2) - X(2)
C     RSUM(3) = RSOL(3) - X(3)
C     RSUM2 = 1.0 / (RSUM(1)**2 + RSUM(2)**2 + RSUM(3)**2)
C     RSUM1 = SQRT (RSUM2)
C     RSUM(1) = RSUM(1) * RSUM1
C     RSUM(2) = RSUM(2) * RSUM1
C     RSUM(3) = RSUM(3) * RSUM1
C   2 FRAC = 1.0
C     RETURN
C
C   CONICAL SHADOW MODEL
C   THE CONICAL SHADOW MODEL HAS BEEN REMOVED.
C
C   3 CONTINUE
C
C...ENTRY POINT TO SET CONSTANTS
C
C   ENTRY SHADMO
C
C   AE2 = AEFF**2
C   Q1 = AEFF/(RS + AEFF)
C   Q2 = AEFF/(RS - AEFF)
C   RSPAE2 = (RS - AEFF)**2
C   RSPAE2 = (RS + AEFF)**2
C   RETURN
C
C...END SHADMO/SHADMO
C   END
C   FUNCTION RAGC (JED, TRBTAD)
C
C...PURPOSE: TO COMPUTE THE RIGHT ASCENSION OF THE GREENWICH
C   MERIDIAN FROM THE MEAN EQUINOX OF DATE
C
C   DOUBLE PRECISION JED
C   DATA TMOPI /6.2831853071796/
C   DATA AL0, AL1, AL2 / 1.7299358937175, 1.720279266007E-02,
C   1 5.0640897110022E-15 /
C   DATA ETMTAI /0.0001725/
C   DATA REFEF, UT1REF, DUT1 /2440224.3, -6.981, -0.00286/
C
C...JULIAN DAYS ELAPSED FROM 1900 JAN 0 DAYS 12 HOURS.
C   DTDAY = ENGL(JED) - REFEF
C   UT1MTAI = (UT1REF + DUT1*DTDAY)/86400.
C   UT1MET = UT1MTAI - ETMTAI
C   TU19001 = JED - 2415020.000 + UT1MET
C   TU19002 = TU19001 + TU19001
C
C...ANGLE FROM MEAN EQUINOX TO GREENWICH MERIDIAN AT CURRENT TIME.
C   ALPBA1 = AL0 + AL1*TU19001 + AL2*TU19002
C
C...FRACTION OF DAY SINCE 0 HOURS UT1
C   UT1 = AMOD(TU19001-.5,1.0)
C
C...HOUR ANGLE OF CONVENTIONAL ZERO MERIDIAN (BETWEEN 0 AND TMOPI)
C   RAGC = AMOD(ALPBA1+UT1*TMOPI, TMOPI)
C   TRBTAD = (1. + DUT1/86400.)*(TMOPI + AL1 + 2.*AL2
C   1 *TU19001)/86400.
C
C   RETURN
C
C   END

```



A NEODYMIUM YAG ACTIVE MIRROR FOR THE
AMPLIFICATION OF MODE-LOCKED LASER PULSES

S.R. Bowman, L.M. Ding, C.O. Alley
F.M. Yang, J. Fogleman
Department of Physics and Astronomy
University of Maryland
College Park, MD 20742 - USA -

Telephone (301) 454 3405

ABSTRACT

We report the development of the first Neodymium YAG active mirror amplifier. This device has advantages over other high average power amplifier geometries when the laser output energy is limited by the peak power damage threshold.

Our research objective is to increase the quantity and quality of data acquired from lunar laser ranging. This requires a combination of single shot laser energy, average power, and pulse duration that was unavailable in previous solid state laser designs. We have therefore conducted research on a new Nd:YAG amplifier configuration that should allow the production of one Joule, 50 picosecond pulses at an average power of 10 to 20 Watts.

Our active mirror configuration is best described by Figures (1) and (2). Three one inch diameter beam footprints lie along the 4 inch crystal length. The crystal thickness is 14 millimeters and the back surface reflections make this an inherently double-pass device. External mirrors transfer the beam from one footprint to the next.

The advantages of this amplifier geometry are three fold. Firstly, with the mirror geometry, large apertures are possible with the presently available crystals of Nd:YAG. Large apertures are essential to avoid damage and beam distortions that occur at high peak intensities and Nd:YAG is still the best solid state material for high average powers. Our mirror dimensions were chosen to make optimum use of a 4 inch diameter boule. Secondly, thermal birefringence and thermal focusing are eliminated by having the laser propagate parallel to the thermal gradients in the mirror.¹ Areas near the mirror's edges where the gradients are nonuniform can be simply avoided. The Nd:YAG active mirror amplifier should have crystal stress fracture limited average power capability without restriction to linear laser polarization. Lastly, the large open faces of the mirror geometry allow for several optically isolated gain paths through the same amplifier. This permits multipass gains of 40 dB for a single device.

Several areas critical to the success of the Nd:YAG active mirror have been investigated. The most important of these is the durability of the dielectric coating on the mirror's back face. This coating must reflect the normally incident high intensity laser without damage and transmit the flashlamp pump band over wide angles. It is exposed to the cooling water and is stressed by the heated YAG substrate. Immersion and laser exposure tests at 1 GW/cm^2 were conducted on samples of commercially supplied coatings. Back surface coatings for the mirror were selected that showed no laser or deterioration after a ten day immersion test. Another area critical to this design is the question of distortions from back surface flatness errors.² This design is very sensitive to such errors because of the high index of refraction of YAG and because of the requirement for multipass operation. Static beam distortions were reduced to below $1/15$ th wave per reflection through the use of compensation polishing on the front face. Dynamic surface distortions as well as gain variations across the beam depend linearly on the nonuniformity of the flashlamp pump intensity. Great care was taken with the pumping cavity in order to obtain less than a 2% RMS variation in the pumping spatial distribution. Other distortion mechanism such as crystal mounting and coolant back pressure were measured and found not to be a serious problem. At the time of this writing thermal distortion, laser gain, and beam quality measurements are in progress.

1. J.A. Abate, "Flashlamp-induced thermal distortions in active-mirror Nd:glass laser amplifier," Wavefront Distortions in Power Optics SPIE (1981) 293, 114.

2. J.A. Abate, et al., "Active mirror: a large-aperture medium-repetition rate Nd:glass amplifier," Appl. Optics (1981) 20, 351.

Active Mirror Amplifier Concept

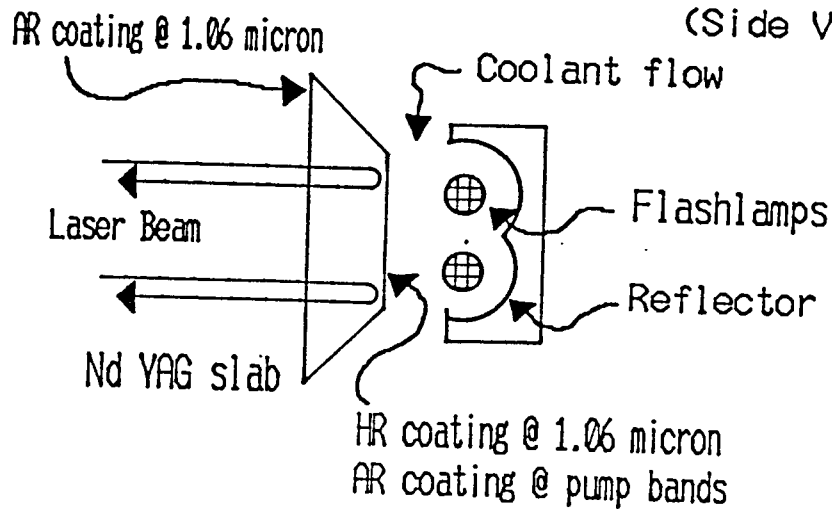


Figure 1

Active Mirror Amplifier Concept

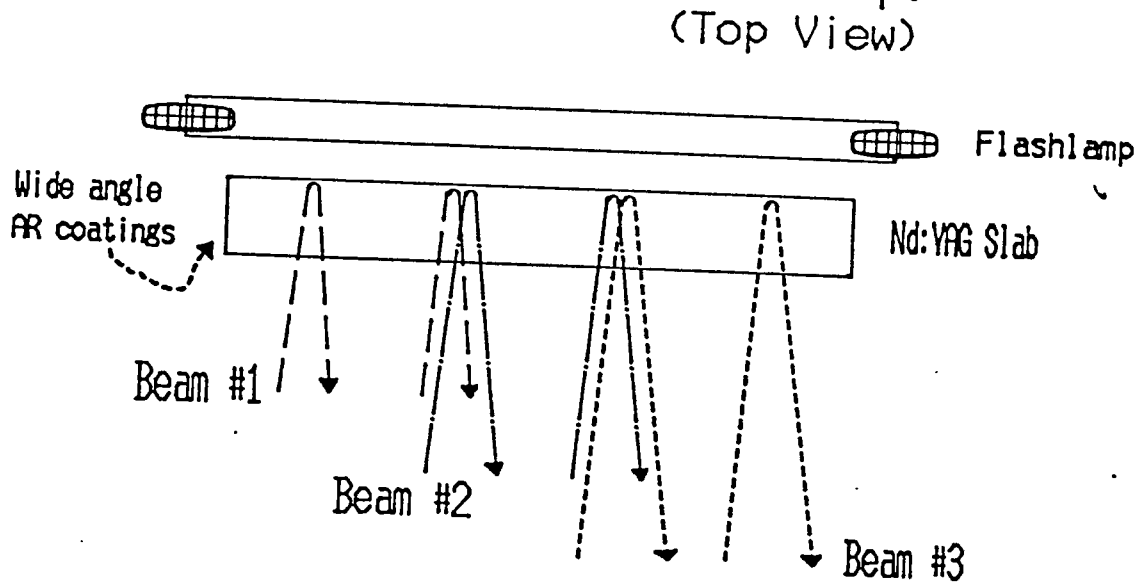
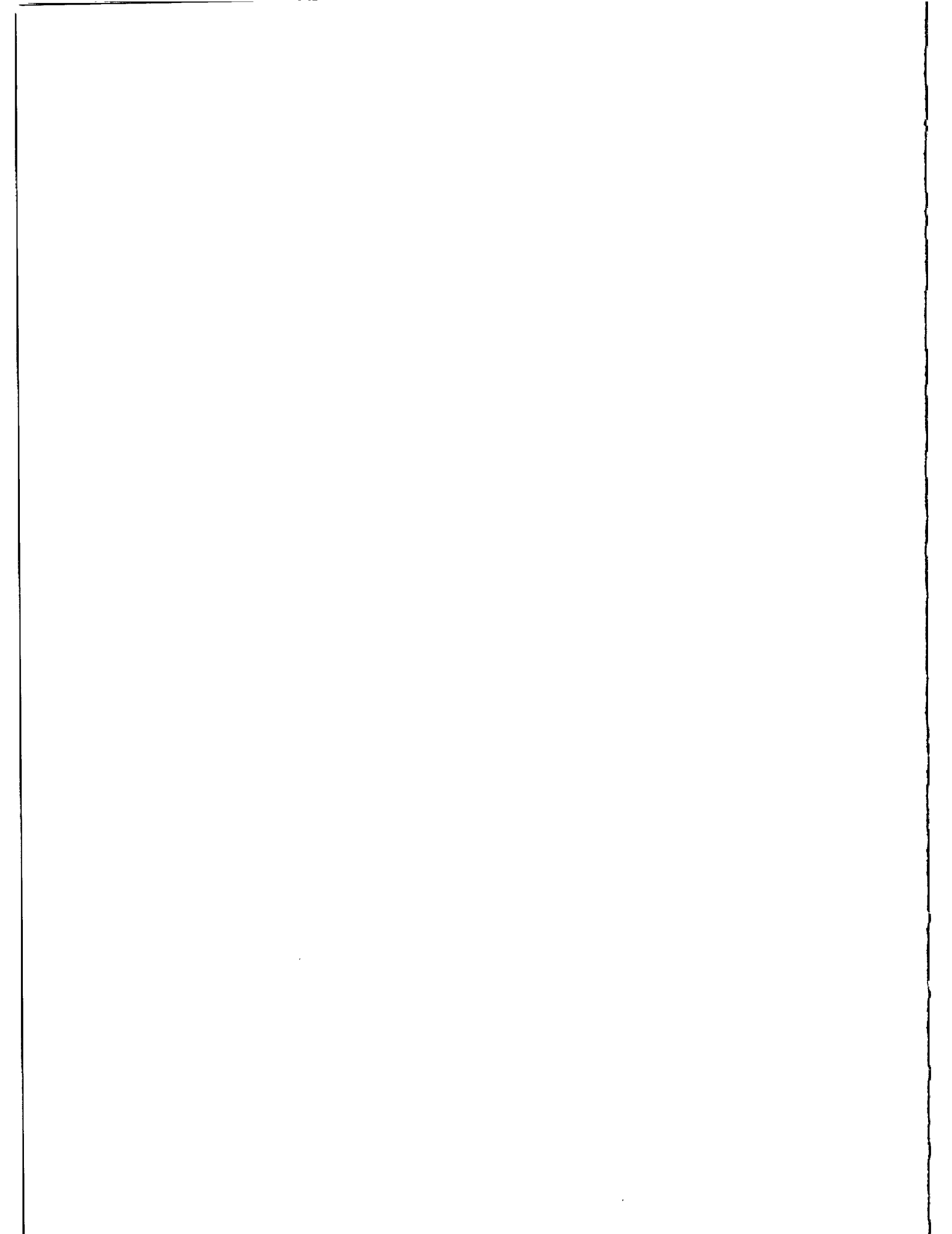


Figure 2



JAPANESE GEODETIC SATELLITE "AJISAI" LAUNCHED IN AUGUST 1986

M. Sasaki
Hydrographic Department of Japan
3-1, Tsukiji 5-Chome, Cho-ku
Tokyo, 104 - Japan -

Telephone (03) 541 3811
Telex 2522452 HDJODC J

ABSTRACT

The Japanese Experimental Geodetic Satellite "AJISAI" with functions for laser ranging and photographing from the ground was launched on August 12, 1986. The tracking observation of AJISAI has been made after the launch by laser ranging and photographing techniques under international cooperation. According to a simulation the range accuracy of one to two centimeters level is attainable by applying edge detection method with narrow laser pulse. A construction of a marine geodetic controls around Japan is to be made by the Hydrographic Department of Japan using the AJISAI satellite and a transportable laser ranging station.

JAPANESE GEODETIC SATELLITE "AJISAI" LAUNCHED IN AUGUST 1986

M. Sasaki
Hydrographic Department of Japan
3-1, Tsukiji 5-chome, Chuo-ku
Tokyo, 104 Japan

Telephone (03) 541 3811
Telex 2522452 HDJODC J

ABSTRACT

The Japanese Experimental Geodetic Satellite "AJISAI" with functions for laser ranging and photographing from the ground was launched on August 12, 1986. The tracking observation of AJISAI has been made after the launch by laser ranging and photographing techniques under international cooperation. According to a simulation the range accuracy of one to two centimeters level is attainable by applying edge detection method with narrow laser pulse. A construction of a marine geodetic controls around Japan is to be made by the Hydrographic Department of Japan using this AJISAI satellite and a transportable laser ranging station.

1. INTRODUCTION

The Japanese Experimental Geodetic Satellite (EGS) was launched at the Tanegashima Space Center by using the first H-I rocket of the National Space Development Agency (NASDA) of Japan on August, 1986 and the satellite was named "AJISAI" which means "HYDRANGEA" of flower in Japanese. The original mission of this satellite was to determine the location of isolated islands, to adjust the triangulation network and to know the relation between the Japanese Geodetic Coordinate System (Tokyo Datum) and those of other parts of the world.

The original design in early 1970s was a balloon of 10 meters diameter for both photographing and laser ranging. The design of the satellite was changed to a rigid type to avoid the air drag and the unreliability at the expansion of balloon to space later. The flight model of the satellite was completed by NASDA and launched. The specifications and observation project of "AJISAI" are presented here.

2. FUNCTIONS AND SPECIFICATION OF "AJISAI"

The function of the satellite "AJISAI" are (1) to reflect input laser light back toward the incident direction by Corner Cube Reflectors (CCRs) and (2) to reflect solar light to the ground by solar reflecting mirrors.

The body of the satellite is hollow sphere made of glassfiber-reinforced

plastics. The surface of the body is covered with CCRs and solar light reflectors (Fig. 1). Twelve pieces of unit CCRs form a set of Laser Reflector (LR) and 120 sets of the LR are distributed on the surface almost uniformly. The effective area for laser light reflection within the full prospect angle of 30 degrees from the center of the satellite is 91.2 cm². The remainder part of the surface is covered with 318 pieces of solar reflectors. The reflectors are mirrors with the radii of the curvature from 8.4 to 8.7 m. The base of the mirror is made of an alloy of aluminum and the surface is coated by an oxide silicon for protection from flanging and diminution of quality. The reflective efficiency of the mirror is 0.85. The diameter of "AJISAI" is 2.15 m and its total weight is 685.2 kg.



Fig. 1 Japanese Geodetic Satellite "AJISAI".

"AJISAI" was given a spinning of 40 rpm before detachment from the rocket. The spin axis was set in parallel to the earth rotation axis and almost every observers on the ground in the dark can observe the flashing light of reflection from the solar reflectors of "AJISAI" in repetition rate of 2 pps if the satellite is exposed to the solar light. The flashing duration is about 5 msec and the brightness of the reflective light is from 1.5 to 4.0 star magnitude as shown as followings:

The intensity of the reflected light from a mirror sphere through atmosphere is given by

$$I = \gamma I_s \frac{a^2}{4r^2} T$$

and the brightness expressed in star magnitude is

$$m = -2.5 \log I$$

where I_s : intensity of input light, γ : reflectivity of a sphere, a : radius of a sphere, r : range from observer to a sphere, T : transparency of atmosphere. The magnitude of the brightness is estimated by using some values of specifications and atmosphere as

I_s : ($m_s = -2.5 \log I_s = -26.8$: star magnitude of the sun), γ : 0.85, a : 8.5 m, T : $\exp(-k \sec z)$ for a model transparency of atmosphere, z : zenith distance, k : atmospheric condition (0.3 : good, 0.4 : medium, 0.5 : not good). The results are shown in Table I.

The flash can be taken in a photo with a number of fixed stars by using a camera on an equatorial mount and the direction of the satellite from the observer can be measured referring the star

Table I Brightness of "AJISAI" expressed in star magnitude

elevation	range	transparency		
		k=0.3 (good)	k=0.4 (medium)	k=0.5 (not good)
deg	km	mag	mag	mag
90	1500	1.44	1.55	1.65
80	1519	1.47	1.58	1.69
70	1577	1.56	1.71	1.80
60	1680	1.73	1.86	1.98
50	1841	1.98	2.12	2.26
40	2080	2.32	2.50	2.67
30	2428	2.81	3.03	3.24
20	2931	3.52	3.84	4.15

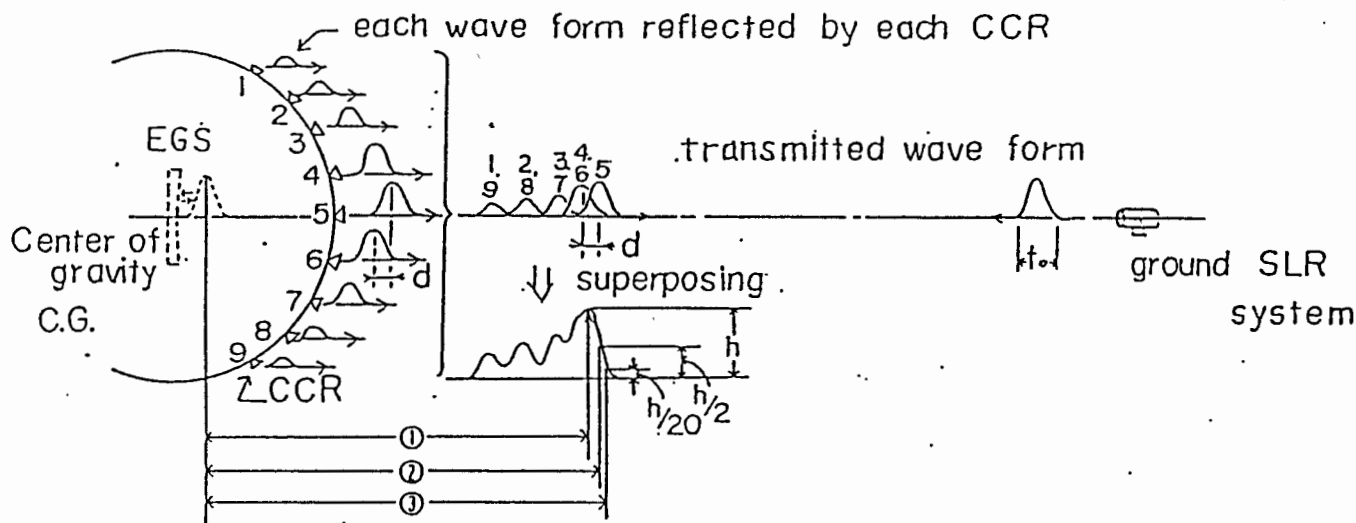


Fig. 2 Concept of simulation to know wave form of return pulse and range bias. Range bias for ① first peak position, ② half height position and ③ rising position.

coordinate system.

For the estimation of the ranging accuracy of "AJISAI", a simulation has been conducted by NASDA. The concept of the simulation is given in Fig. 2. In this simulation no atmospheric fluctuation effect is considered. A kind of the full width at half-maximum (FWHM) of 78 psec (200 psec for total width within three times of the standard deviation of a Gaussian shape) are used. The incident direction of 60 in number are selected geometrically in 30 degrees step from -60 degrees to +60 degrees for latitude and in 30 degrees step for longitude around the spin axis. The resultant change of position (half distance) of the first peak, rising position of half height of the highest peak and rising position of 1/20 height of highest peak are shown in Table II. The mean value of the position of the first peak and its root mean square (RMS) are :

$$1013.3 \pm 11.3 \text{ mm.}$$

The reflection patterns for the three typical cases are given in Fig. 3. The results of the simulation above indicate that the range accuracy to "AJISAI" attains 1 to 2 cm level when a high precision Satellite Laser Ranging (SLR) system with a narrow-pulse-laser-transmitter and with multi-photoelectron-detection or front-edge-detection method. The most of Lageos capable SLR systems can be attainable to the front edge detection of return laser light from "AJISAI" since the lower orbit than Lageos (5900 km) gives much stronger return energy of laser light.

The launch of "AJISAI" was made successfully at 20^h 45^m on August 12, 1986 (UT) and the tracking observations by NASDA, JHD (Hydrographic Department of Japan) and other supporting organizations including the National Aeronautics and Space Administration (NASA) of the United States has been continued. The determined orbit is circular with the inclination of 50.0 degrees and altitude from the ground is 1500 km high.

Table II Change of range bias for reflective pulse from "AJISAI"

pulse width	measuring position	range bias	
		maximum mm	minimum mm
200 ps	first peak	1026	984
	half height	1031	1011
	rising	1037	1031
300 ps	first peak	1026	984
	half height	1034	1019
	rising	1043	1035

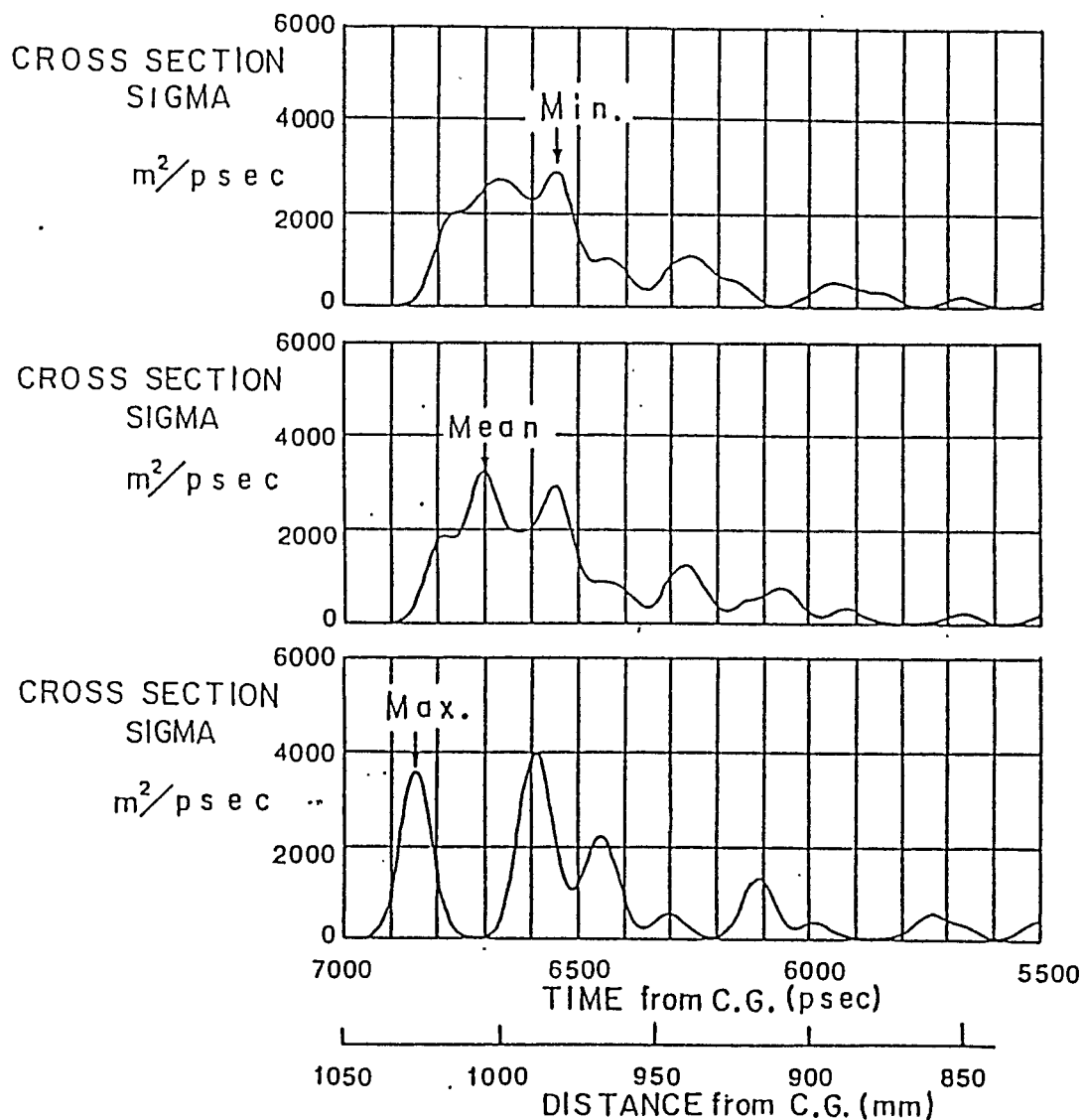


Fig. 3 Examples of laser reflection pattern. For the cases of the first peak position of the minimum-, mean- and maximum-range bias.

3. COMPARISON OF ORBITAL STABILITY WITH OTHER GEODETIC SATELLITES

"AJISAI" satellite is a fully passive satellite for use of both laser ranging and photo direction observation. For the laser ranging there are two passive sphere satellites of Lageos and Starlette. The diameter, weight and orbital height for both satellites are 0.60 m, 411 kg, 5900 km and 0.24 m, 47 km, 900 km respectively. There were three balloon satellites in 1960s.

To realize the stable orbit against air drag and radiation pressure effects, large mass/cross-section-area (M/A) ratio is preferable. M/A ratio is an index to indicate the stability of radiation pressure and $1/\rho M/A$ is an index for air drag stability in the atmospheric density of ρ . The M/A ratio for the satellite. The values of M/A ratio and $1/\rho M/A$ for AJISAI and sphere laser satellites are shown in Table III for comparison.

The air drag effect is more sensitive for orbital stability of the geodetic satellite than radiation pressure. Concerning that higher orbit of satellite is preferable to avoid effect of uncertainty of geopotential, the stability of the orbit of AJISAI seems a little better than or at least almost the same as that of Starlette.

In addition to the availability to geometrical use and dynamical use of AJISAI for geodetic purpose, one more remarkable subject is that the precise determination of orbit of AJISAI in long period improves the accuracy of coefficients of the geopotential.

Table III Comparison of AJISAI with other rigid laser satellite

	mean altitude	M/A mass/area	$1/\rho M/A$ mass/air-density·area
	km	kg/m ²	x 10 ⁴ m
AJISAI	1500	148	2.6
Starlette	900	816	1.9
Lageos	5900	1140	370

4. METHOD OF OBSERVATION

There are several methods in geodetic use of this "AJISAI" satellite. One is fully geometrical method by using simultaneous observations of distance and direction at some stations. Namely, two kinds of observations are made at a base station (known position or given position) and temporary stations (unknown positions, e.g. isolated islands). The position of the satellite is given by distance and direction observation from the known position and unknown positions are determined from the position of the satellite by similar distance and direction observations at these points. A SLR system and a Satellite Camera are also necessary at a temporary station in this method. The location of an unknown position is given by only one set of observation in principle.

The other geometrical method is to use several SLR systems simultaneously in a region of a few thousands kilometers. The range correction of this satellite is well determined as shown in a simulation above and simultaneous precision ranging can determine baselines in a centimeter level.

The dynamical method is also useful to determine the location of SLR stations based on a geocentric coordinate and other geophysical parameters as geopotential coefficients, air drag effect and tidal effects. For each method or combined methods it is effective to hit laser beam well on this satellite because of its brightness.

JHD is under preparation of a SLR system and satellite camera at fixed base station (Simosato Hydrographic Observatory) and a transportable SLR station and satellite camera for temporary stations of which geodetic position should be combined with the base station. For these equipments, another report is presented in this laser workshop. By using these equipments, marine geodetic controls are to be expanded by JHD around Japan to combine isolated islands with the Tokyo Datum.

5. SUPPORTING OBSERVATIONS FOR "AJISAI" AND INTERNATIONAL COOPERATION

The observation of "AJISAI" by using the SLR systems at the Simosato Hydrographic Observatory has been made from just after the launch. 25,300 ranges of 27 passes were obtained at the observatory in August 1986. The preliminary range accuracy for them, 7~8 cm level, seems a little better than those of other geodetic satellite, 9~10 cm level, within early stage after the launch. The supporting observations of Japanese domestic organizations were made. The SLR data and pointing information were transferred to the Tsukuba Space Center of NASDA and the Satellite Geodesy Office in the Headquarters of JHD through a microcomputer network (PC-VAN). The orbital elements have been created continuously at those places and distributed to domestic observation sites.

JHD has an agreement for cooperation of SLR observation and its data exchange with NASA. The Goddard Laser Tracking Network of NASA also started the supporting observation for "AJISAI" from just after the launch and distributes their own orbital elements of AJISAI to cooperative SLR stations. Observation data and results of research work of AJISAI will be exchanged between JHD and NASA.

Other international SLR stations in England, Switzerland and so on also tracking AJISAI and more wider cooperation with France, China, West Germany, Australia and Austria is expected. For these international cooperation for AJISAI observation JHD with NASA will play a role of data distribution center. The work on collection of SLR and photograph data, determination of orbit, distribution of orbital elements, data file management and data analysis has started in JHD.

REFERENCES

- Ganeko, Y., K. Komaki and H. Hashimoto, "On the geodetic satellite GS-1", in Proc. Sympo. on Space Techniques in Positional Astronomy, A. Tsuchiya, Ed. Tsukuba, pp.12-18, 1983 (in Japanese).
- Hashimoto, H. and K. Saito, "Development of the Experimental Geodetic Payload", in Proc. 17th Sympo. for engineering results in NASDA, 1985 (in Japanese).
- Sasaki, M., "Optimum orbit of the Geodetic Satellite GS-1", Rep. Hydrogr. Researches, JHD, no.14, pp.131-144, 1979 (in Japanese).
- Sasaki, M., "Observation Project of Japanese Geodetic Satellite GS-1", in Proc. Sympo. on Application on Space Techniques to Astronomy and Geophysics, H. Kinoshita, I. Murata and K. Nakajima, Ed. Tokyo, pp.27-31, 1986.
- Sasaki, M. and H. Hashimoto, "Launch and Observation Program of the Experimental Geodetic Satellite of Japan", IEEE Transactions on Geoscience and Remote Sensing, to be published.
- Sasaki, M. and Y. Suzaki, "Satellite Ranging System at the Simosato Hydrographic Observatory and the Transportable System", in this issue.

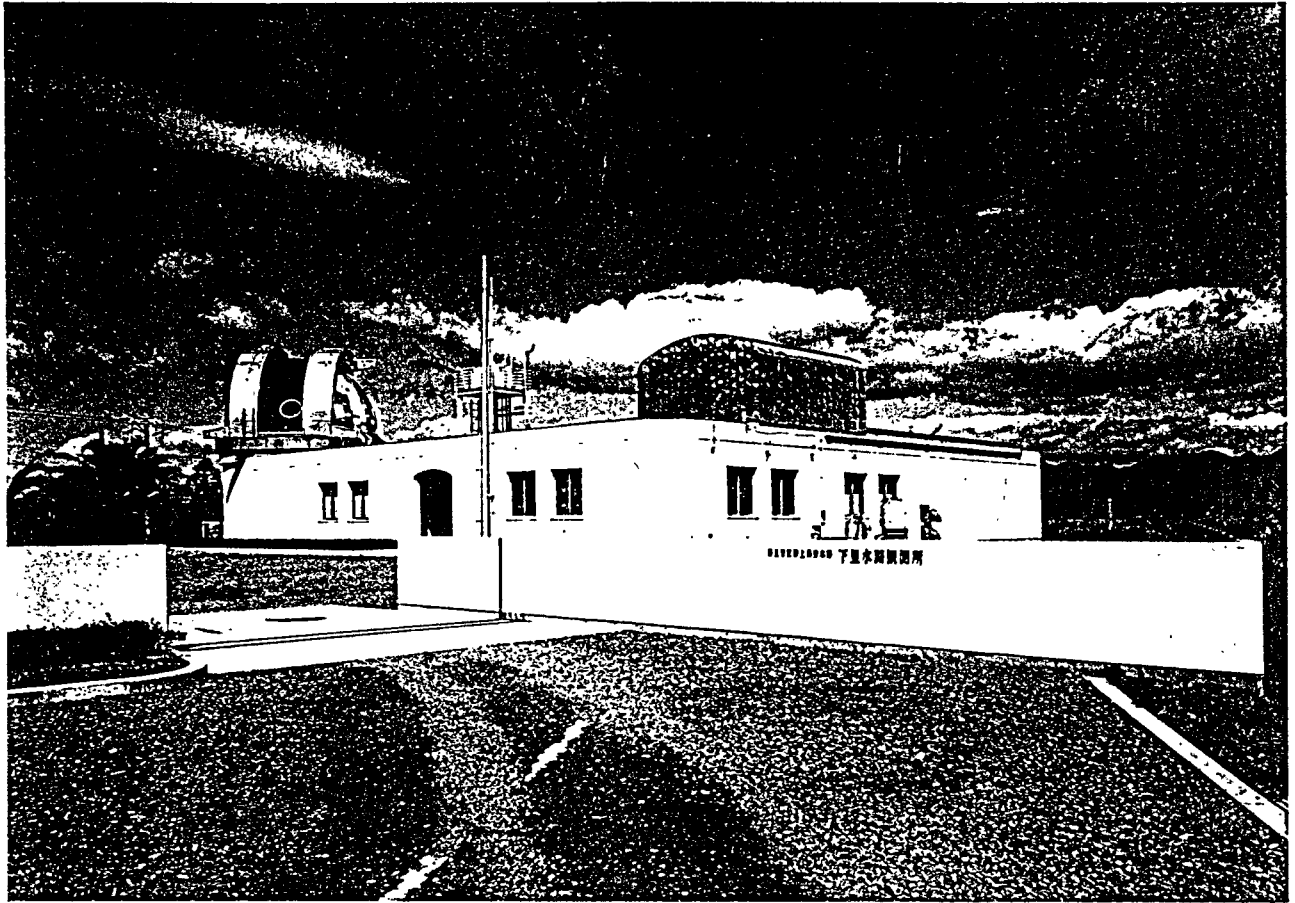


Fig. 1 External View of the Simosato Hydrographic Observatory

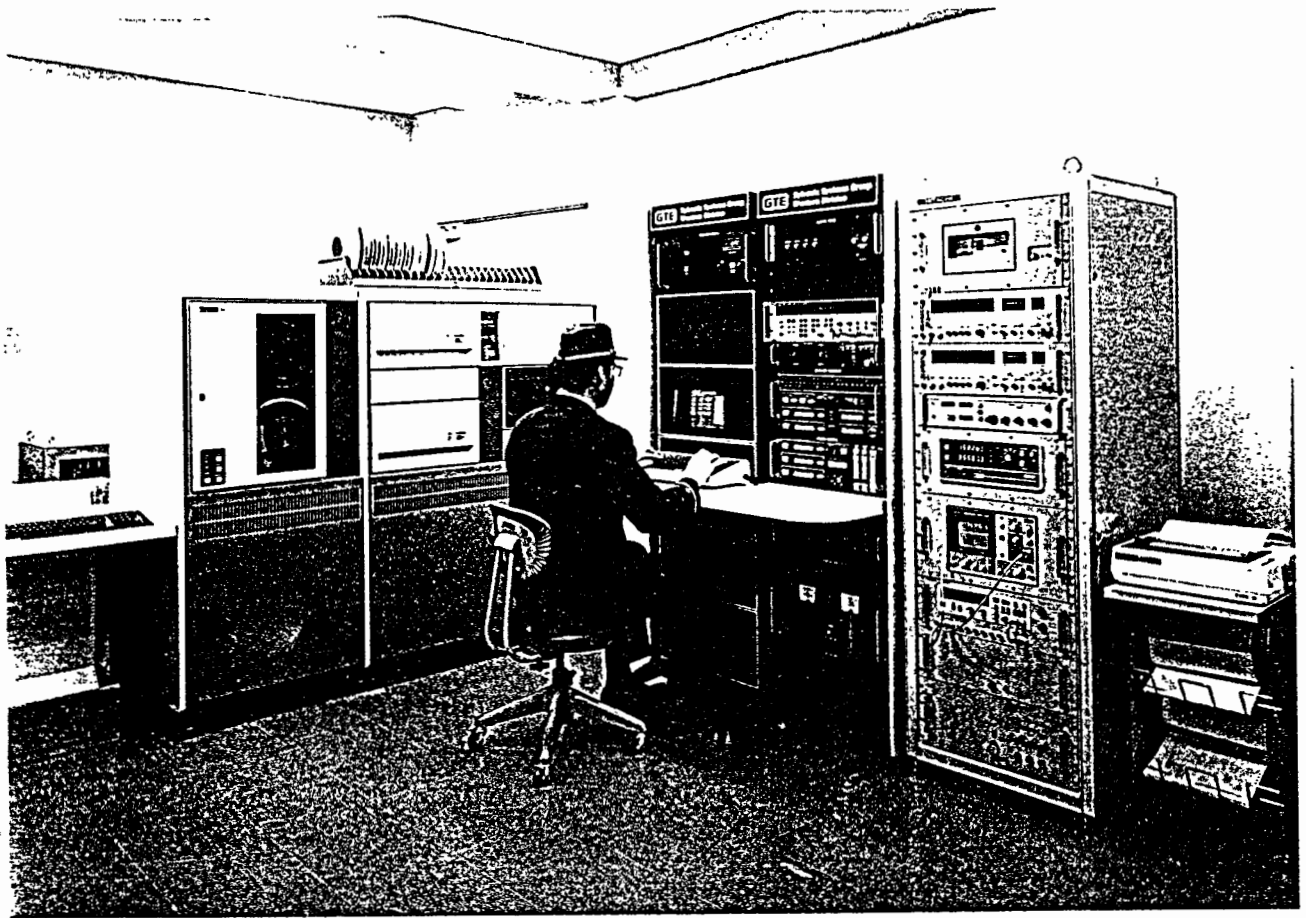


Fig. 2 Electronics

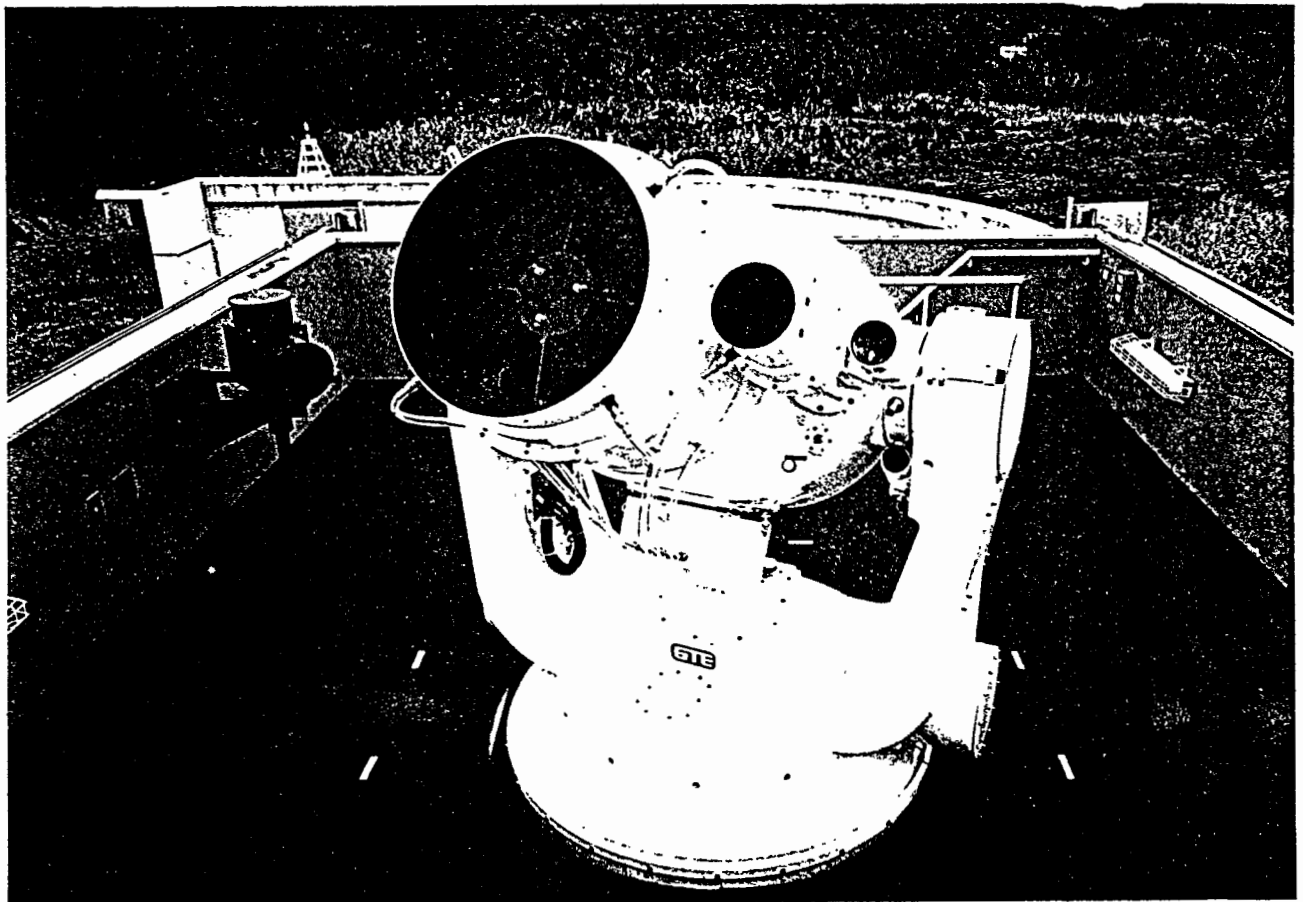


Fig. 3 Optics / Mount

***** SATELLITE TRACKING REPORT *****
 Station : 793E (SIMOSATO)
 (-3822.38448km, 3699.36735km, 3507.57235km)
 (6371.73470km, 135.9370deg, 33.5777deg)
 Satellite : S602101
 Used ORBITAL : 1986.08.14 0:00:00 (UT)
 Pass starts : 1986.08.13 17:43:00 (UT)
 Atmosphere : Sky/Shadow code 1
 Humidity 99.0%
 Temperature 23.2deg
 Pressure 1007.1mmHg
 System control : Leveling angle 0.0061deg(CDS(AZ- 93.0600deg))
 Collimation angle -0.0046deg
 Encoder offset (160.1600deg, 4.5500deg)
 Telescope sag 0.0000deg
 Refraction factor 0.9610
 Laser firing 250msec
 pre Range offset 7.1msec
 post Range offset 7.3msec

Produced by T. Yamasuchi (Phone 045-803-7253)

RHS of Br = 0.079(m) Number of Br = 1501

UT	-2m	-150cm	-1m	-50cm	0	50cm	1m
17:43:10	:	:	:	:	:	:	:
17:43:20	:	:	:	:	:	:	:
17:43:30	:	:	:	:	:	:	:
17:43:40	:	:	:	:	:	:	:
17:43:50	:	:	:	:	:	:	:
17:44:00	:	:	:	:	:	:	:
17:44:10	:	:	:	:	:	:	:
17:44:20	:	:	:	:	:	:	:
17:44:30	:	:	:	:	:	:	:
17:44:40	:	:	:	:	:	:	:
17:44:50	:	:	:	:	:	:	:
17:45:00	:	:	:	:	:	:	:
17:45:10	:	:	:	:	:	:	:
17:45:20	:	:	:	:	:	:	:
17:45:30	:	:	:	:	:	:	:
17:45:40	:	:	:	:	:	:	:
17:45:50	:	:	:	:	:	:	:
17:46:00	:	:	:	:	:	:	:
17:46:10	:	:	:	:	:	:	:
17:46:20	:	:	:	:	:	:	:
17:46:30	:	:	:	:	:	:	:
17:46:40	:	:	:	:	:	:	:
17:46:50	:	:	:	:	:	:	:
17:47:00	:	:	:	:	:	:	:
17:47:10	:	:	:	:	:	:	:
17:47:20	:	:	:	:	:	:	:
17:47:30	:	:	:	:	:	:	:
17:47:40	:	:	:	:	:	:	:
17:47:50	:	:	:	:	:	:	:
17:48:00	:	:	:	:	:	:	:
17:48:10	:	:	:	:	:	:	:
17:48:20	:	:	:	:	:	:	:
17:48:30	:	:	:	:	:	:	:
17:48:40	:	:	:	:	:	:	:
17:48:50	:	:	:	:	:	:	:
17:49:00	:	:	:	:	:	:	:
17:49:10	:	:	:	:	:	:	:
17:49:20	:	:	:	:	:	:	:
17:49:30	:	:	:	:	:	:	:
17:49:40	:	:	:	:	:	:	:
17:49:50	:	:	:	:	:	:	:
17:50:00	:	:	:	:	:	:	:
17:50:10	:	:	:	:	:	:	:
17:50:20	:	:	:	:	:	:	:
17:50:30	:	:	:	:	:	:	:
17:50:40	:	:	:	:	:	:	:
17:50:50	:	:	:	:	:	:	:
17:51:00	:	:	:	:	:	:	:
17:51:10	:	:	:	:	:	:	:
17:51:20	:	:	:	:	:	:	:
17:51:30	:	:	:	:	:	:	:
17:51:40	:	:	:	:	:	:	:
17:51:50	:	:	:	:	:	:	:
17:52:00	:	:	:	:	:	:	:
17:52:10	:	:	:	:	:	:	:
17:52:20	:	:	:	:	:	:	:
17:52:30	:	:	:	:	:	:	:
17:52:40	:	:	:	:	:	:	:
17:52:50	:	:	:	:	:	:	:
17:53:00	:	:	:	:	:	:	:
17:53:10	:	:	:	:	:	:	:
17:53:20	:	:	:	:	:	:	:
17:53:30	:	:	:	:	:	:	:
17:53:40	:	:	:	:	:	:	:

1 17:43:13.283765 0 18.91581012 330.5359 21.6536 -0.00129217 0.155

Fig. 4 "AJISAI" Ranging Data Obtained at Simosato

Table 3 Major Specifications of the HTLRS

receiver diameter	35cm
laser : output energy	50mJ
pulse width	200ps
repetition rate	5 - 10pps
range resolution	20ps
range accuracy	5cm/shot
transportation	air transportable

THE PROPOSAL OF
STRICTLY SIMULTANEOUS SATELLITE LASER RANGING

F.M. Yang
Department of Physics and Astronomy
University of Maryland
College Park, MD 20742 - USA -

Telephone (301) 454 3405
Telex 908787

ABSTRACT

A proposal of synchronized laser ranging to artificial satellites from different stations is presented in this paper. In this operational mode, the laser firing epoch at each station should be strictly controlled by computers so that all laser pulses transmitted from different stations arrive at a satellite at certain moments (such as seconds, or tenths of second) with a minimum time uncertainty. (20 microseconds can be easily obtained for present passive mode-locked lasers).

All full-rate range data attained in this mode can be analysed by dynamic technique as usual. Besides, based on the 3-D multilateration method (1), a strictly geometric solution without polynomial smoothing and complex interpolation may be achieved, and 5 mm accuracy baselines between laser stations could be obtained in near future.

I Introduction

The range accuracy of satellite laser ranging systems has greatly improved in recent years. A few 1 cm accuracy systems (for single measurement) are now operational [2][3][4]. For removing systematic errors, millimeter level real time calibration technique are now in common use at most stations. Streak-camera-based two color satellite laser ranging systems have been under development, and appear capable of measuring the atmospheric delay with an accuracy of 5 mm or better [5].

The analysis of SLR data is now dominated by dynamic method and a great deal of scientific results in geodesy and geodynamics have been achieved in the recent 10 years. But one realizes that there still are some difficulties in the dynamic technique because of complex perturbation factors influencing on orbits of satellites, so some results derived from the same LAGEOS data by different analysis groups are quite different, such as in the intercomparison of 22 baseline lengths determined by SLR and VLBI respectively [6][7]. The authors of [7] found a scale difference of 1.9×10^{-8} , but no difference was found in [6]. It was also shown in Fig.13 of [8] that a few measured baseline values seem suspicious. The errors in the best gravity model we now have will affect baseline estimate with 2 cm uncertainty. In the mentioned comparison of baseline length determinations [6], the uncertainty of baselines from SLR (dynamic method) is 2-4 cm, a little worse than those from VLBI (1-3 cm). However, the fact is that a few SLR systems have already had the capability of 1 cm single shot accuracy. Could one use the geometric simultaneous ranging technique proposed by some investigators over 10 years ago to exploit this high range accuracy and to obtain ground baselines with the same or better accuracy? If one could, the future results would be a very important check to the SLR dynamic method. Although there are many difficulties for simultaneous observations, a large number of updated SLR stations have existed in some regions, especially in Europe and North America, and the reliability of these SLR systems has been greatly improved, so the possibility of successful simultaneous observations are much improved.

II Method and Purposes

In previous geometric solution tests, such as [9], only quasi-simultaneous observations were used which required complex smoothing and interpolation. This could lead to additional errors which could not be ignored in the processing of 1 cm accuracy data.

For SLR stations using 10 Hz laser systems, the arriving time differences of laser pulses from different sites to LAGEOS would be about 50 msec, equal to maximum range differences of about 200 meters. Even for those stations which can synchronize the transmit pulses from different systems to a certain time standard (e.g. UTC USNO), the arriving time epoch of laser pulses from different stations will still be different by up to 10-15 msec owing to variations of relative positions of the satellite and stations. This corresponds to range differences of about 40-60 meters. Due to high frequency perturbation factors, it is not easy to interpolate these quasi-simultaneous observations (40-200 meters range differences) to the 1 mm level accuracy which seems necessary for processing 1 cm accuracy data.

The routine predictions of one way flight time from stations to LAGEOS have been made as good as 0.5 μ sec. During this time uncertainty, the maximum radial motions of LAGEOS relative to stations is only 2 mm. So, if the laser firing epoch at each participating station can be strictly controlled, the epoch of pulses arriving at the satellite from different stations will be the same with this same time uncertainty. For active Q-switch and mode-locked laser systems, firing epoch can be controlled within 100 nsec, but for those mode-locked systems having passive devices (such as dye cell), firing epoch can be controlled to about 20 μ sec, which means only 80 mm maximum variation of slant ranges of LAGEOS. Based on the accurate timing of transmitted pulses and returned signals, and the routine predictions of range rates of LAGEOS, the measured ranges could be easily interpolated to the same time to 1 mm accuracy. In this way, a strictly geometric solution, which includes accurate baselines and 3-D relative coordinates of LAGEOS and stations, can be accessible.

These results can contribute towards the following topics:

- 1) Comparison of SLR dynamic solutions and VLBI baselines results;
- 2) Control of geodetic network and monitoring of tectonic plate motions and deformations, and assessment of earthquake hazards. Especially, the high temporal resolution of this method may be very useful to obtain the variations of baselines;
- 3) Verification of real accuracy of distant laser ranging technique;
- 4) Assist in accurate determination of UT1. By means of determined three-dimensional station coordinates and LAGEOS space positions at different epochs, the directions of the satellite relative to this station network at those epochs with $0.0005''$ ($1 \text{ cm} / 6000 \text{ KM}$) accuracy can be calculated. If the space directions of two baselines in the network can be determined at some epoch by co-location observations with VLBI or LLR technique at the three relevant stations, then the directions to LAGEOS relative to the inertia reference frame at those epochs can be figured out with the same accuracy, so, the technique could help dynamic methods improve the determination of UT1.

III Technical requirements

1) It is necessary to have 6 or more stations which can range to LAGEOS with 1 cm accuracy participating in the observation in order to obtain stable solutions^{[1][10]};

Fig.1 is the geometry of simultaneous LAGEOS laser ranging. Table 1 is the estimate of co-observable time of LAGEOS at different baselines. Assuming the lowest elevation for LAGEOS ranging is 20° , two stations which are separated by 6000 KM can have 10 or more minutes of common visibility. For $P_1 P_3$ baseline (4450 KM), when the elevation of LAGEOS at station P_1 is 20° , the satellite may be at the zenith of station P_3 at the same time.

2) In order to ensure a sequence of 4 or more stations simultaneous strikes, the percentage of LAGEOS returns at most stations must be about 30% (Table 2). This requires multi-photoelectron receiver and nighttime ranging. For example,

if there are 6 participating stations, 5 Hz repetition lasers, 20% percentage of returns for each station, and 10 minutes co-observation period, giving 3000 transmitted pulses. Then from Table 2, the total number of 4 and more stations simultaneous ranges will be 78 (3000×0.026). If the percentage increases to 30% for these same stations, the total number of simultaneous ranges will be 420.

3) The laser firing epoch at all stations must be strictly controlled by computers, so that laser pulses coming from all stations strike LAGEOS simultaneously with an uncertainty of less than 20 μ sec. This operation mode will be different from the current mode and the fire intervals will no longer be exactly constant at each station. For 10 Hz repetition laser systems, we have,

$$\begin{aligned} \text{Firing commands} &= i/10 \text{ seconds} - (1/2) * \text{Predicting flight time} \\ &\quad - \text{Delay time of firing circuit} \\ &\quad (i = 1, 2, 3, \dots, n). \end{aligned}$$

Before ranging, the delay time of each laser firing system must be input into computer as a parameter.

It should be pointed out that this laser operational mode will be adopted in the LASSO experiment with millisecond level uncertainties in firing times.

4) The clocks at each station must be synchronized to 0.3 μ sec (1.2 mm range uncertainty) with respect to a master clock. It can be achieved via Loran-C, TV and portable clocks.

IV Estimate of baseline accuracy

JPL's P.R.Escobal and K.M.Ong had made a lot of numerical simulations for baseline solutions with simultaneous laser ranging. Their conclusion was " the method of multilateration can determine the relative three-dimensional solution coordinates with an accuracy that is limited only by the hardware measurement system. If a highly accurate laser ranging system (1 cm accuracy) is used, then accuracies in the 1 cm range can be expected." [10].

In fact, Ong and Escobal employed only a total of 100 trajectory points from a few passes of two different altitude satellites in the simulations. If more stations join in the strictly simultaneous laser ranging and accumulate numbers of passes, especially from two LAGEOS-like satellites, better results of baselines will be obtained, for example, if 10-20 passes with more strikes can be used to the reduction, it will be reasonable to achieve 5 mm baseline accuracy.

The following accuracy of baselines can be expected:

1 cm ---- Temporal solution (a few passes from different satellites in several hours);

0.5 cm ---- Average solution (over dozen passes in several days).

I would like to thank Prof.C.O.Alley and J.Rayner for helpful discussions.

References

1. P.R.Escobal, H.F.Fliegell, R.M.Muller, K.M.Ong, O.H.vos Roos and M.S.Shumate: 3-D Multilateration: A Precision Geodetic Measurement System, JPL Quarterly Technical Review, Vol.2, No.3, (1972).
2. J.J.Degnan, Satellite Laser Ranging: Current Status and Future Prospects, IEEE Trans. on Geoscience and Remote Sensing, Vol.GE-23, No.4, p.398 (1985).
3. T.Varghese, Recent MOBLAS Upgrades, this proceedings.
4. B.Greene, Recent Development at Orroral, this proceedings.
5. J.B.Abshire and S.Gardner, Atmospheric Refractivity Corrections in Satellite Laser Ranging, IEEE Trans. on Geoscience and Remote Sensing, Vol.GE-23, No.4, p.414 (1985).
6. R.Kolenkiewicz, J.Ryan, and M.H.Torrence, A Comparison Between LAGEOS and Very Long Baseline Interferometry Determined Baseline Lengths, J.G.R., Vol.90, No.B11, p.9265 (1985).
7. B.D.Tapley, B.E.Schutz, and R.J.Eanes, Station Coordinates, Baselines, and Earth Rotation From LAGEOS Laser Ranging: 1976-1984, J.G.R., *ibid*, p.9235 (1985).
8. D.C.Christodoulidis, D.E.Smith, R.Kolenkiewicz, S.M.Klosko, M.H.Torrence, and P.J.Dunn, Observing Tectonic Plate Motions and Deformations From Satellite Laser Ranging, *ibid*, p.9249 (1985).
9. E.C.Pavlis, On the Geodetic Applications of Simultaneous Range Differences to LAGEOS, *ibid*, p.9431 (1985).
10. K.M.Ong and P.R.Escobal, Multilateration: A Nondegenerate Method of Obtaining Station Coordinates and Satellite Ephemerides, J. of Astronautical Sciences, Vol.XXI, No.5&6, p.206 (1974).

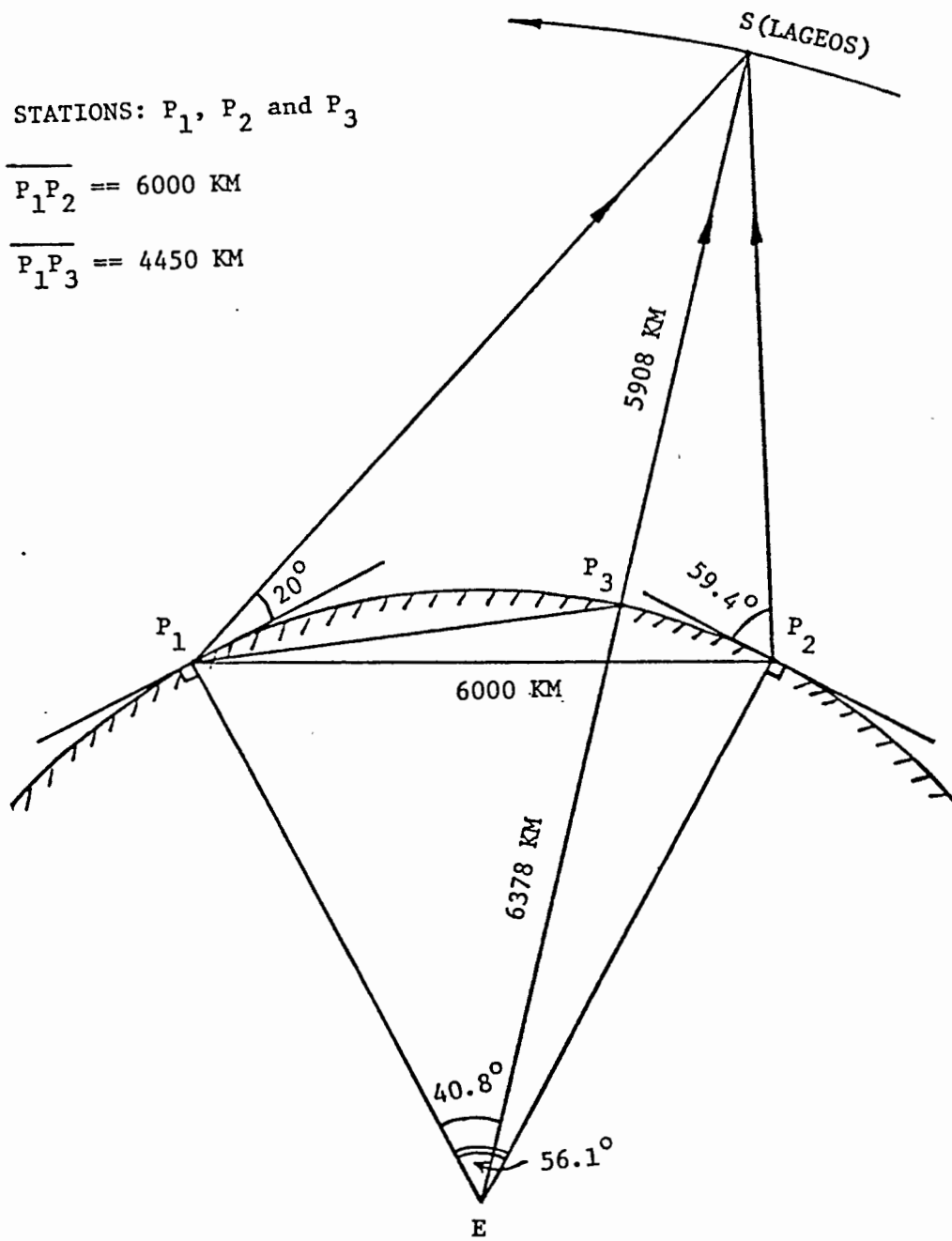


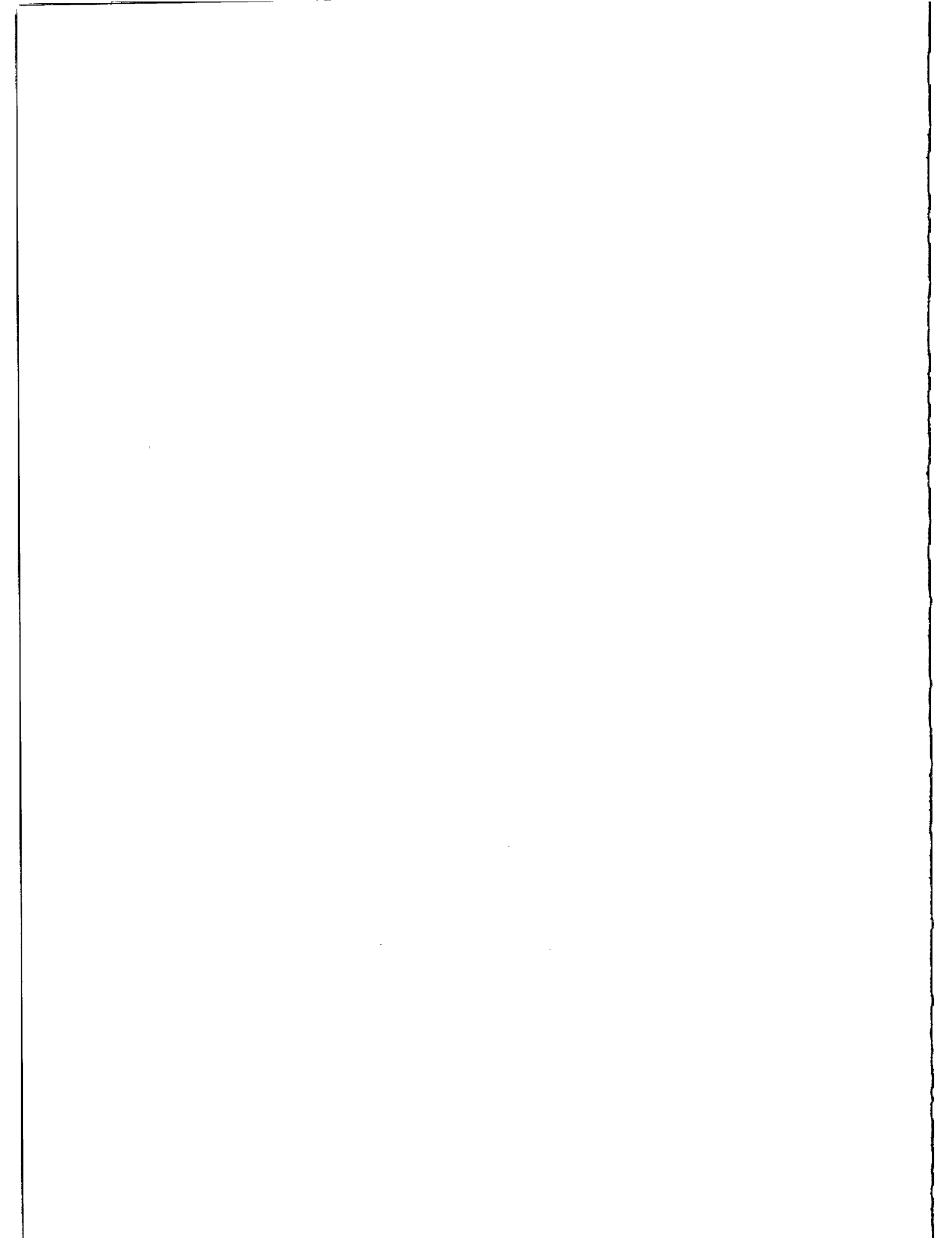
Fig.1 Geometry of Simultaneous Laser Ranging

Table 1
 Estimate of Co-observable Time of LAGEOS
 at Different Baselines

Lengths of Baselines	4450 KM	6000 KM
Co-observable Lengths of Arc with respect to Earth's Center (Elevation: 20° above)	40.8°	25.5°
Estimate Co-observable Time (Minutes, Elevation > 20°)	20-30 min.	10-16 min.

Table 2
 The Probability of at least 4 Stations Simultaneous Ranging
 in the Cases of Different Number of the Participating Stations

Assuming Percentage of Returns at Each Stations	Participating Station Numbers				
	4	5	6	7	8
0.2	.0016	.008	.026	.063	.132
0.3	.008	.04	.14	.34	.73
0.4	.026	.14	.45	1	1
0.5	.062	.34	1	1	1
0.6	.130	.73	1	1	1



STREAK CAMERA BASED LASER RADAR RECEIVER
ITS PERFORMANCE AND LIMITATIONS

I. Prochazka, K. Hamal
Czech Technical University
Faculty of Nuclear Science and Physical Eng.
Brehova 7, 115 19 Prague - Czechoslovakia -

Telephone 848840
TWX 121254 FJFI C

ABSTRACT

The expected streak camera based satellite laser radar receiver performance is discussed. The effects of receiver diameter/field of view, the spatial/temporal relation are described. The noise sources in the receiver were analysed. The low signal - down to a single photoelectron - temporal properties of the C979 Hamamatsu camera and the trigger delay variations were tested.

The streak is one of the candidates for the detector of the laser ranging system with subcentimeter accuracy. To get the subcentimeter ranging accuracy, the two color ranging technique is unavoidable to model the atmosphere on the basis of two colour differential time delay. To achieve the 1mm absolute ranging accuracy, this time delay must be measured with the accuracy about 0.7psec /1/. The streak camera commercially available (August 1986) have the 2 picoseconds temporal resolution. Several two colour ground target ranging experiments using streak cameras have been described /2,3,4,.../. Although, these experiment gave promising results, the application of the streak camera for the satellite laser ranging system introduces some new problems : see WG2. Streak camera simplified scheme is on WG3 together with the signal level calculation /5/.

Receiver field of view limit

For camera top performance , the light spot size on the photocathode must not be wider than 30 μ m. This fact restricts substantially the field of view achievable. Assuming the maximal ratio $f/D > 1$ of the receiver optics, the fields of view for different receiver diameters are tabulated on WG4.

Temporal/angular relation

The streak tube is sensitive to a position within the photocathode, where the photons are absorbed. Assuming the streak speed, the tube magnification and the streak velocity at the screen, the streak velocity at the photocathode was calculated (see WG5) for N895 and N1357 tubes. On the same picture there is a table of temporal/angular sensitivity of the streak camera based receivers with different input optics diameter. For example, let us suppose the receiver system of 1 meter diameter equipped with the "10psec" streak tube N895. If the direction of the signal detected is deviated at 2 arcsec from the expected direction , the induced timing bias will approach 2.4 picosecond.

Noise sources and low signal response

The main noise sources are listed on WG6, the possibilities of noise reduction are included. As only a very small area of the photocathode is involved , its noise contribution is negligible compared to other sources. The SIT TV camera noise contribution may be reduced by cooling, its signal to noise ratio may be increased by the persistence integration over the consequent 6-15TV frames. The A/D conversion noise contribution may be reduced by cooling, as well, by proper shielding from RF interference and by proper signal processing.

The streak camera C979 low signal performance was tested at the following set up : see fig.2 on WG7. The 12psec pulse from frequency doubled Nd YAP was reflected by the $R=4\%/85\%$ etalon 130psec and detected by the streak camera. Thus a pair of 12psec pulses spaced at 130 psec arrived at the photocathode, the second pulse 21 times stronger. The strong pulse response was used as a reference, the low pulse response was investigated. The data were transferred from the streak to the HP1000 computer for storing and

off-line processing. A new, in house built preprocessor/interface board for the Hamamatsu Temporal Analyser C1098, which permits both direction communication, recording rate up to 5 Hz, 1-15 persistence integration has been used. The original Hamamatsu algorithm for the persistence integration/calibration was found to introduce highly correlated noise on the single PE level, that is why a new algorithm was developed and applied /6/. To reduce the dark noise, the whole streak camera system was cooled down to +5 deg Centigrade. The record of the doubled pulse is on fig. 3 (strong signal response). To ephase the first pulse, the streak is slightly saturated and the 1:21 ratio is affected. To measure the low signal response, the laser output was attenuated, for each signal strength the series of 500 records was recorded. Using the strong signal response as a reference, the data were overlapped. The actual signal strength was determined in two ways: measuring the laser output power and applying the calibrated ND filters and by signal strength table supplied by the manufacturer. The agreement of both values was within a factor of 3, the second method was giving more stable results and was used later.

The plot of 300 shots out of 500 overlap with a mean signal strength 3 PE and 0.7 PE per shot entering the MCP is on fig.4 and 5. The signal of 3 PE and 0.7 PE on the MCP input corresponds to about 100 and 20 photons on the photocathode input. Obviously, at the signal strength of 3PE and lower, the pulse response is spread, the "dual peak" pulse shape appears and is reproducible. The 24 pseconds contribution is unexplained.

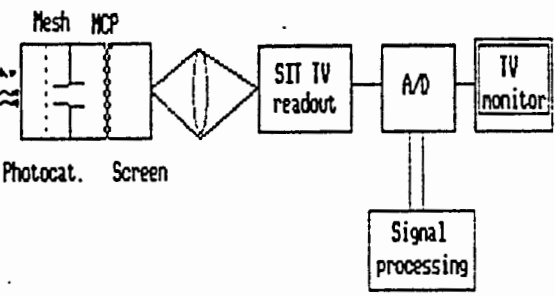
Trigger delay

The trigger delay is the time between the electrical pulse is applied and the streak sweep start. This time is about 10 nsec at the fastest sweep 0.5 nsec/screen. Due to the sweep electrical circuit construction, the delay is drifting in a range up to 1 nanosecond. On fig. 6 there is a plot of the trigger delay drift within 3 hours after ON. The temperature dependence of this effect was tested and found of order lower. No stabilisation of the effect was found within 5 hours after camera ON.

Literature

- 1/ J.J.Degnan, Satellite laser ranging, current status and future prospects, IEEE, Geoscience and remote sensing, Vol. GE-23, No.4
- 2/ J.B.Abshire, J.F.McGarry, H.E.Rowe, J.J.Degnan, Streak camera based laser ranging receiver development proceedings of the 5th IWLRI, Herstmonceux, England, 1984
- 3/ K.Hamal, I.Prochazka, J.Gaignebet, Two wavelength picosecond ranging of ground target, in /2/
- 4/ J.Gaignebet, J.L.Hatat, K.Hamal, I.Prochazka, H.Jelinkova, Two wavelength ranging on ground target using Nd YAG 2HG+Raman in this proceedings
- 5/ Picosecond Steak Camera and its Applications, Picoseconds Vol.14, June 1983, published by Hamamatsu Corp. Japan
- 6/ P.Valach, MS Thesses, FJFI CVUT, Prague, 1986

Goals of using streak camera as a LR receiver	Problem areas of streak camera SLR application															
<p>GOALS :</p> <ul style="list-style-type: none"> - subcentimeter ranging accuracy by picosecond laser ranging - atmospheric correction determination by means of two colour ranging and dispersion measurement. <p>Streak camera performance</p> <table border="1"> <thead> <tr> <th></th> <th colspan="2">tube</th> </tr> <tr> <th></th> <th>N895</th> <th>M1357</th> </tr> </thead> <tbody> <tr> <td>temporal resolution</td> <td>18psec</td> <td>2 psec</td> </tr> <tr> <td>dynamic range</td> <td>> 200</td> <td>> 100</td> </tr> <tr> <td>trigger jitter</td> <td>18psec</td> <td>5 psec</td> </tr> </tbody> </table>		tube			N895	M1357	temporal resolution	18psec	2 psec	dynamic range	> 200	> 100	trigger jitter	18psec	5 psec	<p>Problem areas :</p> <ul style="list-style-type: none"> - receiver aperture/field of view echo signal propagation direction - noise sources - low signal response - trigger delay variations
	tube															
	N895	M1357														
temporal resolution	18psec	2 psec														
dynamic range	> 200	> 100														
trigger jitter	18psec	5 psec														
K.Hanal, I.Prochazka Streak Camera Based LR Receiver Its Performance and ...	K.Hanal, I.Prochazka Streak Camera Based LR Receiver Its Performance and ...															

Streak camera signal/data flow	Receiver field of view limit																												
<p>Hananatsu streak camera scheme</p>  <p>Signal levels</p> <table border="1"> <tbody> <tr> <td>Photocathode</td> <td>(S - 20)</td> <td>IN</td> <td>30 Photons</td> </tr> <tr> <td></td> <td></td> <td>OUT</td> <td>3 PE</td> </tr> <tr> <td>Mesh</td> <td></td> <td>OUT</td> <td>1 PE</td> </tr> <tr> <td>Microchannel plate</td> <td></td> <td>IN</td> <td>1 PE</td> </tr> <tr> <td>A/D (settings G4, MCP4, P15)</td> <td></td> <td></td> <td>3.5 count</td> </tr> </tbody> </table>	Photocathode	(S - 20)	IN	30 Photons			OUT	3 PE	Mesh		OUT	1 PE	Microchannel plate		IN	1 PE	A/D (settings G4, MCP4, P15)			3.5 count	<p>Receiver field of view limit</p> <ul style="list-style-type: none"> - light spot size on photocathode 38 μmeters - assuming the receiver f/D > 1 <p>The maximum receiver field of view</p> <table border="1"> <thead> <tr> <th>receiver diameter</th> <th>field of view</th> </tr> </thead> <tbody> <tr> <td>2 meters</td> <td>3 arcsec</td> </tr> <tr> <td>1 meter</td> <td>6 arcsec</td> </tr> <tr> <td>0.5 meter</td> <td>12 arcsec</td> </tr> </tbody> </table>	receiver diameter	field of view	2 meters	3 arcsec	1 meter	6 arcsec	0.5 meter	12 arcsec
Photocathode	(S - 20)	IN	30 Photons																										
		OUT	3 PE																										
Mesh		OUT	1 PE																										
Microchannel plate		IN	1 PE																										
A/D (settings G4, MCP4, P15)			3.5 count																										
receiver diameter	field of view																												
2 meters	3 arcsec																												
1 meter	6 arcsec																												
0.5 meter	12 arcsec																												
I.Prochazka, K.Hanal Streak Camera Based LR Receiver Its Performance and ...	I.Prochazka, K.Hanal Streak Camera Based LR Receiver Its Performance and ...																												

Tab. 1

Temporal / angular relation		
Streak tube	N895	N1357
	18 ps	2 ps
streak velocity at the screen	67 ps/mm	25 ps/mm
tube magnification	3.5	1.3
streak velocity at the photocathode	235 ps/mm	33 ps/mm

receiver diameter	temporal/angular sensitivity psec/arcsec	
	N895	N1357
2 meters	2.35	0.32
1 meter	1.18	0.16
0.5 meter	0.59	0.08

Noise sources		
Noise source	contribution	reduction possibility
photocathode	low	cooling
MCP intensifier	high	gating, cooling
SIT TV camera	medium	persist. intg., cooling
A/D conversion	medium	persist. integration data processing

I. Prochazka, K. Hanal
Streak Camera Based LR Receiver Its Performance and .. 5

I. Prochazka, K. Hanal
Streak Camera Based LR Receiver Its Performance and .. 6

Streak at low signal, experiment set up

Fig. 2


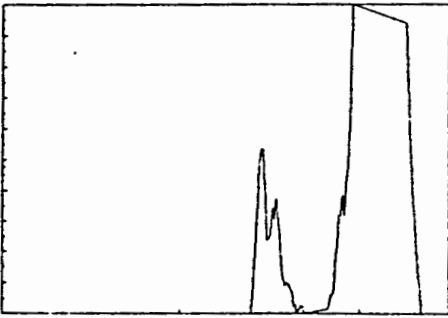
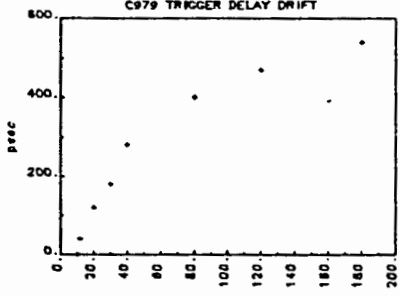
- cooling to +5° C
- no MCP gating available
- inhouse built preprocessor/interface
 - * recording/transfer rate up to 5 pps
 - * 1-15 persistence integrations
 - * new calibration/integration algorithm
- streak records overlap

Streak camera record

Fig. 3

I. Prochazka, K. Hanal
Streak Camera Based LR Receiver Its Performance and .. 7

I. Prochazka, K. Hanal
Streak Camera Based LR Receiver Its Performance and .. 8

<p style="text-align: center;">Streak low signal response, 300 records overlap</p> <p style="text-align: center;">3 PE entering MCP, approx. 100 Photons on photocathode</p>  <p style="text-align: right;">500psec/ screen</p> <p style="text-align: right;">Fig. 4</p> <p style="text-align: center;">0.7 PE entering MCP, approx. 20 Photons on photocathode</p>  <p style="text-align: right;">500psec/ screen</p> <p style="text-align: right;">Fig. 5</p>	<p style="text-align: center;">Low signal pulse spread</p> <table border="0" style="width: 100%;"> <tr> <td>driving pulse length</td> <td style="text-align: right;">12 psec</td> </tr> <tr> <td>streak strong signal response+overlap</td> <td style="text-align: right;">16 psec</td> </tr> <tr> <td>sweep nonlinearity contribution (unmodelled)</td> <td style="text-align: right;">11 psec</td> </tr> <tr> <td>streak low signal response</td> <td style="text-align: right;">31 psec</td> </tr> <tr> <td>unexplained $\sqrt{31^2 - 16^2 - 11^2}$</td> <td style="text-align: right;">24 psec</td> </tr> </table> <p style="text-align: right;">Table 3</p> <p>* dual peak pulse shape for signal strength < 3PE is reproducible</p>	driving pulse length	12 psec	streak strong signal response+overlap	16 psec	sweep nonlinearity contribution (unmodelled)	11 psec	streak low signal response	31 psec	unexplained $\sqrt{31^2 - 16^2 - 11^2}$	24 psec
driving pulse length	12 psec										
streak strong signal response+overlap	16 psec										
sweep nonlinearity contribution (unmodelled)	11 psec										
streak low signal response	31 psec										
unexplained $\sqrt{31^2 - 16^2 - 11^2}$	24 psec										
<p>I.Prochazka, K.Hanal Streak Camera Based LR Receiver Its Performance and ..</p>	<p>K.Hanal, I.Prochazka Streak Camera Based LR Receiver Its Performance and ..</p>										
<p style="text-align: center;">Trigger delay variations</p>  <p style="text-align: right;">Fig. 6</p> <ul style="list-style-type: none"> - the saturation was not found within 3 hours, - the temperature changes +5 C to +35 C have low impact on the trend - the effect complicates the streak camera application in the automated laser radar system 	<p style="text-align: center;">Conclusion</p> <ol style="list-style-type: none"> 1. The temporal resolution of 10/2 (0.4)psec and dynan. ratio 200/100 are attractive for two color laser ranging applications. 2. The "FOV" limitation and the angular/temporal sensitivity are serious problems affecting the system design and its limitations. 3. The use of streak camera at extremely low light levels has been demonstrated for conventional 10psec tube. (Using the new Hamamatsu ps tube+2MCP, the 1PE detection should be possible as a standard technique) 4. The trigger delay time/temperature variations complicate the automation of TV time delay measurements and makes the application of streak camera as a vernier to a ranging counter very difficult 										
<p>K.Hanal, I.Prochazka Streak Camera Based LR Receiver Its Performance and ..</p>	<p>K.Hanal, I.Prochazka Streak Camera Based LR Receiver Its Performance and ..</p>										

TWO WAVELENGTH RANGING ON GROUND TARGET
USING ND:YAG 2HG + RAMAN.0.68 μ M PULSES

J. Gaignebet, F. Baumont, J.L. Hatat
C.E.R.G.A.
Avenue Nicolas Copernic
06130 - Grasse - France -

Telephone 93 36 58 49
Telex 470865 F

K. Hamal, H. Jelinkova, I. Prochazka
Czech Technical University
Faculty of Nuclear Science and Physical Eng.
Brehova 7, 115 19 Prague - Czechoslovakia -

Telephone (1) 848840
Telex 121254FJFI C

ABSTRACT

A two color ranging experiment is described here. The system is designed with the following goals.

- Ground to Ground measurements with a precision at 10^{-7} for distances ranging from 50 km to 300 km
- Ground to satellite ranging with an accuracy of 5 mm (shot to shot basis)
- Possibility to develop a space borne system around the ideas tested on the ground.

0.68 μ m, the upper one to the stimulating 2HG (0.53 μ m). The streak sweep is 4psec/pixel in the dual window mode.

Signal processing results

A mirror mounted upside down led to a temporal/spatial structure with double pulse. This degradation was emplied by the Raman Cell (threshold and staturation effect) and gave us serious difficulties on the processing and application of correlation algorithms.

Thus we think that the results are not very significant and that the experiment must be reimplemented to give true figures.

Literature

- 1/ Picosecond Streak Camera and its applications, Picoseconds, Voll4, June 1983, published by Hamamatsu Corp. Japan
- 2/ P.Valach, Diploma Work, FJFI CVUT, Prague, 1986
- 3/ I.Procházka Start detector for the mode locked train laser radar in this proceedings
- 4/ Y.Tarasov, Laser physics Moscow, 1983
- 5/ I.Procházka, K.Hamal, Streak camera as a LR reseceiver, its performance and limitations in this proceedings
- 6/ K.Hamal, H.Jelinkova, Stable saturable dye for 1.06 μ m in this proceedings

Laser transmitter for 1.06/0.68/0.53 μm

The optical scheme is on fig 1. The oscillator is formed by 100%/5m/concave mirror in the contact with 2mm flowing dye cell and a wedged plate (M1). The design of the cell ensures optimum laminar dye flow. The cell is filled with the saturable dye ML51/6/. The YAG rod 3x50mm 2deg/2deg is Quantel pumping head (OSC). The iris diameter 1.6mm ensures the single mode operation. The front mirror (M2) is a quartz plate 0.025mm thick. Quartz plates (P1,P2) are at the Brewster angle to optimize the polarisation of the output beam for the pulse slicer (SL). The telescope (T) 1:2 matches the beam for the double pass amplifier (G/AMPL/O/M6). The NdYAG rod 7x114 is in Quantel head. The output beam passes the second harmonic generator (SHG), the +1meter focusing lens (L) and enters the Raman hydrogen cell (RAM).

Assuming the purpose - two wavelength ranging in the field conditions - the attention has been focused to the shortest pulse available from the compact set up. The output pulse length from the oscillator/ampl./2HG was 14psec. The pumping energy was varied from the threshold up to 2.3 times above it. No change in the output pulse duration has been observed. The output pulse length at 0.68 μm from the Raman cell was measured 14psec (fig.2), assuming the camera resolution 10psec, the deconvoluted value is 10psec. The Raman cell output was acceptably stable. The 0.68 μm output is collinear with the 0.53 μm input/output and therefore no angle compensation is required.

Two wavelength ranging experimental set up

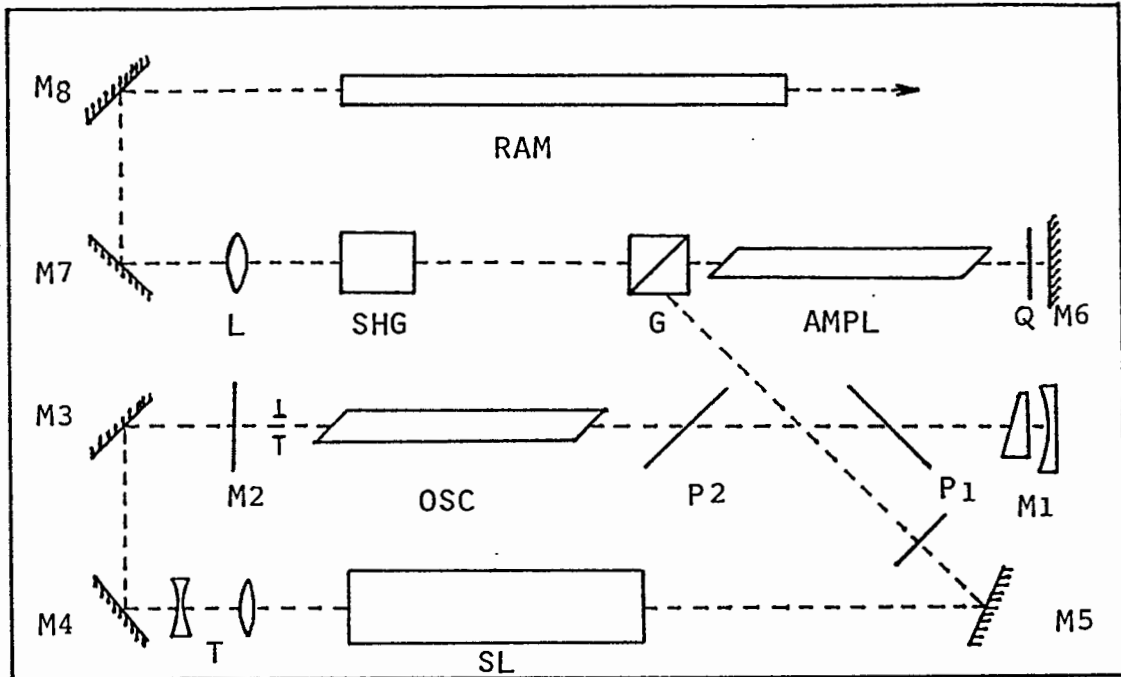
The block scheme of a two wavelength picosecond ranging experiment is on fig 3. The laser output is directed to a corner cube placed at the distance 2m or 110meters for an calibration (indoor) and outdoor passes respectively. A small fraction of the transmitted pulse is picked up and fed to the semiconductor switch /2/ to start the ranging counter and /after an appropriate delay/ the streak camera. The reflected light pulse is passing an optical delay of 20 nsec, ND filters and a dispersion prism. The additional cylindrical lens optics and a streak slit are projecting the input light on two spots on the streak tube photocathode. The Hamamatsu C979 /1/ Temporal disperser system was used. The streak image is monitored by the SIT TV camera and digitized in the Temporal analyser Hamamatsu C1098. Using an in house built preprocessor/interface board in the Temporal analyzer /3/ the digitised data are on line transferred to a computer system HP1000 for display, storing and off line processing. The recording speed exceeds 5 frames/second. The readout system permits to process two windows of one streak image simultaneously. This way, both pulses at different wavelength are recorded at the same time and the trigger jitter contribution to the time delay measurement is suppressed.

The "sweep monitor" camera output signal stops the ranging counter, thus the camera trigger jitter is not involved in the resulting error budget.

Streak camera ranging data

The typical streak record of the TW ranging at 0.53/0.68 μm is on fig.4 . The lower trace corresponds to the Raman down shift

Laser scheme



M1-M8	... mirrors
L	... positive lens $f = 1m$
RAM	... Raman cell
SHG	... second harmonic generator
G	... Glan Thompson polariser
AMPL	... double pass amplifier rod
Q	... quarter wave plate
I	... diaphragm
OSC	... oscillator rod
P1, P2	... quartz Brewster angles plates
T	... beam expanding telescope
SL	... slicer

Fig. 1

Raman cell output temporal/spatial structure

Simultaneous 0.68/0.53um record, indoor pass

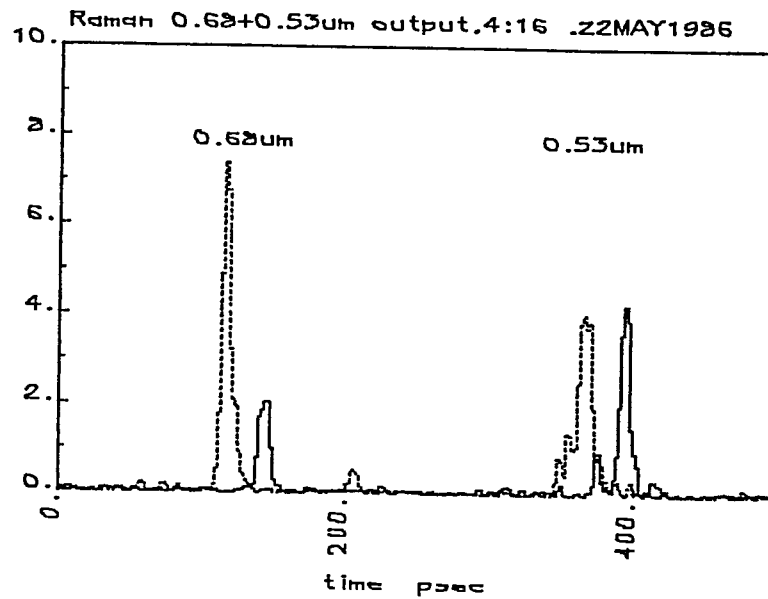
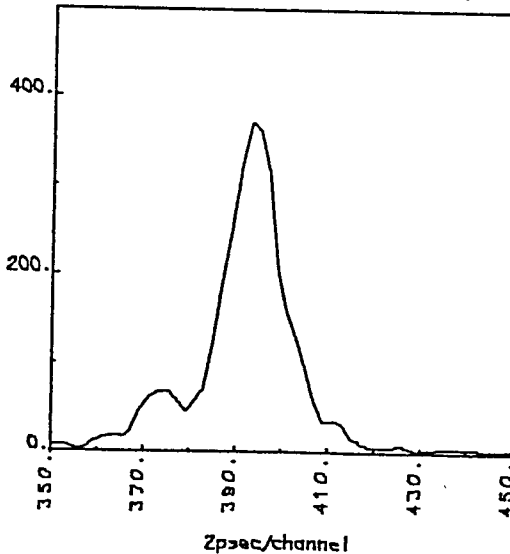


Fig. 6

2HG signal overlap

indoor

Raman TW ranging, indoor, 0.53um overlap



outdoor

Raman TW ranging, 0.53um outdoor overlap

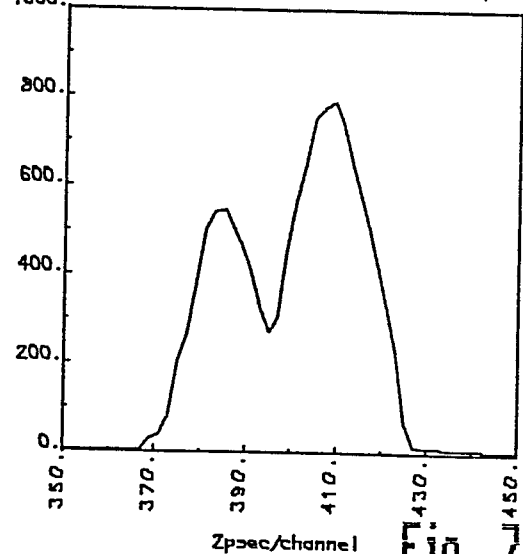
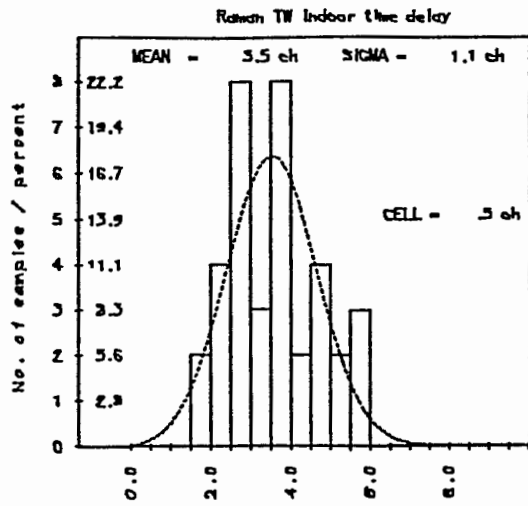


Fig. 7, 8

J. Gaignebet, J. L. Hatat, K. Hamal, I. Prochazka, H. Jelinekova
Two Wavelength Ranging on Ground Target Using Raman...

Two wavelength ranging results

indoor



outdoor

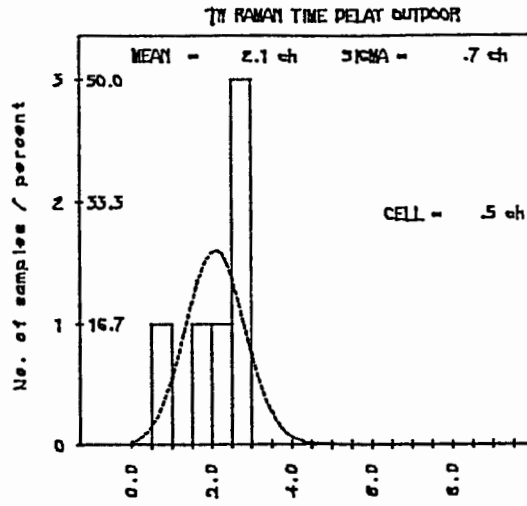


Fig. 9,10

streak speed

4 psec/ channel

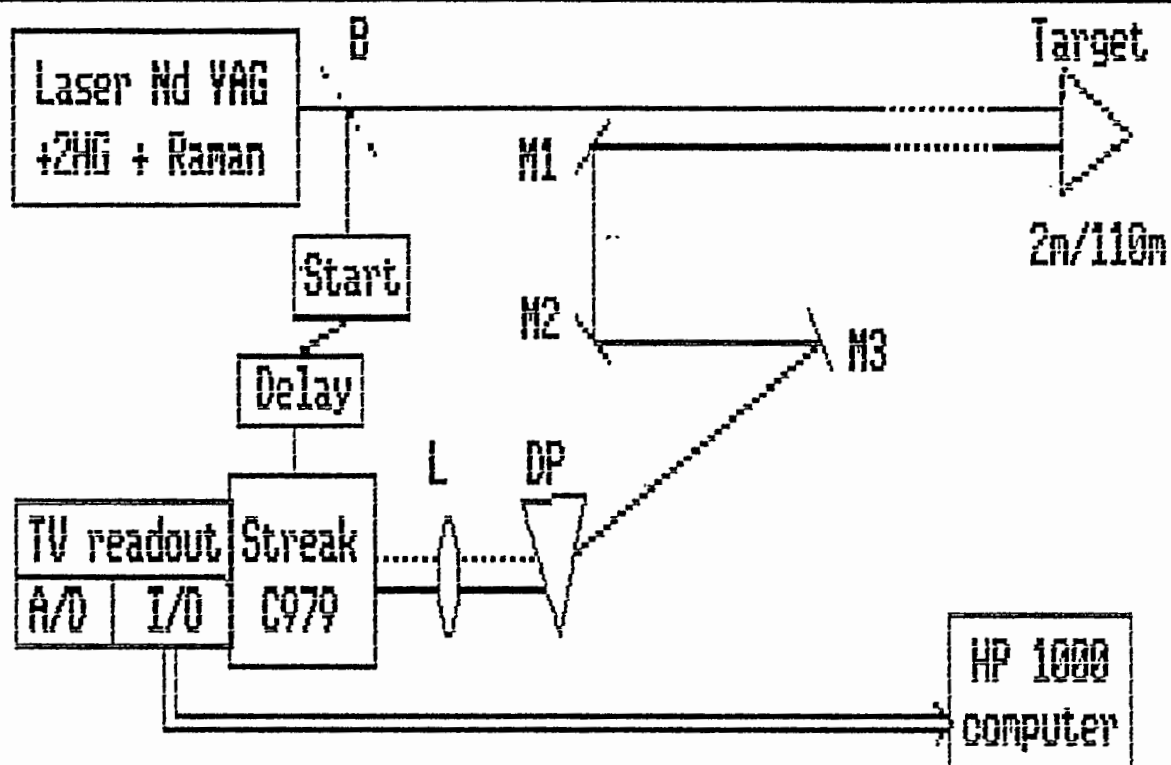
indoor-outdoor

1.4 channel

Time delay : theory 4.3 psec

measured 5.6 psec rms 5.2psec

Two wavelength ranging block scheme



B ... beam splitter

Start ... triggering semiconductor switch

M1, M2, M3. mirrors forming the optical delay 20 nsec

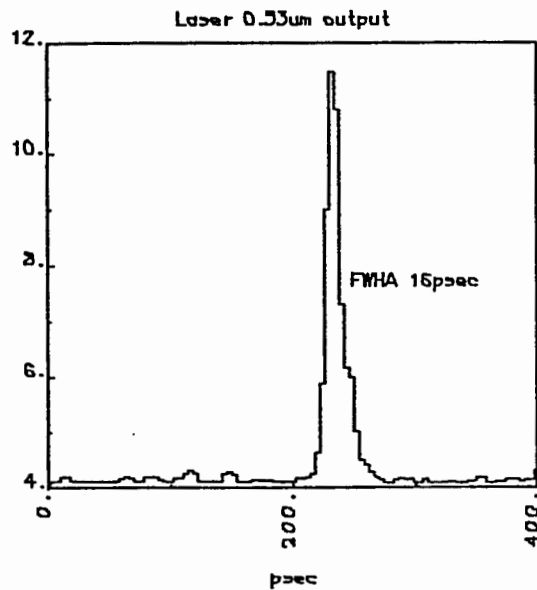
A/D ... part of Hamamatsu Temporal Analyser

I/O ... inhouse built preprocessor/interface

L ... focusing lens

DP ... dispersion prism

Laser output pulses

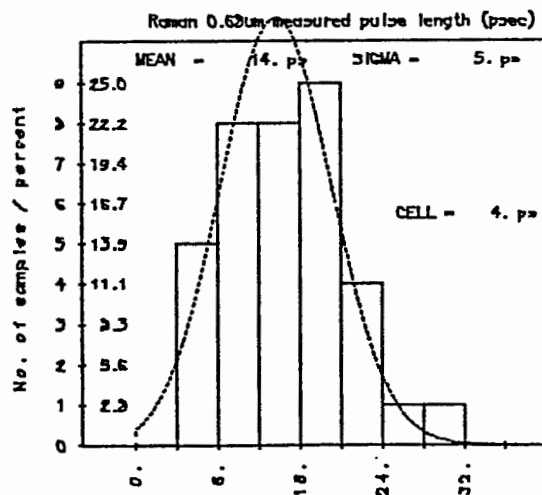


0.53 μm 2HG Nd YAG

FWHA mean : 17 psec

deconvoluted : 14 psec

Fig. 2



0.68 μm Raman

FWHA mean : 14 psec

deconvoluted: 10 psec

Fig. 3

Two wavelength ranging streak records

Indoor pass

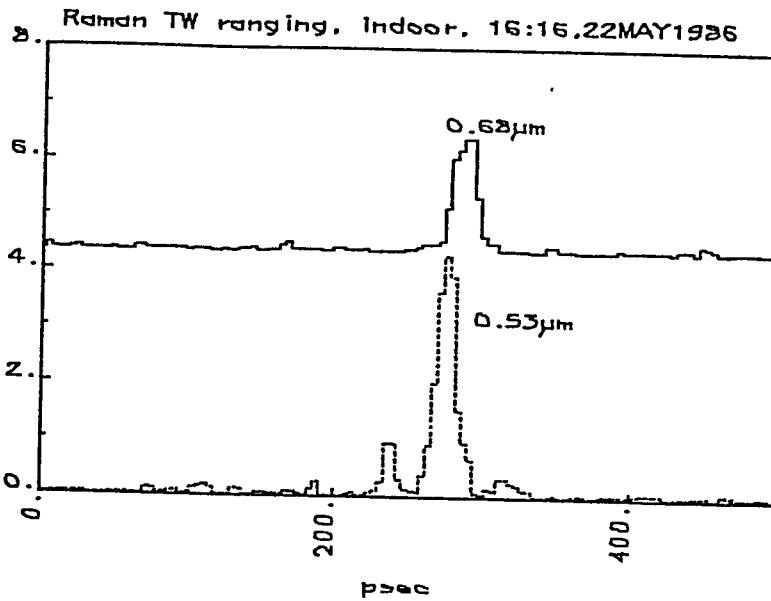
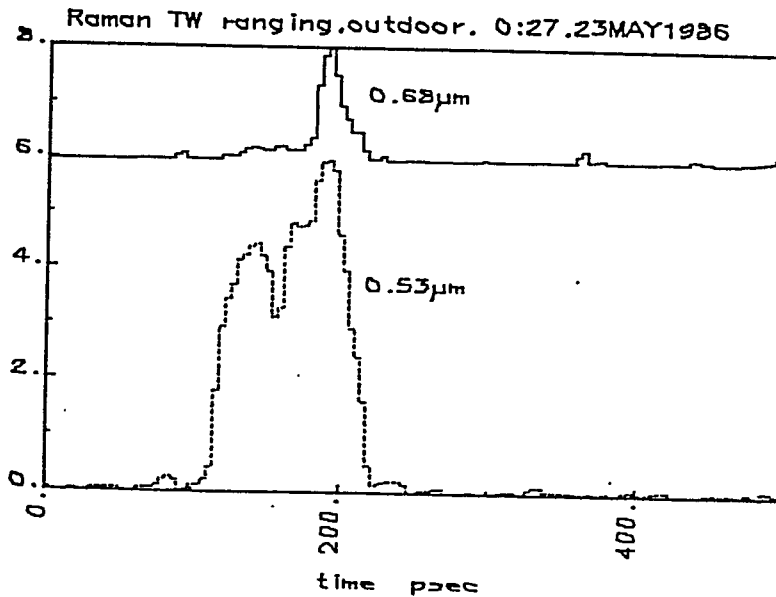
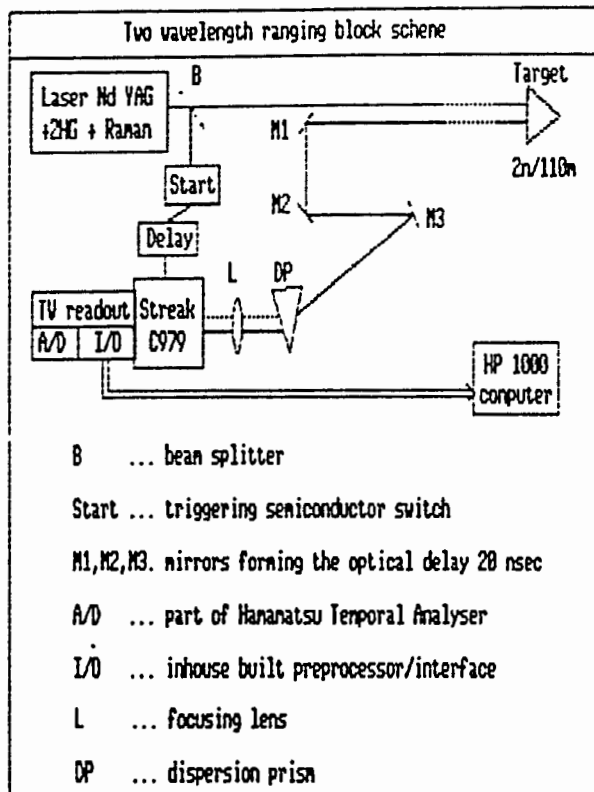


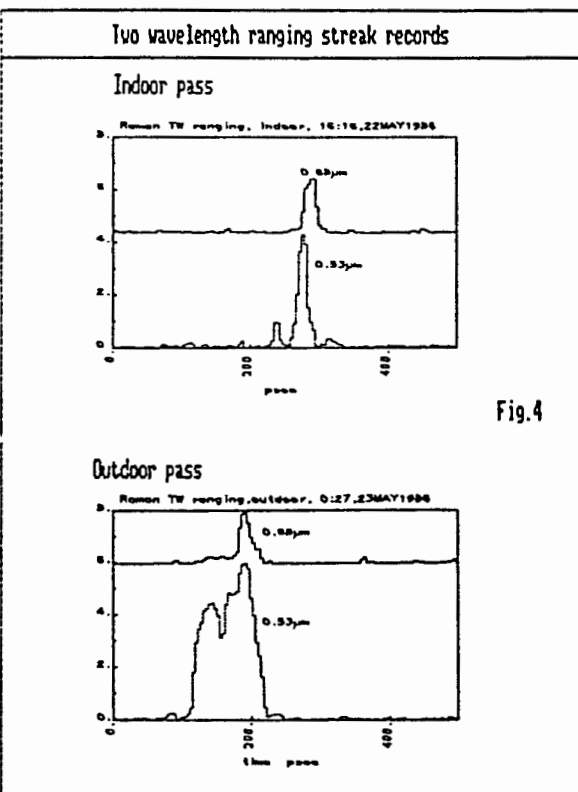
Fig.4

Outdoor pass

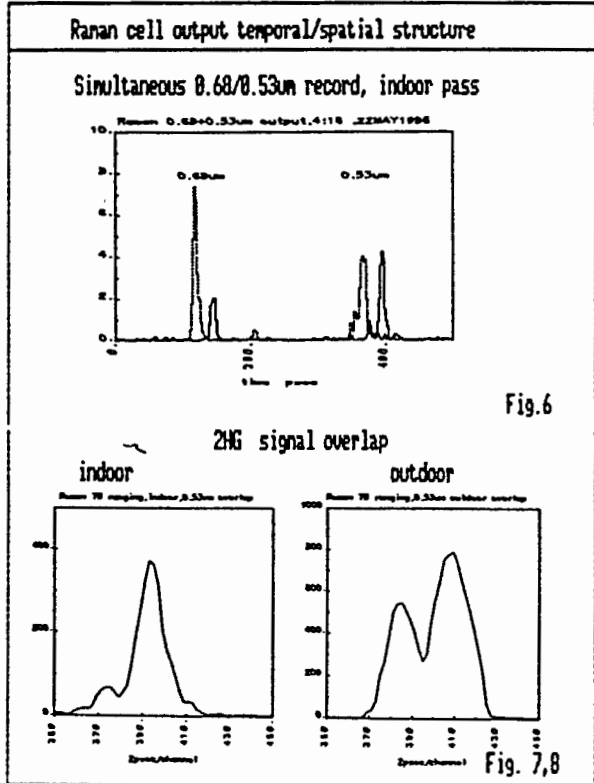




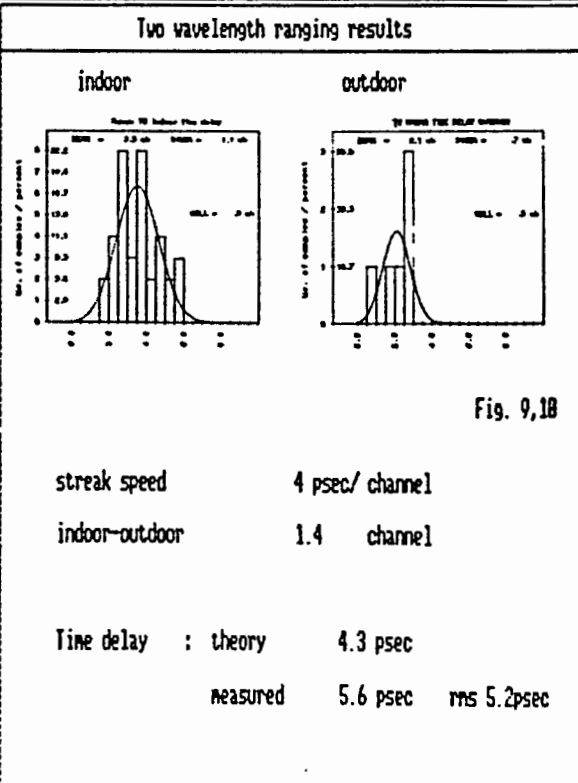
J. Gaignebet, J. L. Hatat, K. Hanal, I. Prochazka, H. Jelinkova
 Two Wavelength Ranging on Ground Target Using Raman... 4



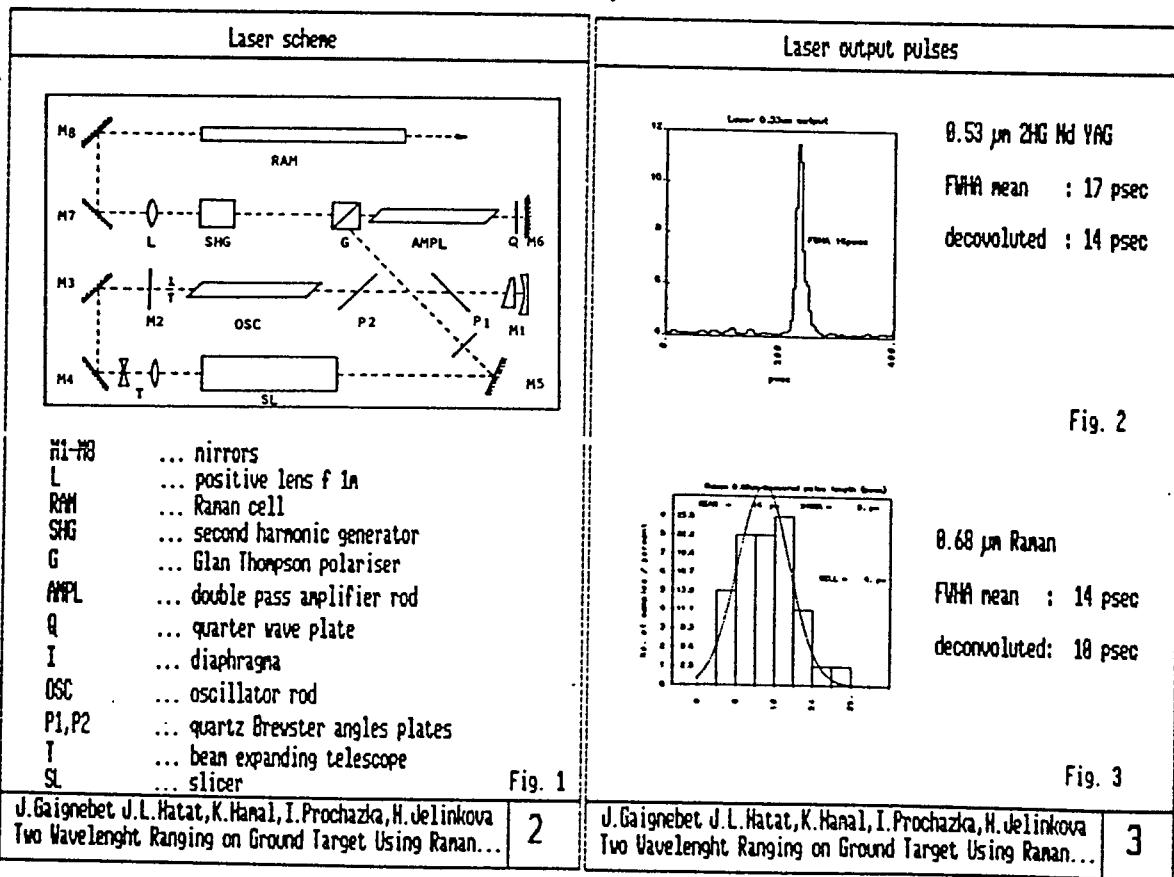
J. Gaignebet, J. L. Hatat, K. Hanal, I. Prochazka, H. Jelinkova
 Two Wavelength Ranging on Ground Target Using Raman... 5

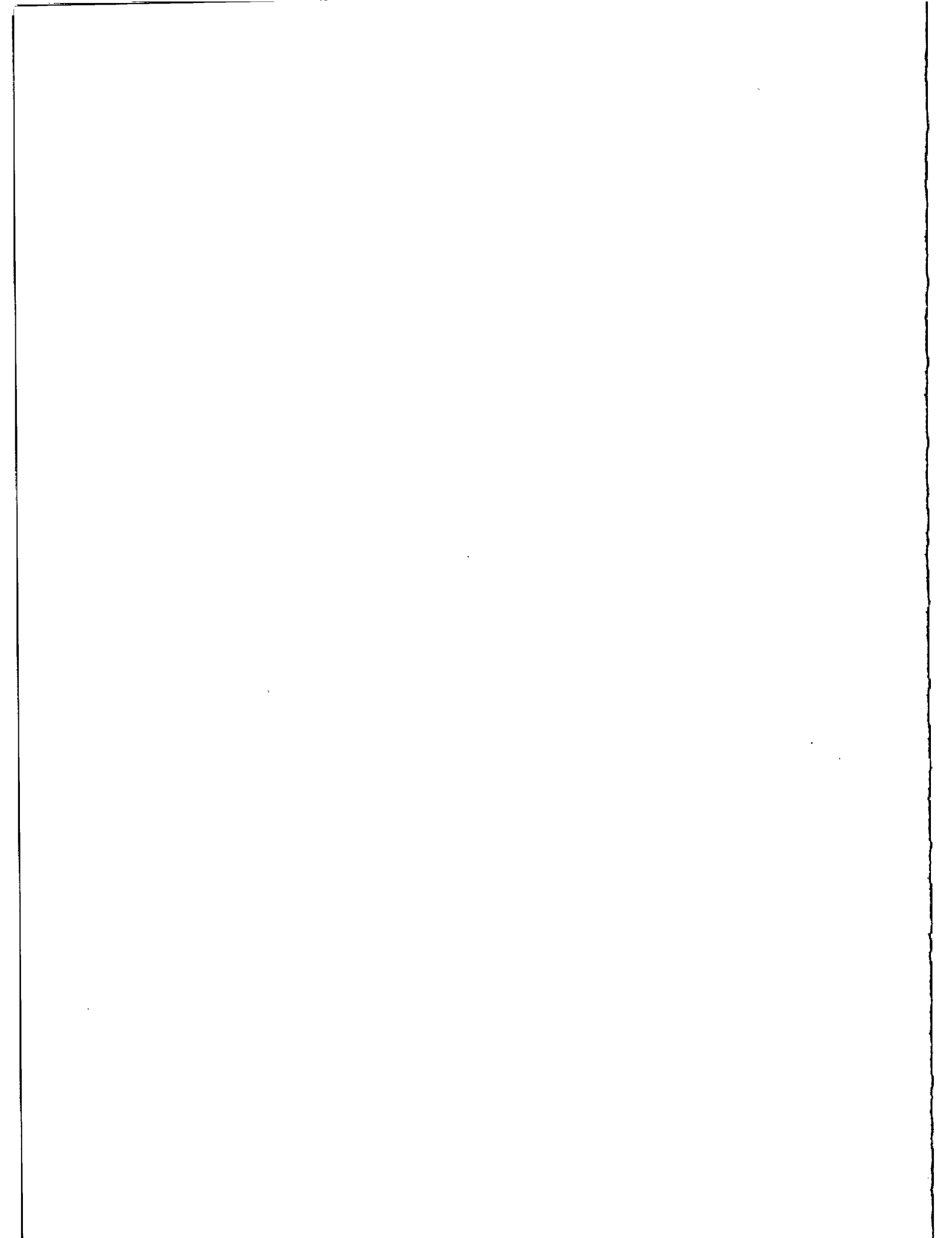


J. Gaignebet, J. L. Hatat, K. Hanal, I. Prochazka, H. Jelinkova
 Two Wavelength Ranging on Ground Target Using Raman... 6



J. Gaignebet, J. L. Hatat, K. Hanal, I. Prochazka, H. Jelinkova
 Two Wavelength Ranging on Ground Target Using Raman... 7





PICOSECOND LASER RANGING USING PHOTODIODE

I. Prochazka, K. Hamal
Czech Technical University
Faculty of Nuclear Science and Physical Eng.
Brehova 7, 115 19 Prague - Czechoslovakia -

Telephone 848840
TWX 121254 FJFI C

ABSTRACT

The two wavelength (1.06 μm and 0.53 μm) laser ranging experiments using photodiode is described. The ultimate jitter limits for different type of photodiodes was measured at the signal strength $1.E4$ to $1.E5$ photons. The jitter limit of 10 psec for TW time delay measurements was found for the in house built HP S5 diode biased 0.1V below break. The minimal signal strength 10,000 photons at 0.53 μm was detected. The jitter of 15 psec rms for two wavelength time delay measurement was achieved.

INTERKOSMOS SATELLITE LASER RADAR NETWORK

PICOSECOND LASER RANGING USING PHOTODIODE

I. Prochazka, K. Hanal

Czech Technical University
Faculty of Nuclear Science and Physical Engineering
Brehova 7, 115 19 Prague, Czechoslovakia

I. Prochazka, K. Hanal
Picosecond Laser Ranging Using Photodiode

0

Goals of picosecond laser ranging using photodiode

GOALS :

- subcentimeter laser ranging
- two colour ranging using single photodiode at high signal strength levels
- measurements :
 - * ultimate jitter limit for photodiode based laser radar receiver
 - * ultimate signal strength for 1.06um and 0.53um ranging

I. Prochazka, K. Hanal
Picosecond Laser Ranging Using Photodiode

1

INTERKOSMOS SATELLITE LASER RADAR NETWORK

Experimental set up

Fig. 1

Example of Transient record

Fig. 2

I. Prochazka, K. Hanal
Picosecond Laser Ranging Using Photodiode

2

Tranzient data processing

Tranzient data processing

Smoothering, sweep nonlinearity compensation

Pulse position determination:

- Mean of pulse half amplitude leading/trailing edge
- * minimal amplitude 1 div (10mV)
- * jitter 13 - 8 psec 1 - 8 div ampl.
- * time walk (20 psec
- * simple and fast

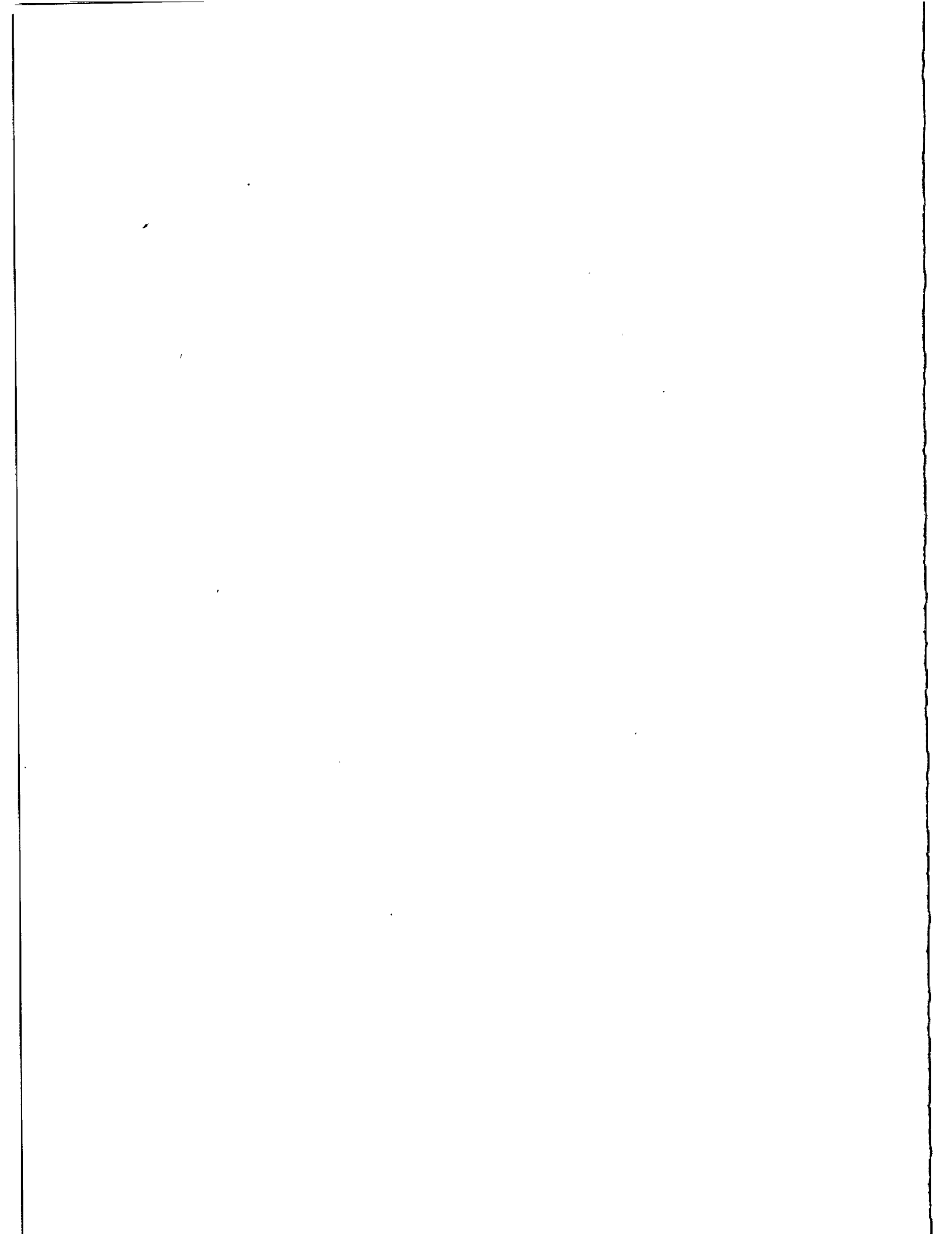
Pulses separation determination:

Correlation algorithm

- * min. amplitude 0.2 div
- * jitter 18 - 6 psec 0.2 - 8 div
- * time walk 100 psec 0.2 - 8 div
- software compensation is required
- * time consuming

I. Prochazka, K. Hanal
Picosecond Laser Ranging Using Photodiode

3



MULTIPLE WAVELENGTH LASER RANGING

B.A. Greene
Division of National Mapping
P.O. Box 31
Belconnen ACT 2616 - Australia -

Telephone (6162) 525095
Telex AA62230

T.A. Herring
Harvard/Smithsonian Center for Astrophysics
60 Garden Street
Cambridge MA 02138 - USA -

Telephone (617) 4959279
Telex 921418

ABSTRACT

The establishment of sub-centimeter accuracy satellite-laser ranging (SLR) systems may require such systems to operate at more than one wavelength in order to ensure that range corrections made to compensate atmospheric dispersion are themselves accurate. Analytic expressions to be applied to the observed dual (or multiple) color ranges are derived with particular emphasis on their application in an operational environment. Full consideration is given to the design needs for sub-centimeter accuracy systems, resulting in system design parameters for operational multiple wavelength SLR stations. Progress on the design and construction of such a system is reported.

1. INTRODUCTION

The refractive index of the earth's atmosphere depends on the wavelength of the signal transmitted through it. At optical wavelengths, this dispersion of the atmosphere should be sufficiently large that two ranges to a body measured with different wavelengths could be used to estimate the contribution of atmospheric refraction to each of the ranges. Since the signals at each of the wavelengths will be affected differently by the atmosphere, the difference in the ranges should be related to the total contribution of the atmospheric refraction at each of the wavelengths. The applications of the such techniques to satellite-laser ranging (SLR) have been discussed by Bender and Owens, 1965; Owens, 1967; Abshire and Gardner, 1985.

In this paper we examine the dual-color correction in detail. In particular we consider the effects of the approximations made in deriving the standard refractive index formulas, the contribution of water vapor, and the effects of ray bending. We also examine the equipment needed for the dual-color correction to make a significant improvement in the accuracy of satellite laser ranging.

2. THEORY OF THE DUAL-COLOR CORRECTION

The oneway range to a satellite measured with a signal which is affected by the earth's atmosphere is approximately given by (here we neglect the effects of the motion of the satellite relative to the transmitting station)

$$R_o = \int_{atm} n_g(s) ds \quad (1)$$

where \int_{atm} is the integration along the path followed by the signal, and $n_g(s)$ is the group refractive index at each point s along the path. Ideally, we would like to estimate the contribution of the atmospheric refraction to the integral given in equation (1) so that we could estimate the geometric part of the range, R_g , given by

$$R_g = \int_{vac} ds \quad (2)$$

where \int_{vac} is the integration along the straight line path between the transmitter and the satellite. We will define the contribution of atmospheric refraction, R_a , to the observed range to be $R_o - R_g$. R_a will be wavelength dependent (see e.g., Owens, 1967) because of the wavelength dependence of both n_g and the integration path in equation (1). If we can write equation (1) in the form

$$R_{oj} = R_g + F(\lambda_j)G_a(P, T, e, \dots) \quad (3)$$

where the subscript j denotes a specific wavelength, F is a function only of wavelength λ_j , and G_a is only a function of atmospheric parameters such as pressure, P ; temperature, T ; and water vapor partial pressure, e ; then we could obtain estimates

of R_g from measurements of R_o at two wavelengths. Measurements R_{o1} and R_{o2} made at wavelengths λ_1 and λ_2 can be combined using

$$\hat{R}_g = \frac{F(\lambda_2)R_{o1}}{F(\lambda_2) - F(\lambda_1)} - \frac{F(\lambda_1)R_{o2}}{F(\lambda_2) - F(\lambda_1)} \quad (4)$$

to obtain an estimate of the geometric range. \hat{R}_g will differ from R_g due to measurement errors in R_{o1} and R_{o2} , and due to equation (3) not fully representing the effects of the atmospheric contribution to the observed range.

To assess the likely improvement of using equation (4) instead of relying on other means to calibrate R_a , we will examine the effects of the approximations made in manipulating equations (1) and (2) into the form of equation (3), and the effects of noise in the measurements R_{o1} and R_{o2} on \hat{R}_g . We commence our discussion by examining the group refractivity of a mixture of gases (such as those in the earth's atmosphere). The group refractivity is derived from the phase refractivity, n_p , which for non-polar gases, is given approximately by the Lorenz-Lorentz equation (Bottcher, 1952)

$$\frac{n_p^2 - 1}{n_p^2 + 2} = \sum_i \mathcal{R}_i(\lambda)\rho_i \quad (5)$$

in which \mathcal{R}_i is the specific refraction and ρ_i is the partial density of the i th component of the mixture. The specific refraction is derived from a measurement of $\frac{n_p^2 - 1}{n_p^2 + 2}$ for a single constituent of the mixture at a specific value of ρ_i and λ . From equation (5) we see that the determination of n_p reduces to determining the function $\mathcal{R}_i(\lambda)$ and the determination of ρ_i for any atmospheric conditions. For our study we take the formulas of Owens (1967) for $\mathcal{R}_i(\lambda)$ and ρ_i for dry, CO₂ free air; water vapor; and CO₂. These formulas and their ranges of validity are summarized in Table 1.

To derive an equation of the form of equation (3) we need to make some assumptions (which we will evaluate the effects of later in this paper). The first approximation we need to make will allow us to convert equation (5) from its non-linear form to a linear one. If we expand the left hand side of equation (5), assuming n_p is close to 1, then the equation reduces to

$$2(n_p - 1)/3 - (n_p - 1)^2/9 = \sum_i \mathcal{R}_i(\lambda)\rho_i. \quad (6)$$

If the second order term is neglected, then we may express the phase refractivity of each constituent, n_{pi} , in the mixture as a function only of the $\mathcal{R}_i(\lambda)$ and ρ_i for that constituent *i.e.*,

$$2(n_{pi} - 1)/3 = \mathcal{R}_i(\lambda)\rho_i. \quad (7)$$

Owens (1967) derived a simplified set of refractivity formulas based on the expansion given in equation (7). In this linearized form, refractivity formulas can be given for each constituent of the atmospheric mixture separately. However, since the mixing ratios of many of these constituents remain constant through out the atmosphere, many of them can be grouped together.

Table 1. Equations for atmospheric refractive index (compiled from Owens, 1967)

Dry air, CO₂ free air

$$((\mathcal{R}_o)_1 - 1) \times 10^8 = 8340.78 + \frac{2405640.}{(130 - \sigma^2)} + \frac{15994.}{(38.9 - \sigma^2)}$$

$$\rho_1 = 348.328 \frac{P_1}{T} \left[1 + P_s (57.90 \times 10^{-8} - \frac{9.3250 \times 10^{-4}}{T} + \frac{0.25844}{T^2}) \right]$$

$$(\rho_o)_1 = \rho_1 (P = 1013.25 \text{ mb}, T = 288.16 \text{ K})$$

Range of validity: 2303–20,586 Å; 240 K < T < 330 K; 0 < P < 4 atm.

Water vapor

$$((\mathcal{R}_o)_2 - 1) \times 10^8 = 295.235 + 2.6422\sigma^2 - 0.03138\sigma^4 + 0.004028\sigma^6$$

$$\rho_2 = 216.582 \frac{e}{T} \left[1 + e \left[1 + 3.7 \times 10^{-4} \left[-2.37321 \times 10^{-3} + \frac{2.23366}{T} - \frac{710.792}{T^2} + \frac{7.75141 \times 10^4}{T^3} \right] \right] \right]$$

$$(\rho_o)_2 = \rho_2 (P = 13.33 \text{ mb}, T = 293.16)$$

Range of validity: 3611–6440 Å; 250 K < T < 320 K; 0 < P < 100 mb.

Carbon dioxide

$$((\mathcal{R}_o)_3 - 1) \times 10^8 = 22822.1 + 117.8\sigma^2 + \frac{2406030.}{(130 - \sigma^2)} + \frac{15997.}{(38.9 - \sigma^2)}$$

$$\rho_3 = 829.37 \frac{P_3}{T}$$

$$(\rho_o)_3 = \rho_3 (P = 1013.25 \text{ mb}, T = 288.16 \text{ K})$$

Range of validity: 2379–6010 Å; 240 K < T < 330 K; 0 < P < 17 mb.

P_1 is partial pressure of dry air (mbar),
 e is partial pressure of water vapor (mbar),
 P_3 is partial pressure of CO₂ (mbar),
 T is temperature (K),
 σ is $\frac{1}{\lambda}$ (μm^{-1}).

In Table 2 we give Owens formulas for the group and phase refractivities for dry air with 0.03 % CO₂ (standard air), and for water vapor. The form of the refractivities is

$$n_{gi}(\lambda) = f(\lambda)D_i \quad (8)$$

where $f(\lambda)$ depends only on λ , and D is independent of λ . Substituting equation (8) into the definition of R_a , we obtain

$$R_a(\lambda) = \int_{atm} (1 + \sum_i f_i(\lambda)D_i) ds - \int_{vac} ds. \quad (9)$$

If we assume that $\int_{atm} = \int_{vac}$ then equation (9) reduces to

$$R_a(\lambda) = \sum_i f_i(\lambda) \int_{vac} D_i ds \quad (10)$$

where we show the integration path to be through vacuum to emphasize that we have assumed that the integration along the atmospheric path and the vacuum path are the same in order to obtain equation (10).

For the Owen's simplified formulas i takes on two values, one for standard air and one for water vapor. We may now write an equation for R_{oj} almost in the form of equation (3), *vis.*

$$R_{oj} = R_g + f_d(\lambda_j) \int_{vac} D_d ds + f_w(\lambda_j) \int_{vac} D_w ds \quad (11)$$

where we show explicitly the terms for standard air with a subscript d and those for water vapor with a subscript w . If the water vapor terms are neglected in equation (11) then $f_d(\lambda_j)$ corresponds to $F_d(\lambda_j)$ in equation (3), and $\int_{vac} D_d ds$ corresponds to $G(P, T, E, \dots)$. $f_d(\lambda_j)$ then becomes the frequency dependent function we should use in computing the dual color correction.

3. ACCURACY OF THE DUAL-COLOR CORRECTION

The usefulness of the dual color correction will depend on two factors: the effects of noise in the range measurements, and the effects of the approximations we have made in deriving equation (11). The effects of noise can be simply computed by evaluating the coefficients in equation (4) for pairs of wavelengths commonly used in satellite laser ranging. In Table 3, we give the coefficients of the linear combinations for four laser wavelengths. Even for largest separation of wavelengths ($\lambda = 1.064$ and $0.355 \mu\text{m}$), the dual color estimate of the range will 11 times noisier than in individual range measurements at the two wavelengths (assuming equal range error for the two wavelengths). Also, any biases in the range measurements will also be amplified by a similar amount.

In addition to the noise in the dual color system, we need to examine the effects of the assumptions we have made in deriving the correction formulas. We

Table 2. Simplified equations for atmospheric refractive index (compiled from Owens, 1967)

Dry air with 0.03 % CO₂ (Standard air)

$$(n_p - 1) \times 10^8 = \left[2371.34 + \frac{683939.7}{(130 - \sigma^2)} + \frac{4547.3}{(38.9 - \sigma^2)} \right] D_s$$

$$(n_g - 1) \times 10^8 = \left[2371.34 + \frac{683939.7(130 + \sigma^2)}{(130 - \sigma^2)^2} + \frac{4547.3(38.9 + \sigma^2)}{(38.9 - \sigma^2)^2} \right] D_s$$

$$D_s = \frac{P_s}{T} \left[1 + P_s(57.90 \times 10^{-8} - \frac{9.3250 \times 10^{-4}}{T} + \frac{0.25844}{T^2}) \right]$$

Water vapor

$$(n_p - 1) \times 10^8 = [6487.31 + 58.058\sigma^2 - 0.71150\sigma^4 + 0.08851\sigma^6] D_w$$

$$(n_g - 1) \times 10^8 = [6487.31 + 174.174\sigma^2 - 3.55750\sigma^4 + 0.61957\sigma^6] D_w$$

$$D_w = \frac{e}{T} \left[1 + e \left[1 + 3.7 \times 10^{-4} \times \left[-2.37321 \times 10^{-3} + \frac{2.23366}{T} - \frac{710.792}{T^2} + \frac{7.75141 \times 10^4}{T^3} \right] \right] \right]$$

investigated these effects by ray tracing through model atmospheres and computing the dual-color correction from the ranges computed in the ray trace. In the ray trace model, the full Lorenz-Lorentz equation for the refractivity of the mixture was used. Thus, we were able to assess the effects of all of the assumptions we had made. The summary of the results obtained from the ray tracing are given in Table 4.

The two largest sources of error in Table 4 arise from the presence of water vapor, and the effects of the bending of the ray as the signal propagates through the atmosphere. These two effects affect the dual color correction because their wavelength dependence is different from that for standard air. The wavelength dependence of water vapor is given in Tables 2 and 3. The contribution of water vapor to the error was almost independent of the choice of wavelength pairs. However, this result should be treated cautiously because only one the wavelengths we examined was within the range of validity of the refractive index formulas for water vapor. The errors due to water vapor could be reduced by removing the water-vapor contribution to the observed ranges before the dual color correction was computed. However, the dual-color correction would then be influenced by errors in modeling the distribution of water vapor in the atmosphere. As a general rule, the error in the dual-color correction will be approximately 50-100% larger than the error in computing the water vapor contribution to the ranges.

Table 3. Refractive index dispersion and dual color combinations

<u>Dispersion functions, $f(\lambda)$</u>				
λ		$f_d(\lambda)$	$f_w(\lambda)$	
(μm)				
1.064		7866.06	6638.81*	
0.694		8028.77	6839.15*	
0.532		8235.85	7085.63	
0.355		8925.00	7954.92*	
<u>Dual color combination</u>				
λ_1	λ_2	$\frac{f_d(\lambda_2)}{f_d(\lambda_2)-f_d(\lambda_1)}$	$\frac{f_d(\lambda_1)}{f_d(\lambda_2)-f_d(\lambda_1)}$	Noise ratio†
(μm)	(μm)			
1.064	0.694	49.34	48.34	69.0
1.064	0.532	22.27	21.27	30.8
1.064	0.355	8.43	7.43	11.2
0.694	0.532	39.77	38.77	55.5
0.694	0.355	9.96	8.96	13.4
0.532	0.355	12.95	11.95	17.6

* These wavelengths fall outside the range of validity of the water vapor refractive index formula

† The noise ratio is computed assuming that the ranges at the two wavelengths are measured with the same standard deviation. The noise ratio gives the ratio the standard deviations of the dual-color-corrected range to the standard deviation of the range measurements.

In the case of bending, the error in the dual-color correction arises because the bending contribution to the range depends on both the group- and phase-refractivities. The error due to bending is approximately equal to the difference in the range along the curved path followed by the ray and the straight line path. Again, this error can be reduced by either by correcting the observed ranges for the effects of bending, or by developing elevation-angle dependent coefficients for combining the ranges at the two wavelengths. Each of these approaches would introduce a dependence in the dual-color correction on the model of the atmosphere used to compute the bending. For observations made with elevation angles greater than 20°, the effects of errors in the bending correction should be small.

There are several other cautions which should be issued concerning dual-color corrections. For laser systems with very short pulses (5-10 ps), the bandwidth of the pulses will be large (6-3 Å). If the pulse shape in the wavelength domain is very irregular, then the effective wavelength to be used in computing the coefficients

Table 4. Errors in dual-color ranging

Source	Error at Z=0° (mm)	Error at Z=70° (mm)	Comments
Use of simplified formulas	< 0.3	< 1	λ 1.064, 0.355 μm P= 1013.25-900 mbar T= 293 - 273 K
%CO ₂	< 0.01	< 0.03	for 0.03 % changes
water vapor	\approx 6	\approx 17	20 mbar H ₂ O for all λ pairs
bending	0	\leq 4	all conditions
wavelength	0.3	1	for 1 Å change in λ

for the dual-color correction may not be the wavelength of the laser itself. The sensitivity of the dual-color corrections to wavelength changes is given in Table 4. A few millimeters of error could be introduced by such effects. Also, the most accurate refractivity formulas should be used in any computation of the corrections. As an example, if the standard IUGG refractivity formulas are used to compute the coefficients for the dual-color correction, then errors of several centimeters can be introduced into the corrected ranges.

The dual-color correction will amplify any noise in the range measurements, generally by at least an order of magnitude. To achieve 1 centimeter dual-color ranges, the ranges at the two wavelengths will need to be measured with sub-millimeter accuracy.

4. SYSTEM DESIGN CONSIDERATIONS

There is no known technique for determining the true flight time difference to 0.5 mm (3 ps) on a single shot. This level of precision can be approached by averaging. The two principal techniques available are:

- average range differences (ARD), and
- difference average ranges (DAR).

These two techniques have fundamentally different observables, and different noise ratios. The average range difference (ARD) method utilizes direct observations of range difference, which are averaged to produce the required precision. The second technique (DAR) simply measures the actual ranges at two or more wavelengths with high precision, and determines the range difference by subtraction of normal points for range at a given epoch. Because subtraction of two observables is involved, the noise ratio is around 1.4 times worse than for the ARD method.

To achieve 1 cm range corrections using ranging wavelengths which are within the range of validity of the formulas used, a range difference error of less than 0.5 mm, or 3 ps is required.

The principal characteristics of state-of-the-art ARD and DAR systems designed to produce this precision for ranging to LAGEOS are given in Table 5. The ARD system utilizes a combination of MCP PMT and streak camera to yield 45 ps single shot uncertainty in range difference. Thus 225 observations are required to produce 3 ps uncertainties in range difference. A drawback of the ARD technique is that range returns at both wavelengths are required, from the same shot, to produce an observation. Thus if the probabilities of obtaining range measurements at wavelengths λ_1 and λ_2 are n_1 and n_2 respectively, then the probability of obtaining these events simultaneously is $n_1 n_2$. In practice, because of the requirement to split the signal to a range detector (PMT) and a range difference detector (streak camera) the probability is even lower. The measurement frequency will be around 1 Hz for a system which could produce range measurements in each color individually at 4 Hz from a 10 Hz laser system. Thus it takes such a system 225 seconds to determine range difference to 3 ps.

Table 5. Characteristics of ARD and DAR systems.

	Average Range Difference (ARD)	Difference Average Range (RAD)
Required observation precision	3 ps	2 ps
Single observation precision	45 ps	50 ps
No. of observations required	225	625
Observation frequency	1 Hz	4 Hz
Time required	225 sec	156 sec
Error tolerance	good	poor
Complexity	poor	good
Data modeling	poor	good
Calibrations	poor	good
Automation	poor	good

The DAR system requires many more measures to obtain the same result. This is because single shot observation error is slightly larger, and the precision ultimately required is 1.4 times smaller (2 ps). However, this system accumulates range at 4 Hz (same power as the ARD system above) and thus can obtain the range difference required in 156 seconds.

It can be seen that the systems are comparable in performance. Both currently would require 3-4 minutes to obtain a single measure of the range difference suitable for atmospheric correction. This elapsed time is approaching the time density of normal point observations of range data, and would be satisfactory for elevation angles above 20°, and all except the lowest satellites.

There are major differences between the two techniques in some area which may ultimately decide which, if any, finds its way into the operational domain. Points to be considered in this context are:

- tolerance of systematic errors,
- system complexity,
- capability for further modeling of data,
- ease and rigor of calibration, and
- automation.

The ARD technique tolerates systematic errors in the actual range measurement (as opposed to the range difference) and order of magnitude higher (20 ps) than the DAR technique. Since it is extremely difficult to construct a ranging system with less than 2 ps systematic error in the range measurement (excluding atmosphere), this may be a telling factor.

System complexity considerations favor the DAR technique, as ARD requires a state-of-the-art streak camera and considerably more optics. A wider analysis of the probable applications of dual-color ranging suggest that a major application will be in mobile SLR systems. This is because errors or biases (in laser ranging products) due to errors in atmospheric correction will tend to integrate towards zero over time. Most of this error is thought to arise from azimuthal asymmetry in the atmosphere, which, for most locations, should be random with respect to time. For a fixed station, it is likely (although not proven) that the resultant error in the laser ranging products will be small compared to their uncertainty. However, for a mobile station, this consideration may require lengthy site stays (many weeks to months) just to ensure that these errors are "randomized", when the time required on site to obtain sufficient tracking data may be only a few days. Thus a dual-color capability could enhance mobile SLR productivity by a considerable amount. The complexity of currently viable ARD designs is not compatible with mobile operations.

The DAR technique has another slight advantage in the area of satellite (target) modeling. The individual color range data can be analyzed to extract the satellite target depth by Fourier/deconvolution techniques. The higher density of data available, as well as good satellite models, facilitate this. The ARD technique has observables doubly convoluted with the satellite target depth function, making extraction of the desired observable more difficult.

Calibration of DAR systems is straightforward. Techniques exist (Greene, 1986a; 1986b) to rigorously calibrate ranging systems to 0.1 mm. The DAR system is essentially only two perfectly colocated ranging systems operating at different colors: calibration of ARD systems can use the same techniques. ARD systems cannot yet be satisfactorily calibrated, and it remains to be seen whether some errors associated with streak cameras can be satisfactorily modeled (Prochazka and Hamal, 1986).

Finally, automation will be a major factor in the future evolution of dual-color systems. While it may be feasible to automate ARD systems with streak cameras, DAR systems now exist which are fully automated. This automation

process required several years of development on systems considerably less complex than ARD systems.

5. LASER DESIGN CONSIDERATIONS

The selection of operating wavelength, pulse energy, pulse width, and pulse repetition frequency are all facilitated by the foregoing considerations.

The choice of wavelength should be made from within the validity range of the formulas used. This limits operating wavelengths to the spectrum from 2300 Å – 20,000 Å and sets a lower bound on the noise ratio which is achievable.

The choice of laser pulse widths is also restricted. Any technique for dual-color ranging presently requires very high SNR to achieve good results. For example, neither of the techniques discussed above can achieve the single shot precision quoted in Table 5 unless a large (>100 photons/color) signal is received at the receiver.

However, SNR is almost directly proportional to the square of the pulse width for pulses from 5 ps to 100 ps. This is because, as the pulse width is reduced, the filter bandwidth must be increased, admitting more noise. At the same time, less energy can be transmitted because of the energy density limitations in the laser and the optics. Data volume, upon which both ARD and DAR depend, is also proportional to laser pulse energy. Thus there is a clear case for using longer rather than shorter laser pulses, within this domain (5–100 ps), with currently available laser and optics technology (*e.g.* 5 GW/cm² coating limits).

The uncertainty in determining the power spectrum of the laser for pulse widths below 30 picoseconds, and the consequent errors in dual-color range corrections, are a final encouragement to select a pulse width in the upper half of the range considered.

6. EXPERIMENTAL RESULTS

With the sole exception of its poor tolerance for systematic error, the DAR technique seems superior for practical implementation. The possibility of ranging in two more colors with a systematic error of 2 ps in each has been explored on the Natmap Laser Ranging System (NLRS). During 1986 it was progressively enhanced to the point where one-color ranging could be executed with less than 2 ps systematic error for ranging operations not exceeding 20 minutes duration (Greene, 1986a). It now remains to replicate parts of this system to allow multiple wavelength operations, and the experimental determination of atmospheric range correction.

CONCLUSIONS

We have examined the dual-color correction to determine if such a technique will yield improved range accuracy by calibrating the contribution of atmospheric refraction to satellite range measurements. Our analysis indicates that sub-millimeter accuracy in the range measurements will be required to achieve one centimeter accuracy in the dual-color ranges. There are also systematic effects in the correction,

due mainly to water vapor and ray-bending which may in the future limit the accuracy of the dual-color ranges. For ranges made at 20° elevation angle, these systematic effects could introduce errors of ≈ 2 centimeters in the dual-color range. These errors could be reduced by modeling the water vapor and bending contributions to the ranges.

Acknowledgements

This work was supported in part by the U.S. Air Force Geophysics Laboratory, contract F-19628-86-K-0025; NASA grant NAG5-538; and NSF grant EAR-83-06380.

References

- Abshire, J.B., and C.S. Gardner, *IEEE Trans Geoscience and Remote Sensing*, GE-23, 414-425, 1985.
- Bender, P.L. and J.C. Owens, *J. Geophys. Res.*, 70, 2461, 1965.
- Böttcher, C.J.F. *Theory of Electric Polarization*, Elsevier Publ. Co. Amsterdam, 1952.
- Greene, B.A., "Calibration of sub-millimeter precision satellite laser ranging system", *6 th International Workshop on Laser Ranging Instrumentation*, Antibes, France, 1986a.
- Greene, B.A., "Calibration of sub-picosecond timing systems", *6 th International Workshop on Laser Ranging Instrumentation*, Antibes, France, 1986b.
- Owens, J.C., *Appl. Opt.*, 6, 51-58, 1967.
- Prochazka, I., and K. Hamal, "Streak camera based laser radar receiver: its performance and limitations", *6 th International Workshop on Laser Ranging Instrumentation*, Antibes, France, 1986

PROBLEMS INDUCED BY MULTICOLOUR TELEMETRY
ON LASER RETROREFLECTOR DEVELOPMENT

F. Guerin, G. Cerutti-Maori
AEROSPATIALE
100 Boulevard du Midi
06322 Cannes La Bocca Cedex - France -

Telephone (33) 92 92 71 27
Telex 470902 F

ABSTRACT

Aerospatiale's concept of retröreflectors coated with silver -
Aerospatiale experience over 20 years - is optimized for laser
wavelengths in the range 500-800 nm.

Further investigation is needed to adapt the thermal and optical
concept for use in a spectral range extended to ultraviolet (380 nm).

1 - History

AEROSPATIALE (AS) experience in laser retroreflectors started in 1965 for D1-C satellite. For more than 10 years, AS developed laser retroreflector arrays designed for use with Ruby Lasers ($\lambda = 694 \text{ nm}$) : PEOPLE, D2-B, TL2, STARLETTE.

In 1978, the laser retroreflector array designed for LASSO experiment was specified for two lasers : Ruby $\lambda = 694 \text{ nm}$ and doubled Neodyme $\lambda = 532 \text{ nm}$.

Following the evolution of laser technology, the laser ranging users are interested by multicolour laser ranging, for instance Alexandrite lasers ($\lambda = 760 \text{ nm}$, $\lambda = 380 \text{ nm}$).

Today, the ERS-1 laser retroreflector array is specified for $\lambda = 694 \text{ nm}$ and 532 nm and will be used with the 2 wavelengths of Alexandrite laser.

2 - AEROSPATIALE's concept

AS has been using cube corners made of high homogeneity synthetic silica (Heraeus Suprasil) in order to achieve a very high optical transmission and a good insensitivity to space radiations.

The entrance pupil can be an hexagone (D1-C, PEOPLE, D2-B), a triangle (TL2) or a circle (STARLETTE, LASSO, ERS-1).

Low thermal conductance fixations to the frame were developed in each case.

The silica trihedron rear faces are coated with protected silver.

The angular tolerances on the 90° trihedron are optimized for the mission (velocity aberration) and the thermal gradients inside the cube corner's material.

3 - Laser retroreflector to station link budget

According to Fournet's formula (Reference n° = 1), the number of photons received back in the ground station after 2 ways travel in the atmosphere is :

$$N_{\text{photons}} = K \frac{T_a \frac{2}{\cos Z}}{D^4} R \sum_{\text{C.C.}} F(G_i, \rho)$$

Z = zenith angle of the satellite from the laser station

T_a = atmosphere transmission

R = corner cube reflection coefficient

ρ = velocity aberration

G_i = apparent corner cube area

D = distance from ground station to satellite.

The first term is a function of satellite to station geometry.

The second term is dependent only on the laser retroreflector array.

Hence, the optimization of the link budget will be achieved by optimization of the product of the two. Very severe specifications on the laser retroreflector array will not compensate for very faint return signals caused by large zenith angles.

The reflection coefficient is the ratio of the retroreflected energy to the incident energy.

The last expression is the sum of the individual corner cube's efficiencies considered as light sources incoherent to each other. The efficiency informs about the distribution of light in the cube corner's diffraction pattern.

4 - Thermal environment

The distribution of light inside the diffraction pattern is a function of :

- pupil's diameter
- dihedral angular offsets
- laser wavelength
- thermal state of the cube corner

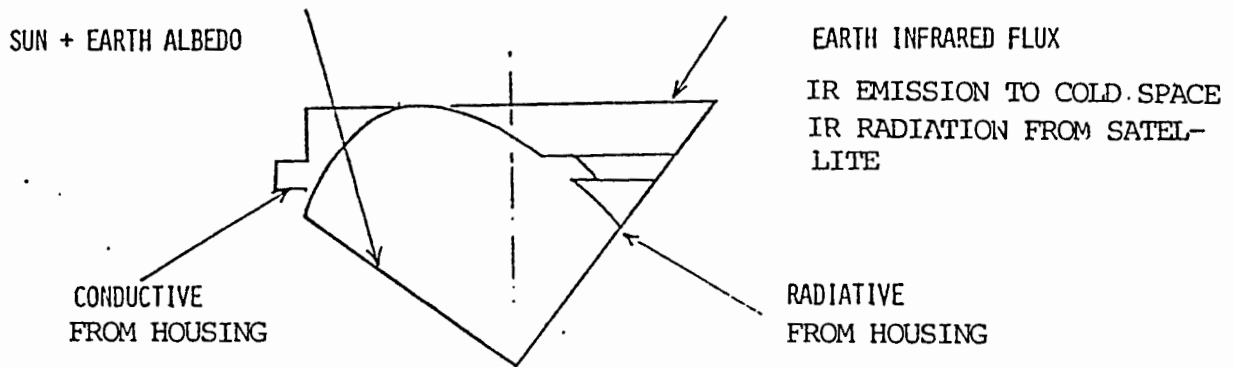


Fig. 1 : Thermal inputs

The thermal inputs on the corner cubes are :

- radiative :
 - . the solar and earth albedo fluxes, in the visible range, mainly absorbed by the silvered faces,
 - . the thermal infrared flux from the Earth and the satellite, the radiation to cold space,
 - . radiative exchanges between the housings and the silvered faces of the corner cubes,
- conductive : between the housing and the "ears" of the corner cube.

Because the silica is a bad heat conductor, thermal gradients appear in the corner cube's material and distort the diffraction pattern. In orbit, the cube corners are rarely in thermal equilibrium because their thermal environment is changing (see fig. 6).

In the case of a spinned satellite, the laser retroreflector successively views Sun, Earth, deep space.

In the case of a low orbit satellite like ERS-1, the laser retroreflector views permanently Earth with 3 phases :

- Solar flux with high incidence,
- Earth albedo flux from sunlit Earth,
- Thermal infrared flux from Earth.

AS developed a software taking into account the thermal gradients inside the real cube corner in the computation of the diffraction pattern (see fig. 1 bis).

5 - Velocity aberration

Velocity aberration represents the small angular shift between the incident and retroreflector beams caused by the relative motion of the satellite in relation to the ground station (fig. 2) for :

- Lunar laser ranging $0,7 \leq \rho \leq 1,4$ arcseconds
- Geostationary orbit $3,5 \leq \rho \leq 4,2$ arcseconds
- Low orbit (ERS-1) $5,2 \leq \rho \leq 10,5$ arcseconds

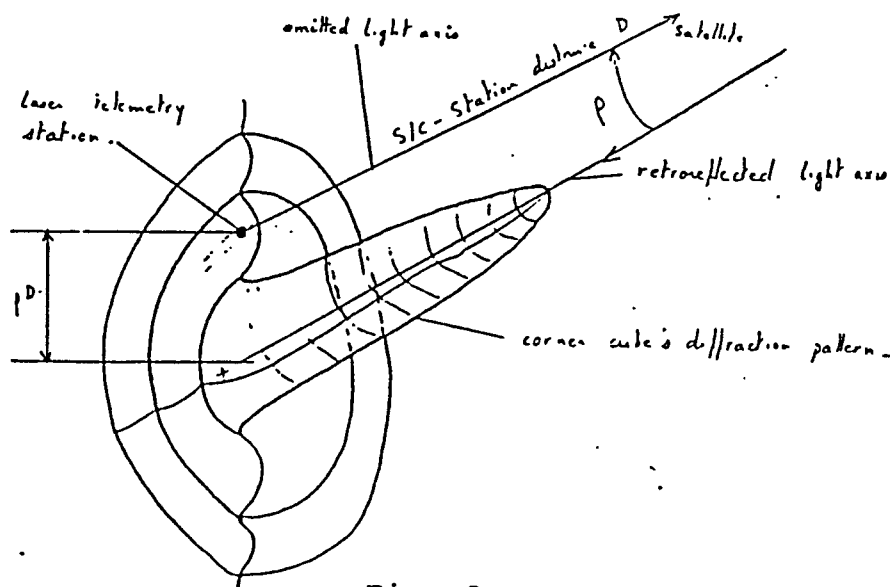
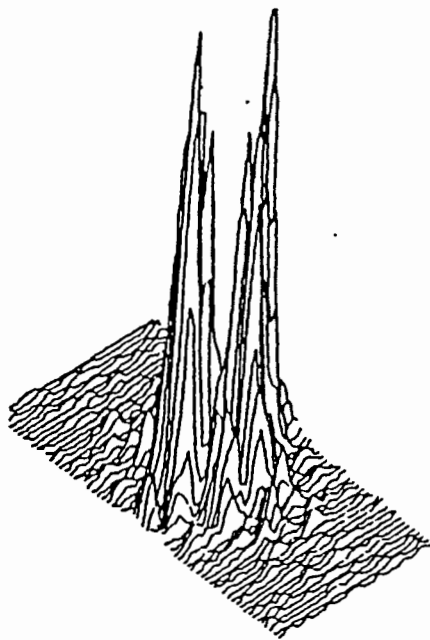
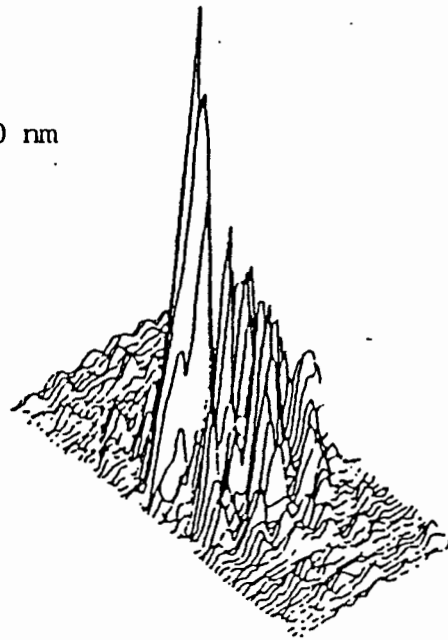


Fig. 2

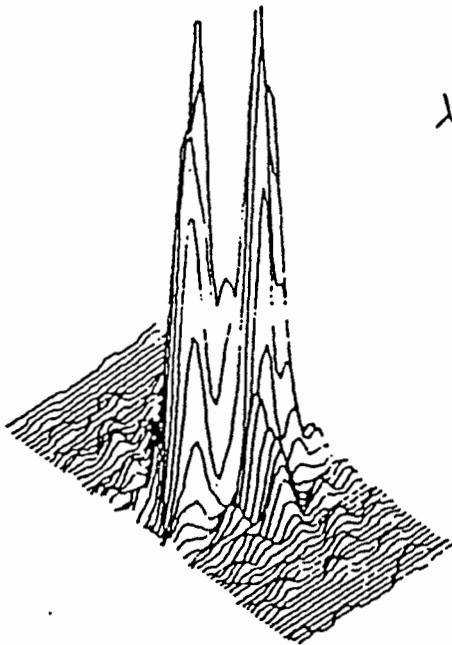


$\lambda = 380 \text{ nm}$

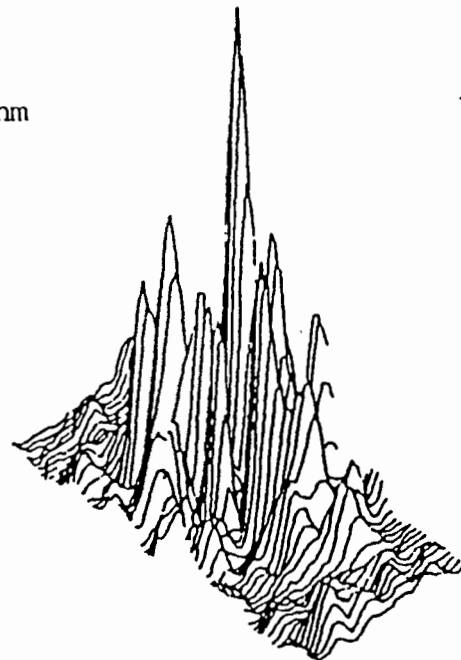


Thermal equilibrium

Thermal gradients



$\lambda = 633 \text{ nm}$



Thermal equilibrium

Thermal gradients

Fig. 1 bis : Computed diffraction patterns for a real cube corner (diameter \varnothing 33 mm) - Scale 64 x 32 arcseconds

6 - Corner cube's efficiency

The efficiency represents the mean value of the retroreflected flux at an angular distance ρ from the center of the diffraction pattern :

$$F(G_i) = 3.05 \times 10^{-10} \frac{S_{cc}}{\Omega_\rho} \frac{E_\rho}{E}$$

E = total retroreflected flux

E_ρ = retroreflected flux in an angular ring, radius ρ

S_{cc} = surface area of the corner cube's pupil (cm^2)

Ω_ρ = solid angle of the ring ρ viewed from the cube corner (sr)

Efficiency depends on :

- corner cubes' geometry (diameter, dihedral angular offsets),
- velocity aberration ρ
- beam incidence angle i (Fig. 3),
- laser wavelength,
- thermal state of the corner cube.

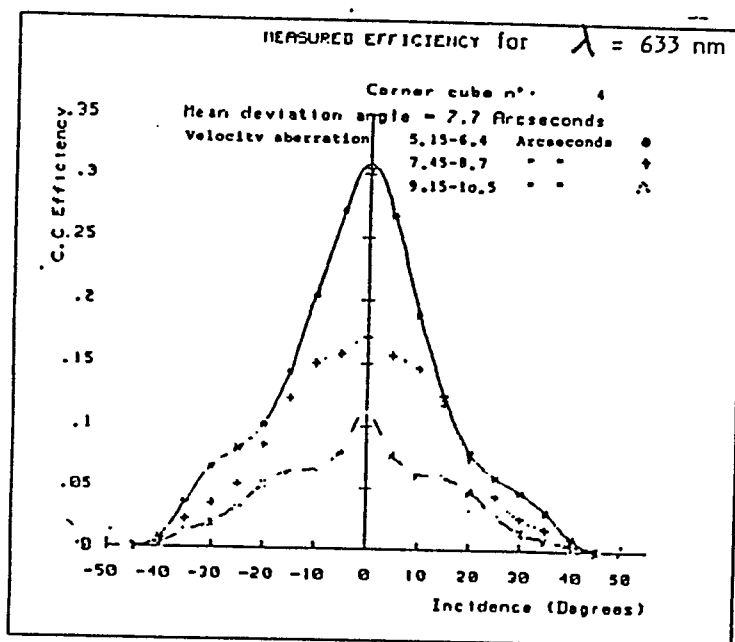


Fig. 3 : Example of ERS-1 Laser Retroreflector

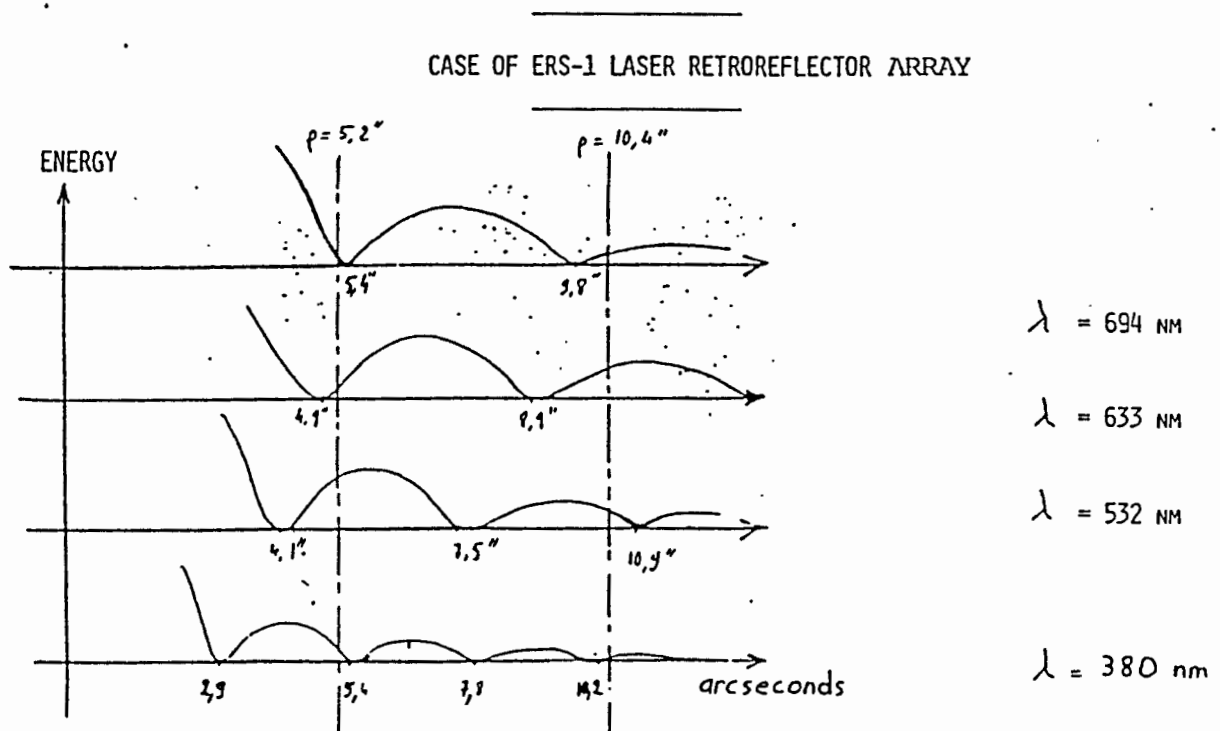
7 - Efficiency is highly dependent on wavelength

In the case of a perfect cube corner (perfect 90° trihedron), the diffraction pattern is nearly an Airy disk : it varies with wavelength (fig. 4).

When λ varies from 694 nm to 380 nm, the velocity aberration range for ERS-1 [5.2 ; 10.4 arcseconds] passes from the first bright ring to the 2nd and 3rd bright rings.

For the real cube corners, the diffraction patterns are very different from Airy disk if the dihedral angle offsets are larger than 3 arcseconds (typically). The aim of the retro-reflectors designer is to obtain less energy in the central peak, no dark rings, energy spread on pattern a little larger than the velocity aberration rings. Similarly, the diffraction pattern -hence efficiency- changes very much when λ varies from $\lambda = 694$ nm to 380 nm.

Fig. 4 : AIRY DISK AS A FUNCTION OF WAVELENGTH



8 - Reflection coefficient decreases in the blue-UV region

The reflectivity of silver decreases very rapidly when λ becomes smaller than 0.4 μm . Fig. 5 shows the corner cubes' reflection coefficient R as a function of wavelength.

R is slightly above specification for $\lambda = 400 \text{ nm}$.

On the other hand, the atmospheric transmission is lower for wavelength 400 nm than for wavelengths 500-700 nm.

Hence, the link budget -ground station to satellite- decreases rapidly when wavelength becomes smaller than 400 nm.

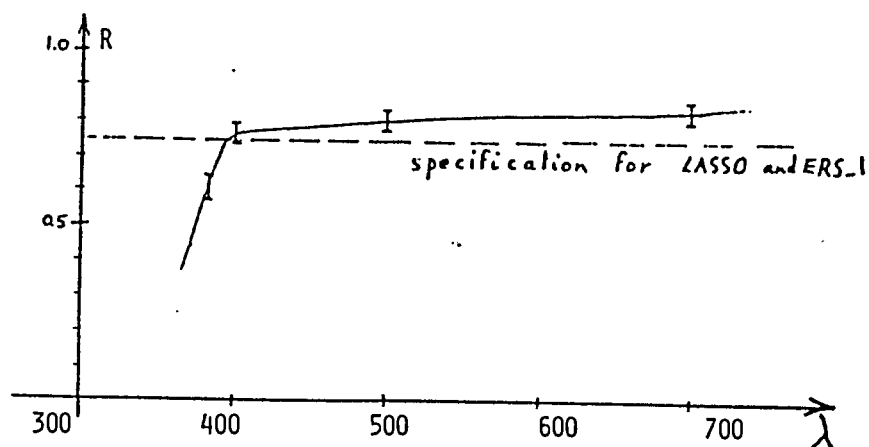


Fig. 5 : Reflection coefficient versus wavelength

For use with 380 nm lasers, a coating with higher UV reflectivity will be investigated -Al for example-. Solar absorptance α_s being 0.12 for Al and 0.05 for Ag, the thermal behaviour of the cube corners will be different. Higher thermal gradients will appear with Al coated cube corners : the thermo-optical concept needs to be adapted.

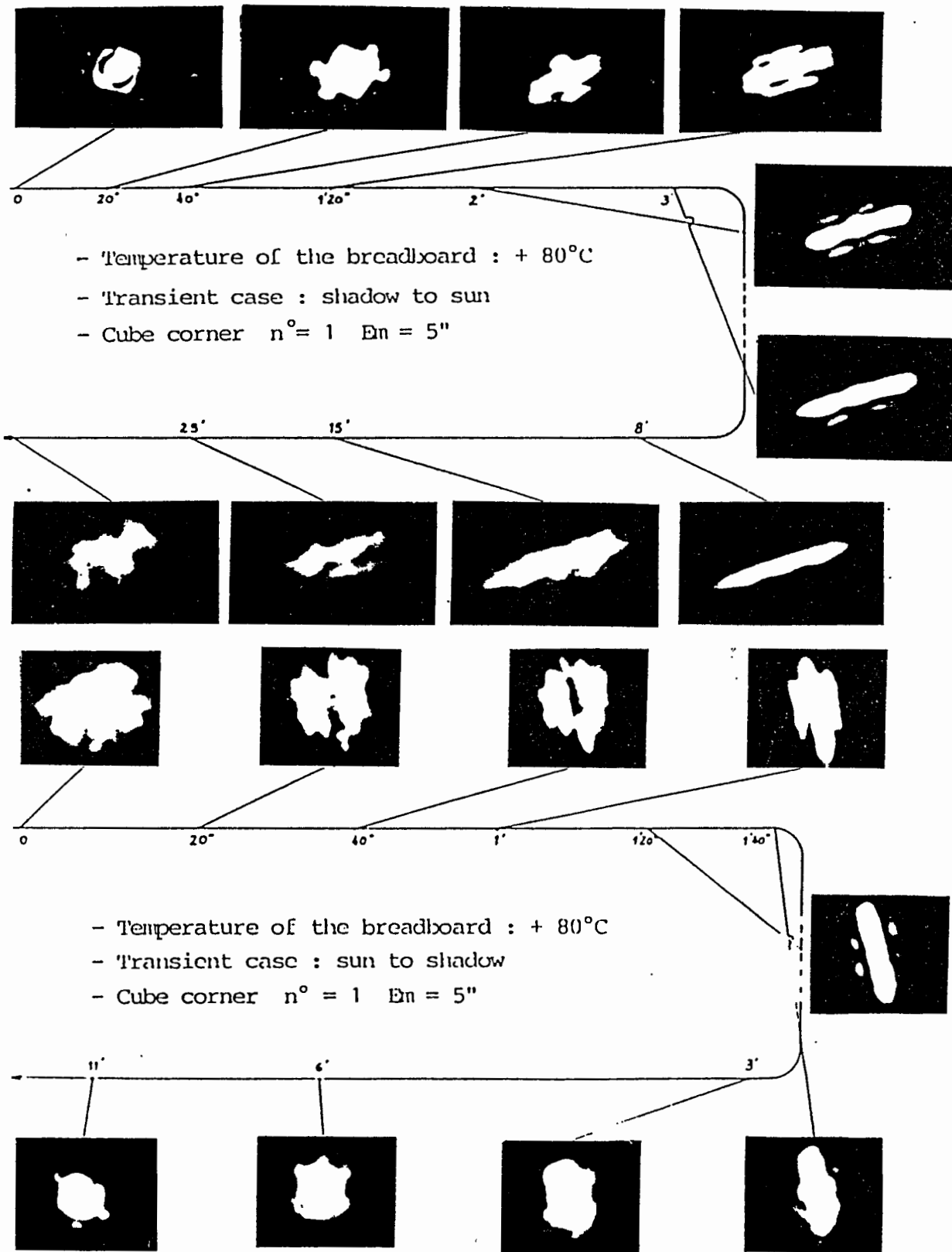


Fig. 6 : Evolution of the C.C. diffraction pattern with thermal environment : Results of Starlette thermoptical tests

9 - Conclusion

The concept of retroreflectors coated with silver is optimized (reflectivity/thermal behaviour) for laser wavelengths in the range 500-800 nm.

A larger spectral range -up to ultraviolet wavelengths- needs further investigation in order to optimize the optical and thermal behaviour of the laser retroreflector array. In 1984, AS was contracted for the design of ERS-1 laser retroreflector array : the test results will be known in a few months.

References :

1. Bulletin du Groupe de Recherches en Géodésie Spatiale n° 1, juin 1971 : Techniques Laser en Géodésie Spatiale.

LASER RANGING INSTRUMENTATION

6th INTERNATIONAL WORKSHOP

PROBLEMS INDUCED BY MULTICOLOUR TELEMETRY
ON LASER RETROREFLECTOR DEVELOPMENT

BY G. CERUTTI-MAORI - F. GUERIN, ETABLISSEMENT DE CANNES



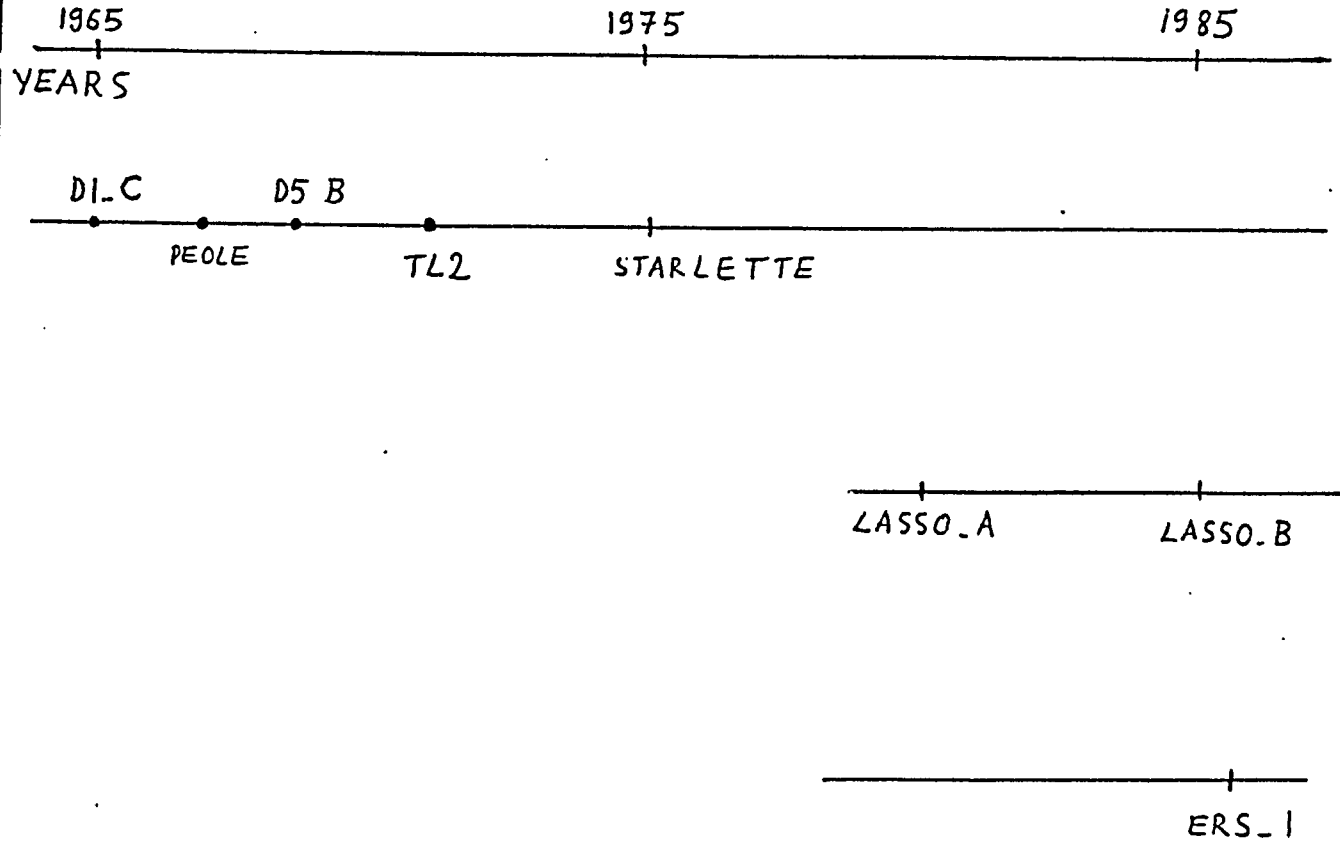
HISTORY

TYPE OF LASER.

RUBY

RUBY + DOUBLED NEODYME

RUBY + DOUBLED NEODYME +
ALEXANDRITE (760 nm + 380 nm)

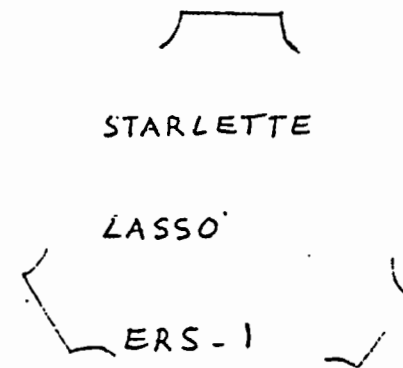
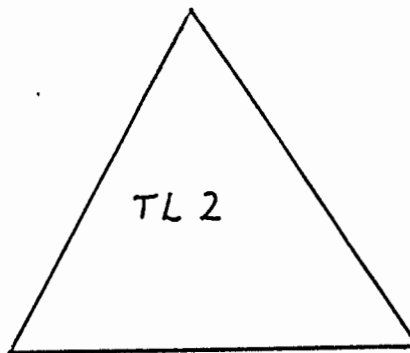
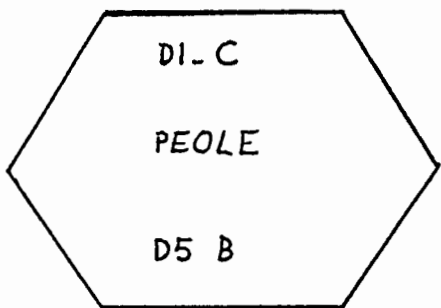




AEROSPATIALE LASER REFLECTOR

- CUBE CORNER
- HIGH HOMOGENEITY SYNTHETIC SILICA (HERAEUS SUPRASIL)

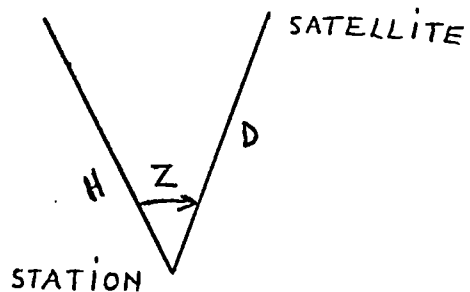
- ENTRANCE PUPIL



- LOW CONDUCTANCE FIXATION
- REFLECTIVE FACES COATED WITH SILVER PROTECTED BY INCONEL.



LASER RETROREFLECTOR TO STATION LINK BUDGET



NUMBER OF PHOTONS RECEIVED BACK AT GROUND STATION : FOURNET'S FORMULA

$$N_{\text{photons}} = K \underbrace{\frac{T_a \frac{2}{\cos Z}}{D^4}}_{\text{S/C STATION GEOMETRY}} \underbrace{R \sum_{\text{c.c.}} f(G_i; \rho)}_{\text{L.R.}}$$

T_a : ATMOSPHERIC TRANSMISSION

R : c.c. REFLECTION COEFFICIENT

ρ : VELOCITY ABERRATION

G_i : APPARENT c.c. AREA

LINK BUDGET OPTIMIZATION \Rightarrow OPTIMIZATION OF $\frac{T_a \frac{2}{\cos Z}}{D^4} R \sum_{\text{c.c.}} f(G_i)$



aerospatiale

LASER RETROREFLECTOR EFFICIENCY

DEFINITION

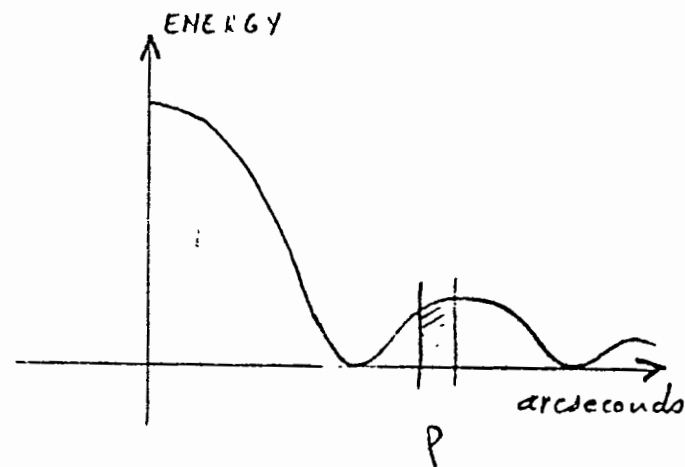
E_p = RETROREFLECTED ENERGY HAVING A CERTAIN
VELOCITY ABERRATION

E = TOTAL RETROREFLECTED ENERGY

$$F(G_i) = K \frac{E_p}{E}$$

DEPENDS ON :

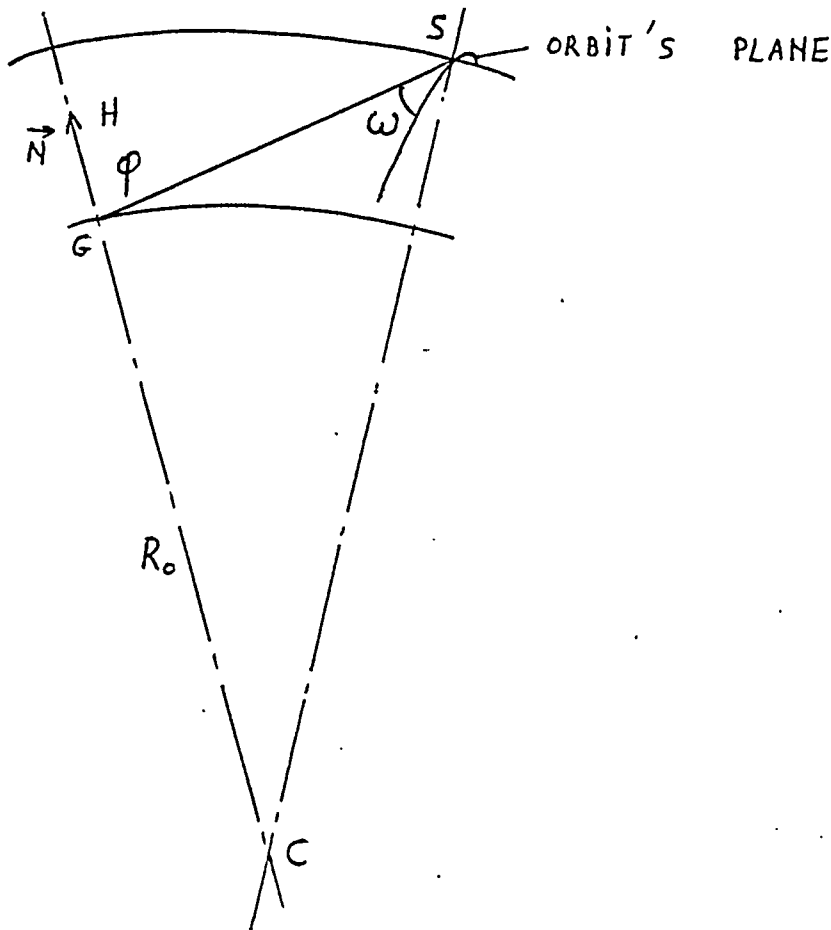
- VELOCITY ABERRATION ρ
- INCIDENCE
- WAVELENGTH
- c.c. DIAMETER
- c.c. DEVIATION ANGLES
- THERMAL ENVIRONMENT





VELOCITY ABERRATION

SMALL ANGULAR SHIFT (ρ) BETWEEN INCIDENT AND RETROREFLECTED LASER BEAMS, DUE TO THE RELATIVE MOTION OF SATELLITE/STATION



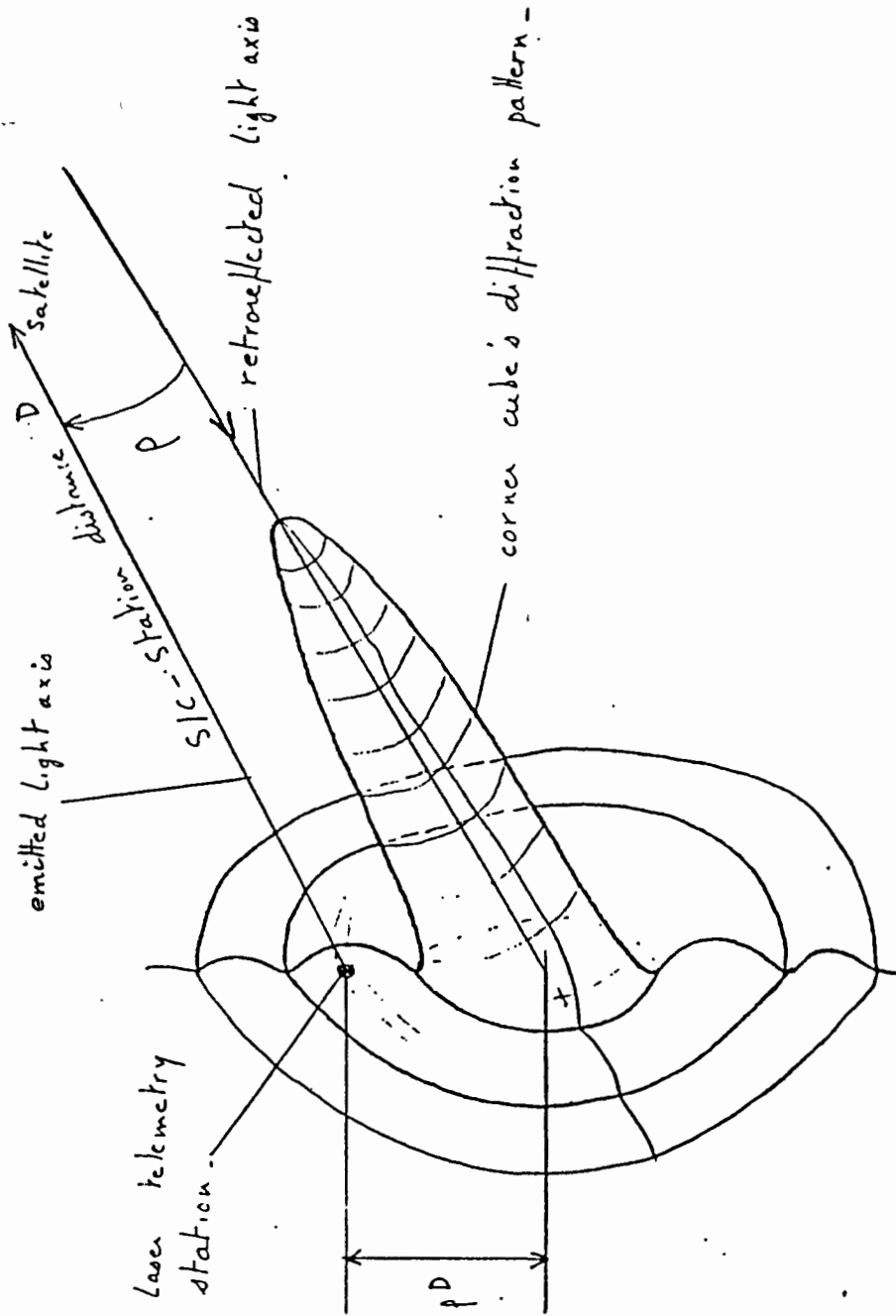
: ANGLE BETWEEN ORBIT'S PLANE AND PLANE CONTAINING G, \vec{N}, S

$$\sin \rho \approx \rho = \frac{2v}{c} \sqrt{1 - \frac{R_0}{R_0 + H}} \sin^2 \varphi \cos^2 \omega$$

FOR LASER RETROREFLECTOR :

- ON MOON $0,7'' \leq \rho \leq 1,4''$
- ON GEOSTATIONARY ORBIT (LASSO) $3,5'' \leq \rho \leq 4,2''$
- ON LOW ORBIT (ERS-1) $5,2'' \leq \rho \leq 10,5''$

INFLUENCE OF VELOCITY ABERRATION ON EFFICIENCY



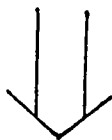


INFLUENCE OF INCIDENCE

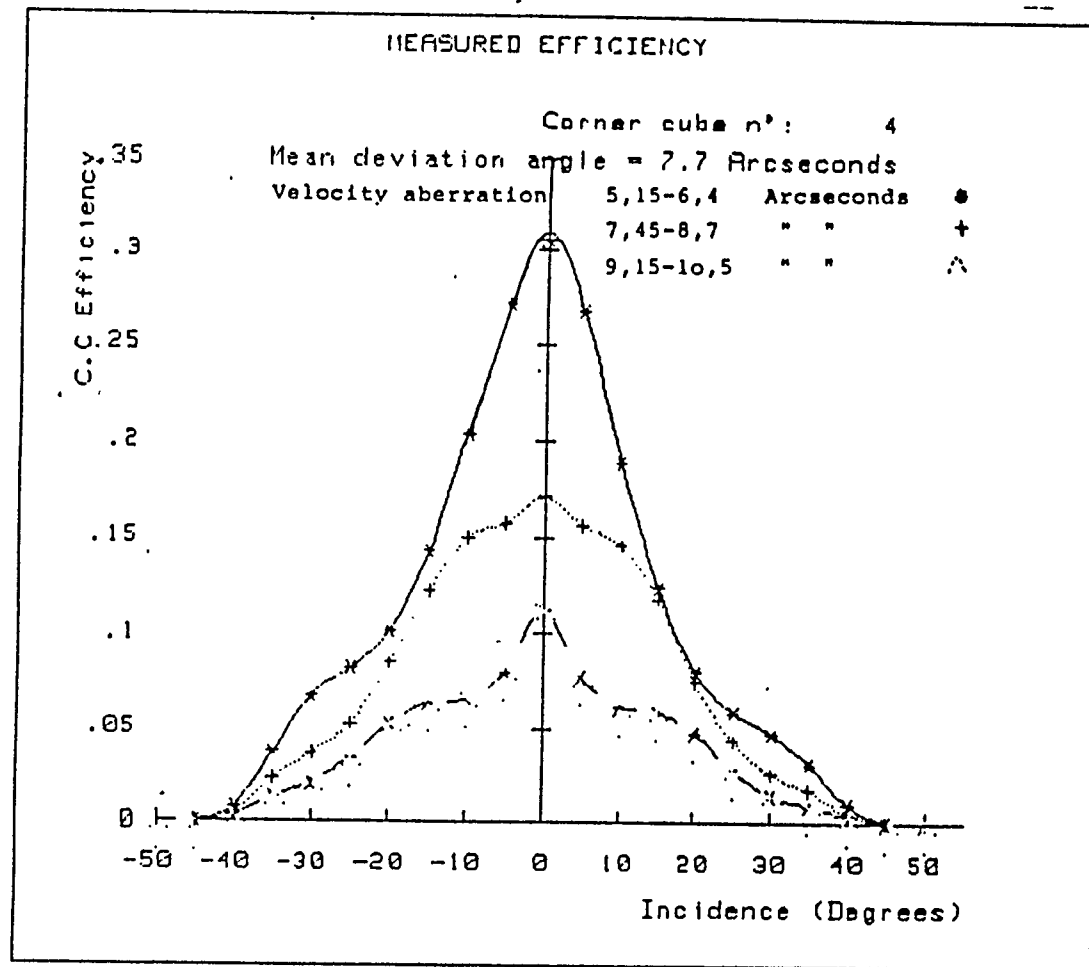
VARIATION OF PUPIL



VARIATION OF RETROREFLECTED ENERGY



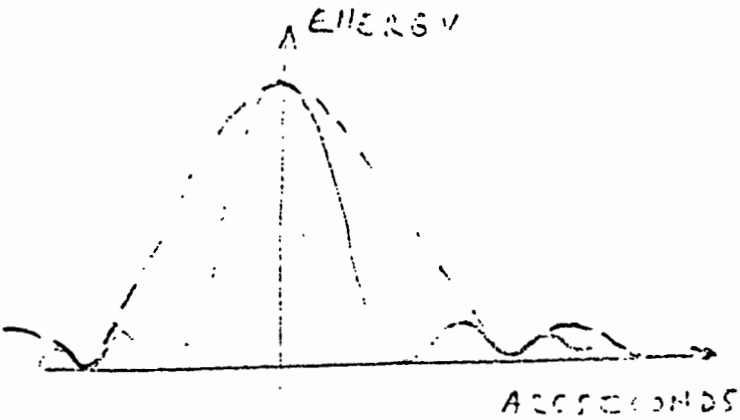
IMPACT ON LASER RETROREFLECTOR GEOMETRY



EXAMPLE OF ERS-1 LASER RETROREFLECTOR



INFLUENCE OF WAVELENGTH AND CUBE CORNER DIAMETER



DIFFRACTION PATTERN (AIRY DISK) IS A FUNCTION OF

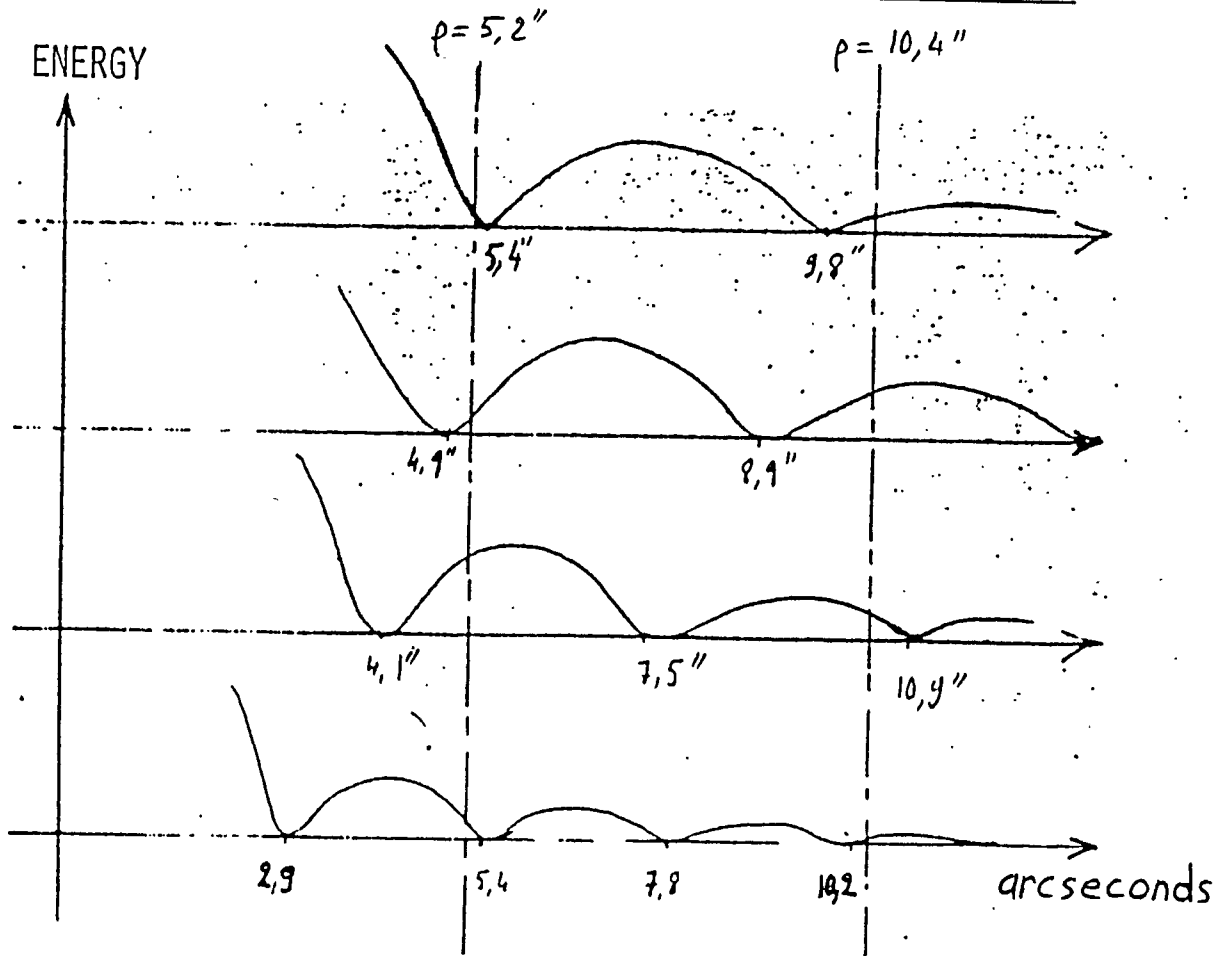
$$\lambda/a$$

FOR THE REAL CUBE CORNER, DIFFRACTION PATTERN IS A FUNCTION OF :

- DEVIATION ANGLES
- WAVELENGTH
- THERMAL ENVIRONMENT

AIRY DISK AS A FUNCTION OF WAVELENGTH

CASE OF ERS-1 LASER RETROREFLECTOR



$\lambda = 694 \text{ nm}$

$\lambda = 633 \text{ nm}$

$\lambda = 532 \text{ nm}$

$\lambda = 380 \text{ nm}$

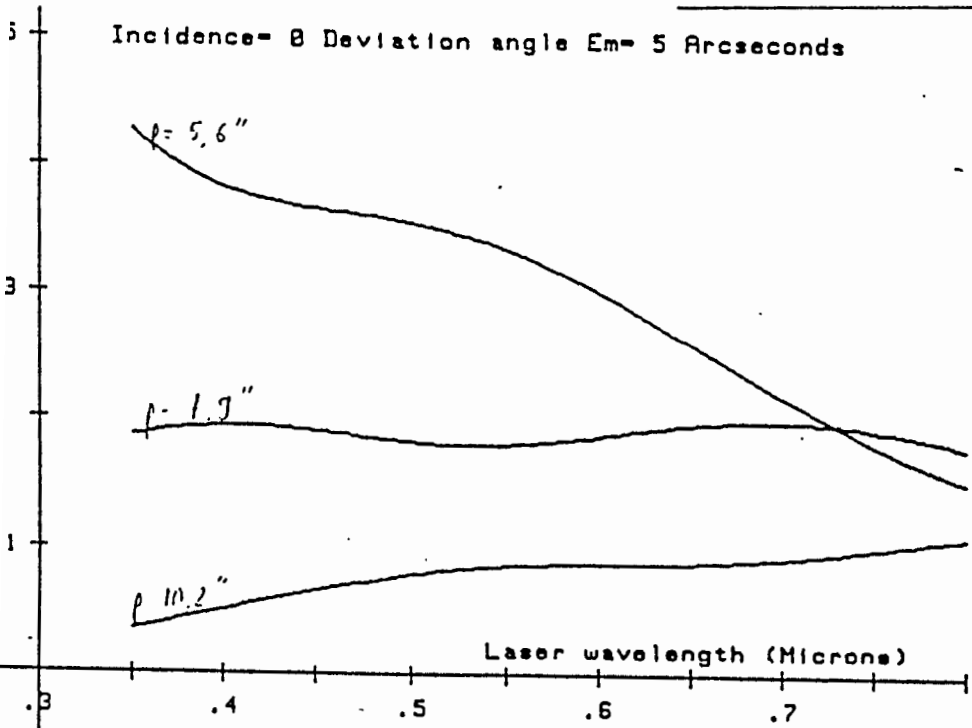
WHEN WAVELENGTH VARIES FROM $\lambda = 694 \text{ nm}$ TO $\lambda = 380 \text{ nm}$, THE VELOCITY ABERRATION RANGE VARIES FROM 1ST BRIGHT RING TO 2ND AND 3RD BRIGHT RINGS.



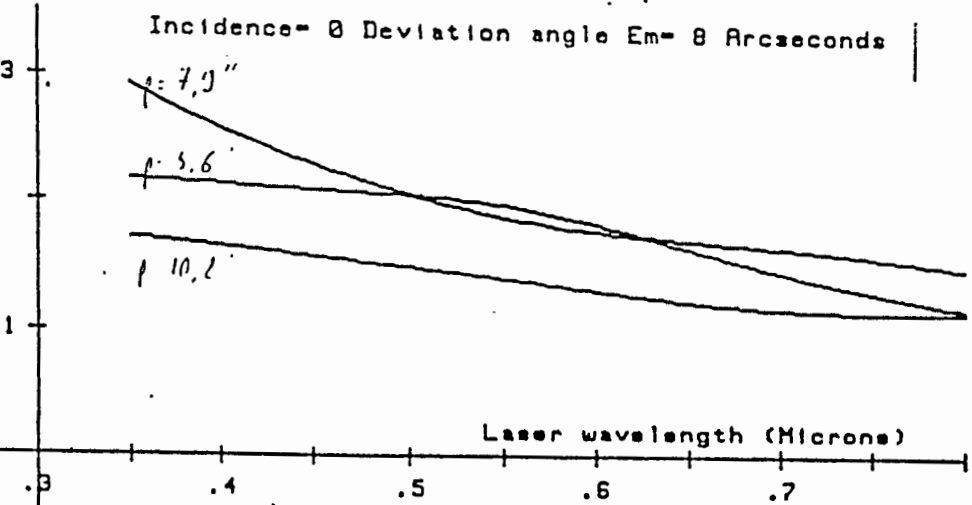
EFFICIENCY AS A FUNCTION OF WAVELENGTH

APPLICATION OF FOURNET'S FORMULA

Incidence = θ Deviation angle $E_m = 5$ Arcseconds



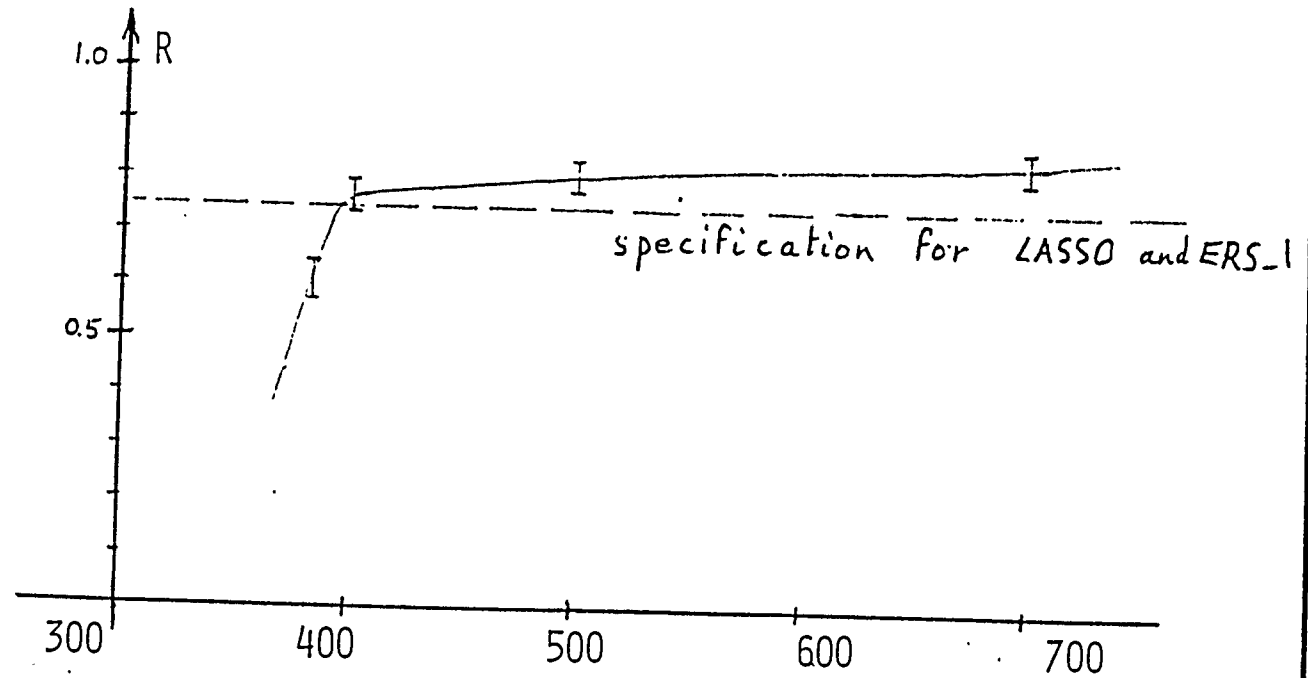
Incidence = θ Deviation angle $E_m = 8$ Arcseconds



INFLUENCE OF WAVELENGTH

R = CUBE CORNER REFLEXION
COEFFICIENT

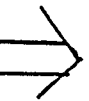
$$= \frac{\text{RETROREFLECTED FLUX}}{\text{INCIDENT FLUX}}$$



FOR $\lambda < 0,4 \mu\text{m}$

R IS LOW

ATMOSPHERIC TRANSMISSION IS LOW



LOW LINK BUDGET



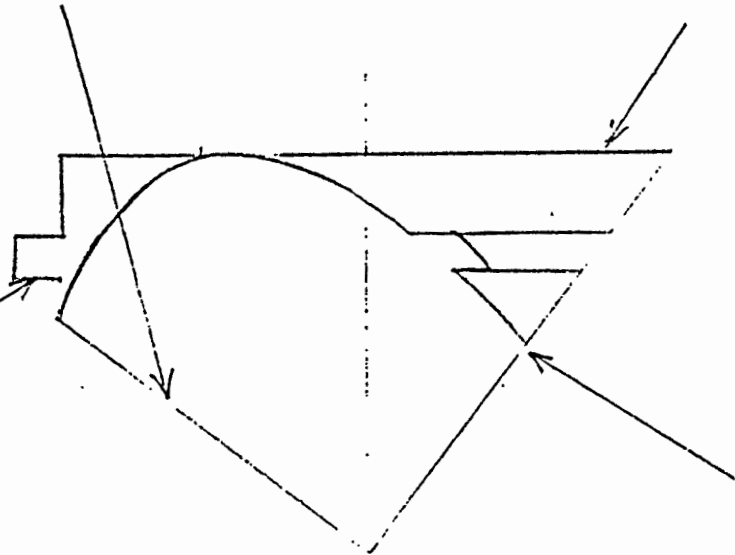
INFLUENCE OF THERMAL ENVIRONMENT

SUN + EARTH ALBEDO

EARTH INFRARED FLUX

CONDUCTIVE

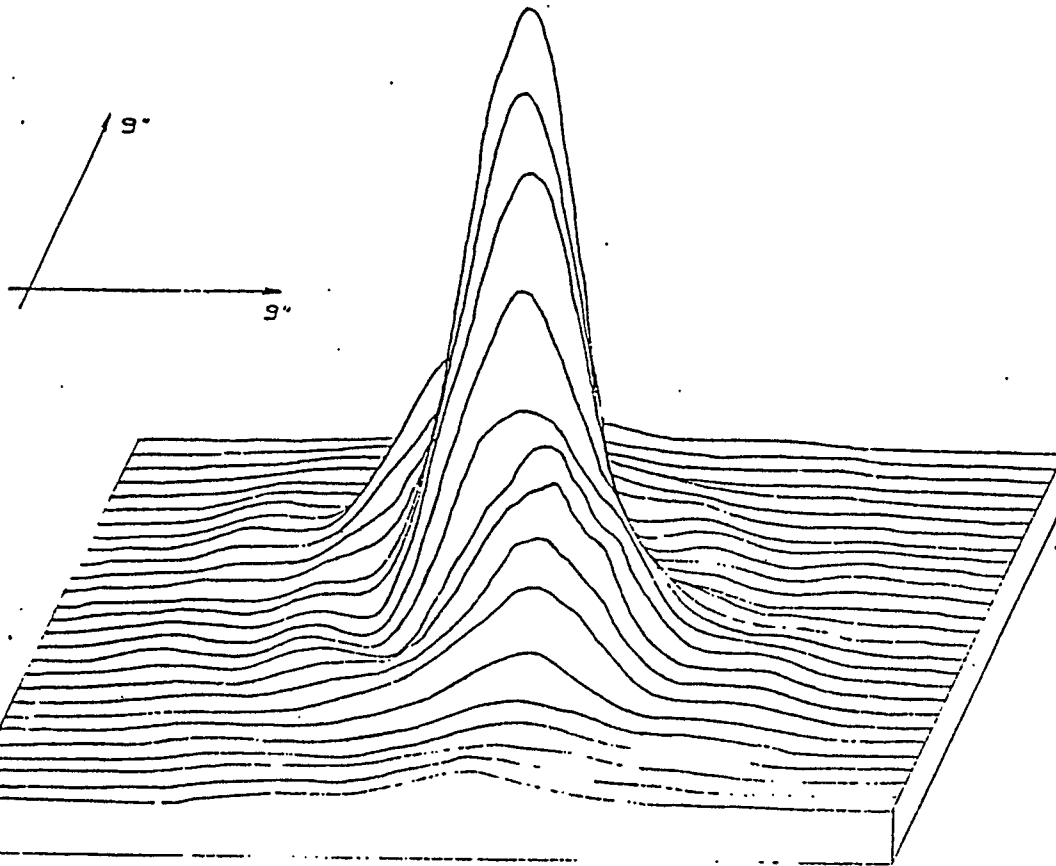
RADIATIVE





RESULTS FROM STARLETTE THERMOPTICAL TEST

CUBE CORNER WITH $E_M = 8''$



SHADOW CASE

FRAME TEMPERATURE : 20°C

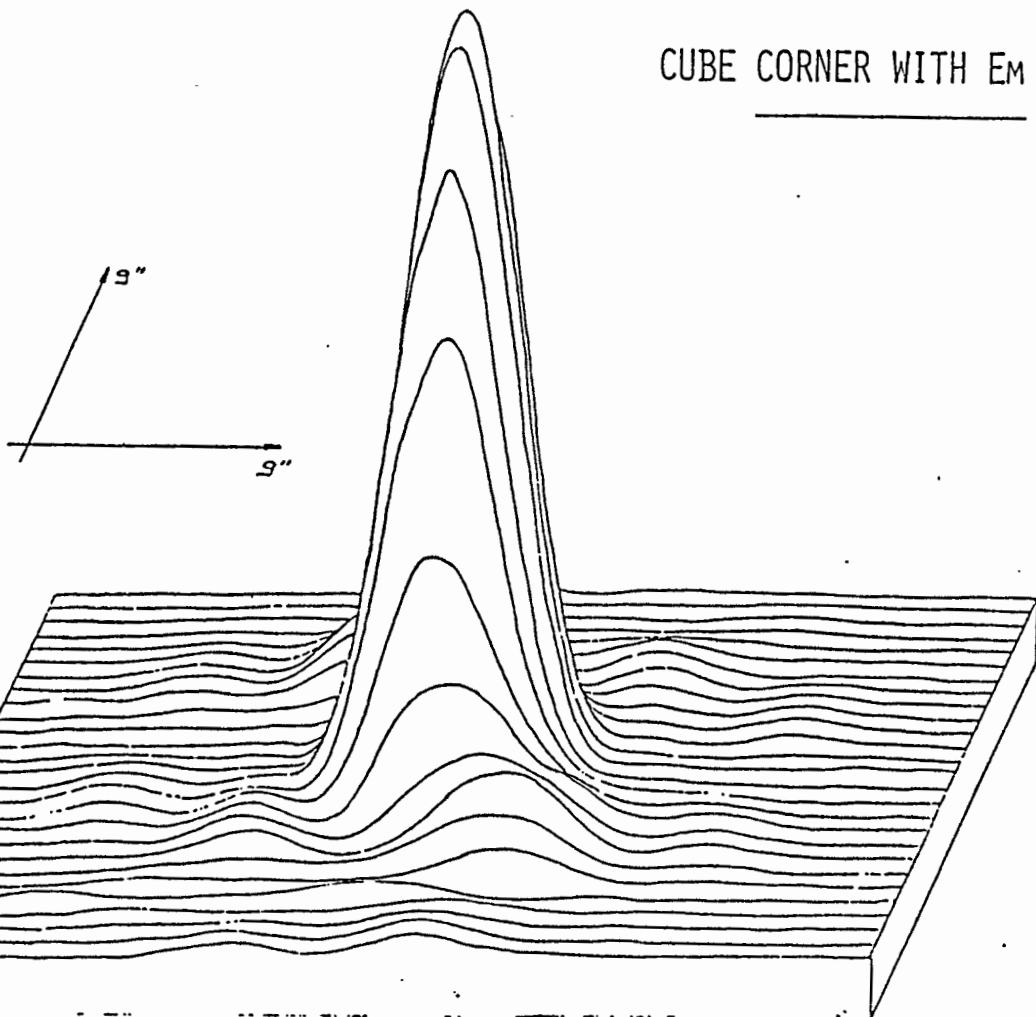
CUBE CORNER TEMPERATURE : 10°C

EFFICIENCY = 0.27 FOR $p = 5''$
= 0.06 FOR $p = 9''$



RESULTS FROM STARLETTE THERMOPTICAL TEST

CUBE CORNER WITH $E_M = 8''$



SHADOW CASE

FRAME TEMPERATURE : 80°C

CUBE CORNER TEMPERATURE : 60°C

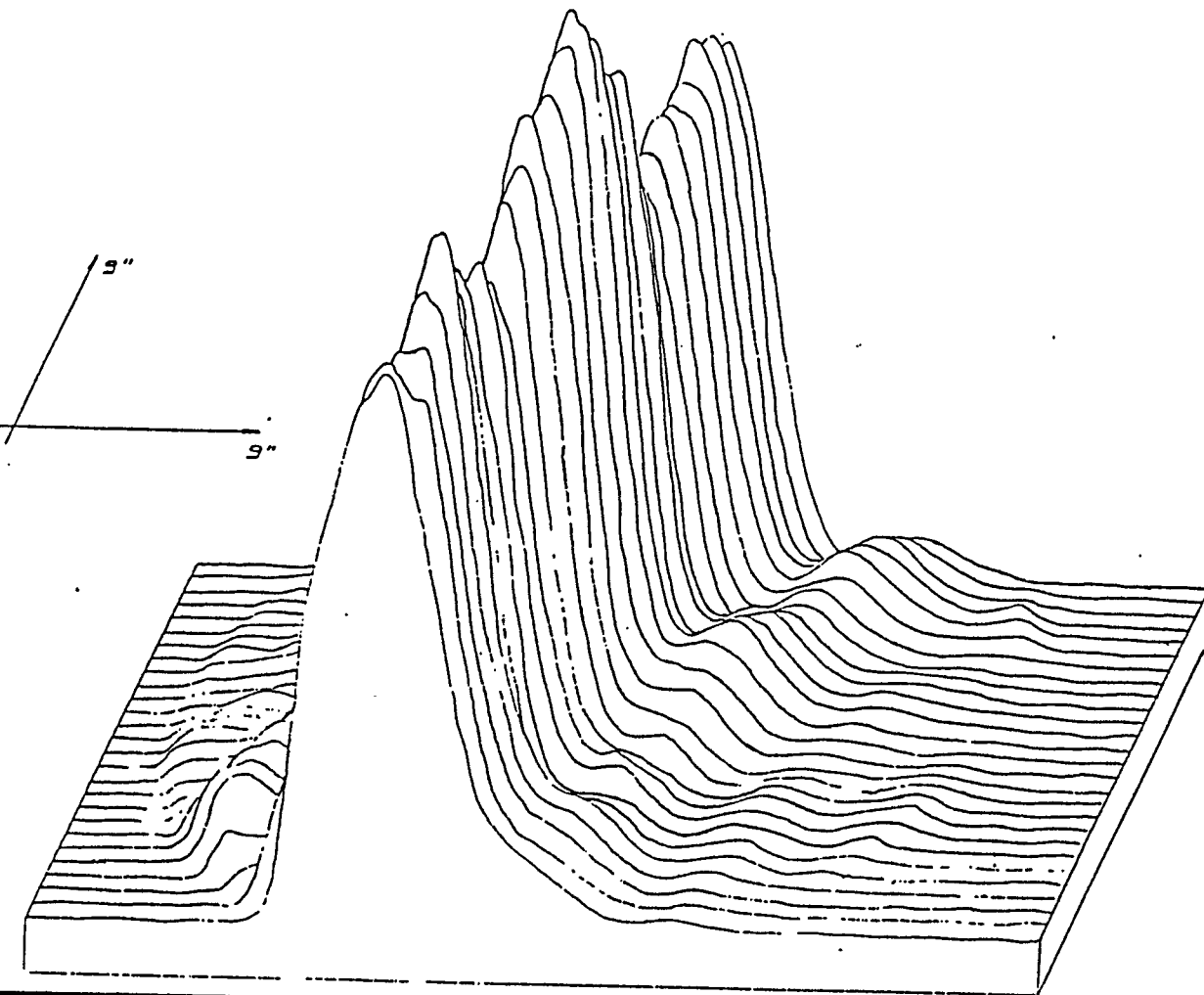
EFFICIENCY = 0,12 FOR $\rho = 5''$

= 0,04 FOR $\rho = 9''$

RESULTS FROM STARLETTE THERMOPTICAL TEST

CUBE CORNER WITH $E_M = 8''$

SUN CASE

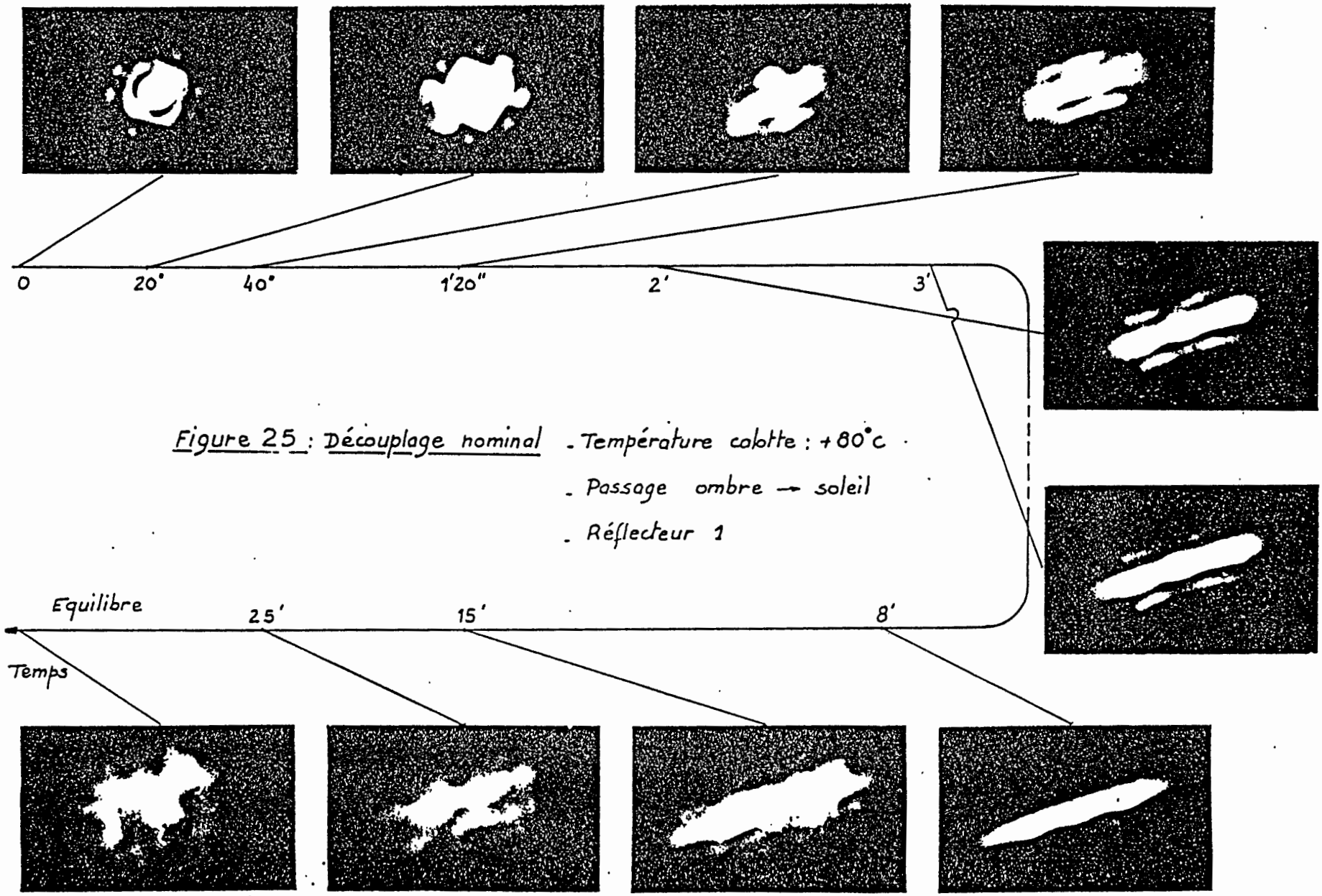


FRAME TEMPERATURE : 19°C

CUBE CORNER TEMPERATURE : 20°C

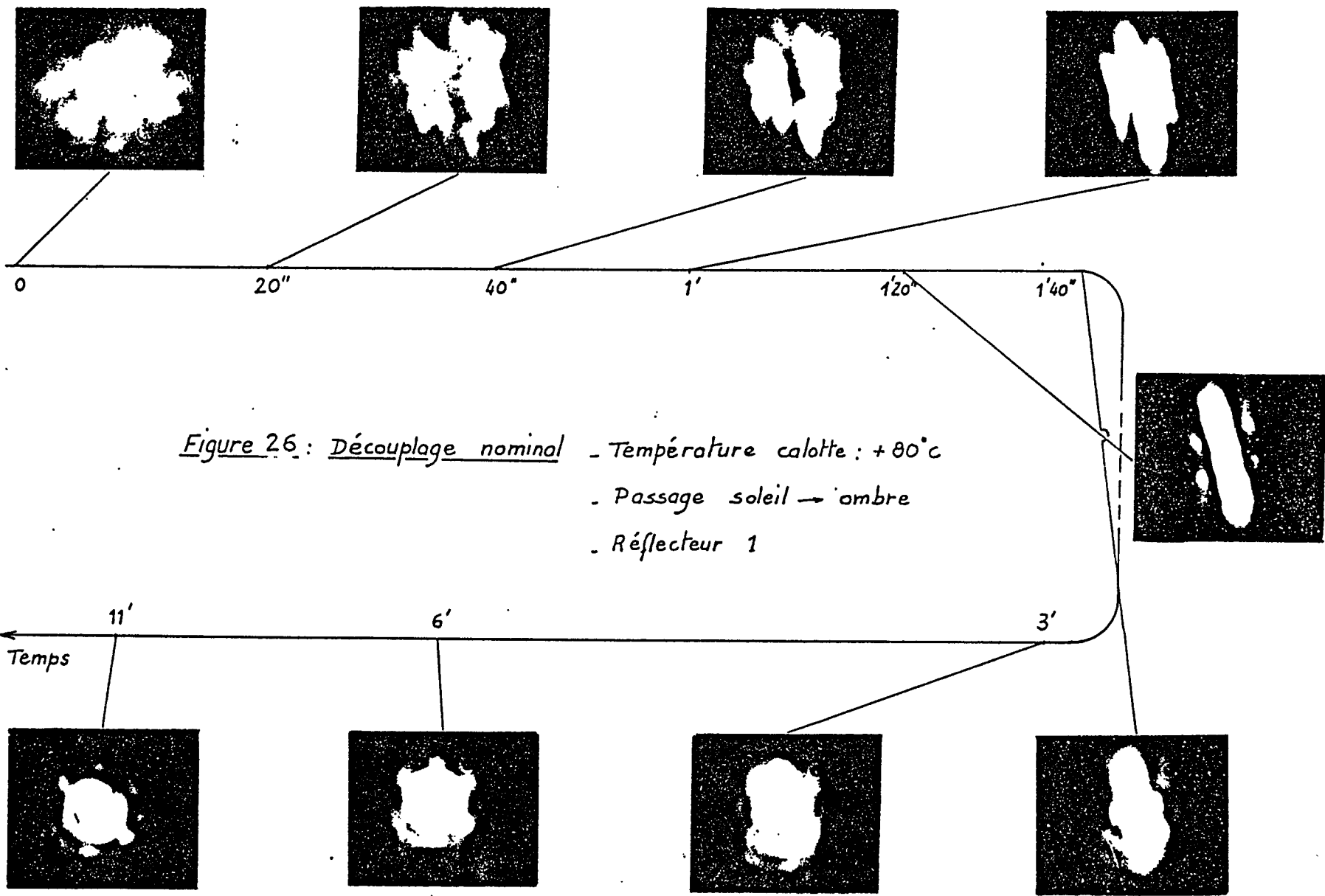
EFFICIENCY = 0,11 FOR $P = 5''$
= 0,09 FOR $P = 9''$

RESULTS OF STARLETTE THERMOPTICAL TEST



EVOLUTION OF DIFFRACTION PATTERN / THERMAL ENVIRONMENT

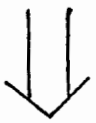
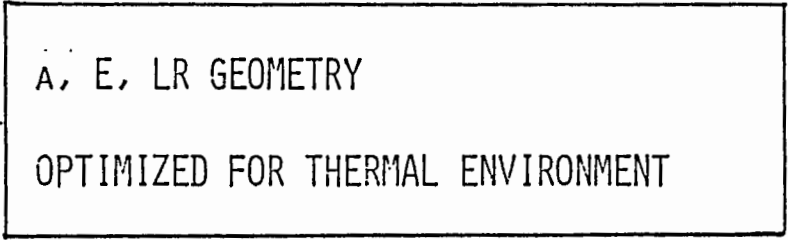
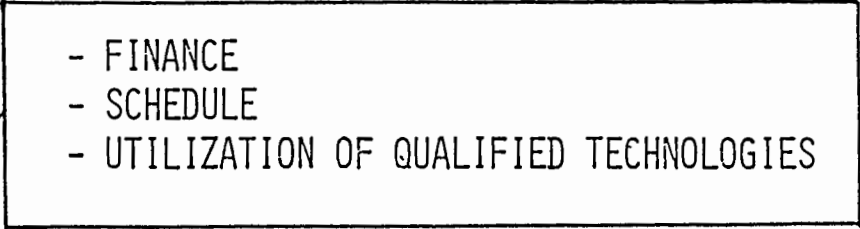
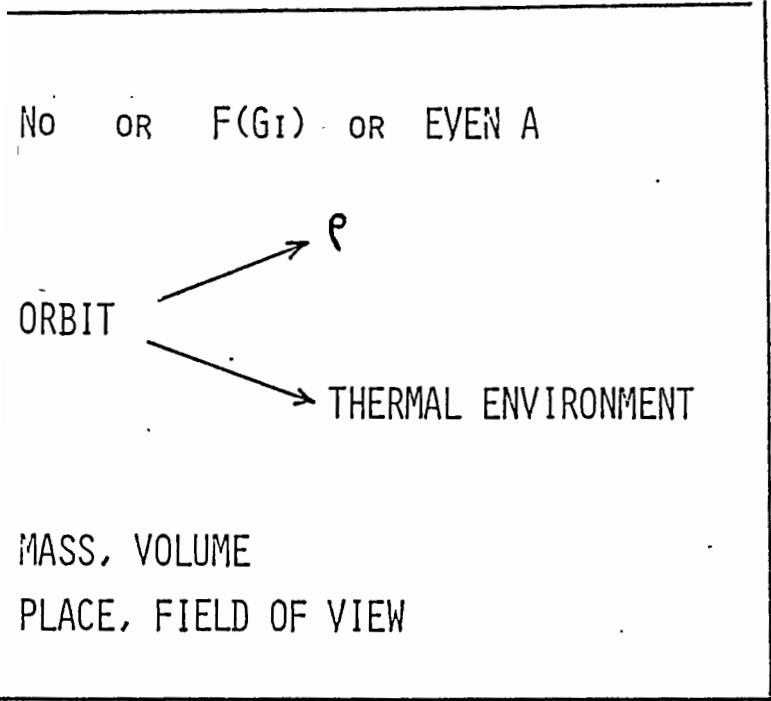
RESULTS OF STARLETTE THERMOPTICAL TEST



CONCLUSION

IMPOSED

LIMITATIONS



MULTICOLOR LASER TELEMETRY HAS A DIRECT IMPACT ON LASER RETROREFLECTOR CONCEPT

THE LASER RETROREFLECTOR FOR ERS-1 IS UNDER DEVELOPMENT AT AEROSPATIALE/CANNES.

SPECIAL STUDY GROUP ON LUNAR LASER RANGING

Report prepared by
Ch. Veillet
CERGA
Av. Copernic
06130 GRASSE

C. Alley (Maryland) - B. Greene (Orroal) - S. Bowman (Maryland) - J.F. Mangin (CERGA) - X
X Newhall (JPL) - J. Pham-Van (CERGA) - J. Rayner (Maryland) - P. Shelus (Mc Donald) - W.
Schlüter (Wetzzel) - C. Steggarda (Maryland) - J.M. Torre (CERGA) - T. Varghese (Bendix) - C.
Veillet (CERGA) - M. White (Maui) - J. Wiant (Mc Donald)

1/ LLR observing strategy - needed accuracy

All stations are working at first on Appolo XV and don't try generally any other reflector before having returns from that target. The largest hour angle coverage should be obtained for Earth rotation parameter determination, and as many reflectors as possible on the same time for libration studies. Thus the best strategy finally adopted (in good observing conditions) is to focus on two reflectors (Apollo XV and another) in order to have at the end of the observing session two long series of data for ERP, and to range the other targets more sporadically if time is available. The second ERP target should change from night to night for libration purposes. Lunakhod 1 has been once more mentionned. The fruitless systematic search for returns from this target made a few years ago at the Mc Donald 2.7-m reflector seems to prevent any station with smaller receiving area from loosing time with new attempts.

A two centimeters accuracy for Lunar normal points seems achievable in a near future, and is important at least for a complete ERP determination including not only UT0, but also the Pole coordinates. A MCP detector at Maui could be one of the means to reach this accuracy very soon. This implementation is strongly supported by the Lunar community.

2/ Normal point format

A new format defined by R. Ricklefs after many exchanges with stations and users, has been presented to CSTG and COSPAR last July. It is decided to overlap both the old and the new format for three months from January through March 1987. A report presenting the new format will be sent to all stations and users before the end of the year. During the overlap period it is possible that minor changes could be accommodated if that is necessary.

It is also planned to have a format for ERP transmission. It will be studied starting from the JPL format.

3/ Rapid data exchanges

C. Veillet suggests that exchanges of normal points or ERP determinations could be done rapidly on a regular basis. BIH is looking for ERP data on Thursday morning. Thus the data could be put on Mark 3 on Tuesday night to give one day for analyzing and transmitting ERP results to BIH and the other interested centers. As Maui will be able very soon to process the Lunar returns and to build normal points at the station, it is planned to try such a quick data transmission at the beginning of 1987.

4/ LLR capability at Orroral

B. Greene presents the Lunar situation at Orroral. GPS work made busy a large part of the team for the last year, and the development of good capabilities for SLR took most of the time. Upgrades seem necessary for increasing the return rate (actually one per minute), among which a larger laser energy (400 or 500 mJ per pulse) should be the most efficient.

5/ LLR at Wettzel

Two contracts for a LLR/SLR station have been signed recently, one for the instrument (75 cm reflector, Zeiss), and the other one for hardware and software (EOS, B. Greene). The delivery is planned for 21 months after contract signature.

6/ MLRS site

P. Shelus presents objective comparative measurements of the seeing made at the present MLRS location and at Flat Top by echosond. They show clearly that Flat Top is always better, and most often much better than the actual site. It is now time to prepare schedule and finance proposals for an eventual move of MLRS. Such a move is wished by all the participants. More on this matter will be discussed during the CDP meeting at GSFC in October.

7/ Miscellaneous remarks

P. Shelus mentions that the astronomical community needs very accurate UT1 values in real time for absolute pointing on very sophisticated telescopes.

S. Bowman presents a study on the efficiency of the reflectors as a function of numerous parameters (libration, illumination, etc ...).

Mount modelling and absolute pointing are discussed. Some pointing differences between stars and the Moon are mentionned for both Orroral and Maryland stations. This problem will be examined by an exchange of lunar position predicions between CERGA and MLRS.

FIRST LUNAR RANGING RESULTS FROM THE
UNIVERSITY OF MARYLAND RESEARCH STATION AT THE
1.2 METER TELESCOPE OF THE GODDARD SPACE FLIGHT CENTER

C.O. Alley, S.R. Bowman, J.D. Rayner,
C.A. Steggerda and J.A. Fogleman
Department of Physics and Astronomy
University of Maryland
College Park, Maryland 20742

Telephone: (301) 454-3405
Telex: 90 87 87 PHY UN MD CORK

B.C. Wang
Yunnan Observatory, Academia Sinica
Kunming, People's Republic of China

Telephone: 71347
Telex: 64040 YUOBS CN

F.M. Yang
Shanghai Observatory, Academia Sinica
Shanghai, People's Republic of China

Telephone: 386191
Telex: 33164 SHAO CN

ABSTRACT

The first lunar laser ranging returns with our new laser and detection system attached to the 1.2 meter telescope at the Goddard Optical Research Facility were recorded on August 26, 1986 from the Apollo 15 Laser Ranging Retro-Reflector (LR³) at Hadley Rille. Eleven photons were detected over a five minute interval with a firing rate of 10 Hertz. The energy per shot was about 130 millijoules, the pulse duration was 100 picoseconds, and the event timer resolution was 50 picoseconds. The standard deviation of the range was 2.5 cm, corresponding closely to the predicted spread from the calculated libration tilt of the Apollo 15 LR³ of ± 3.5 cm. The standard deviation of the mean was 0.75 cm. We believe this to be the "tightest" lunar range data point ever measured.

INTRODUCTION

The first detection of light quanta reflected from the Moon with our research station at the 1.2 meter telescope located at the Goddard Optical Research Facility of the U.S. National Aeronautics and Space Administration was achieved on August 26, 1987 at 08:44 UT. The target was the Apollo 15 Laser Ranging Retro-Reflector at Hadley Rille. Eleven returns were recorded from 3000 shots fired at 10 Hertz for a period of five minutes. The pulse duration was 100 picoseconds and the energy per pulse was about 130 millijoules.

The new laser system has been under development for several years (S.R. Bowman et al, 1982; 1985), and was first tested with LAGEOS ranging in 1984. Some details of the system are discussed in other papers at this Workshop:

"The Use of Geiger Mode Avalanche PhotoDiodes for Precise Laser Ranging at Very Low Light Levels: An Experimental Evaluation"

by S. R. Bowman, Y. H. Shih, and C. O. Alley

"Zero Range Real Time Calibration"

by J.D. Rayner, S.R. Bowman, C.O. Alley and F. M. Yang

"Analysis and Performance of a Passive Polarization Coupling Switch for Lunar Laser Ranging"

by S. R. Bowman, J. D. Rayner, and C. O. Alley.

A complete description of the new system is contained in the Maryland Ph.D. Dissertation of S.R. Bowman, "The Design, Construction and Testing of a High Precision Lunar Laser Ranging Station," April, 1986.

Telescope and Coupling Optics

The 1.2 meter telescope is shown in a cut-away view in Figure 1. It was used by our group in 1978 with a 0.5 millijoule per pulse, 10 Hz, frequency doubled Nd:YAG laser to achieve the first single-photon ranging to artificial satellites (reported at the Third International Workshop on Laser Ranging Instrumentation in Lagonisi, 1978). The 45° bending mirror can be placed in different azimuthal positions, allowing as many as eight different experiments to be accommodated at the telescope. Part of the Maryland equipment is shown in Figure 2, coupled by the passive polarization switch to one of the ports.

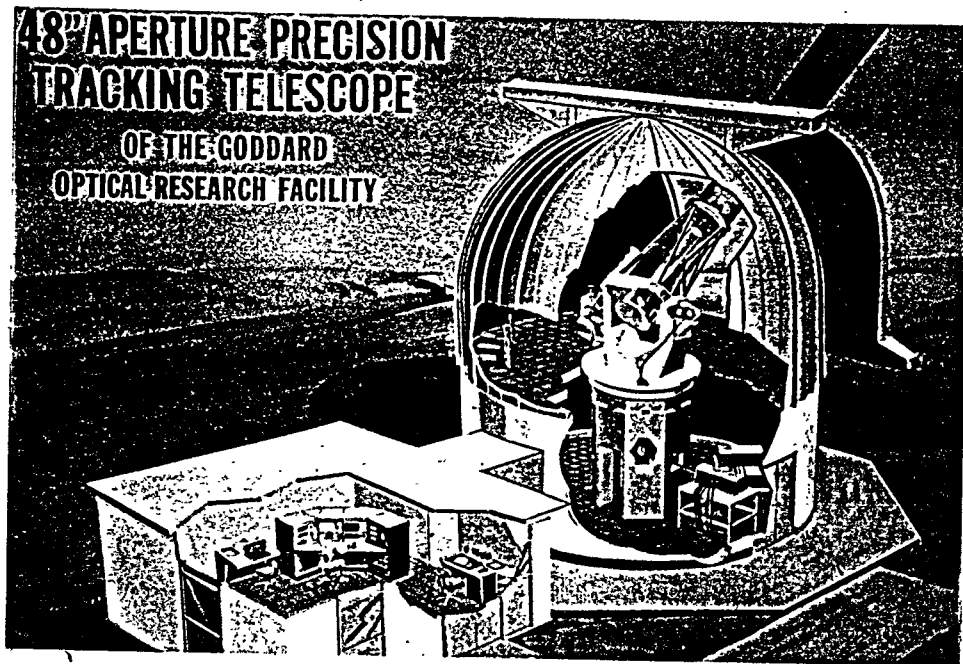


Figure 1

The telescope is computer controlled with 22 bit resolution optical encoders on the elevation and azimuth axes. Using a mount model calibrated by pointing to stars in known directions, absolute pointing is possible at a level of two or three seconds of arc. However the accuracy tends to degrade rapidly as temperature conditions change even during an observing run. Some limited success with absolute pointing to the lunar reflectors has been achieved, but will not be discussed here.

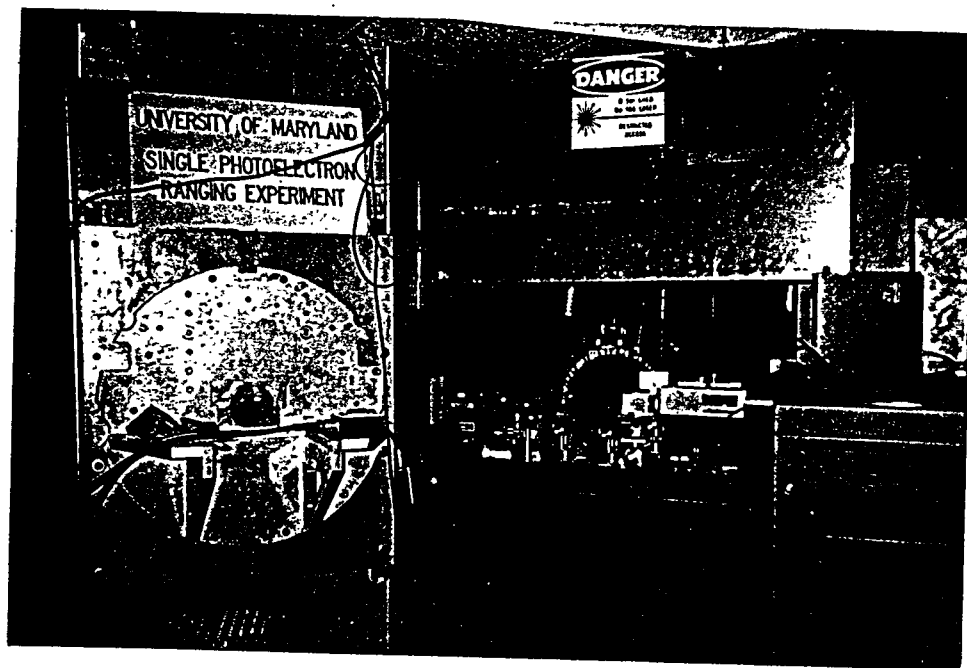


Figure 2

New Laser

The frequency-doubled, Nd:YAG laser, which uses spatial filters and re-imaging optics to minimize damage from the high peak power densities, was designed expressly for lunar ranging and has operated successfully with 350 millijoules output in a green pulse of 100 ps duration at 10 Hz. However the probability of damage is too large at this energy level. In the measurements reported here the output was limited to about 130 millijoules per pulse.

An active mirror slab geometry Nd:YAG laser has been designed and constructed to allow more energy at high repetition rates. It has not yet been added to the ranging system. This laser is discussed in another paper at this workshop:

"An Active Mirror Geometry Laser Amplifier
for High Average Power Laser Ranging"
by S. R. Bowman, L. M. Ding, and C. O. Alley

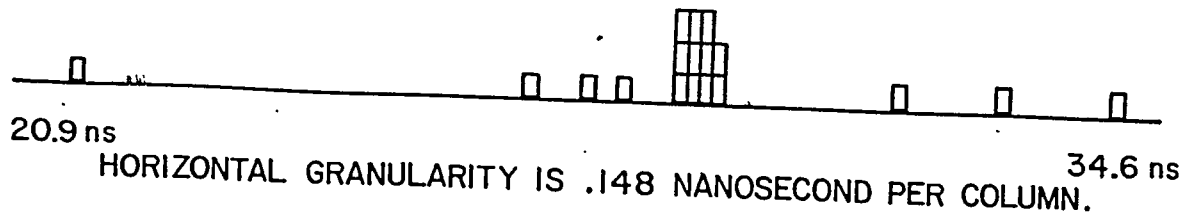
Geiger Mode Avalanche Photo-Detector

Following a suggestion at the Fifth Laser Ranging Instrumentation Workshop (B. Hyde, 1985), this type of detector was studied by us and used successfully in the new lunar laser ranging system. High quantum efficiency for single photon detection (20-30%), fast response, and large output voltage (5 volts) are among its desirable features. Details are given in the workshop paper by Bowman et al, referenced in the Introduction.

Timing and Calibration

The Maryland Event Timer, improved to 50 picosecond resolution (Steggerda, 1985), was used. The real time zero range calibration which is made possible by the large output voltage of the avalanche photo-detector is discussed by Rayner et al in the paper at this workshop referenced in the Introduction.

The zero range calibration for the measurement reported here is 103.5 ± 0.05 ns for the round trip range time.



ROUND TRIP RESIDUALS FROM THE JPL ANALYSIS OF THE RETURNS OF AUG. 26, 1986 (COURTESY OF X X NEWHALL)

Figure 3

Data

Figure 3 shows the histogram produced at the Jet Propulsion Laboratory during the analysis of the round trip times of the detected light quanta. Eleven returns are displayed in four contiguous bins 0.148 ns wide. The other entries in the histogram represent the background noise just before fourth quarter. The spatial filter was set at 5 arcseconds, the spectral filter width was 1.5 Angstroms, and the range gate was opened 300 ns before the prediction.

Mean = 29.24 ns
 Standard Deviation = 0.166 ns
 Standard Deviation of the Mean = 0.05 ns

For the one-way range, these times give

Standard Deviation = 2.5 cm
 Standard Deviation of the Mean = 0.75 cm.

It is interesting to note that the expected front to back spread from the libration tilt of the Apollo 15 LR³ on August 26, 1986 was 7 cm, or ± 3.5 cm. This is in reasonable agreement with the measured spread.

We believe this set of returns, although small in number of photons, to be the "tightest" in terms of spread yet achieved in lunar ranging.

Acknowledgments

It is a pleasure to acknowledge important contributions to this work by W. L. Cao, M. Z. Zhang and N. H. Wang of the Shanghai Institute of Optics and Fine Mechanics during their visits to the University of Maryland. We also thank our

colleagues D. G. Currie and J. D. Mullendore of the University of Maryland for many valuable contributions during the early days of this research. We are indebted to many people associated with the Goddard Space Flight Center: to John Degnan for his early technical contributions to this work and for his continuing expert interest; to Mike Figzmaurice for allowing the use of the 48 inch telescope; to Jan McGarry, Arnie Abbott, and Dick Chabot for technical support of the telescope; and to Tom Zagwowski for sharing the LAGEOS ranging experience at the telescope. We thank also our friends at the Jet Propulsion Laboratory, Jim Williams, Jean Dickey, and Skip Newhall for their invaluable help in identifying initial mistakes in the station coordinates and for the computer analysis of the measured data.

We acknowledge with gratitude not only the financial support of the U.S. Naval Observatory which has made this research possible, but also the strong technical contributions and interest of members of its Time Services Department.

References

S. R. Bowman, W. L. Cao, J. J. Degnan, C. O. Alley, M. Z. Zhang, and C. L. Steggerda, "The New University of Maryland Laser," Fourth International Workshop on Laser Ranging Instrumentation, Austin, Texas, edited by Peter Wilson by the Geodetic Institute, University of Bonn, 1982.

S. R. Bowman, C. O. Alley, J. T. Degnan, W. L. Cao, M. Z. Zhang, and N. H. Wang, "New Laser Developments towards a Centimeter Accuracy Lunar Ranging System," Fifth International Workshop on Laser Ranging Instrumentation, Herstmonceux Castle, England, edited by Jean Gaignebet of the by Groupe de Recherches de Geodesie Spatiale, Grasse, 1985.

B. Hyde, "Further Thoughts on a Minimal Transmitter for Laser Ranging", Fifth International Workshop on Laser Ranging Instrumentation, Herstmonceux Castle, England, Groupe de Recherches de Geodesie Spatiale, Grasse, 1985.

C. A. Steggerda, "Current Developments in Event Timers at the University of Maryland," Fifth International Workshop on Laser Ranging Instrumentation, Herstmonceux Castle, England, Groupe de Recherches de Geodesie Spatiale, Grasse, 1985.